

GENETICS OF REPRODUCTIVE SYSTEM DEVELOPMENT IN *C. BRIGGSAE*

**MOLECULAR GENETIC STUDY OF REPRODUCTIVE SYSTEM
DEVELOPMENT IN THE NEMATODE *CAENORHABDITIS BRIGGSAE***

By

DEVIKA SHARANYA PERAIYUR PREMKUMAR, M.SC

A Thesis submitted to the School of Graduate Studies In Partial Fulfillment of the
Requirements for the Degree Doctor of Philosophy

McMaster University

© Copyright by Devika Sharanya Peraiyur Premkumar, 2015

DOCTOR OF PHILOSOPHY (2015)
(Biology)

McMaster University
Hamilton, Ontario

TITLE: Molecular genetic study of reproductive system development in the nematode *Caenorhabditis briggsae*

AUTHOR: Devika Sharanya Peraiyur Premkumar M.Sc. (University of Madras)

SUPERVISOR: Dr. Bhagwati P. Gupta

NUMBER OF PAGES: 196

ABSTRACT

The nematode *C. briggsae*, a relative of *C. elegans*, is a widely used animal model for comparative studies to understand evolution of gene function and developmental mechanisms. To investigate differences in the mechanism of reproductive system development, genetic screens were conducted in our laboratory to isolate *C. briggsae* mutant strains that display abnormal vulva and vulva-uterine connection. The screens yielded at least seven genes whose loss of function results in a multivulva phenotype and 13 genes that result in egg-laying defective and protruding vulva phenotypes. Molecular cloning experiments were carried out to determine the identities of these genes, leading to the identification of five *C. elegans* orthologs that function at different steps of vulval development process. Three of these, *Cbr-lin-1*, *Cbr-lin-31* and *Cbr-pry-1*, encode components of Ras and Wnt pathways. The remaining genes are uncloned and include novel regulators of *C. briggsae* vulval development. Our comparative study of vulval development in *C. briggsae* and *C. elegans* has revealed differences in three homologous processes – inter-VPC distance, fate specification and anchor cell migration. Together these studies demonstrate that despite the overall similarity in vulval cell numbers and morphology between the two *Caenorhabditis* species, the underlying genetic programs include both conserved and divergent functional components. Additionally, this work highlights key resources such as mapping tools, mutant strains and CRISPR genome editing technology that have been developed to facilitate the use of *C. briggsae* in a comparative and individual context.

ACKNOWLEDGEMENTS

I would first like to thank my family for all their support during the course of my Ph.D. My father and mother have played a big role in becoming the person I am today. My mother especially, she instilled in my mind, and by her actions, that education is freedom and with it, anything is possible (The world is your oyster). Through my parents, I have learnt to step out of my comfort zone and that education is a liberating force that allows one to think clearly and look far ahead. To this day with their phone calls, they have always reminded me to try my very best and never give up.

To my brother, Rajesh, thank you. You have been my rock and my inspiration through my crusade for higher education. From far away, you have helped me with my endless application process in India six years ago. Even in Canada, every step of my life has started with your presence. I am grateful for all your support and I hope I continue to make you proud. To my sister-in-law Radhika, thank you for your encouragement and for putting up with my absence for all these years. Lastly, to my awesome niece Riya, while you are currently too young to realize this, your videos and baby talk over the phone have always made my day and I will treasure you always.

As William James once said, “Wherever you are, it is your friends who make your world”. A lot of my friends (Sharmila Sathiasothy, Marisa Isaacs, Jessica Knox, Phil Carrella , Sangeena Salam, May Yeo, Lynn Kennedy, Divya Bajoria, Akhila Prakash) have been pivotal for finishing this degree. Marisa Isaacs, who kidnapped me to her home during Christmas, so that I would not have to spend it alone and made me a part of her family. Sharmila Sathiasothy has been my constant companion and confidante. Through

our ritualistic phone calls, she has always motivated me to go after what I want and has been a comforting presence through all my ups and downs. Sangeena Salam, my roommate and who has been like family for the last few years. Jessica Knox and Phil Carella for their unwavering support and encouragement during my periods of writer's block and for our innumerable coffee and tea sessions. Also Divya Bajoria, we started our Bachelors, Masters and Ph.D. together and this year we are completing it once again together.

For research assistance and much needed guidance during my early years in McMaster, I am extremely grateful to Bavithra Thillainathan and Phil Cumbo. Phil Carella, Katelyn Link and Sara Nolte have been really awesome and I am thankful for all their assistance and time during the final stages of my thesis editing and preparation. I am also thankful to my lab mates and friends Ayush, Scott, Sangeena, Justin, Cory and Romy who have helped me out on every occasion despite my endless questions and complaints. A special shout-out to the undergraduate students Jaeyoung Kim, Ria Oommenn and Nayasta Kusdaya for all their assistance in changing this work to a story,

Finally, I would like to express my gratitude for the support of my supervisor Dr. Bhagwati Gupta, my committee members-Dr. Andre Bedard and Dr. Juliet Daniel who have showed confidence in me and for all their help given in shaping my work and thesis. I am especially grateful to Dr. Gupta who has always been available for my questions and also for encouraging me to explore the other facets of science.

Thank you all.

TABLE OF CONTENTS

Title Page	i
Descriptive Note	ii
Abstract	iii
Acknowledgements	iv-v
Table of Contents	vi-x
List of Figures	xi-xii
List of Tables	xiii-xiv
List of Abbreviations	xv-xvi
CHAPTER 1: INTRODUCTION	1
1.1 Overview	1
1.2 Formation of organs	2
1.2.1 Organogenesis: Insight into conserved signaling pathways and genes	3
1.3 Comparative studies: Conserved and divergent developmental mechanisms	5
1.4 Nematodes as model organisms to investigate evo-devo mechanisms.....	7
1.4.1 <i>Caenorhabditis elegans</i> isolate N2	9
1.4.2 <i>Caenorhabditis briggsae</i> in comparison to <i>C. elegans</i>	10
1.5 <i>C. elegans</i> reproductive system	13
1.5.1 Components of the reproductive system.....	13
1.5.2 Formation of the vulva and vulva-uterine connection.....	14
1.5.2.1 Cellular events	14
1.5.2.2 Molecular mechanisms	19
1.6 Signaling pathways involved in vulval development	22
1.6.1 Wnt signaling.....	27
1.6.2 RAS/MAPK signaling	31

1.6.2.1	Components of RAS/MAPK pathway	33
1.6.2.2	Downstream targets	34
1.6.2.3	Regulators of the Ras pathway	35
1.6.2.3.1	Positive regulators of RAS/MAPK signaling	36
1.6.2.3.2	Negative regulators of RAS/MAPK signaling	38
1.6.2.4	Chromatin mediated regulation.....	39
1.6.3	Notch signaling.....	41
1.7	Reproductive system development in <i>C. briggsae</i>	45
1.7.1	Developmental processes and similarities and differences from <i>C. elegans</i> ...	45
1.8	Genetic dissection of vulval development in <i>C. briggsae</i>	48
1.9	Summary of intent.....	50
CHAPTER 2: MATERIALS AND METHODS		53
2.1	Strains and culture conditions	53
2.2	Genetic screens	54
2.3	Mapping	55
2.4	Complementation.....	56
2.5	Serotonin and fluoxetine drug assays	56
2.6	Heat shock experiment.....	57
2.7	Egl penetrance assay	57
2.8	Muv penetrance assay	57
2.9	Generation of sgRNA constructs	58
2.10	Sequencing.....	59
2.11	Generation of transgenic strains.....	59
2.12	Microscopy	60
2.13	Ablation experiments	61
2.14	Statistical analysis	62
2.15	U0126 assays	62
2.16	Quantitative RT-PCR assays.....	62

CHAPTER 3: GENETIC CONTROL OF VULVAL DEVELOPMENT IN <i>CAENORHABDITIS BRIGGSAE</i>	64
Introduction	66
Results	70
Class 1 mutants have defects in egg-laying components other than the vulva and utse	71
Class 2 mutants have defects in nuclear migration and include <i>Cbr-unc-84</i>	71
Class 3 mutants exhibit reduced VPC induction	72
Overexpression of <i>lin-3</i> suppresses the VPC induction defect in a subset of class 3 mutants	73
Class 3 mutations <i>bh20</i> and <i>bh23</i> are alleles of <i>Cbr-lin-39</i>	74
Pn.p cells lack competence and are irregularly placed in <i>Cbr-lin-39</i> mutants	75
<i>bh20</i> is epistatic to <i>Cbr-pry-1(sy5353)</i>	75
Class 4 mutations affect vulval invagination and morphology	75
<i>Cbr-lin-11</i> mutations disrupt vulva and utse morphogenesis	77
Discussion	77
Acknowledgements	80
Supporting information	83-86
CHAPTER 4: MUTATIONS IN <i>CAENORHABDITIS BRIGGSAE</i> IDENTIFY NEW GENES IMPORTANT FOR LIMITING THE RESPONSE TO EGF SIGNALING DURING VULVAL DEVELOPMENT	87
Introduction	89
Results	93
A genetic screen for Multivulva mutants in <i>C. briggsae</i> identifies alleles of seven genes	93
Ectopic vulval cells in <i>C. briggsae</i> Muv mutants can adopt primary as well as secondary vulval cell fates	94
Genetic mapping and a streamlined approach for gene mapping in <i>C. briggsae</i>	95
Mutations in three <i>C. elegans</i> Muv gene orthologs also confer a Muv phenotype	96

The Muv phenotype of <i>C. briggsae</i> mutants is gonad independent	96
The Muv phenotype of new <i>C. briggsae</i> mutants is dependent on MEK	96
The Muv phenotype of some new <i>C. briggsae</i> mutants does not result from increased transcript abundance of lin-3/EGF	99
Discussion	99
Acknowledgements	101
Supporting information	104-109
CHAPTER 5: GENOME EDITING IN <i>CAENORHABDITIS BRIGGSAE</i> USING THE CRISPR/CAS9 SYSTEM	110
Introduction	114
Results	115
Discussion	119
Acknowledgements	120
Supporting information	123-128
CHAPTER 6: DISCUSSION AND FUTURE DIRECTIONS	129
6.1. Genes involved in P-cell migration.....	130
6.2. Genes affecting cell proliferation.....	131
6.2.1. Vulvaless genes	131
6.2.2. Multivulva genes	132
6.2.3. Identification of conserved <i>C. elegans</i> orthologs in <i>C. briggsae</i>	132
6.2.4. New genes that function in an EGF dependent manner	134
6.3. Genes affecting vulval morphology.....	136
6.4. Genetic variations underlying a robust system	136
6.5. Phenotypic spectrum of mutants obtained in different nematode species	140
6.6. Concluding remarks	142
6.7. Future directions	143

APPENDIX.....	146
REFERENCES	156

LIST OF FIGURES

Chapter 1:

Figure 1	Specification of invariant cell fate pattern (3°3°2°1°2°3°) among the vulval precursor cells (VPCs) through Ras, Wnt and Notch signaling pathways in <i>C. elegans</i> .	17
Figure 2	Overview of conserved Wnt, Ras/MAPK and Notch signaling pathways and the core pathway homologs in <i>C. elegans</i>	24-26
Figure 3	Percent identity between the Wnt orthologs in <i>C. elegans</i> and <i>C. briggsae</i>	30
Figure 4	Percent identity between the Ras pathway orthologs in <i>C. elegans</i> and <i>C. briggsae</i>	32
Figure 5	Interaction of Ras and Notch signaling pathways during vulval development	43
Figure 6	Percent identity between the Notch pathway orthologs in <i>C. elegans</i> and <i>C. briggsae</i>	44
Figure 7	Vulval development from L3 to mid L4 stage in <i>C. briggsae</i> .	46
Figure 8	Vulval morphology of <i>C. elegans</i> and <i>C. briggsae</i>	47

Chapter 2:

N/A

Chapter 3:

Figure 1	Egg-laying responses of class 1 mutants	72
Figure 2	Nuclear migration defects in class 2 mutants and molecular analysis of <i>Cbr-unc-84</i>	72
Figure 3	Vulva phenotypes of class 2 and 3 mutants	73
Figure 4	Effect of <i>lin-3</i> overexpression on VPC induction in class 3 mutants	75
Figure 5	Genomic organization and mutant phenotypes of <i>lin-39</i>	76

Figure 6	Vulval morphology defects in class 4 mutants	77
Figure 7	Genomic organization of <i>Cbr-lin-11</i> and mutant phenotypes	78
Figure 8	Vulval development in <i>C. briggsae</i> and the proposed roles of genes described in this study	79
<u>Chapter 4:</u>		
Figure 1	Wild-type vulval development in <i>C. elegans</i> and <i>C. briggsae</i> .	90
Figure 2	<i>C. briggsae</i> Muv mutants exhibit ectopic development of primary and secondary vulval cells	95
Figure 3	Genetic linkage map of <i>C. briggsae</i> Muv genes described in this study	96
Figure 4	A streamlined genetic mapping method allows for efficient genetic mapping and gene identification of <i>Cbr-lin-1</i>	97
Figure 5	Genetic mutations associated with <i>Cbr-lin-31</i> and <i>Cbr-pry-1</i> are identified from the set of <i>C. briggsae</i> Muv mutants	98
Figure 6	The Muv phenotype associated with <i>C. briggsae</i> mutants is gonad-independent	99
Figure 7	The Muv phenotype of four new <i>C. briggsae</i> mutants is dependent on MEK.	99
Figure 8	The abundance of <i>lin-3/EGF</i> transcripts in <i>C. briggsae</i> and <i>C. elegans</i> Muv mutants determined by qRT-PCR	100
<u>Chapter 5:</u>		
N/A		
<u>Chapter 6:</u>		
N/A		
<u>Chapter 7:</u>		
N/A		
<u>Appendix</u>		
Figure 1	Expression of <i>nhr-67</i> in <i>C. briggsae</i> at L3 and early L4 stages	151

LIST OF TABLES

Chapter 1:

N/A

Chapter 2:

N/A

Chapter 3:

Table 1	Results of complementation experiments	69
Table 2	Linkage mapping of <i>Cbr-lin-11</i> using phenotypic markers	69
Table 3	Linkage mapping of mutations by BSA and SNP-chip techniques	70
Table 4	Overview of <i>C. briggsae</i> egg-laying defective mutants	71
Table 5	Vulval induction pattern in Class 2 and 3 mutants	73
Table 6	Vulval cell lineage analysis of class 3 and 4 mutants	74
Table 7	Effect of cell ablations on VPC fates in class 3 mutants	74
Table 8	Vulval morphology defects in class 4 mutants	77
Table 9	Expression of vulval cell fate markers in <i>Cbr-lin-11</i> mutants	78

Chapter 4:

Table 1	An overview of <i>C. briggsae</i> Muv mutants described in this study	91
Table 2	The Muv phenotype of <i>Cbr-lin(gu102)</i> and <i>Cbr-lin(gu167)</i> is temperature sensitive	91
Table 3	Vulval defects in Muv animals derived from homozygous and heterozygous mothers	94
Table 4	Analysis of the VPC induction pattern in Muv mutants	94

Chapter 5:

Table 1	Phenotypes of transgenic animals generated using the CRISPR/Cas9 technique	117
Table 2	Alleles generated by the CRISPR/Cas9 approach	118

Table 3	Genome editing events detected using CRISPR-mediated HR	119
----------------	---	-----

Chapter 6:

N/A

Chapter 7:

Table A1	Main components and targets of Ras, Wnt and Notch signaling pathways in <i>C. elegans</i> and <i>C. briggsae</i> .	153
-----------------	--	-----

LIST OF ABBREVIATIONS

AC	Anchor cell
APC	Adenomatous polyposis coli
BMP	Bone morphogenetic protein
Cbr	<i>Caenorhabditis briggsae</i>
Cel	<i>Caenorhabditis elegans</i>
CK1	Casein kinase I
CRISPR	Clustered, regularly interspaced, short palindromic repeats
CSL	CBF1/Suppressor of Hairless/LAG-1
Dpy	Dumpy
DSD	Developmental system drift
DSL	<i>Drosophila</i> (Delta, Serrate) and <i>C. elegans</i> (LAG-2)
EGF	Epidermal growth factor
Egl	Egg-laying defective
EMS	Ethyl methyl sulfonate
Evo-Devo	Evolution and Development
FGF	Fibroblast growth factor
Fz	Frizzled
GEF	Guanine nucleotide exchange factor
GRB-2	Growth factor Receptor-Bound protein-2
GSK-3	Glycogen synthase kinase-3
GTP	Guanosine Triphosphate
HR	Homologous recombination
Hyp	Hypodermis
ivp	Inappropriate vulval cell proliferation
LEF	Lymphoid enhancer-binding factor
LINC	Linker of nucleoskeleton and cytoskeleton
MAPK	Mitogen-activated protein kinase
MEK	Mitogen-activated protein kinase kinase
Muv	Multivulva
NHEJ	Non-homologous end joining
PAM	Protospacer adjacent motif
Ppa	<i>Pristionchus pacificus</i>
PLZF	Promyelocytic leukaemia zinc finger protein
Pvl	Protruding vulva
sg	Single guide
Shh	Sonic hedgehog
SNP	Single nucleotide polymorphism
Sog	short gastrulation
ssODN	single stranded oligonucleotides
synMuv	Synthetic Multivulva

TALEN	Transcription activator-like effector nuclease
TCF	T-cell factor
Unc	Uncoordinated
Utse	Uterine seam cell
VC	Ventral cord
VPC	Vulval precursor cell
VU	Ventral uterine
Vul	Vulvaless
ZFN	Zinc finger nuclease
ZPA	Zone of polarizing activity

CHAPTER 1: INTRODUCTION

1.1 Overview

The formation of organized structures such as tissues and organs is a striking feature of multicellular organisms. The morphogenesis of these structures is tightly linked to the organization of individual cells during early stages of development. Given the diverse and complex nature of development within the animal kingdom, the study of morphogenesis can be extremely difficult. Remarkably, underneath most of this morphological diversity lies a common set of genetic and cellular mechanisms. However, exactly how the information is processed for cells to organize and form a specific structure in individual organisms still remains an open area of investigation.

The use of model organisms has greatly enhanced our understanding of organ formation. Analysis of mutant animals defective in a particular behavior can provide insight into the components of the organ system and shed light on the genetic programs underlying cell fate specificity. This thesis focuses on the development of the egg laying organ (vulva) in the nematode *Caenorhabditis briggsae* (*C. briggsae*). Taking a forward genetics approach, I investigated the genetic components required for vulval development. Additionally, the studies described herein sets the background for future comparative studies with *Caenorhabditis elegans* (*C. elegans*), a well-established model nematode, to understand how developmental processes change during evolution.

1.2 Formation of organs

Most multicellular organisms begin their life as a single celled zygote. The single cell divides and differentiates to form tissues and organs and ultimately results in the formation of a living organism capable of performing specialized tasks. With nearly 8 million animal species on earth (Mora *et al.*, 2011), it is amazing how cells process genomic information to form distinct structures such as organs in different animal species.

Organogenesis in multicellular animals mostly occurs after gastrulation through the formation of the three germ layers; ectoderm, endoderm and mesoderm (Gilbert, 1997; Solnica-Krezel and Sepich, 2012). Organs are comprised of various cell types and tissues derived from the different germ layers. This process involves the interaction, proliferation and differentiation of cells, and importantly, also requires their organization into distinct patterns for proper organ development. These myriad cellular processes are regulated by multiple signaling pathways to ensure precise control of cell fate and behavior. Alterations in any of these cellular or molecular mechanisms can lead to embryonic defects, congenital abnormalities and structural deficiencies. Due to this intrinsic complexity, organogenesis poses one of the greatest challenges in developmental biology. Nevertheless, the study of organogenesis holds the key to gaining insight into genes controlling cellular organization, development of new strategies to improve health care management and the differences leading up to evolutionary change (Langer and Vacanti, 1993; Whitsett *et al.*, 2004; Zorn and Wells, 2009; Egeblad *et al.*, 2010; Carroll *et al.*, 2013; Fahed *et al.*, 2013).

1.2.1 Organogenesis: Insight into conserved signaling pathways and genes

Previous studies of organogenesis have identified conserved genes and signaling pathways that spatiotemporally regulate a number of biological processes and have improved our understanding of organ development and function in humans and other organisms. For instance, developmental studies on tooth structure have identified a conserved signaling center involving Bone morphogenetic protein (BMP) and Fibroblast growth factor (FGF) signaling that is also expressed in the organizing centers of the embryo, notochord and limb buds (Roelink *et al.*, 1995; Tickle, 1995; Thesleff, 1996). Organogenesis study of the mammalian renal system provided the biological basis for examining molecular events underlying induction and differentiation in kidneys with healthy and impaired function (Saxen and Sariola, 1987).

Further developmental studies using representative model systems like *Drosophila melanogaster* (*D. melanogaster*) have revealed that major components of intercellular signaling pathways also have vertebrate counterparts, e.g. the *short gastrulation* (*sog*) gene is the *D. melanogaster* homolog of vertebrate *chordin* which interacts with the transforming growth factor beta (TGF- β) family of signaling proteins to specify the dorsoventral axis in embryos (Francois *et al.*, 1994). Other signaling proteins include Sonic hedgehog (Shh), a homolog of the *D. melanogaster* Hedgehog signaling protein that is expressed in the growing vertebrate limb bud at the Zone of Polarizing Activity (ZPA) as a morphogen. Comparative studies have identified that changes in Shh signaling could be a major driver in evolutionary diversification of vertebrate limbs (Tickle and Barker, 2013; Lopez-Rios *et al.*, 2014). In *C. elegans*, a number of mutagenesis studies

centered on the identification of genes required for vulval development have identified a signaling network formed by the Epidermal growth factor (EGF), Wnt, and Notch pathways, resulting in an invariant fate pattern among the ventral epithelial precursor cells (Trent *et al.*, 1983; Ferguson and Horvitz, 1985; Sternberg and Horvitz, 1986; Eisenmann, 2005; Greenwald, 2005; Sundaram, 2006).

Hox genes are another prime example of conserved genes in metazoans. They were first identified in *D. melanogaster*, when mutations resulted in homeotic transformation causing a body part or organ to be transformed into another type, e.g. antennae transformed into legs or halteres instead of wings (Lappin *et al.*, 2006). Hox genes function as regulatory transcription factors and are responsible for specifying segmental identity along the anterior-posterior axis (Lewis, 1978; Nüsslein-Volhard and Wieschaus, 1980; McGinnis *et al.*, 1984). Their relative positioning on the chromosomes reflects their anterior-posterior patterning along the organism's body and variations in copy number or spatiotemporal expression correlates with differences in body plan (McGinnis and Krumlauf, 1992; Gellon and McGinnis, 1998). These Homeobox-containing genes are fundamental components of the genetic toolkit responsible for development in all animals and with their discovery in evolutionary distant species, comparative studies involving evolution and development (evo-devo) became prominent (McGinnis *et al.*, 1984; Carroll *et al.*, 2013; Heffer and Pick, 2013).

1.3 Comparative studies: Conserved and divergent developmental mechanisms

Beginning just over a century ago, the approach of model organism-based developmental studies has enhanced our understanding of metazoan development immeasurably. By acting as a representative for a larger group of species, model organisms have provided a fundamental architecture to understand how the components of a biological system form and function. With progressing genomic technologies and scientific methods, the number of model organisms has vastly increased and comparative studies have grown to become a powerful approach in examining developmental diversity. They can facilitate a better understanding of the underlying genetic framework of a given structure and help us understand how modifications to these frameworks evolve to give rise to new structures or novel phenotypes in related species. For example, functional comparisons of the Ultrabithorax orthologs have resulted in the identification of a conserved domain that is present in insects, but absent in other arthropods, which is responsible for the diversification of thoracic and abdominal segments in insects (Galant and Carroll, 2002). Another example is the *HoxC8* gene in vertebrates (Belting *et al.*, 1998; Cohn and Tickle, 1999). Temporal shifts in expression and divergence of a cis-regulatory element in *Hoxc8* is associated with differences in axial morphology between chickens and mice (Belting *et al.*, 1998). In snakes, the absence of *Sonic Hedgehog* (*Shh*) expression along with the expansion of HOXB5 and HOXC8 expression domains accounts for the extended thorax and absence of limbs (Cohn and Tickle, 1999). Other prominent instances of large scale morphological variation between species determined by comparative studies include differences in the number of repeated parts (segmentation)

in arthropods, diversification of homologous structures as in limb development between vertebrate lineages, and evolution of new characteristics such as butterfly wing spots, hair, and antlers in mammals (True and Haag, 2001; Carroll *et al.*, 2013).

On the other hand, underlying developmental mechanisms often diverge over time without phenotypic change, a process known as ‘Developmental System Drift’ (DSD). This is often manifested in highly conserved features like body patterning (True and Haag, 2001). In the nematodes *C. elegans* and *Pristionchus pacificus*, the *lin-39* Hox gene controls vulval cell fate specification in the central body region of the worm (Clark *et al.*, 1993; Sommer *et al.*, 1998). In *P. pacificus*, the vulval cells of *lin-39* mutants undergo programmed cell death, while in *C. elegans*, *lin-39* vulval cells fuse to the hypodermis (Clark *et al.*, 1993; Sommer *et al.*, 1998). In both cases, loss of LIN-39 function gives rise to a non-vulval fate resulting in a vulvaless phenotype, but the cell fate decisions between these two species have diverged (Clark *et al.*, 1993; Eizinger, 1997; Sommer *et al.*, 1998). Signaling mechanisms also differ between these two species. In *C. elegans*, the vulval cell fate is induced mainly by EGF/LIN-3 signal from the anchor cell (AC) along with Wnt signaling, whereas Wnt signaling plays a predominant role during vulval induction in *P. pacificus* (Sternberg, 2005; Zheng *et al.*, 2005; Tian *et al.*, 2008). Furthermore, analysis of a neomorphic allele of *P. pacificus lin-17* where the receptor has acquired an additional domain for regulatory linkage provides evidence of a novel aspect of Wnt signaling that is different from *C. elegans* (Wang and Sommer, 2011). This observation reveals the modular nature of proteins which could potentially rewire signaling mechanisms (Dueber *et al.*, 2003; Howard *et al.*, 2003; Park *et al.*, 2003;

Bhattacharyya *et al.*, 2006; Wang and Sommer, 2011). Genome sequence comparisons to resolve the phylogenetic relationships among the *Caenorhabditis* nematodes suggest that the hermaphroditic mode of reproduction evolved independently in *C. elegans* and *C. briggsae* – the two closely related species that look morphologically identical (Kiontke *et al.*, 2004). *C. briggsae* lacks an ortholog of *fog-2*, a gene responsible for hermaphrodite spermatogenesis in *C. elegans* (Nayak *et al.*, 2005), and RNAi experiments have revealed functional differences among the *fem* genes that are responsible for masculinization of the germline (Stothard and Pilgrim, 2003).

Comparative studies also aid in the identification of regulatory elements (Bergmann *et al.*, 2004). Phylogenetic footprinting enabled the identification of conserved *cis*-regulatory sequences responsible for expression in specific vulval cell types in *C. elegans* and *C. briggsae*, providing tools for expression analysis and mutational analysis (Kirouac and Sternberg, 2003).

1.4 Nematodes as model organisms to investigate evo-devo mechanisms

Nematodes are attractive model systems for comparative evo-devo studies given their prevalence in nature (from the tropics to the polar region) and amenability to genetic manipulation. They offer great potential to gain an understanding in the fields of ecology, evolution, genetics, development, aging, and behavior. They provide several experimental advantages, including ease of maintenance, short generation time, and large brood size, facilitating the study of numerous biological processes that are difficult to study in other

model systems or humans. The prototypical model of the *Caenorhabditis* genus that has been studied in great detail is *C. elegans* (Brenner, 1974).

Comparative studies involving different nematode species and *C. elegans* have identified several differences in gene expression, cell lineages, and morphogenetic processes such as gonadogenesis and vulval development. For instance, the adult *C. elegans* hermaphrodite contains exactly 959 somatic cells, with the lineage of every cell during embryonic and post-embryonic development completely traced (Sulston and Horvitz, 1977). On comparison of this cell lineage map with nematodes like *Panagrellus redivivus*, several cell lineage transformations with respect to polarity reversal, cell fate switch, and division number can be observed (Sulston and Horvitz, 1977; Rudel and Sommer, 2003; Wanninger, 2015). Thus, differences in cell lineage could be used to explain variations in morphological structures. Nematodes also display substantial variation during gonad development. The gonads in males across species are always monodelphic (one-armed), while the gonads in females or hermaphrodites can be mono or didelphic (two-armed) (Chitwood and Chitwood, 1974). *C. elegans* has two gonadal arms developing from four progenitor cells, Z1-Z4. However, in nematodes, such as *Oscheius guentheri*, *Panagrellus redivivus*, *Panagrolaimus sp.* PS1579, and *Mesorhabditis sp.* PS1179, the Z4 lineage is shortened by programmed cell death (Félix and Sternberg, 1996). This results in a monodelphic gonadal structure (Félix and Sternberg, 1996). Monodelphy has evolved repeatedly in these nematodes and in all these species the events are preceded by an asymmetric division in timing between the gonadal cells Z1 and Z4 (Félix and Sternberg, 1996). Another example of how natural genetic

variation influences nematode development is in vulval development. Nematodes can display a wide range of variations with respect to vulval positioning (central versus posterior) and composition (number of vulval precursor cells) (Sommer and Sternberg, 1996). These variations are attributed to changes in the number of gonadal arms, gonad migration and cell signaling events. Given the wide range of variation in developmental processes, combined with the knowledge from *C. elegans*, nematodes form an ideal system for studies involving evolution and development

1.4.1 *Caenorhabditis elegans* isolate N2

C. elegans was first introduced as a model organism in 1973 by Sydney Brenner to study eukaryotic development and the nervous system (Brenner, 1973, 1974). It has a hermaphroditic mode of reproduction and a short life cycle (Brenner, 1974; Riddle *et al.*, 1997). It takes three days to progress from egg to adult, moving through four larval stages (L1 to L4) (Brenner, 1974; Byerly *et al.*, 1976; Riddle *et al.*, 1997). Each hermaphrodite is capable of laying up to 300 eggs under self-fertilization, and substantially more if mating occurs with males (Brenner, 1974; Byerly *et al.*, 1976). The small size (1mm) and transparency of the nematode body, alongside the constancy of cell number and position from one individual to another are unique properties that have enhanced studies in this organism (Riddle *et al.*, 1997). These initial studies, combined with the nematode's genetic tractability in forward and reverse genetic analyses have enabled researchers to elucidate the fine details of the cellular events in *C. elegans* development.

1.4.2 *Caenorhabditis briggsae* in comparison to *C. elegans*

Over the last decade, focus has shifted from *C. elegans* to several other nematode species like *Pristionchus sp.*, *Oscheius sp.*, and *Caenorhabditis briggsae* (*C. briggsae*) to further understand how genetic networks and signaling mechanisms function and evolve (Dichtel *et al.*, 2001a; Dichtel-Danjoy and Félix, 2004; Hong and Sommer, 2006). In the studies described below, we use *Caenorhabditis briggsae* (*C. briggsae*) isolate AF16, a close relative of *C. elegans*, as a genetic system to investigate various processes during vulval development.

C. briggsae is a hermaphroditic nematode that diverged from *C. elegans* approximately 30 million years ago (MYA) (Cutter, 2008). Both nematode species share almost identical morphology and a similar ecological niche, growing within rotten fruits, stems, and in invertebrate carriers, with the exception that *C. briggsae* can thrive in higher temperatures (up to 28°C) (Félix and Duvéau, 2012). Studies sampling natural populations of *C. elegans* and *C. briggsae* have shown that *C. elegans* has a low global diversity whereas *C. briggsae* has a clear pattern of population differentiation between tropical and temperate clades (Barrière and Félix, 2005; Cutter *et al.*, 2006; Dolgin *et al.*, 2008). Several other reports have identified differences between *C. elegans* and *C. briggsae* developmental processes. Some examples include the vulval development process, RNAi uptake, embryonic patterning, and excretory system anatomy (Wang and Chamberlin, 2002; Félix, 2007; Lin *et al.*, 2009; McEwan *et al.*, 2012). With the release of its sequenced genome in 2003 and subsequent RNA-seq analysis in 2012, *C. briggsae* has become a popular species for comparative analysis with *C. elegans* and for

deciphering mechanisms of development involving gene evolution and function (Stein *et al.*, 2003; Uyar *et al.*, 2012).

The genomes of *C. elegans* and *C. briggsae* are similar in organization and size, with both nematodes containing six chromosomes that total a size of 100.3 MB and 104 MB, respectively (Stein *et al.*, 2003). Almost 60% of *C. briggsae* genes have clear orthologs in *C. elegans* (Stein *et al.*, 2003; Uyar *et al.*, 2012). The remaining genes are species-specific or have multiple orthologs in *C. elegans* and other species (Stein *et al.*, 2003; Strange, 2006). Among the 1105 operons detected, approximately 51% are conserved in *C. elegans*, while the rest are divergent or *C. briggsae*-specific (Stein *et al.*, 2003; Uyar *et al.*, 2012). Additionally, there is limited conservation of genes with alternative splice forms (Uyar *et al.*, 2012). Alternative splicing plays a major role in species specificity by regulating and diversifying gene function (Blencowe, 2006). The limited conservation of alternative splice forms still needs to be validated by comparing transcriptomes of nematodes at different developmental stages and in varying environmental conditions (Uyar *et al.*, 2012). Functional conservation among many genes has also been highlighted through rescue experiments between the two species. However, this does not indicate that all genes will function or be expressed in a similar manner in both of the nematode species (Krause *et al.*, 1994; Verster *et al.*, 2014).

In the last decade, alongside the release of the *C. briggsae* genome, recombination maps were generated using SNPs, indels, and mutations to improve mapping and gene identification with forward genetic screens (Stein *et al.*, 2003; Baird and Chamberlin, 2006; Hillier *et al.*, 2007; Koboldt *et al.*, 2010; Ross *et al.*, 2011). More recently,

additional resources have become available that include a *C. briggsae* RNAi library of genes that exhibit 1:1 orthology to *C. elegans* and a fosmid-based transgene resource that allows for examination of protein function, cell lineage tracing, and gene expression profiling (Sarov *et al.*, 2006, 2012; Zhao *et al.*, 2010; Verster *et al.*, 2014).

In addition to the above resources, new genome editing technologies involving the use of nucleases with transcription activator-like effector nucleases (TALENs) and RNA-guided Clustered, Regularly Interspaced, Short Palindromic Repeats (CRISPR) to engineer double stranded breaks at specific locations in the genomes (Dickinson *et al.*, 2013, 2015; Wei *et al.*, 2014; Witte *et al.*, 2015) have allowed for the creation of targeted mutants in *C. briggsae*. In the case of CRISPR, a single guide RNA (sgRNA) expressed from a U6 RNA polymerase III promoter and a DNA endonuclease (Cas9) specifically target genomic sequences preceding a Protospacer Adjacent Motif (PAM) 3'NGG site to cause double strand breaks. The breaks are repaired by an error-prone non-homologous end joining (NHEJ) mechanism (Frøkjær-Jensen, 2013). While the CRISPR protocol has been well established in *C. elegans* (Friedland *et al.*, 2013), its use in other nematodes is just beginning. Witte *et al.*, 2015 have reported successful adoption of CRISPR in *Pristionchus sp.* Chapter 5 in this thesis reports a working CRISPR method in *C. briggsae* that I, along with other members of the Gupta lab, have developed and used to generate mutant alleles of several genes. The CRISPR approach provides a powerful tool to study the function of desired genes involved in vulval development in *C. briggsae*.

1.5 *C. elegans* reproductive system

1.5.1 Components of the reproductive system

The hermaphrodite vulva is one the best studied organ systems in *C. elegans*. Several features make vulval development an attractive paradigm for study. For one, it is a reproductive organ necessary for mating and egg-laying. The vulva is comprised of 22 cells that are derived from seven different cell types following an invariant lineage (Sulston and Horvitz, 1977; Sternberg and Horvitz, 1986; Sharma-Kishore *et al.*, 1999). The organ develops at approximately 28 hours post-L1 larval stage at a precise location in the mid-body region of the worm (Sulston and Horvitz, 1977; Sternberg and Horvitz, 1986). The developmental patterning of this organ requires a network of genes and signaling pathways including Ras, Wnt, and Notch that control the generation, migration, competence, induction, interaction, proliferation, and differentiation/fate specification of cells during morphogenesis (Greenwald *et al.*, 1983; Sternberg and Horvitz, 1986; Sternberg and Han, 1998; Fay and Han, 2000; Eisenmann, 2005; Greenwald, 2005; Cui *et al.*, 2006a, 2006b).

To initiate egg-laying, the vulva requires a functional connection with the gonad, uterine and vulval muscles, as well as two classes of motor neurons; the ventral cord (VC) motor neurons and hermaphroditic-specific motor neurons (White *et al.*, 1986; Li and Chalfie, 1990). Together, these tissues comprise the egg-laying system. The anchor cell (AC) in the somatic gonad plays a major role in vulval morphogenesis and ultimately connects the uterus to the vulva through the formation of the uterine seam cell (Utse) (Newman and Sternberg, 1996). Fertilized eggs are passed to the outside environment

through the vulva with the aid of the vulval and uterine muscles, which control the vulval opening and contraction of the uterus (White *et al.*, 1986; Li and Chalfie, 1990). Muscle activity is controlled by the motor neurons, which form a neuropil (White *et al.*, 1986). The development of this reproductive system follows a series of conserved events that is comparable in *C. briggsae* (Gupta and Sternberg, 2003; Félix, 2004, 2007; Seetharaman *et al.*, 2010; Pénigault and Félix, 2011b; Sharanya *et al.*, 2012, 2015).

1.5.2 Formation of the vulva and vulva-uterine connection

1.5.2.1 Cellular events

In *C. elegans*, vulval fate is initiated with the migration of 12 epidermal P-cells from a ventrolateral position into the ventral cord (Sulston and Horvitz, 1977). Once cell migration is complete, division occurs. The posterior daughter cells of P3-P8 form the vulval precursor cells VPCs (P3.p-P8.p) and together, they establish the precise pattern of VPC fates (3°-3°-2°-1°-2°-3°) (Figure1) (Sternberg and Horvitz, 1986; Sternberg, 2005). The posterior daughters of P1.p, P2.p, and P9.p-P11.p fuse with the hypodermis (hyp7) in the L1 stage (Sulston and Horvitz, 1977). P12.p divides to form two cells – P12.pa undergoes programmed cell death, while P12.pp forms the preanal hypodermis (hyp12) (Sulston and Horvitz, 1977).

Early work by Sulston and White (1980) showed that the gonad plays a crucial role in the formation of the vulva. The removal of the gonad (by ablating gonad precursors during the L1 stage) resulted in vulvaless animals due to VPC daughter cell fusion to the surrounding syncytium. Subsequent work by Kimble (1981) showed that a specialized

gonadal cell, anchor cell (AC), is the key regulator of VPC induction. The AC is formed during the L2/L3 stage through the interaction of two gonadal cells, Z1.ppp and Z4.aaa, which become the AC and a ventral uterine (VU) cell (Hirsh *et al.*, 1976; Kimble and Hirsh, 1979; Kimble, 1981; Seydoux and Greenwald, 1989). During the L3 larval stage, the AC induces P6.p to acquire a 1° fate, while P5.p and P7.p adopt a 2° fate through lateral signaling (Figure 1) (Sternberg and Horvitz, 1986; Greenwald, 2005; Sternberg, 2005). VPCs that do not receive the inductive signal (P3.p, P4.p and P8.p) acquire a non-vulval 3° fate (Figure 1) (Sulston and Horvitz, 1977; Kimble, 1981; Sternberg and Horvitz, 1986; Sternberg, 2005). The 3° VPCs divide once to generate two daughter cells that fuse to the hyp7 in the L3 stage (Figure 1) (Sulston and Horvitz, 1977; Kimble, 1981; Sternberg and Horvitz, 1986; Sternberg, 2005). The P3.p occasionally fuses to hyp7 during the L2 stage before it has a chance to divide, a fate that is termed “Fused” (F) or 4° fate (Sulston and Horvitz, 1977; Kimble, 1981; Sternberg and Horvitz, 1986; Sternberg, 2005).

After induction by the AC, the 1° VPC P6.p undergoes three rounds of cell division in a TTTT lineage (where T is transverse axis of cell division) to generate eight progeny (P6.pxxx) that generate two differentiated cell types in adults – vulE and vulF in a mirrored symmetric pattern (Sternberg and Horvitz, 1986; Wang and Sternberg, 2000; Sternberg, 2005). The 2° VPCs P5.p and P7.p also undergo three rounds of cell division, each in a NTLL lineage (where N - no division, T – transverse and L – longitudinal axis) in opposite orientations, producing seven progeny cells (P5.pxxx and P7.pxxx) that differentiate to produce five cell types (vulA, vulB1, vulB2, vulC and vulD) (Sternberg

and Horvitz, 1986; Sharma-Kishore *et al.*, 1999; Sternberg, 2005). The division patterns of 2^o VPCs P5.p and P7.p are due to the action of the Wnt signaling pathway that changes the polarity of P7.p cells (Deshpande *et al.*, 2005).

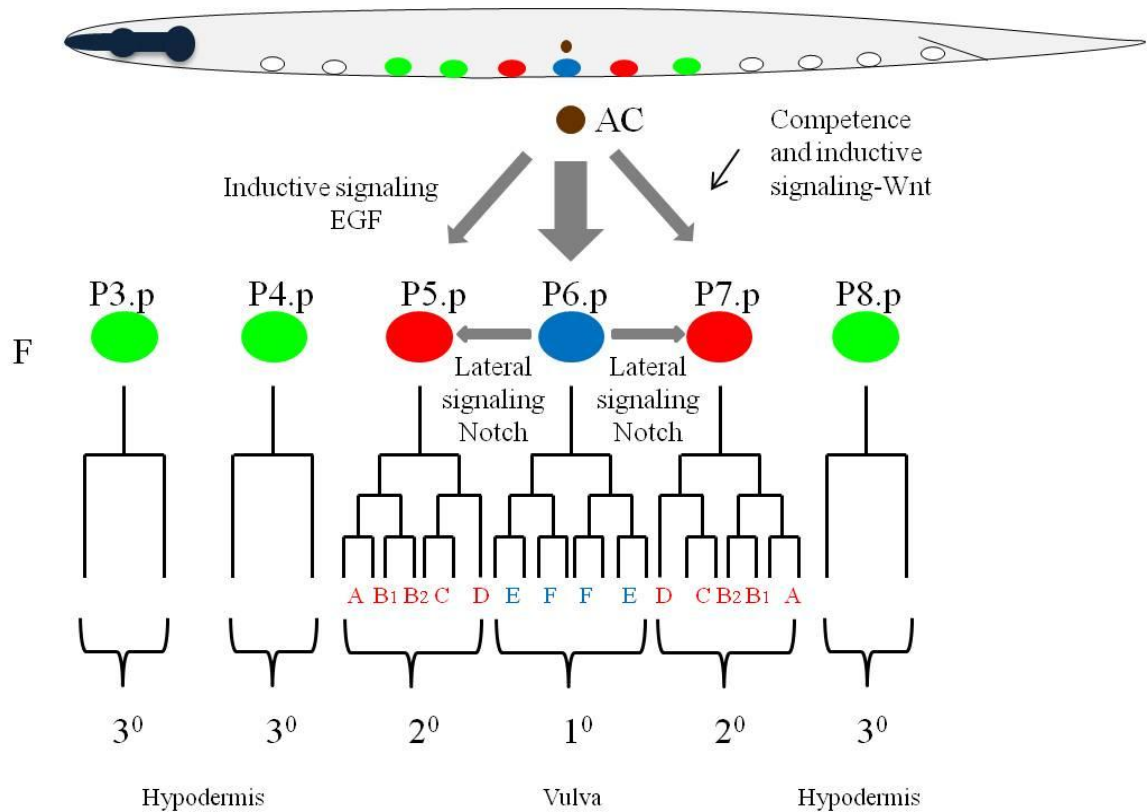


Figure 1. Specification of invariant cell fate pattern (3°3°2°1°2°3°) among the vulval precursor cells (VPCs) through Ras, Wnt and Notch signaling pathways in *C. elegans*.

Among the 12 P cells, 6 (P3.p-P8.p) form the Vulval competence group. The VPC (P6.p) closest to the anchor cell acquires 1° cell fate generating vulE and vulF cells, while the two adjacent VPCs (P5.p and P7.p) acquire the 2° fate through lateral Notch signaling generating five vulval cell types-vulA, vulB1, vulB2, vulC and vulD. VPCs (P3.p, P4.p and P8.p) further away from the AC induced signal acquire the non-vulval fate and fuse with the syncytial hypodermis. Here P3.p can acquire a Fused “F” or tertiary “3o” fate by fusing to the hypodermis (hyp7) either in L2 stage or L3 stage respectively. The other VPCs (P5.p-P7.p) divide further in the L3 and L4 stage to develop into the 22 cell vulval structure.

After competence and commitment to adopt a vulval fate, the great granddaughter Pn.pxxx cells derived from P5.p-P7.p invaginate inward to form the vulval structure in the L4 larval stage (Sternberg and Horvitz, 1986; Sternberg, 2005). This invagination results in the formation of a lumen below the AC and between the vulval cells (Shemer *et al.*, 2000; Sherwood and Sternberg, 2003). The vulval cells further extend processes and selectively fuse to form seven doughnut-shaped vulval toroids (vul A to vulF) (Sharma-Kishore *et al.*, 1999; Shemer *et al.*, 2000). The toroid formation is regulated by protrusions of cell membranes and fusions that occur between the sister cells of their contralateral halves (Sternberg and Horvitz, 1986; Sharma-Kishore *et al.*, 1999; Shemer *et al.*, 2000; Sternberg, 2005).

Besides its indispensable role in vulva formation, the AC is also necessary for establishing a functional connection between the vulva and the uterus. This process involves induction of VU cell grand progeny to become π cells. Subsequently, a multinucleated uterine seam cell (utse), a syncytium in the form of a thin membrane separating the vulval and uterine lumen, is formed by the fusion of π grand progeny with the AC (Newman and Sternberg, 1996; Gupta *et al.*, 2012b). This is followed by the attachment of the vulval muscles that control the vulval opening by contact with the vulval cells and uterus (Sharma-Kishore *et al.*, 1999). The final stage of development is vulval eversion, where the vulva turns inside out to form a slit (Sharma-Kishore *et al.*, 1999).

1.5.2.2 Molecular mechanisms

The specification of the AC is mediated by the LIN-12/Notch signaling pathway. The interaction between the somatic gonadal cells Z1.ppp and Z4.aaa, mediated by the DSL [*Drosophila* (Delta, Serrate) and *C. elegans* (LAG-2) family] ligand LAG-2 and its receptor LIN-12, results in one of the cells adopting the AC fate (Greenwald *et al.*, 1983; Seydoux and Greenwald, 1989; Lambie and Kimble, 1991; Wilkinson and Greenwald, 1995). The cell expressing *lag-2* becomes the AC, while the other cell expressing *lin-12* becomes the ventral uterine (VU) cell (Greenwald *et al.*, 1983; Seydoux and Greenwald, 1989; Lambie and Kimble, 1991; Wilkinson and Greenwald, 1995). First identified in *D. melanogaster*, the Notch protein family is highly conserved (Poulson, 1937, 1940) comprising multiple epidermal growth factor (EGF) like motifs and LIN-12/Notch repeats (LNR) (Wharton *et al.*, 1985; Seydoux and Greenwald, 1989).

During the L1 stage, components of the LINC (linker of nucleoskeleton and cytoskeleton) complex, comprised of KASH and SUN domain proteins *unc-83* and *unc-84* in the nuclear envelope, function to control the nuclear migration of the P-cells into the ventral cord (Malone *et al.*, 1999; Starr *et al.*, 2001; Tapley and Starr, 2013). Soon after arriving in the ventral cord, P-cells divide once. The anterior daughters (Pn.a, n = 1-12) take on the neural fate whereas the posterior daughters (Pn.p) commit to an epidermal fate (Sulston and Horvitz, 1977). The P(3-8).p cells (VPCs) remain unfused, unlike the remaining Pn.p cells that fuse to the hypodermis (Sternberg and Horvitz, 1986). This fusion event is blocked in the P(3-8).p cells through the action of *lin-39*, which represses the fusogen *eff-1* (Shemer and Podbilewicz, 2002). In the absence of the *lin-39* Hox gene

VPCs fuse with the surrounding hypodermal syncytium *hyp7*, resulting in a vulvaless phenotype (Clark *et al.*, 1993).

Genetic studies have revealed a requirement for three evolutionarily conserved signal transduction pathways during vulval development, termed inductive signaling (mediated by LIN-3/EGF-LET-23/EGFR-RAS-60/RAS-MPK-1/MAPK), lateral signaling (mediated by DSL ligands and receptor LIN-12/Notch) and Wnt signaling (Eisenmann, 2005; Greenwald, 2005; Sundaram, 2006). Wnt signaling maintains the competence of the six VPCs (P3.p to P8.p) through L2 alongside the LIN-3/EGF cascade in the L3 stage (Eisenmann *et al.*, 1998; Myers and Greenwald, 2007). Subsequently the P5.p-P7.p cells are induced by a graded *lin-3/EGF* signal generated by the AC (Sternberg and Horvitz, 1986; Katz *et al.*, 1995). The VPC (P6.p) closest to the AC receives most of the inductive signal and acquires 1° cell fate (Sternberg and Horvitz, 1986; Sternberg, 2005). Activation of the LIN-3 induced Ras pathway in *C. elegans* causes the upregulation of DSL ligands and downregulation of LIN-12/Notch receptor in P6.p resulting in a 1° cell fate (Sternberg and Horvitz, 1989; Berset *et al.*, 2001; Shaye and Greenwald, 2002; Yoo *et al.*, 2004a). The DSL ligands in P6.p in turn activate LIN-12 in P5.p and P7.p resulting in the inhibition of the Ras pathway and the adoption of a 2° fate (Figure 4) (Sternberg and Horvitz, 1989; Berset *et al.*, 2001; Shaye and Greenwald, 2002; Yoo *et al.*, 2004a). The components of these three pathways and their mechanism of action are summarized in section 1.6.

Several genes have been identified that regulate the fates of the seven different vulval cell types (Vul A, VulB1, VulB2, VulC, VulD, VulE and VulF) downstream of the three

signaling pathways. The LIM homeodomain transcription factor *lin-11* is a key regulator of vulval morphogenesis and functions at L3 and L4 stages to pattern the 1° and 2° vulval cell fate lineages (Gupta and Sternberg, 2002; Gupta, 2003). *lin-29* (Zinc finger family) is another gene expressed in all progeny from P5.p-P7.p during the L3 and L4 stages (Bettinger *et al.*, 1997). It also regulates *lin-11* expression in 2° lineage cells during L4 stage (Bettinger *et al.*, 1997). Other genes that function specifically in the vulval progeny cells include *egl-38* (PAX2/5/8-like family) and *lin-3* (EGF ligand), which are expressed in vulF cells (Chang *et al.*, 1999; Inoue *et al.*, 2005), and *cog-1* (Nkx6.1 transcription factor family) which is expressed initially in vulE and vulF cells in the L3 stage and in 2° lineage cells during L4 stage (Palmer, 2002). From *C. briggsae* genetic screens, we have identified seven vulval morphogenesis genes including *Cbr-lin-11* (described in Chapter 3).

In wild-type animals, the vulva is connected to the uterus through a thin membrane termed utse. Formation of utse begins at the L3 stage, with the AC inducing six VU granddaughters to adopt π cell fates. (Newman *et al.*, 1995, 2000; Verghese *et al.*, 2011). The present model for π cell generation and utse differentiation proposes that LIN-12/NOTCH receptor activation by the DSL ligand LAG-2 activates *lin-11* and *egl-13* (SOX2 family) in π precursors (Gupta *et al.*, 2012b). The NHR family member NHR-67 and *evi1* proto-oncogene homolog EGL-43 function at multiple stages to specify π cell fate in VU progeny (Hwang *et al.*, 2007; Rimann and Hajnal, 2007; Verghese *et al.*, 2011). Among other possible mechanisms, both these genes have also been shown to regulate *lin-12* signaling (Hwang *et al.*, 2007; Rimann and Hajnal, 2007). The enhancers

of *lin-11* and *egl-13* contain binding sites for LIN-12 target LAG-1 (*Su(H)/CBF family*) and another proto-oncogene FOS-1, suggesting that *lin-11* and *egl-13* are in part directly regulated by LIN-12/Notch signaling specification (Oommen and Newman, 2007; Marri and Gupta, 2009).

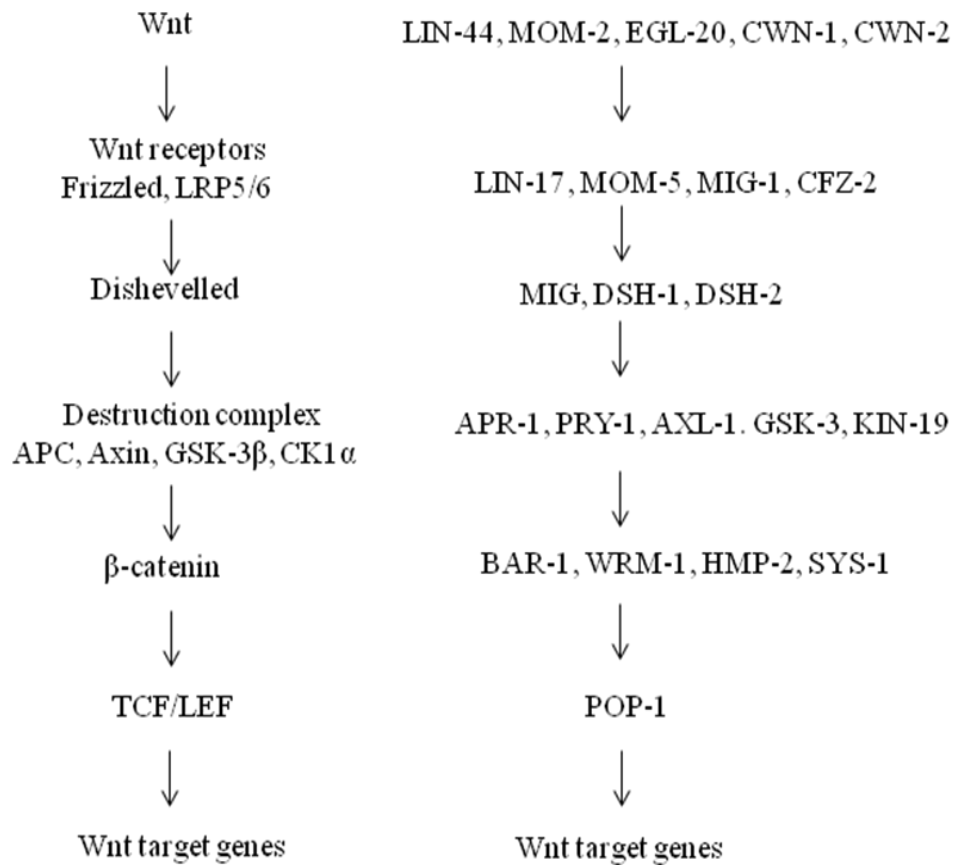
The π cells divide during L3 lethargus and generate 12 π grand progeny cells. Of these, eight cells fuse together to form utse. A channel is established between the uterus and the vulva, breaking the utse when the first egg is laid from the hermaphrodite (Newman *et al.*, 1996). Mutations in *egl-13* and *lin-11* cause a failure of utse formation due to defects in the differentiation of π cells (Newman *et al.*, 1995, 1999; Hanna-Rose and Han, 1999; Cinar *et al.*, 2003; Gupta *et al.*, 2012a).

1.6 Signaling pathways involved in vulval development

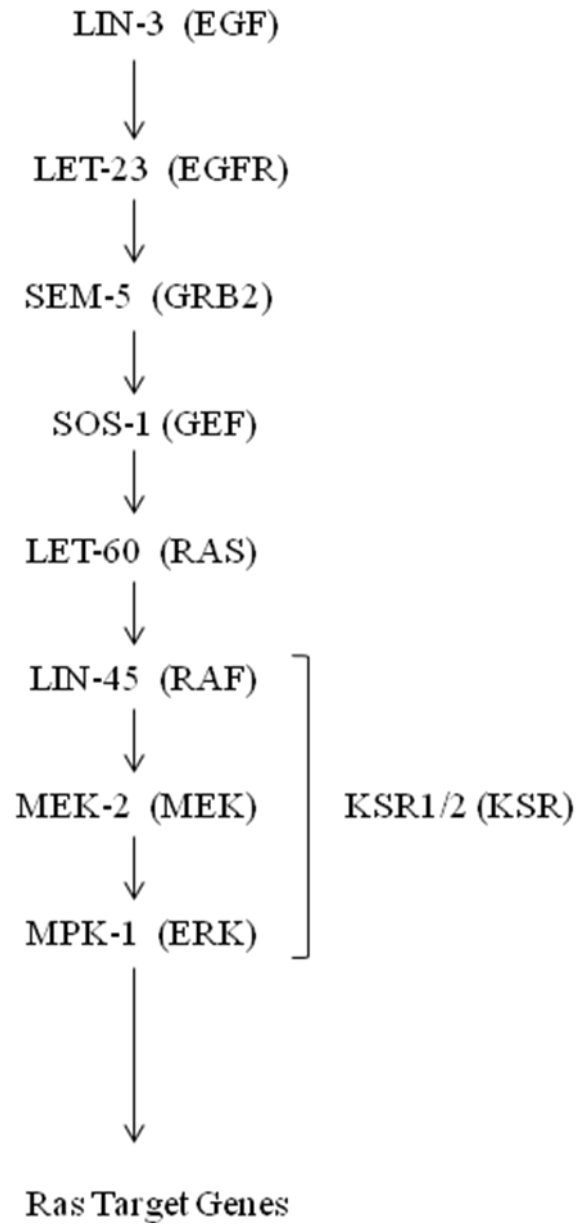
Mutations in genes required for vulval development can cause one of the three phenotypes: failure of VPC induction (termed Vulvaless or Vul), inappropriate induction of P3.p, P4.p and P8.p (termed Multivulva or Muv), or failure of VPC progeny to differentiate correctly (termed Protruding vulva or Pvl). All of these defects may compromise the mutant animal's ability to lay eggs. This results in the accumulation of fertilized eggs inside the uterus (termed egg-laying defective or Egl phenotype), which may hatch and ultimately devour the mother (Trent *et al.*, 1983; Ferguson and Horvitz, 1989). In a Vul animal, VPCs that normally generate the vulva fail to get induced. Instead, they fuse to hyp7 (Horvitz and Sulston, 1980; Ferguson and Horvitz, 1985). In a Muv animal, VPCs that normally fuse to the hypodermis divide further to form vulva-like

protrusions (Ferguson and Horvitz, 1985). These pseudo-vulvae arise due to abnormal and uncontrolled cell division (Ferguson and Horvitz, 1985, 1989). In *C. elegans*, studies based on these mutant phenotypes have resulted in the identification of genes involved in at least three different conserved signaling pathways- EGF-receptor /LET-23 and Ras/LET-60; LIN-12 /Notch, and Wnt (Figure 2) (Greenwald *et al.*, 1983; Ferguson and Horvitz, 1985, 1989; Sternberg and Han, 1998; Eisenmann and Kim, 2000; Fay and Han, 2000; Chen and Greenwald, 2004; Cui *et al.*, 2006a; Fay and Yochem, 2007). The orchestration of these signaling components results in the precise patterning of vulval cells and their fate specification.

A



B



C

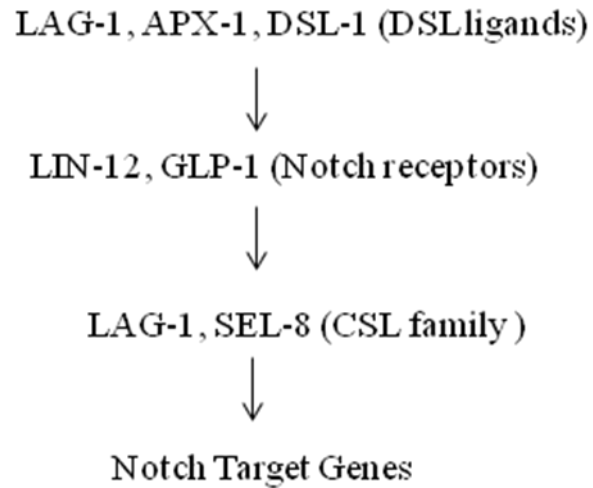


Figure 2. Overview of conserved Wnt (A), Ras/MAPK (B) and Notch (C) signaling pathways and the core pathway homologs in *C. elegans*.

1.6.1 Wnt signaling

The Wnt pathway is an evolutionarily conserved signal cascade involved in a wide range of developmental processes including cell fate specification, polarity, differentiation, migration, stem cell maintenance, and tissue regeneration during metazoan development. Due to its wide spread role in development, alterations in Wnt signaling is often associated with a range of human pathologies including cancer, limb deformities and degenerative diseases (Polakis, 2000; Nusse, 2005; Clevers and Nusse, 2012).

Canonical Wnt signaling acts through β -catenin. Wnt signaling is initiated when a Wnt ligand binds to the receptor complex comprised of the seven-transmembrane protein Frizzled (Fz) and the lipoprotein receptor family co-receptor LRP5/6/Arrow (Bhanot *et al.*, 1996; Wehrli *et al.*, 2000). The destruction complex comprising of Adenomatous Polyposis Coli (APC) (Hart *et al.*, 1998), glycogen synthase kinase (GSK3 β) (Yost *et al.*, 1996), casein kinase 1 (CK1) (Amit *et al.*, 2002; Liu *et al.*, 2002) and the Axin scaffold protein (Kishida *et al.*, 1998) is then recruited to the plasma membrane. Binding of Axin to the cytoplasmic tail of LRP5/6 and Dsh to Fz stabilizes β -catenin and prevents its degradation, allowing it to accumulate (Mao *et al.*, 2001; Wong *et al.*, 2003). β -catenin translocates to the nucleus where it interacts with TCF/LEF family transcription factors to activate Wnt target genes (Takemaru, 2000; Nusse, 2005).

In the absence of a Wnt ligand, β -catenin undergoes ubiquitination and is rapidly degraded by the proteasome resulting in the repression of Wnt target genes (Cavallo *et al.*, 1998; Clevers and Nusse, 2012).

In *C. elegans*, there are five Wnt ligands (*lin-44*, *egl-20*, *mom-2*, *cwn-1*, *cwn-2*), four Wnt receptors (*Frizzled family members lin-17*, *mom-5*, *mig-1*, *cfz-2*) and three Dishevelled proteins (*mig-5*, *dsh-1*, *dsh-2*) (Sawa and Korswagen, 2013). Key differences to the traditional Wnt pathway include the presence of four β -catenins (*bar-1*, *sys-1*, *wrm-1* and *hmp-2*) that regulate different processes in contrast to the single β -catenin in *Drosophila* and vertebrates (Cadigan and Nusse, 1997; Clevers and Nusse, 2012).

In *C. elegans*, Wnt signaling is involved in numerous developmental processes such as neuronal differentiation, male hook formation, fate specification of the hypodermal P12.p cell, and vulval development (Sawa and Korswagen, 2013). During vulval development, Wnt signaling is required for maintaining VPC competence through upregulation of the Hox gene *lin-39* in the L2 and L3 stages (Eisenmann *et al.*, 1998; Myers and Greenwald, 2007). *cwn-1* and *egl-20* are the main Wnt ligands involved in maintaining VPC competence in the L2 stage (Myers and Greenwald, 2007). *bar-1/ β -catenin* prevents inappropriate fusion of the VPCs to *hyp7* by regulating the *lin-39* Hox gene (Eisenmann *et al.*, 1998; Gleason *et al.*, 2002, 2006). Ras signaling also acts alongside Wnt in the L2 and L3 stage to regulate VPC competence (Myers and Greenwald, 2007).

Wnt signaling also regulates VPC induction. The *pry-1(mu38)* mutant exhibits a multivulva phenotype due to hyperactivation of Wnt signaling (Gleason *et al.*, 2002) with all ectopic VPCs adopting a 2^o cell fate (Seetharaman *et al.*, 2010). A similar phenotype has been observed in *bar-1/ β -catenin* overactivation mutants (Gleason *et al.*, 2002). These phenotypes are not suppressed by Ras pathway mutants (Gleason *et al.*, 2002;

Eisenmann, 2005), although it remains to be seen if complete elimination of inductive signaling (e.g., by gonad ablation) will have any impact. The Wnt receptor *lin-17* (*Frizzled*) may also play a redundant role in 1^o lineage cell (VulE and VulF) distinction along with the Ras pathway (Wang and Sternberg, 2000). Thus, the Wnt signaling pathway is important for VPC competence and vulval induction.

Wnt signaling is also necessary to orient the cell lineage pattern in 2^o VPCs to give rise to a symmetrical vulval invagination. This process is regulated by the *lin-17*(*Frizzled*) and *lin-18*(*Ryk*) Wnt receptors through *pop-1*, which acts in the P7.p lineage (NTLL) to specify a polarity opposite to that of the P5.p lineage (LLTN) (Deshpande *et al.*, 2005).

Figure 3 depicts the percent identity between the main Wnt pathway components of *C. elegans* and *C. briggsae* based on UniProtKB and WormBase BlastP results (See table A1 for percent identity). Sequence comparison of these genes reveals that their percent identity is similar to the genome wide median identity 80% (mean, 75%; SD, 18%) estimated for all orthologs in *C. elegans* and *C. briggsae* (Stein *et al.*, 2003).

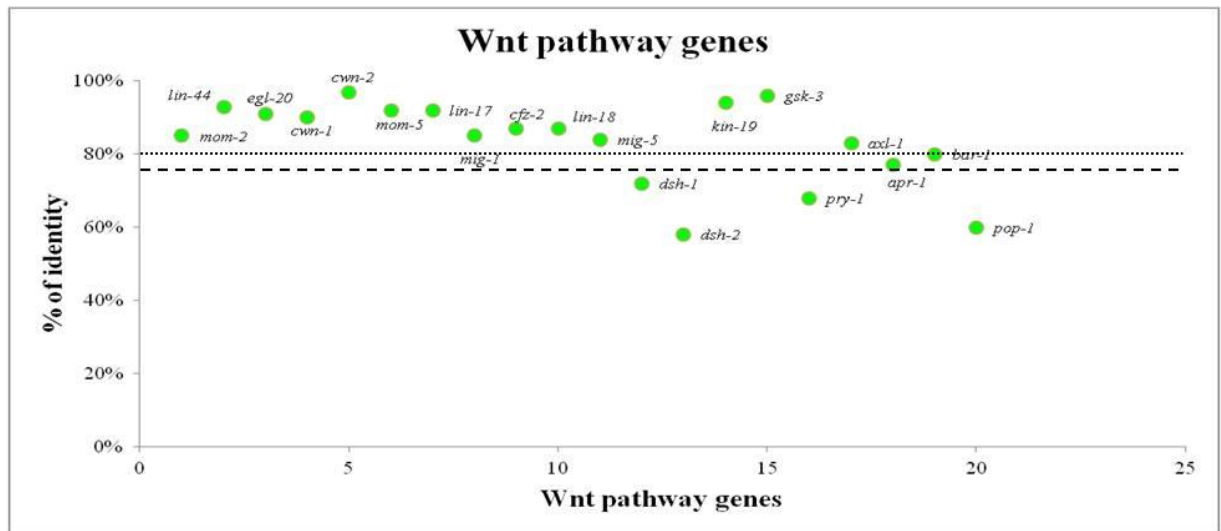


Figure 3. Percent identity between the Wnt pathway orthologs in *C. elegans* and *C. briggsae* (based on UniProtKB results). Genome wide median and mean is highlighted as dotted and hyphenated line.

1.6.2 RAS/MAPK signaling

The RAS protein, belonging to the GTP-binding protein family, was first identified as a viral oncogene in Harvey murine sarcoma virus and Kirsten murine sarcoma virus when it induced tumor transformations (Cox and Der, 2010). Due to its role in tumorigenesis, it has been extensively studied in a number of model systems, including *C. elegans*, to identify its upstream and downstream pathway components. The culmination of these studies has helped determine how mitogenic signals from outside the cell cause aberrant alterations in tumor cells (Malumbres and Barbacid, 2003). Along with its role in cell proliferation, this evolutionarily conserved signal cascade is responsible for many cellular functions, which include apoptosis, migration, growth and differentiation (Malumbres and Barbacid, 2003; Sundaram, 2006). In *C. elegans*, along with vulval development, the Ras pathway is involved in various development processes such as axon guidance, P12.p specification, excretory duct cell fate, germline meiosis, uterine and spicule development (Brenner, 1973; Fixsen *et al.*, 1985; Chamberlin and Sternberg, 1994; Church *et al.*, 1995; Yochem *et al.*, 1997; Jiang and Sternberg, 1998; Chang *et al.*, 1999; Bülow *et al.*, 2004).

Figure 4 shows minimum sequence conservation of major Ras pathway orthologs in *C. briggsae* and *C. elegans* based on UniProtKB and WormBase BlastP results (See table A1 for percent identity). The percent identity for most of the Ras pathway genes is similar to the genome wide median identity for orthologs between *C. elegans* and *C. briggsae* (Stein *et al.*, 2003).

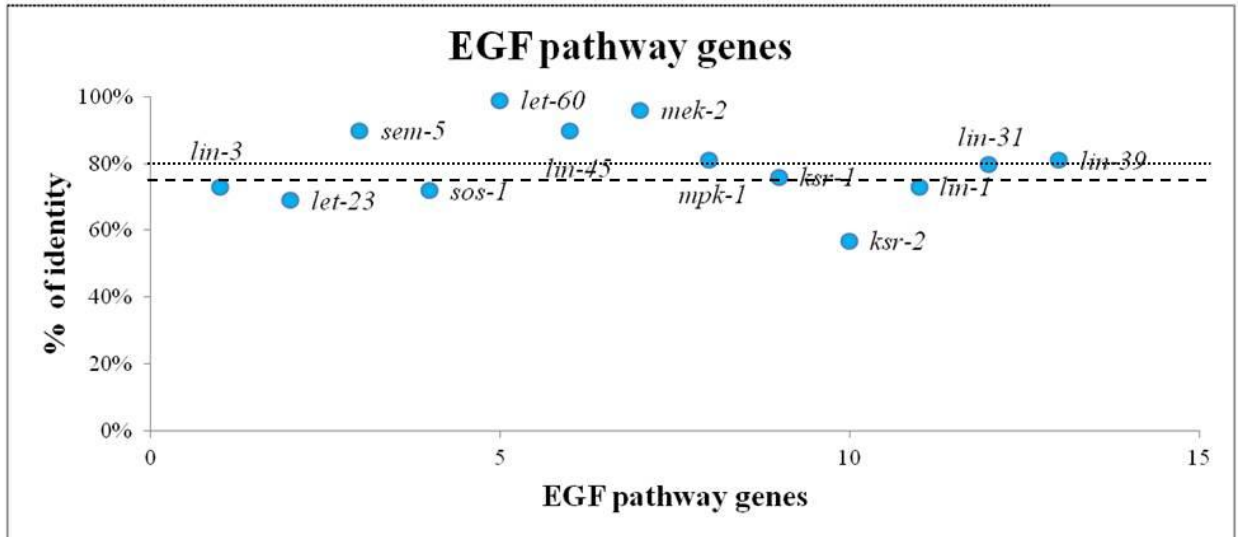


Figure 4. Minimum percent identity between the Ras pathway orthologs in *C. elegans* and *C. briggsae* (based on UnitProtKB and WormBase BlastP results). Genome wide median and mean is highlighted as dotted line and hyphenated line.

1.6.2.1 Components of RAS/MAPK pathway

C. elegans let-60 encodes the RAS protein (Han and Sternberg, 1990). It is activated in response to the binding of LIN-3/EGF signal to LET-23/EGFR in the receiving VPCs (Sundaram *et al.*, 1996; Sternberg, 2005; Sundaram, 2005). Activation of LET-23 by the ligand on the cell membrane induces a conformational change in the cytoplasmic portion of the receptor causing it to dimerize and autophosphorylate tyrosine residues at its C-terminal (Lesa and Sternberg, 1997). In turn, the phosphotyrosine residues are recognized by the GRB-2-like (Growth factor Receptor-Bound protein 2) adaptor protein SEM-5 with its Src homology domains (SH2 and SH3) (Clark *et al.*, 1992). The SH2 domain of the SEM-5 adaptor molecule binds to the receptor, while the two SH3 domains activate the guanine nucleotide exchange factor (GEF) SOS-1 by binding to proline rich sequences, thus activating RAS (Clark *et al.*, 1992). In this way, the domains mediate the association between the cytosol and the cell membrane. RAS acts as a binary switch, converting from a RAS-GDP (inactive state) to a RAS-GTP (active state) (Chang *et al.*, 2000). Activated LET-60/RAS then turns on the kinase activity of LIN-45/RAF (Han *et al.*, 1993). This cascade results in RAF phosphorylating MEK-2 (MAPK kinase), which in turn phosphorylates MPK-1 (MAP kinase) (Lackner *et al.*, 1994; Kornfeld *et al.*, 1995). Phosphorylation of MPK-1 by MEK-2 results in its translocation to the nucleus where it phosphorylates transcription factors like LIN-1 and LIN-31 to influence downstream responses. (Miller *et al.*, 1993; Beitel *et al.*, 1995).

1.6.2.2 Downstream targets

LIN-1 belongs to the E26 (ETS) family of transcription factors that transcriptionally activate and repress vulval induction genes (Beitel *et al.*, 1995). LIN-31 is a Winged Helix (WH) transcription factor that can also positively and negatively regulate vulval development (Miller *et al.*, 1993). LIN-1 and LIN-31 interacts directly to form a repressor complex which inhibits vulval induction (Jacobs *et al.*, 1998; Tan *et al.*, 1998). During vulval induction, MPK-1 phosphorylates the C-terminus of LIN-1, converting it into a transcriptional activator that promotes vulval development by activating the downstream target *lin-39* (Wagmaister *et al.*, 2006).

The *lin-39* Hox gene is the *C. elegans* ortholog of *Drosophila* – *sex combs reduced* (*scr*) that specifies cell fates in the central body region of the worm (Clark *et al.*, 1993; Maloof and Kenyon, 1998). During the L1 stage, this Hox gene is required to maintain VPC competence and avoid the “F” fate by repressing EFF-1 (Shemer and Podbilewicz, 2002) . During the L2 stage, this competence is regulated through LIN-39 by the BAR-1 (β -Catenin)-mediated canonical Wnt signaling pathway (Eisenmann *et al.*, 1998; Gleason *et al.*, 2006). In the L3 stage, LIN-39 acts downstream of the LIN-3-Ras signal to mediate vulval development (Eisenmann *et al.*, 1998). Mutations affecting *lin-39* give rise to a vulvaless phenotype, as VPCs fuse to *hyp7* because they lack competence to respond to inductive signal (Clark *et al.*, 1993; Eisenmann and Kim, 2000).

Other downstream targets of MPK-1 include the BTB/ Zinc finger protein EOR-1, an ortholog of human PLZF, and a novel nuclear protein EOR-2, which both positively regulate vulval development (Howard and Sundaram, 2002; Rocheleau *et al.*, 2002;

Sundaram, 2006). *eor-1* and *eor-2* were identified in a forward genetic screen for Ras pathway components in *C. elegans* (Rocheleau *et al.*, 2002). Mutations in either of these genes suppress the multivulva phenotype of *let-60/Ras* and *mpk-1/mapk* (Howard and Sundaram, 2002; Rocheleau *et al.*, 2002; Sundaram, 2006). *lin-25* and *sur-2* also function downstream of MPK-1 redundantly with EOR-1 and EOR-2 (Singh and Han, 1995; Tuck and Greenwald, 1995; Nilsson *et al.*, 1998; Howard and Sundaram, 2002). SUR-2 is a mediator subunit and LIN-25 is another novel nuclear protein (Singh and Han, 1995; Tuck and Greenwald, 1995; Nilsson *et al.*, 1998). Both *lin-25* and *sur-2* function together in vulval development and a loss of function in either gene causes strong vulvaless phenotypes (Singh and Han, 1995; Tuck and Greenwald, 1995).

1.6.2.3 Regulators of the Ras pathway

The RAS pathway functions by integrating its core components with those from other signaling pathways and is subject to regulation at every step (Sundaram, 2006). Genetic screens for enhancer and suppressor mutations have identified several genes that regulate EGF signaling (Moghal, 2003). These types of modifier screens are important because mutations in the regulators alone often have little to no impact on vulval development (Moghal, 2003). However, in the background of a weak hypomorphic allele of core component components like *let-60*, *lin-45* or *mpk-1*, they can result in strong vulvaless or multivulva phenotypes (Moghal, 2003).

1.6.2.3.1 Positive regulators of RAS/MAPK signaling

A number of positive acting modulators have been identified which include scaffold proteins KSR-1, KSR-2 (Kinase Suppressor of Ras), and SUR-8 (Suppressor Of Clear homolog). These positive regulators act between Ras/Raf and other regulatory proteins like CDF-1 and SUR-6, which enhance signaling through the MAPK cascade (Sieburth *et al.*, 1998; Ohmachi *et al.*, 2002; Kao *et al.*, 2004; Yoder *et al.*, 2004; Rocheleau *et al.*, 2005; Sundaram, 2006).

The importance of scaffolds to regulate and provide specificity to MAPK signaling was discovered through studies on the Ste5p scaffold in yeast (Elion, 2001). Ste5p selectively binds MAP kinases in response to pheromone stimuli to activate the mating pathway (Elion, 2001). One well known scaffold protein is KSR, which associates with RAF, MEK, ERK (Denouel-Galy *et al.*, 1998). In *C. elegans*, two KSR isoforms have been identified, KSR-1 and KSR-2, which positively regulate vulval development (Ohmachi *et al.*, 2002). The *ksr-1* and *ksr-2* genes are individually required for specific Ras-dependent processes like sex myoblast migration (*ksr-1*) and germline meiotic progression (*ksr-2*) (Ohmachi *et al.*, 2002). However, both proteins are necessary for most processes controlled by Ras, such as the development of the excretory system, hermaphrodite vulva, and male spicules (Ohmachi *et al.*, 2002). Single *ksr-1* or *ksr-2* mutants do not affect vulval development, but double mutants of *ksr-2;ksr-1* display a strong vulvaless phenotype that is associated with reduced levels of phosphorylated MPK-1 (Ohmachi *et al.*, 2002). Thus, they function redundantly to promote the activation and

maintenance of RAF/MEK/ERK kinase cascade during vulval development (Ohmachi *et al.*, 2002).

SUR-8 contains multiple leucine-rich repeats (LRR) similar to yeast adenylate cyclases, a downstream target of Ras (Kataoka *et al.*, 1985; Sieburth *et al.*, 1998). Reduction of *sur-8* function suppresses activated *let-60/ras*, but does not suppress *lin-45* gain of function mutation, indicating that *sur-8* is upstream of *lin-45* (Sieburth *et al.*, 1998). Studies with SHOC-2, the human homolog of SUR-8, have shown that it functions as a scaffold by forming a ternary complex with Ras and Raf to enhance ERK activation (Li *et al.*, 2000). Overexpression of *shoc-2* results in increased duration of EGF-dependent ERK activation (Leon *et al.*, 2014).

Studies in *Drosophila* and mammalian cells have shown that Protein Phosphatase 2A (PP2A) can influence the Ras pathway both positively and negatively. SUR-6 is a *C. elegans* homolog of the regulatory B subunit of PP2A and is a positive regulator of Ras-mediated vulval development that was identified in suppressor screen of *let-60/Ras* (Kao *et al.*, 2004). It acts upstream of Raf activation and functions along with LET-92/PP2A-c to remove inhibitory phosphates on KSR1/2 or LIN-45/Raf (Kao *et al.*, 2004).

Other positive regulators of Ras include CDF-1, a cation diffusion facilitator and SUR-7, a divergent CDF family member, which regulate the transport of heavy metal ions like Zinc (Bruinsma *et al.*, 2002; Yoder *et al.*, 2004).

1.6.2.3.2 Negative regulators of RAS/MAPK signaling

Genetic screens have also identified a number of genes that negatively regulate Ras signaling. Many were identified in genetic screens using *lin-3/egf* and *let-23/egfr* mutant strains. Two such genes are *sli-1* and *sli-3* (Jongeward *et al.*, 1995; Gupta *et al.*, 2006). SLI-1, an E3 Ubiquitin ligase and Cbl homolog, promotes LET-23/EGFR degradation through ubiquitination (Jongeward *et al.*, 1995). *sli-3* is currently uncloned but genetic studies have shown that *sli-3* acts either downstream or in parallel to *lin-1* and *sur-2* (Gupta *et al.*, 2006).

Another negative regulator of Ras is UNC-101, which encodes one of the medium chains of the AP-1 clathrin-associated protein complex that promotes LET-23 endocytic recycling (Lee *et al.*, 1994; Shim *et al.*, 2000). These genes were identified through suppressor screens in a hypermorphic *let-23/egfr* background (Lee *et al.*, 1994; Jongeward *et al.*, 1995).

AGEF-1, a homolog of yeast Sec7p and the mammalian Arf GEFs, is also a negative regulator that functions to regulate LET-23/EGFR localization (Skorobogata *et al.*, 2014). Loss of function of AGEF-1 causes increased LET-23 localization in the VPCs (Skorobogata *et al.*, 2014). AGEF-1 likely functions together with UNC-101 to negatively regulate signaling (Skorobogata *et al.*, 2014). Other negative regulators which function near or at the level of LET-23 include ARK-1 (Ack-related tyrosine kinase) and RAB-7 (GTPase) (Hopper *et al.*, 2000; Skorobogata and Rocheleau, 2012).

One of the well characterized negative regulators of RAS/MAPK signaling in *C. elegans* is the GTPase activating protein (GAP) GAP-1 that stimulates LET-60 GTP hydrolysis (Hajnal *et al.*, 1997). In *C. elegans*, there are three GAP proteins; GAP-1 which is similar to GAPs from *Drosophila* and vertebrates, GAP-2 which is similar to SynGAP family of RasGAPs, and the p120 RasGAP family member GAP-3 (Gaul *et al.*, 1992; Maekawa *et al.*, 1994; Hajnal *et al.*, 1997; Hayashizaki *et al.*, 1998). Loss of function mutations in *gap-1* and *gap-3* can suppress the vulvaless phenotype in *let-60* (Hajnal *et al.*, 1997; Stetak *et al.*, 2008), while the role of GAP-2 in vulval development is still unclear (Stetak *et al.*, 2008).

Additional proteins that negatively regulate RAS/MAPK signaling have been identified. These include the G-protein coupled receptor SRA-13, its $G\alpha$ target GPA-5, PAR-1 kinase, MPK-1-binding protein LST-1 and the MAP kinase phosphatase LIP-1 (Berset *et al.*, 2001; Müller *et al.*, 2001; Battu, 2003; Kao *et al.*, 2004; Yoo *et al.*, 2004b).

1.6.2.4 Chromatin mediated regulation

The Synthetic Multivulva (*synMuv*) class of genes implicates the chromatin structure as a mechanism for regulating LIN-3/EGF signaling. Based on genetic interactions, these genes have been placed into three classes - A, B and C (Ferguson and Horvitz, 1989; Cui *et al.*, 2006a). Normally, single *synMuv* gene mutants appear normal, but simultaneous disruption of two genes from different *synMuv* classes causes the *Muv* phenotype (Ferguson and Horvitz, 1989; Clark *et al.*, 1994; Cui *et al.*, 2006a). The exception to this is the *lin-15* gene that produces two transcripts (*lin-15A* and *lin-15B*) from a single promoter (Ferguson *et al.*, 1987; Clark *et al.*, 1994; Huang *et al.*, 1994). The *lin-15*

mutations that affect both transcripts cause the Muv phenotype (Clark *et al.*, 1994; Huang *et al.*, 1994).

Class A includes six synMuv genes, of which many are novel. The mechanism by which these genes inhibit vulval development is not well understood. Class B synMuv is the largest class comprising of at least 25 genes, which include *efl-1* (*C. elegans* E2F ortholog) and *lin-35* (*C. elegans* pRB ortholog) (Lu and Horvitz, 1998b; Ceol and Horvitz, 2001). Other class B genes include components of the NuRD (nucleosome remodeling and histone deacetylase) complex as well as SET domain proteins that are mainly involved in transcriptional repression associated with cell proliferation, transgene silencing, larval development and pharyngeal morphogenesis (Lu and Horvitz, 1998a; Romagnolo *et al.*, 2002; Unhavaithaya *et al.*, 2002; Bender *et al.*, 2004; Cui *et al.*, 2006a; Vastenhouw *et al.*, 2006; Andersen and Horvitz, 2007). Class C genes belong to different families, some of which encode components of the TIP60 histone acetyltransferase HAT complex. They function redundantly with Class B genes and may be required to negatively regulate vulval development (Ceol and Horvitz, 2004).

The SynMuv genes function by repressing LIN-3 during vulval development (Cui *et al.*, 2006a). In wild type animals *lin-3* is specifically restricted certain tissues, namely the pharynx, anchor cell, gonad and tail. However, in synMuv double mutants *lin-3* is ectopically expressed in low levels throughout the animal resulting in abnormal activation of the signal cascade (Cui *et al.*, 2006a; Saffer *et al.*, 2011a). SynMuv genes function in the hyp7 syncytium and throughout the animal to keep LIN-3 repressed, but their site of action in repressing LIN-3 is not completely clear (Saffer *et al.*, 2011b). The

identification of a dominant synMuv A mutation in the *lin-3* promoter has led to the proposal that LIN-3 is the key target of synMuv A genes (Saffer *et al.*, 2011b). In comparison, class B gene products likely repress *lin-3* by preventing somatic to germline transformation (Wang *et al.*, 2005; Saffer *et al.*, 2011b).

1.6.3 Notch signaling

The Notch pathway is an evolutionarily conserved intercellular signalling cascade critical for embryonic and post-embryonic developmental processes in all multicellular organisms. Notch signalling influences mechanisms such as cell fate decisions in response to developmental signals, cell proliferation and apoptosis. The function of Notch signaling in development was first demonstrated in *Drosophila*, where a partial loss of function in the *notch* gene resulted in a dominant notched wing phenotype (Morgan, 1917). Its role in human development was recognized only in the late twentieth century when mutations in *notch* genes were associated with leukemia and several developmental disorders (Ellisen *et al.*, 1991).

In *C. elegans*, LIN-12/NOTCH signaling facilitates cell-cell communication during the development of the vulva and vulva-uterine connection. During late L2 stage, it functions in the AC-VU decision process to generate the AC and in later stages is involved in the formation of the uterine-vulval connection regulated by *nhr-67* (*tailless* homolog of NHR family) and *egl-43* (*evi1* family) (Seydoux and Greenwald, 1989; Verghese *et al.*, 2011; Gupta *et al.*, 2012b). LIN-12 signaling in vulval cells confers a 2° fate on P5.p and P7.p VPCs following the specification of the 1° fate of P6.p (Greenwald *et al.*, 1983; Seydoux and Greenwald, 1989; Greenwald, 2005). The P6.p cell produces

DSL ligand LAG-2 that binds to and activates the LIN-12 receptor on neighboring P5.p and P7.p cells (Berset *et al.*, 2001; Chen and Greenwald, 2004; Greenwald, 2005; Sternberg, 2005) (Figure 5). The activated LIN-12 receptor is internalized and cleaved by SEL-12 Presenilin (gamma-secretase) to produce an intracellular LIN-12 fragment that interacts with CSL (CBF1/Suppressor of Hairless/LAG-1) proteins- LAG-1 and SEL-8 (*Drosophila* Mastermind family) to regulate target genes (Lambie and Kimble, 1991; Tax *et al.*, 1997; Doyle *et al.*, 2000). The components of the LIN-12/Notch signaling pathway include a MAP kinase phosphatase LIP-1 that antagonizes MPK-1 activity in 2° lineage cells thereby inhibiting these cells from taking on a 1° fate (Figure 5) (Berset *et al.*, 2001). The down regulation of LIN-12 in the P6.p VPC by endocytosis and lysosomal degradation results in the adoption of a 1° fate (Shaye and Greenwald, 2002).

The core components and downstream genes of Notch signaling pathway in *C. elegans* have clear *C. briggsae* orthologs based on UniProtKB and WormBase BlastP results (See table A1 for percent identity). Sequence analysis of *lin-12/Notch* pathway genes in *C. briggsae* has revealed that the percent identities for almost all Notch pathway component orthologs are considerably lower than the median percent identity across the genome (median, 59%) (Figure 6) suggesting a greater divergence (Stein *et al.*, 2003).

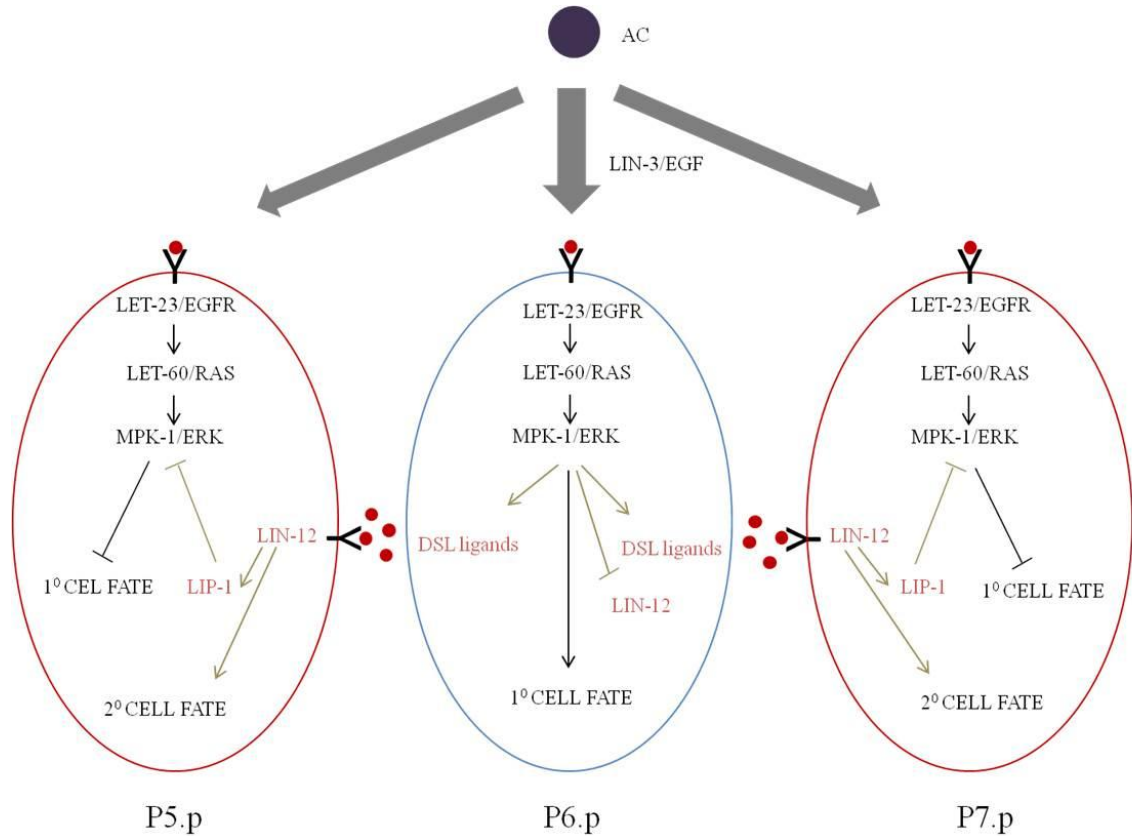


Figure 5. Interaction of Ras and Notch signaling pathways during vulval development

Activation of the EGF induced Ras signal cascade in P6.p triggers the DSL ligands and causes downregulation of LIN-12 Notch receptors resulting in 1° cell fate. Activation of LIN-12 receptors causes the lateral inhibition of 1° cell fate in P5.p and P7.p through LIP-1.

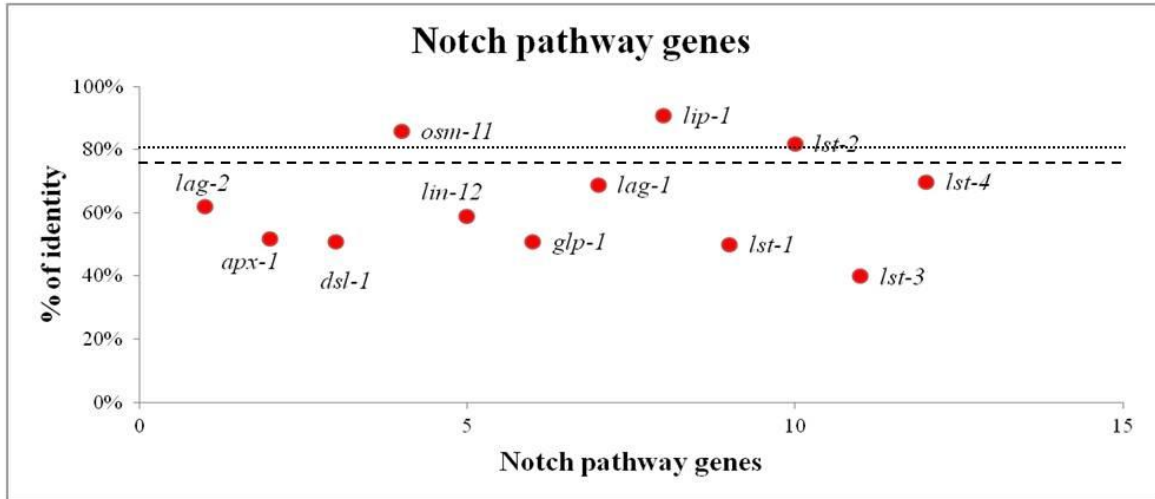


Figure 6. Percent identity among the Notch pathway genes orthologs in *C. elegans* and *C. briggsae* (based on UnitProtKB results). Genome wide median and mean is highlighted as dotted and hyphenated line.

1.7 Reproductive system development in *C. briggsae*

1.7.1 Developmental processes and similarities and differences from *C. elegans*

The egg-laying system in *C. briggsae* is largely identical to *C. elegans* (Figure 7). The vulva is located in the centre body region and several characteristics like anchor cell position, P cell migration, vulval cell number, and cell fusion are similar between the two species. The vulva is formed by the progeny of 6 Pn.p cells [P(3-8).p] that adopt a 2°1°2° fate pattern from the divisions of the three innermost P(5-7).p cells.

Initially, P3.p was not included as part of the VPC equivalence group, as the cell did not appear to adopt an induced fate following the ablation of other VPCs (Delattre and Félix, 2001b). However, subsequent studies involving *C. briggsae* Muv mutants showed that P3.p can be induced to adopt a vulval fate, suggesting that P3.p is indeed a VPC (Seetharaman *et al.*, 2010; Sharanya *et al.*, 2015).

It has been reported that the P3.p division frequency differs between *C. elegans* and *C. briggsae*. In the wild *C. briggsae* isolate *AF16*, P3.p was found to be induced in approximately 15% of the animals, whereas the same cell was induced in 50% of the *C. elegans* animals examined (Delattre and Félix, 2001b; Sharanya *et al.*, 2012). In addition, the morphology of the uterine vulval connection (utse), which connects the uterus and vulva, is thicker in *C. briggsae* (Figure 8) (Gupta and Sternberg, 2003). Differences in brood size, sheath-contraction rate, and reproductive efficiency between the two species have also been noted (Eisenmann *et al.*, 1998; Miller *et al.*, 2004; Félix, 2007; Pénigault and Félix, 2011a).

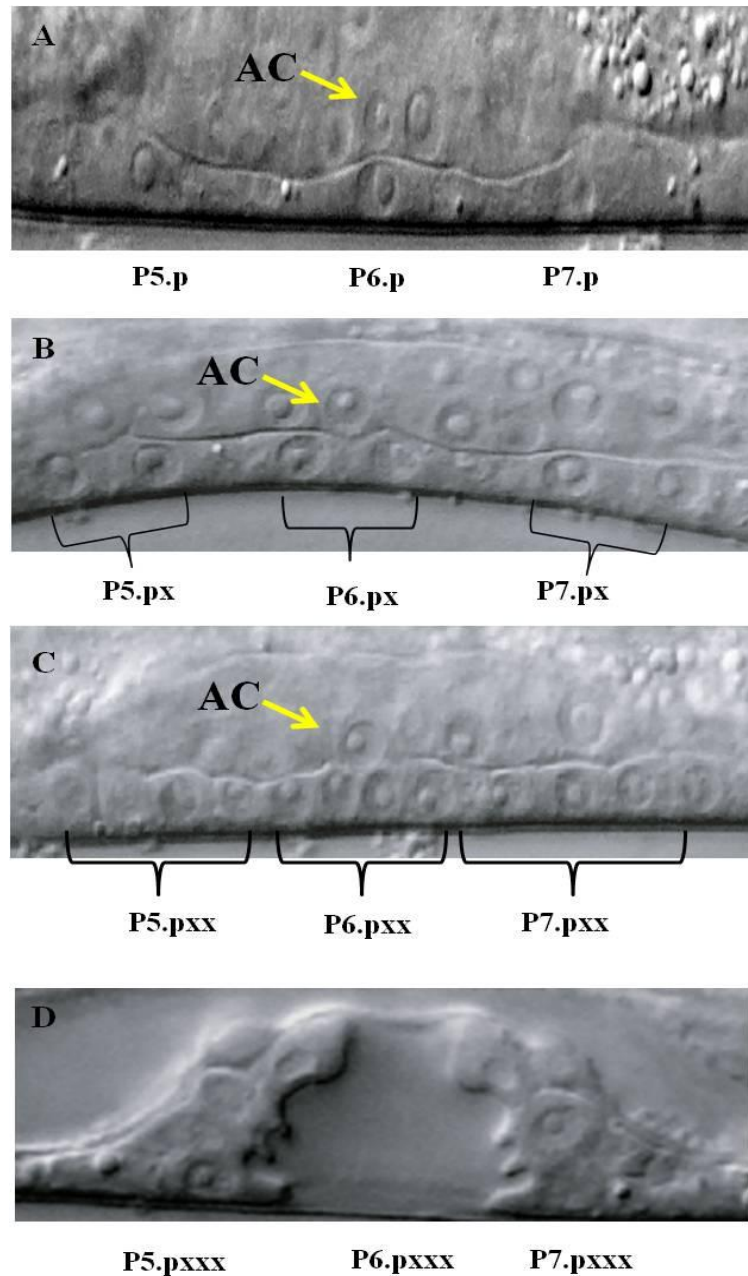


Figure 7. Vulval development from L3 to mid L4 stage in *C. briggsae*.

Differential Interference Contrast (DIC) images from A to D showcase the VPCs P5.p-P7.p dividing three times to form the 22-cell stage vulva. AC is the anchor cell and the Pn.px, Pn.pxx and Pn.pxxx represent the daughter, granddaughter and great granddaughter cells of the VPC.

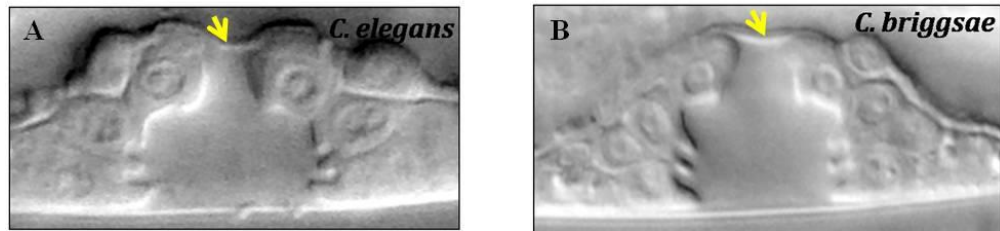


Figure 8. Vulval morphology of *C. elegans* and *C. briggsae*. At mid L4 larval stage, the VPCs(P5.p-P7.p) divide and form the 22-cell vulva (Christmas tree-like appearance). The arrow (yellow) indicates the utse connecting the uterus and vulva.

1.8 Genetic dissection of vulval development in *C. briggsae*

Genetic studies of Ras, Wnt and Notch components in *C. briggsae* have demonstrated conserved roles in promoting vulval fates.

Gonad ablation and LIN-3/EGF overexpression experiments have provided evidence that *Cel-lin-3* can induce 1^o and 2^o vulval fates in *C. briggsae*, and that VPCs fuse to the hypodermis in the absence of the AC (Félix, 2007; Sharanya *et al.*, 2012). This pattern was observed in comparable studies performed in *C. elegans* (Myers and Greenwald, 2007). Heat shock experiments precisely timed the VPC response to the inductive signal in *C. briggsae*. The VPCs respond to the inductive Cel-LIN-3 signal from 20-28 hours post L1 stage and the highest response is seen at 24 hours, with the animals displaying increased Muv penetrance (Sharanya *et al.*, 2012). Thus, the LIN-3/EGF signal induces vulval development in *C. briggsae*.

The function of the *lin-12/Notch* signaling pathway in anchor cell formation and 2^o cell fate specification also appears to be conserved in *C. briggsae* (Félix, 2007). RNAi knock down of *Cbr-lin-12* results in the development of multiple anchor cells, with all AC-adjacent cells acquiring 1^o cell fates (Félix, 2007). This suggests that *Cbr-lin-12* is needed for cell-cell communication during this process.

The canonical Wnt signaling pathway is involved in VPC competence and cell proliferation in *C. briggsae* (Seetharaman *et al.*, 2010). Genetic studies involving Axin homolog *Cbr-pry-1* have revealed its function in a canonical Wnt pathway upstream of *Cbr-bar-1* and *Cbr-pop-1*, where it regulates the downstream target gene *Cbr-lin-39*

(Seetharaman *et al.*, 2010). *Cbr-pry-1* hypomorphs exhibit a multivulva phenotype due to the constitutive activation of Wnt signaling in all VPCs (Seetharaman *et al.*, 2010). Examination of VPC fate pattern indicated that ectopic VPCs adopt a 2^o fate. This ectopic fate specification is independent of gonad-derived signals and LIN-12/Notch since *pry-1* mutants lacking gonad and *lin-12* signal still show ectopic 2^o lineage cells (Gleason *et al.*, 2002; Seetharaman *et al.*, 2010). Thus, activated Wnt signaling can confer 2^o cell fate on VPCs. Additional experiments showed that the role of Wnt signaling in VPC fate is conserved between *C. elegans* and *C. briggsae* (Seetharaman *et al.*, 2010).

Analyses of the vulval genes in *C. briggsae* have also revealed differences in function. Examination of the Notch receptor *glp-1* showed that its role in vulval development has diverged (Rudel and Kimble, 2002). In *C. briggsae*, *glp-1* RNAi causes the Muv phenotype, however *C. elegans glp-1* alleles show no effect on vulval development (Rudel and Kimble, 2002). Similar RNAi experiments with *lin-12* in *C. briggsae* have demonstrated that loss of *lin-12* causes L1 larval arrest, while no such phenotype is seen in *C. elegans* (Rudel and Kimble, 2002). In other instances involving signal variation, slight overexpression of *lin-3* can cause the adjacent cells to acquire 1^o cell fate in *C. briggsae*, however the adjacent cells still acquired the 2^o cell fate in *C. elegans* (Félix, 2007). Thus, lateral inhibition is easily overcome in *C. briggsae* (Félix, 2007). In another example, treatment of worms with EGF pathway inhibitors completely inhibits VPC induction in *C. elegans*, but only partially eliminated induction in wild type *C. briggsae* and EGF pathway mutants (Zitnik, 2014). These observations reveal subtle variations in the roles of these signaling pathways during the mechanism of vulva

formation between *C. elegans* and *C. briggsae*. Together, these studies demonstrate that although some information is available on the function of genes and pathways in vulval development in *C. briggsae*, it is very limited. Significantly more work will be required to gain a comprehensive, functional understanding of signaling pathways and regulatory networks controlling vulval development in *C. briggsae*.

1.9 Summary of intent

Although vulval development is conserved between *C. elegans* and *C. briggsae*, several subtle differences at the cellular and genetic level drive this biological process in each nematode species. This study aims to uncover the unique and shared features of this pathway through the genetic characterization of *C. briggsae* vulval mutants. The objectives of this thesis were to **(i) identify and characterize the genes and genetic networks driving the vulval development process in *C. briggsae* (ii) investigate the similarities and differences in developmental mechanisms between the two nematode species *C. elegans* and *C. briggsae*, and (iii) develop an efficient CRISPR-based genome editing method to generate targeted *C. briggsae* vulval mutants.**

To isolate genes required for vulval development in *C. briggsae*, forward genetic screens were undertaken in our lab. This study, described in Chapter 3, reports the identification of 19 mutants representing 13 genes, including 3 that are orthologs of *Caenorhabditis elegans* *unc-84* (SUN domain), *lin-39* (Dfd/Scr-related homeobox), and *lin-11* (LIM homeobox). This is the first report of a large collection of vulva mutants in this species. By analyzing the *C. briggsae* vulva mutants, I discovered developmental

systems drift (DSD) in three homologous processes. As described in Section 1.3 of Chapter 1, DSD is the process where developmental mechanisms diverge with time without any change in the phenotypic outcome (True and Haag, 2001). One of the DSD processes involves inter-VPC distance. Specifically, the distance between P5.p and P6.p. in *lin-39* mutants is lower in *C. briggsae* than in *C. elegans*. Second, *lin-39* does not interact with *pry-1* to enhance the small nuclear size phenotype of posterior Pn.p cells in *C. briggsae* as it does in *C. elegans*. And third, unlike *Cel-lin-11* mutants *Cbr-lin-11* animals do not exhibit a defect in anchor cell migration (**Chapter 3**).

Next, in collaboration with Dr. Helen Chamberlin's lab (Ohio State University), I assisted in the identification and mapping of seven vulval development genes, defining a new gene class 'ivp' (inappropriate vulval cell proliferation). Once again, it is the first report of a large number of genes that function to limit cell proliferation. Loss of function in these genes causes inappropriate division of VPCs and results in a Muv phenotype. The molecular identities of three of these Muv genes include orthologs of *lin-1* (ETS), *lin-31* (Winged-Helix) of the EGF-Ras pathway, and *pry-1* (Axin) of the Wnt pathway. The remaining four genes are EGF dependent and reside in regions of the genome that lack orthologs of known *C. elegans* Muv genes. As such, these Muv genes may represent novel regulators of *C. briggsae* vulval development (**Chapter 4**).

In addition to characterizing the roles of Vul, Pvl and Muv genes, I also contributed to the development of the CRISPR/cas9 system in *C. briggsae* to generate targeted mutations in genes of interest. This technology is based on protocols and reagents developed in the *C. elegans* system. In this study, through NHEJ, several *C.*

briggsae mutants (*Cbr-unc-22*, *Cbr-dpy-1*, *Cbr-unc-119*, and *Cbr-bar-1*) were generated. The results show that while the CRISPR approach works in *C. briggsae*, it appears less efficient in directing homologous recombination based events compared to *C. elegans*. In this work, my contribution was in donor vector design, generation of reporter constructs, and generating PCR amplicons for the *Cbr-lin-17* and *Cbr-dpy-1* genes to determine their efficiency in genome editing (**Chapter 5**).

In summary, the results described in this thesis indicate that despite the developmental and morphological similarity in wildtype vulval development between *C. elegans* and *C. briggsae*, the underlying genetic programs that govern this development include both conserved and divergent components. Also, the use of emerging genome editing technologies such as CRISPR, along with forward genetics and approaches like RNAi knock down will add strength to comparative studies using these nematodes (Dickinson *et al.*, 2013; Verster *et al.*, 2014). These powerful tools will not only revolutionize comparative studies, but also enable the study of *C. briggsae* in an individual context. Additionally, they can lead to the identification of new pathway components and regulatory networks that are not present in *C. elegans*.

CHAPTER 2: MATERIALS AND METHODS

2.1 Strains and culture conditions

C. briggsae strains were cultured under standard conditions used for *C. elegans* (Brenner, 1974; Wood, 1988). All experiments were performed at 20°C, unless otherwise noted. The wild-type *C. briggsae* strain used was *AF16*, and the polymorphism genetic mapping strain used was *HK104*. The ‘Cbr’ prefix denotes the *C. briggsae* orthologs of known *C. elegans* genes.

The mutants in this study include

Egl mutants: *Cbr-egl(bh21)*, *Cbr-egl(bh6)*, *Cbr-egl(bh21)*, *Cbr-egl(sy5395)*, *Cbr-lin(bh7)*, *Cbr-lin(bh13)*, *Cbr-lin(bh14)*, *Cbr-lin(bh25)*, *Cbr-lin(sy5197)*, *Cbr-lin(sy5212)*, *Cbr-lin-11(sy5336)*, *Cbr-lin-11(sy5368)*, *Cbr-lin-39(bh20)*, *Cbr-lin-39(bh23)*, *Cbr-lin(sy5425)*, *Cbr-lin(sy5426)*, *Cbr-unc(sy5505)*, *Cbr-unc-84(sy5506)*, *Cbr-egl-13lin(bh26)*.

Muv mutants: *Cbr-pry-1(sy5353)*, *Cbr-pry-1(gu137)*, *Cbr-ivp-1(gu163)*, *Cbr-lin-31(sy5342)*, *Cbr-lin-31(sy5344)*, *Cbr-lin-31(gu138)*, *Cbr-lin-31(gu168)*, *Cbr-lin-1(gu198)*, *Cbr-lin-1(sa993)*, *Cbr-lin-1(bh9)*, *Cbr-ivp-2(gu167)*, *Cbr-ivp-3(sy5216)*, *Cbr-ivp-3(sy5392)*, *Cbr-ivp-4(gu102)* and *Cbr-ivp-4(gu168)*.

Mutants generated in the CRISPR study: DY503 *Cbr-unc-22(bh29)*, DY504 *Cbr-dpy-1(bh30)*, DY530 *Cbr-bar-1(bh31)*, DY544 *Cbr-unc-119(bh34)* and DY545 *Cbr-unc-119(bh35)*.

The *C. briggsae* markers and mapping strains used in genetic experiments:

Cbr-sma(sy5330), *Cbr-sma-6(sy5148)*, *Cbr-unc-4(sy5341)*, *Cbr-dpy-1(sy5022)*, *Cbr-daf-4(sa973)*, *Cbr-unc-22(s1270)*, *Cbr-unc-22(gu205)*, *Cbr-dpy(sy5027)*, *Cbr-unc(sa997)* V, *Cbr-unc(sy5329)*, *Cbr-unc(sy5077)*. *bhEx166[Cel-daf-6::YFP+Cel-myo-2::GFP]*, *mfIs5[Cbr-egl-17::GFP + Cel-myo-2::GFP]* (Félix, 2007), *mfIs8[Cbr-zmp-1::GFP + Cel-myo-2::GFP]*, *bhEx31[pRH51(hs::lin-3)+myo-2::GFP]*, *bhEx78[pGF50(lin-11)+myo-2::GFP]*, *bhEx117[mec-7::GFP+myo-2::GFP]*, *bhEx123[C07H6 + myo-2::GFP]*, *bhEx124[C07H6 + myo-2::GFP]*, *bhEx132[F44F12 + myo-2::GFP]*, *bhEx134[F44F12 + myo-2::GFP]*, *bhEx139[pSL38(unc-84) + myo-2::GFP]*, *bhEx141[pSL38(unc-84) + myo-2::GFP]*, *bhEx142[pSL38(unc-84) + myo-2::GFP]*, *bhEx148[pGF50(lin-11) + myo-2::GFP]*, *bhEx152[pSL38(unc-84) + myo-2::GFP]*.

The *C. elegans* strains include N2 (wild type), *Cel-lin-31(n301)* (Ferguson and Horvitz, 1985), *Cel-lin-1(e1777)* (Ferguson and Horvitz, 1985), *Cel-lin-15AB(n309)* (Ferguson and Horvitz, 1985), *Cel-lin-11(n389)* (Ferguson and Horvitz, 1985) and transgenes include *ayIs4[Cel-dpy-20(+)+Cel-egl-17::gfp]* (Burdine *et al.*, 1998), *bhEx53[Cel-unc-119(+)+pGLC9 (Cel-daf-6::YFP+Cel-myo-2::GFP)]* (Seetharaman *et al.*, 2010).

2.2 Genetic screens

Ethyl methyl sulfonate (EMS) mutagenesis was performed by soaking *AF16* animals in a 25 mM M9 buffer solution of EMS for up to 4 hours (Brenner, 1974). The worms were

then washed four times with M9 solution and transferred onto standard nematode growth media (NGM) plates (Brenner, 1974).

For the Egl screen, animals exhibiting Egl phenotype were screened for in the F2 generation. From four independent F2 screens (in the range of 100,000-125,000 haploid genome sets in total), 39 independent Egl clones were isolated. This study focused on 19 mutations residing in 13 genes. For the Muv study, animals exhibiting Muv phenotype were isolated in the F2 generation and their progeny were evaluated. The lines exhibiting a heritable phenotype were retained for further study. Each strain was outcrossed at least three times before initiating genetic experiments. The 13 Muv strains were recovered by screening the offspring of approximately 40000 F1 animals (80000 mutagenized gametes). The additional mutation, *sa993*, was kindly provided by Takao Inoue (National University of Singapore).

2.3 Mapping

Mutations were mapped to linkage groups by several genetic mapping techniques. For polymorphism based mapping, the mutants were mapped to specific chromosomes by single worm and bulk segregant methods using indels and SNPs (Koboldt *et al.*, 2010). In addition, a 12X oligo microarray chip containing 4500 SNPs was used to map mutations (Flibotte *et al.*, 2009). Linkage of the Egl mutations were tested with several phenotypic markers as listed in www.briggsae.org. For genetic introgression, hermaphrodites from the *AF16* derived Muv strain was crossed to HK104 males. The selected F1 progeny hermaphrodites were allowed to self-cross and the resulting F2 Muv animals were

allowed to grow to establish round 1 backcross line. The round 1 line was further crossed to HK104 males to repeat the same process for a minimum of 5 rounds. Genomic DNA recovered after the 5 rounds will then be genotyped using a series of polymorphisms or phenotypic markers to establish and narrow the physical location of the mutation

2.4 Complementation

Complementation tests were performed between two vulval mutants (*m1* and *m2*) by crossing *m1/+* heterozygote males to *m2/m2* hermaphrodites. The crosses were done using visible recessive (e.g., Dpy or Unc) or *gfp*-based markers to identify the cross progeny. In the F2 generation, the vulval phenotype of L4 worms or the Egl/Muv phenotype of adult worms was scored under Nomarski optics. Based on these findings, the mutations have been placed into various complementation groups.

2.5 Serotonin and fluoxetine drug assays

Drug assays were carried out using Serotonin and fluoxetine to analyze the pharmacological response of the Class 1 Egl mutants. Serotonin (35 mM) and fluoxetine (1 mg/mL) solutions were prepared in M9 buffer freshly on the day of the experiment. In a 96-well microtiter plate, 50 μ L of drug was added in individual wells with appropriate controls. A day before the assay, L4 animals were picked and allowed to grow for 18-24 hr. They were then placed individually into drug and M9 containing wells. After 1 hr at room temperature, the number of eggs laid by each worm was counted to assess the effect of the drug on egg laying behavior. All assays were repeated a minimum of three times.

2.6 Heat shock experiment

For this experiment, L1 animals of the *bhEx31* strain grown on standard NG agar plates were heat shocked in a water bath. Various heat shock conditions were tested by fixing the temperature at 37° and varying the duration of the exposure. The effects of two different types of pulses were examined. A single long pulse (between 0:30 hour and 1:30 hour) and multiple short pulses (either consisting of four 30 minute pulses each separated by 1 hour rest period or two 1 hour pulses separated by 1 hour rest period), were tested. 37°C was chosen for all subsequent analysis after initial experiments. Once the heat shock treatment was complete, the animals were shifted 20°C. The vulval phenotype with respect to induction and morphology was examined at L4 by Nomarski. All of the heat shock experiments were done by Carle Ching.

2.7 Egl penetrance assay

In 6-well nematode growth agar plates, L4 animals were placed individually and observed over a 3-day period. The Egl phenotype was classified into 3 categories as Egl (no laid eggs, “bag of worms” appearance), semi-Egl (few eggs initially but eventually formed “bag of worms”), and non-Egl (no defect, phenotypically wild type).

2.8 Muv penetrance assay

The Muv penetrance was calculated by scoring adult worms at plate-level using a stereomicroscope, as well as in L4 animals using Nomarski optics. Adult animals exhibiting two or more protrusion were scored as Muv and those with a single protrusion

as Pvl . The Pvl animals were included in the non-Muv category. For *gul02* and *gul67* mutants, the Muv penetrance was calculated for temperatures 15 °C, 20 °C and 25 °C to test for temperature sensitivity.

2.9 Generation of sgRNA constructs

For the generation of the sgRNA constructs, gene sequences were first identified from Wormbase. The exons were searched for the target sgRNA following the form G/A(N)19NGG using ZiFiT Targeter Version 4.2 software (Sander *et al.*, 2007) and optimized using the scoring algorithm by (Doench *et al.*, 2014; Xie *et al.*, 2014) or the presence of a 3' GG motif at positions 19 and 20 of the NGG site (Farboud and Meyer, 2015). Constructs were generated using either two-step overlap-extension PCR on a *pU6::Cbr-unc-119_sgRNA* template (Friedland *et al.*, 2013) or Q5 site-directed mutagenesis on a *pU6::Cbr-lin-10_sgRNA* template (Paix *et al.*, 2014) using the NEB Q5 site-directed mutagenesis kit (E0554). Substitution at the target site was confirmed by AclI digestion. Donor templates were made with different sized homology arms using single stranded oligonucleotides (ssODN) (primers), PCR amplicons or plasmids containing fluorescent reporters (GFP and dsRED). The ssODNs were designed to insert a 22bp sequence containing a *NcoI* target site with homology arms of 75 and 49bp overlapping the sgRNA site (Paix *et al.*, 2014). PCR amplicons having 30-40bp short homology arms were generated to insert GFP (864 bp) and dsRED (830 bp) sequences into the gene of interest. The donor vector *myo-2::dsRED::unc-54 3'UTR* with 1Kb

homology arms flanking the target site was designed to insert a *myo-2::dsRED* reporter using Gibson Assembly Cloning Kit NEB catalog #E5510.

2.10 Sequencing

The primers and mutations associated with each identified gene are tabulated and listed in chapter 3, 4 and 5. The sequencing associated with ‘*gu*’ alleles was done by Helen Chamberlin lab members.

2.11 Generation of transgenic strains

By injecting DNA into the gonads of young adult hermaphrodites with injection mixes containing *myo-2* as transformation pharyngeal markers, transgenic worms were generated. The injections were done using a Zeiss Axiovert 200 microscope and Eppendorf FemtoJet. The microinjection technique was followed as described in Mello *et al.*, 1991.

For rescue experiments in the Egl study, transgenic worms were generated by injecting pSL38 (4ng/ μ L)(Mcgee *et al.*, 2006), *C. elegans* cosmids C07H6 (20 ng/ μ L) and F44F12 (0.7 ng/ μ L), pGF50 (20 ng/ μ L) (Freyd, 1991). Transgenic animals were further examined for the rescue of P-cell, vulval induction, invagination and Egl defects.

bhEx31 transgenic animals carry the pRH51 plasmid, which contains the EGF domain of *lin-3* under the control of the hsp16-41 promoter (pPD49.83). This heat shock experiment was done by Carle Ching.

Transgenic strain for the Muv study was generated by injecting the *daf-6::YFP* plasmid pGLC6 (100 ng/μL) (Seetharaman *et al.*, 2010).

For the CRISPR/cas9 study, the injection mixes were prepared containing *myo-2::GFP* (10 ng/μL), pU6::sgRNA (100 ng/μL) (customized for each gene) and *Peft-3::Cas9-SV40NLS::tbb-2 3'UTR* (100 ng/μL). Linear sgRNAs were injected at 60 ng/μL and 100 ng/μL. Mutants were detected either by plate level screening at F2 generation or by PCR screening of F1 and F1 mutant progeny with primers spanning the sgRNA site. These experiments except for linear sgRNA injections were done by Elizabeth Culp and Cory Richman.

2.12 Microscopy

The fates of each VPC were examined in L3 and L4 stages animals mounted on agar pads using Zeiss Axioimager D1 and Nikon Eclipse 80i microscopes. 1M sodium azide (1M) was used to anaesthetize the worms.

Based on the number of cells observed in *hyp7*, the fate was noted. If the VPC fused to the *hyp7* without dividing, it was assigned a Fused (F) fate. If the VPC divided once and fused with *hyp7*, it was assigned a tertiary (3°) fate. If the VPC was induced to give rise to more than 4 vulval progeny, it was assigned an Induced (I) fate. In *sy5353* and *sy5353;bh20* mutants, a few Pn.p cells appeared small and with a cell fate similar to P12.pa (Seetharaman *et al.*, 2010). These were termed as “small” cells.

In Muv animals, more than 3 VPCs get induced resulting in an induction score >3 . The fates of Muv animals were observed using primary and secondary cell fate fluorescent markers at mid and late L4 stage. *Cbr-egl-17::GFP* is a secondary cell fate marker expressing in Vul C and Vul D cells. *Cbr-zmp-1::GFP* and *Cel-daf-6::YFP* are primary cell markers expressing in VulE, VulF and VulA, VulE cells respectively. GFP analysis was done using a Zeiss Axioplan microscope equipped with the GFP filter HQ485LP (Chroma Technology), a power source (Optiquip 1500) and a 200 W OSRAM Mercury bulb.

The inter-VPC distances in *lin-39* mutants of *C. elegans* and *C. briggsae* was measured by calculating the distances among the 5 VPC pairs (P3.p-P4.p, P4.p-P5.p, P5.p-P6.p, P6.p-P7.p, P7.p-P8.p) in mid-to-late L2 stage animals using Nikon NIS Elements software.

2.13 Ablation experiments

Animals were first anaesthetized with 1–10 mM sodium azide. Cells of interest were then ablated using a class IIb laser system (Photonic Instruments Inc.) attached to a Nikon Eclipse 80i Nomarski fluorescence microscope. (Avery and Horvitz 1987). For the Egl study, P6.p was ablated at L2 stage to examine the fate of the neighbouring VPCs. For the Muv study, the gonad precursors (Z1 to Z4) were ablated during the L1 stage. Once the ablation was complete, the worms were recovered from the slides and allowed to grow in OP50 containing NG plates. Vulval phenotypes of the ablated worms were

examined for both experiments using Nomarski optics at either L4 or adult stage. The ablations for the Muv study were done by Jaeyoung Kim.

2.14 Statistical analysis

InStat 2.0 (GraphPad) Software was used for statistical analysis. For the unpaired *t*-tests, the tailed *P* values were calculated and values less than 0.05 were measured as statistically significant.

2.15 U0126 assays

A 10 mM U0126 solution dissolved in DMSO was diluted with 1X M9, with 150 µl of the solution spread on NGM plates on day one. The solution was left overnight at room temperature to be absorbed into the agar with final concentration of 10 µM and 30 µM. On day two, three drops of OP50 *E. coli* were added to the centre of each plate, and allowed to dry overnight. The next day, approximately 20 L1 worms were added to each plate. From here forth, the plates were maintained at 20°C. After three days, the adult worms were scored for the Muv phenotype. This experiment was done by Dr. Helen Chamberlin lab.

2.16 Quantitative RT-PCR assays

C. elegans, mutagenesis studies involving the egg-laying system have identified a signaling network RNA was extracted from Late L2 and early L3 cultures of *C. briggsae* wild type (*AF16*), *Cbr-lin(sy5216)*, *Cbr-lin(gu102)*, *Cbr-lin(gu167)*, *Cbr-lin(gu163)*, *Cbr-lin-31(sy5342)*, *Cbr-lin-1(gu198)*, *C. elegans* N2, *Cel-lin-15AB(n309)* using a TRIzol

based method. The developmental stage of the animals in culture was confirmed by observing the size of the gonad and the AC. All samples were DNase treated (Ambion Turbo DNA-free AM1907). cDNA were prepared using Protoscript AMV first strand cDNA synthesis kit- #E6500S. Reaction mixes for qRT-PCR for the reference and target genes were prepared using LuminoCt SYBR Green qPCR ReadyMix- L6544. Primers GL909/GL910 was used for amplifying *lin-3* fragment in *C. elegans*, while for *C. briggsae* primers GL911/GL912 were used. The reference genes were *Cbr-pmp-3* and CBG22375 in *C. briggsae* and *Cel-pmp-3* and Y45F10d.4 in *C. elegans*. *Cel-pmp-3* and *Cbr-pmp-3* were used in the final analyses Data were generated and analyzed using BioRad CFX manager software 3.1.

CHAPTER 3: GENETIC CONTROL OF VULVAL DEVELOPMENT IN *CAENORHABDITIS BRIGGSAE*

Preface:

This chapter includes the following article in its originally published format: “*Genetic control of vulval development in Caenorhabditis briggsae*”, by Devika Sharanya, Bavithra Thillainathan, Sujatha Marri, Nagagireesh Bojanala, Jon Taylor, Stephane Flibotte, Donald G. Moerman, Robert H. Waterston and Bhagwati P. Gupta. (G3 (Bethesda). 2012 Dec;2(12):1625-41. doi: 10.1534/g3.112.004598). This is an open-access article distributed under the terms of the Creative Commons Attribution Unported License, which permits unrestricted use, distribution, and reproduction in any medium, provided the original work is properly cited.

In this study, mutagenesis screens were undertaken to study the genes and the genetic pathways underlying the egg laying system in *C. briggsae*. In this work, we have isolated 39 Egl mutants and have characterized 19 mutants. The 19 *C. briggsae* mutants define 13 genes whose loss of function results in an Egl phenotype due to defects in neuronal or muscular components of the egg laying system, failed P-cell migration, reduced VPC induction and errors in cell division axes, anchor cell migration and invagination. Among the 13 genes, three *C. briggsae* genes *unc-84* (SUN domain), *lin-39* (Dfd/Scr-related homeobox), and *lin-11* (LIM homeobox) have been identified to be orthologous and functionally conserved with *C. elegans*. Additionally, DSD has been identified in three processes where the orthologous genes *lin-11* and *lin-39* display

different phenotypes with respect to VPC spacing, P7.p fate transformation and uterine vulval connection formation.

Contributions:

I performed most of the experiments for this paper with assistance from Bavithra Thillainathan (Figures 1, 2, 3, 5, 6, 7A, 7C and tables 1, 3, 4, 5, 8 and SNP chip-based genetic mapping). The mutagenesis screens and mutant isolation were done by Bhagwati Gupta along with Shahla Gharib and Takao Inoue. The cell lineage analysis of mutants was done by Nagagireesh Bojanala and Bhagwati Gupta (Table 7, Figure 7B). The cell fate analysis data in Table 9 was provided by Sujatha Marri. Don Moerman lab (Jon Taylor and Stephane Flibotte) and Robert H. Waterston performed the SNP-chip mapping of mutants (part of Table 3 and Supplementary Figure S2). Bhagwati Gupta and Carly Ching did the heat shock experiment involving LIN-3 overexpression (Figure 4). Bhagwati Gupta and I wrote the paper.



INVESTIGATION

Genetic Control of Vulval Development in *Caenorhabditis briggsae*

Devika Sharanya,* Bavithra Thillainathan,* Sujatha Marri,* Nagagireesh Bojanala,*¹ Jon Taylor,[†] Stephane Flibotte,[†] Donald G. Moerman,^{1,2} Robert H. Waterston,[§] and Bhagwati P. Gupta*²

*Department of Biology, McMaster University, Hamilton, Ontario L8S 4K1, Canada, [†]Michael Smith Laboratories and ²Department of Zoology, University of British Columbia, Vancouver, British Columbia V6T 1Z4, Canada, and [§]Department of Genome Sciences, University of Washington, Seattle, Washington 98195-5065

ABSTRACT The nematode *Caenorhabditis briggsae* is an excellent model organism for the comparative analysis of gene function and developmental mechanisms. To study the evolutionary conservation and divergence of genetic pathways mediating vulva formation, we screened for mutations in *C. briggsae* that cause the egg-laying defective (Egl) phenotype. Here, we report the characterization of 13 genes, including three that are orthologs of *Caenorhabditis elegans unc-84* (SUN domain), *lin-39* (*Dfd/Scr*-related homeobox), and *lin-11* (LIM homeobox). Based on the morphology and cell fate changes, the mutants were placed into four different categories. Class 1 animals have normal-looking vulva and vulva-uterine connections, indicating defects in other components of the egg-laying system. Class 2 animals frequently lack some or all of the vulval precursor cells (VPCs) due to defects in the migration of P-cell nuclei into the ventral hypodermal region. Class 3 animals show inappropriate fusion of VPCs to the hypodermal syncytium, leading to a reduced number of vulval progeny. Finally, class 4 animals exhibit abnormal vulval invagination and morphology. Interestingly, we did not find mutations that affect VPC induction and fates. Our work is the first study involving the characterization of genes in *C. briggsae* vulva formation, and it offers a basis for future investigations of these genes in *C. elegans*.

KEYWORDS

C. briggsae
C. elegans
vulva
development
cell proliferation
differentiation
morphogenesis
egg-laying
defective

Invertebrate model organisms such as the nematode *Caenorhabditis elegans* are excellent model organisms for investigating the genetic basis of development. Studies in *C. elegans* have provided insights into the cellular and molecular basis of organ formation and have revealed similarities and differences in the formation of homologous structures in metazoans.

Nematodes are an attractive system for studying the evolution of developmental mechanisms because they offer many useful features, including rapid development, transparency, and large brood size.

Comparative studies in nematodes have revealed similarities and differences in the vulva, the egg-laying organ. For example, the vulval precursor cell (VPC) equivalence group in *Oschies tipulae* and *Pristionchus pacificus* is smaller than that of *C. elegans* (Sommer 2005; Sternberg 2005). Furthermore, in *Pristionchus*, the mechanism of restricting vulval precursor competence is different. Although cell fusion limits precursor competence in *C. elegans*, programmed cell death controls this process in *P. pacificus* (Sommer 2005). In addition to these two species, vulval morphology has been examined in a large number of other nematodes, and differences have been found in the number of vulval progeny and the placement of the vulva (Felix *et al.* 2000; Felix and Sternberg 1997; Sommer *et al.* 1994; Sommer and Sternberg 1996). More recently, Kiontke *et al.* (Kiontke *et al.* 2007) examined 51 rhabditid species and identified variations in different steps of vulva development. In the *Caenorhabditis* genus, *Caenorhabditis briggsae* is an excellent model for comparative and evolutionary studies (Gupta *et al.* 2007). Sequence analyses of *C. elegans* and *C. briggsae* have suggested a divergence of approximately 30 million years (Cutter 2008). Morphologically, *C. briggsae* is almost identical to *C. elegans*; however, sequence comparison has revealed that almost one-third of all predicted genes in its genome are highly divergent (Gupta

Copyright © 2012 Sharanya *et al.*

doi: 10.1534/g3.112.004598

Manuscript received May 31, 2012; accepted for publication October 19, 2012

This is an open-access article distributed under the terms of the Creative Commons Attribution Unported License (<http://creativecommons.org/licenses/by/3.0/>), which permits unrestricted use, distribution, and reproduction in any medium, provided the original work is properly cited.

Supporting information is available online at <http://www.g3journal.org/lookup/suppl/doi:10.1534/g3.112.004598/-/DC1>.

¹Present address: Biology Center, ASCR, Institute of Parasitology, Budweis, Czech Republic, 37005.

²Corresponding author: Department of Biology, McMaster University, Hamilton, ON L8S 4K1, Canada. E-mail: guptab@mcmaster.ca

and Sternberg 2003; Stein *et al.* 2003). Both organisms offer powerful tools for dissecting gene function, including rapid development, invariant cell lineages, fully sequenced genomes, and amenability to both genetic and molecular manipulation (Antoshechkin and Sternberg 2007; Gupta *et al.* 2007; Hillier *et al.* 2007; Stein *et al.* 2003; Zhao *et al.* 2010). The hermaphroditic mode of reproduction of these species is another advantage because it allows for the maintenance of mutations that affect mating and egg laying. Organisms with divergent genomes but overall morphological similarity may offer intriguing examples of how networks of genes can be regulated differently while yielding the same ultimate structure.

Comparative studies of *C. elegans* and *C. briggsae* have revealed that alterations in developmental mechanisms do not always affect morphology. For example, the expression pattern of *lin-39*, an important Hox family member (*Dfd/Scr*-related) that regulates VPC competence, differs between the two species, yet VPC induction and cell fates are conserved (Penigault and Felix 2011a). The role of the Wnt pathway effector *pop-1* (TCF/LEF family) in *C. briggsae* endomesoderm specification represents yet another case of altered gene function with no obvious change in embryonic cell divisions or tissue morphology (Lin *et al.* 2009). In another case, knockdown of the *lin-12/Notch* receptor family member *glp-1* causes a multivulva (*Muv*) phenotype in *C. briggsae* but not in *C. elegans* (Rudel and Kimble 2001). Thus, *glp-1* appears to have acquired a new function in negative regulation of VPC fate specification in *C. briggsae*. Such alterations in gene function without apparent changes in homologous characters were described originally as developmental system drift (DSD) (True and Haag 2001).

The egg-laying system of *C. briggsae* is well suited for comparative analysis of gene function in organ formation, and it is helpful in elucidating DSD. Morphologically, the system is identical to *C. elegans* and follows a similar sequence of developmental events. Several of the vulval characters, such as cell number, position in the midbody region, and cell fusions are shared between these two species. However, some differences also have been noted. For example, the division frequency of the P3.p vulval precursor is higher in *C. elegans* than in *C. briggsae* (Delattre and Felix 2001). Other differences that have been found include the role of anchor cell (AC) in the vulval induction process, uterine seam (*utse*) cell morphology, brood size, sheath-contraction rate, and reproductive efficiency (Delattre and Felix 2001; Felix 2007; Gupta and Sternberg 2003; Miller *et al.* 2004). Subtle variations in VPC responses to inductive and lateral signaling cascades also have been reported (Felix 2007; Hoyos *et al.* 2011). Thus, there are some distinct differences in the mechanisms of vulva formation and egg-laying between *C. elegans* and *C. briggsae*.

In *C. elegans*, the egg-laying system is composed of five different cell types, namely, the vulva, somatic gonad (uterus), vulva and uterine muscles, and neurons (Li and Chalfie 1990). The vulva is connected to the uterus via a multinucleated *utse* cell (Newman and Sternberg 1996) and serves as a passageway for egg laying. Defects in any of the egg-laying components can cause eggs to accumulate in the uterus, resulting in an Egg-laying defective (*Egl*) phenotype. The *C. elegans* vulva is formed by the descendants of three of six equipotent VPCs. The VPCs are the posterior daughters of P cells. At hatching, the L1 larva contains six bilaterally symmetrical pairs of P cells in the ventrolateral region. By the mid-L1 stage, P cells migrate into the ventral cord region and become arranged in a single row (numbered P1 to P12) (Sulston 1976 and Sulston and White 1980). This process involves an orchestrated series of events initiated by the directed migration of P-cell nuclei. As a nucleus migrates, it drags the rest of the cell body along with it. Several genes have been identified that

affect P-cell nuclear migration, including *UNC-83* (KASH domain) and *UNC-84* [SUN domain (Starr 2011)]. These two proteins are localized to the outer and inner nuclear membranes, respectively (McGee *et al.* 2006), and they bridge the nuclear envelope and facilitate nuclear migration by transferring forces from the cytoskeleton to the nuclear lamina.

Soon after arriving at the ventral cord region, all 12 P cells divide once along the anteroposterior axis. Of the posterior daughters, five (P1.p, P2.p, P(9-11).p) fuse with the *hyp7* syncytium during the L1 stage. P12.p produces two daughters: P12.pp, which undergoes programmed cell death, and P12.pa, which adopts a unique epidermal fate, *hyp10*. The remaining 6 Pn.p cells ($n = 3$ to 8, VPCs) remain unfused in L1 due to the action of the Hox gene *lin-39*. These VPCs respond to later developmental cues. P3.p loses competence in the L2 stage in roughly half of animals and fuses with *hyp7* (termed 'F' fate).

Although all six VPCs are equally capable of giving rise to vulval tissue, only P5.p, P6.p, and P7.p do so in wild-type animals. This is due to the action of three evolutionarily conserved signal transduction pathways mediated by LET-60/Ras-MPK-1/MAPK (inductive signaling), LIN-12/Notch (lateral signaling), and Wnt-BAR-1/ β -catenin (Eisenmann 2005; Greenwald 2005; Sternberg 2005). In the L3 stage, the gonadal AC secretes the ligand LIN-3/EGF that binds to LET-23/EGFR on VPCs, leading to the activation of LET-60/Ras signaling in P6.p and to a lesser extent in P5.p and P7.p. Induced P6.p serves as a source of lateral signal that activates the LIN-12/Notch receptor in P5.p and P7.p. The inductive and lateral signaling together specify 1° (P6.p) and 2° (P5.p and P7.p) cell fates. In addition, Wnt signaling also participates in this process (Gleason *et al.* 2006; Seetharaman *et al.* 2010). The remaining uninduced VPCs fuse with *hyp7* after one cell division (termed 3° fate).

Forward genetics is an elegant method by which to study vulva formation in *C. briggsae* and to compare its developmental mechanisms with *C. elegans*. We have isolated mutations in *C. briggsae* AF16 by using the *Egl* phenotype as an assay. In this study, we describe 19 mutants, 17 of which fall into four phenotypic categories and represent 13 different genes. Class 1 mutants exhibit the *Egl* phenotype with normal vulval cells and morphology. Class 2 mutants lack some or all of the Pn.p cells in the ventral hypodermal region, suggesting that these genes play important roles in maintaining the correct number of P cells in the ventral hypodermal region. Class 3 mutants have a normal number of VPCs, but some precursor cells fail to be induced. Class 4 mutants affect the differentiation of vulval progeny and lead to abnormal vulval morphology in L4 larvae and a protruding vulva (*Pvl*) phenotype in adults. We also provide evidence that three of the genes recovered in our screen, *Cbr-lin(sy5506)* (class 2), *Cbr-lin(bh20)* (class 3), and *Cbr-lin(sy5336)* (class 4), are orthologs of *C. elegans unc-84*, *lin-39*, and *lin-11*, respectively.

The mutants and phenotypic classes described here serve as the nucleus of our effort to investigate the genes involved in vulva formation in *C. briggsae*. In addition, they provide a tool for identifying interacting genes through enhancer and suppressor screens. These findings will facilitate the comparison of cellular and molecular processes between *C. briggsae* and *C. elegans* in studying conservation and divergence in developmental mechanisms.

MATERIALS AND METHODS

Strains and culture conditions

Wild-type *C. briggsae* AF16 was used as a reference strain in all experiments. Strains were maintained at 20° using culture methods described for *C. elegans* (Brenner 1974; Wood 1988). To obtain synchronized

animals, gravid hermaphrodites were bleached. The bleach solution was prepared using sodium hypochlorite (commercial bleach) and 4 N sodium hydroxide (NaOH) at a ratio of 3:2. For 2 volumes of worms washed with M9 buffer, 1 volume of the bleach solution was added. The solution was vortexed and left to stand for 3 min at room temperature. After three consecutive washes with M9 solution, a pellet with 1 mL of remaining M9 buffer was transferred to an Eppendorf tube and placed in a shaker. Twenty-four hours later, the F1 worms were plated onto a new NG plate.

The strains used in this study are listed below (linkage groups of mapping markers are also mentioned; see www.briggsae.org for details). The *egl(bh6)* strain [allelic to *egl(bh2)*] was lost during the course of this study. The 'Cbr' prefix denotes the *C. briggsae* orthologs of known *C. elegans* genes.

Mapping mutants: *dpy(sy5148) II*, *dpy(sy5022) III*, *sma(sy5330) I*, *unc(s1270) IV*, *unc(sa997) V*, *unc(sy5077) X*.

Egl and Vul mutants: *egl(bh2)*, *egl(bh6)*, *egl(bh21)*, *egl(sy5395)*, *lin(bh7)*, *lin(bh13)*, *lin(bh14)*, *lin(bh20)*, *lin(bh23)*, *lin(bh25)*, *lin(bh26)*, *lin(sy5197)*, *lin(sy5212)*, *lin(sy5336)*, *lin(sy5368)*, *lin(sy5425)*, *lin(sy5426)*, *unc(sy5505)*, *unc(sy5506)*.

Transgenic strains: *bhEx31[pRH51(hs::lin-3) + myo-2::GFP]*, *bhEx78[pGF50(lin-11) + myo-2::GFP]*, *bhEx117[mec-7::GFP + myo-2::GFP]*, *bhEx123[C07H6 + myo-2::GFP]*, *bhEx124[C07H6 + myo-2::GFP]*, *bhEx132[F44F12 + myo-2::GFP]*, *bhEx134[F44F12 + myo-2::GFP]*, *bhEx139[pSL38(unc-84) + myo-2::GFP]*, *bhEx141[pSL38(unc-84) + myo-2::GFP]*, *bhEx142[pSL38(unc-84) + myo-2::GFP]*, *bhEx148[pGF50(lin-11) + myo-2::GFP]*, *bhEx152[pSL38(unc-84) + myo-2::GFP]*, *mfls5[Cbr-egl-17::GFP + myo-2::GFP]*, *mfls8[Cbr-zmp-1::GFP + myo-2::GFP]*.

mfls5 and *mfls8* animals carry a *gfp* reporter driven by the vulva-specific enhancers of *Cbr-egl-17* (748 bp) and *Cbr-zmp-1* (755 bp), respectively (Kirouac and Sternberg 2003). *bhEx117* is a transgenic HK104 line that was used in polymorphism-based mapping experiments (see below).

Mutagenesis

AF16 animals were mutagenized by soaking in 25 mM ethyl methane sulfonate (EMS) and screening for Egl and Pvl mutants in the F2 generation. To prevent worms from burrowing into the agar, we used 9-cm NG-Agarose plates (1 L of media containing 3 g of sodium chloride, 2.5 g of bacteriological peptone, and 17 g of agarose; the other components were the same as nematode growth medium). Mutagenized worms were individually transferred onto plates, and the F2 progeny were screened for Egl worms. Such animals formed the characteristic "bag of worms" phenotype as a result of the progeny hatching inside the uterus and devouring the mother (Horvitz and Sulston 1980).

From four independent F2 screens (in the range of 100,000-125,000 haploid genome sets in total), we recovered 39 independent Egl clones that bred true. An additional 34 Egl clones could not be propagated because they were either sterile or gave rise to dead progeny. Apart from animals with the Egl phenotype, we also recovered dumpty and uncoordinated mutants. One of these, twitcher, was isolated from at least three independent plates (B. P. Gupta, unpublished results). In *C. elegans* and *C. briggsae*, the twitcher phenotype is associated with *unc-22*, a gene with more than 20 kb of open reading frame that is readily mutated in EMS screens (Benian *et al.* 1993). All three twitcher mutations are recessive and have been found to be allelic (data not shown), which suggests that our screens were capable of recovering viable recessive mutations with a visible phenotype.

This study focuses on a collection of 19 mutations that reside in 13 genes (see *Results*). Compared with the original *C. elegans* Egl screen (Trent *et al.* 1983), the number of Egl mutants in our case is considerably lower. It is unclear whether this is due to differences in the population of screened worms, as Trent *et al.* did not provide an estimate of the number of worms that were screened. Based on the mapping and complementation experiments, 70% of *C. briggsae* genes (9 of 13) are represented by single mutations (see *Results*). Although this result is indicative of the screen being unsaturated, the proportion of genes defined by a single allele in our case is very similar to that of Trent *et al.* (Trent *et al.* 1983). Furthermore, it is worth pointing out that additional alleles of the existing *C. briggsae* genes may be present among the remaining 20 mutations that have yet to be characterized. This analysis is the focus of our current study.

Similar to *C. elegans* (Ferguson and Horvitz 1985; Trent *et al.* 1983), not all *C. briggsae* mutants described here affect vulva formation, indicating that defects in other egg-laying components (such as neurons and muscles) can also lead to the Egl phenotype. Each mutant was backcrossed at least three times before we performed genetic experiments. All alleles were recessive and caused no obvious maternal effect phenotype.

Microscopy, cell ablations, and VPC fates

Worms were mounted on agar pads as described previously (Wood 1988) and examined under Nomarski optics using Zeiss Axiomager D1 and Nikon Edipse 80i microscopes. Sodium azide (1 M) was used as an anesthetic. To examine vulval lineages, L3 and L4 stage animals were mounted without any anesthetic, and coverslip edges were sealed with Vaseline to prevent dehydration. For GFP reporter-expressing strains, epifluorescence was visualized with a Zeiss Axioplan microscope equipped with the GFP filter HQ485LP (Chroma Technology), a power source (Optiquip 1500) and a 200 W OSRAM Mercury bulb. Cell ablation experiments were performed as described (Avery and Horvitz 1987).

VPC fates were examined in L3 and L4 stage animals under a Nomarski microscope. If a VPC fused with *hyp7* as a single cell without dividing, it was assigned an 'F' (Fused) fate. If the VPC divided once and its daughters (Pn.px, where x denotes both anterior and posterior cells) fused with *hyp7*, it was assigned a 3° (tertiary) fate. If the VPC was induced to give rise to more than 4 vulval progeny (Pn.pxxx cells), it was considered fully induced and assigned an 'I' (induced) fate [includes 1° and 2° fates as described previously (Sternberg and Horvitz 1986)]. Vulval induction score was calculated as described previously (Gupta *et al.* 2006). In *sy5353* and *sy5353*; *bh20* mutants some of the Pn.p appeared small and morphologically similar to P12.pa (Seetharaman *et al.* 2010). These were termed as "small" cells.

To determine inter-VPC distances in *lin-39* mutants, animals were bleached synchronized. Distances among the 5 VPC pairs (P3.p-P4.p, P4.p-P5.p, P5.p-P6.p, P6.p-P7.p, P7.p-P8.p) were measured in mid-to-late L2 stage animals using Nikon NIS Elements software.

Pharmacological assays

Serotonin and fluoxetine were used to analyze the pharmacological response of some of the Egl mutants. Serotonin (35 mM) and fluoxetine (1 mg/mL) solutions were freshly prepared in M9 buffer. The assay was performed in 96-well microtiter dishes using 50 μ L of drug in individual wells. As a control, the same volume of M9 buffer was placed in adjacent wells. L4 animals were picked a day before the assay and allowed to grow for 18-24 hr before placing them individually into drug and M9 containing wells. After incubating worms for 1 hr at

■ Table 1 Results of complementation experiments

m1/+	m2/m2	Animals Showing Phenotype	Phenotype Scored
bh2/+	bh6	39% (n = 28)	Egl
bh7/+	bh14	0% (n = 60)	Vul
bh7/+	bh20	0% (n = 23)	Vul
bh14/+	bh20	0% (n = 31)	Vul
sy5197/+	bh13	62% (n = 8)	Sma, vulval invagination abnormal
bh13/+	bh25	0% (n = 30)	Egl, Sma, vulval invagination abnormal
sy5336/+	sy5368	58% (n = 12)	Egl, vulval invagination abnormal

room temperature, the number of eggs laid by each worm was counted. Assays were repeated at least three times.

Heat shock protocol

L1 animals of the *bhEx31* strain were transferred to standard NG agar plates containing *Escherichia coli* OP50 bacteria and grown for a desired period of time. Plates were sealed with Parafilm M (American National Can) and heat shocked in a water bath. We tested various heat shock conditions by fixing the temperature at 37° and varying the duration of the exposure. Two different types of pulses, i.e. a single long pulse (between 0:30 hr and 1:30 hr) and multiple short pulses (either consisting of four 30-min pulses each separated by 1-hr rest period or two 1-hr pulses separated by 1h, i.e., 1-hr-r rest period), were tested. Animals were heat shocked at different time points after transferring L1 worms on bacteria-containing plates. After the initial trials, we chose 37° for 1 hr for all subsequent experiments. After heat shock treatment, animals were shifted back to 20°. Vulval induction and morphology were examined at stage L4.

Egl penetrance assay

L4 animals were placed individually into six-well nematode growth medium-agar plates and observed over a 3-day period. Egl phenotype was classified as Egl (no laid eggs, “bag of worms” appearance), semi-egl (few eggs initially but eventually formed “bag of worms”), and Non-Egl (no defect, phenotypically wild type).

Complementation tests

Complementation tests between two vulval mutants (*m1* and *m2*) were performed by crossing *m1/+* heterozygote males (obtained by crossing *m1/m1* hermaphrodites to *myo-2::gfp* carrying *nfls5* or *nfls8* males) to *m2/m2* hermaphrodites. The presence of the *gfp* transgene allowed us to identify cross progeny. In the F2 generation, vulval phenotype in L4 worms was scored under Nomarski optics. Complementation tests were carried out for mutations belonging to the same phenotypic categories. Table 1 lists all combinations that were tested and the results.

Phenotypic marker-based genetic mapping

We tested the linkage of *lin-11(sy5336)* with several phenotypic markers that were assigned to various chromosomes. The website www.briggsae.org shows a larger list of mapping experiments involving these markers. The *sy5336* mutation was linked to *sma(sy5330)* (Table 2). Together these two genes define a single linkage group that was assigned chromosome 1 based on *sy5336* molecular identity and synteny of the *lin-11* genomic region (<http://www.wormbase.org>). The *unc(sy5506)* mutation was linked to chromosome X based on the *Unc* phenotype of F1 males derived from a cross of *sy5506* hermaphrodites to AF16 males.

Insertion-deletion (indel) and snip-SNP-based genetic mapping

All mutations except *lin(bh14)* and *Cbr-lin-11* alleles were mapped to chromosomes by bulk segregant analysis (BSA) using Indels and snip-

SNPs (Table 3, Supporting Information, Figure S1). The cross scheme was as follows. Hermaphrodites of a given mutant strain were crossed with either normal or GFP fluorescing (*bhEx117*) HK104 males. F1 cross progeny were picked and cloned. In the next generation (F2), phenotypically mutant and wild-type animals (20 each) were picked separately and processed to obtain genomic DNA. Genomic DNA was prepared by placing worms into 5 to 10 μ L of lysis buffer (containing Proteinase K). The solution was incubated at 60° for 1 hr followed by heat inactivation of Proteinase K at 95°. This crude genomic DNA prep was frozen at -20° and used as a template in polymerase chain reaction experiments. The detailed indel mapping protocol and primers have been published previously (Koboldt *et al.* 2010). We reported earlier the single recombinant analysis of *lin(sy5506)* using the indel *bhP26*. The distance between the two loci was determined to be 10% (Koboldt *et al.* 2010).

SNP chip-based genetic mapping

In addition to the aforementioned polymorphism-based BSA mapping, we used a microarray chip mapping approach to localize the mutations on chromosomes (Table 3). For this, a 12x oligo microarray chip containing approximately 4500 SNPs was designed using methods similar to those for *C. elegans* (Flibotte *et al.* 2009). An earlier version of the *C. briggsae* chip contained almost 9700 SNPs and was successfully used to map mutations (Zhao *et al.* 2010). *C. briggsae* Egl animals were mated with HK104 males, and F1 heterozygotes were cloned. In the F2 generation, 100 mutant worms were picked and allowed to grow on 10 6-cm Petri plates close to starvation. The worms were washed off with M9 buffer. Genomic DNA was extracted using the QIAGEN Blood and Tissue DNeasy kit (cat. no. 69504). DNA hybridization, measurement of fluorescence intensity and ratio analysis were performed as described previously (Flibotte *et al.* 2009; Maydan *et al.* 2007). Based on the mapping signal intensity and the arc of the signal (Figure S2), the approximate chromosomal locations of mutations were determined (Zhao *et al.* 2010). In some cases, such as *sy5505*, arc pattern was not obvious, rendering the analysis less reliable. Overall, the SNP-chip data agreed with seven of the indel and snip-SNP BSA mapping results (Table 3). Independent verification of these results by phenotypic-marker-based classical mapping has not been performed.

■ Table 2 Linkage mapping of *Cbr-lin-11* using phenotypic markers

Marker	LG	Data
<i>sma(sy5330)</i>	I	2/39 Sma were Egl
<i>dpy(sy5148)</i>	II	19/29 Egl segregated Dpy
<i>dpy(sy5022)</i>	III	11/18 Egl segregated Dpy
<i>unc(sy1270)</i>	IV	16/24 Egl segregated Unc
<i>unc(sy997)</i>	V	24/32 Unc segregated Egl
<i>unc(sy5077)</i>	X	15/32 Unc segregated Egl

■ Table 3 Linkage mapping of mutations by BSA and SNP-chip techniques

Gene	Allele	Chromosomal Location	
		BSA-Based	SNP Chip-Based
<i>egl</i> (<i>sy5395</i>)	<i>sy5395</i>	1: left arm (bhP19)	–
<i>lin</i> (<i>bh7</i>)	<i>bh7</i>	1 (cb-m142, cb650)	1: 4.5 Mb
<i>lin</i> (<i>bh13</i>)	<i>bh13</i>	1: left arm (bhP42)	1: 4 Mb
<i>lin</i> (<i>bh25</i>)	<i>bh25</i>	1 ^a (cb650)	–
<i>egl</i> (<i>bh2</i>)	<i>bh2</i>	1: center (bhP42)	1: 7.5 Mb
<i>Cbr-lin-11</i>	<i>sy5336</i>	–	1: 7.9 Mb ^b
<i>Cbr-lin-39</i>	<i>bh20</i>	3: right arm ^c (bhP40)	–
<i>unc</i> (<i>sy5505</i>)	<i>sy5505</i>	5: center/right arm (bhP5, cb-m103)	5: 8.5 Mb
<i>lin</i> (<i>sy5425</i>)	<i>sy5425</i>	5: center (bhP5)	–
<i>Cbr-unc-84</i>	<i>sy5506</i>	X: right arm ^c (bhP26)	–
<i>egl</i> (<i>bh21</i>)	<i>bh21</i>	X (bhP25)	X: 11.5 Mb
<i>lin</i> (<i>bh14</i>)	<i>bh14</i>	I (bhP1)	–
<i>lin</i> (<i>bh26</i>)	<i>bh26</i>	X: right arm (bhP26)	X: 12.5 Mb

Tightly linked indel and snip-SNP markers are shown in brackets. Dashes (–) indicate a lack of map information.

^a Likely to be located on the left arm.

^b Previous study (Zhao et al. 2010).

^c Previous study (Koboldt et al. 2010).

Molecular biology and transgenics

Transgenic worms were generated by injecting DNA into the syncytial gonad of adult hermaphrodites using *myo-2::GFP* (pPD118.33) as a transformation marker (S. Q. Xu, B. Kelly, B. Harfe, M. Montgomery, J. Ahnn, S. Getz, and A. Fire, personal communication). The micro-injection technique was described previously (Mello et al. 1991).

The pSL38 plasmid, which contained a *C. elegans unc-84* rescuing fragment (McGee et al. 2006), was injected at 4 ng/μL in *unc*(*sy5505*) and *unc*(*sy5506*) animals. Stable lines (*sy5505: bhEx141* and *bhEx142*, *sy5506: bhEx139* and *bhEx152*) were analyzed for the rescue of *Unc*, P cell migration, and *Egl* phenotypes.

The *hsc::lin-3* transgenic animals, *bhEx31*, carry the pRH51 plasmid [50 ng/μL (Katz et al. 1995)]. pRH51 contains the EGF domain of *lin-3* along with a synthetic signal peptide. The expression of *lin-3* is under the control of the *hsp16-41* promoter (pPD49.83).

For the rescue of *Cbr-lin-39* mutants, *C. elegans* cosmids C07H6 and F44F12, containing the entire *lin-39* genomic region, were injected into *bh20* animals. Two stable lines were obtained for each cosmid (*bhEx123* and *bhEx124* with C07H6 at 20 ng/μL; *bhEx132* and *bhEx134* with F44F12 at 0.7 ng/μL). VPC induction and *Egl* phenotypes were analyzed in transgenic animals. A greater proportion of F44F12 stable lines showed rescue of the *Egl* phenotype compared to C07H6. Therefore, we focused on *bhEx132* and *bhEx134* transgenic animals for all subsequent analyses.

Cbr-lin-11 cDNA was amplified using the ProtoScript first strand kit (NEB, #E6500S). The primers cb-lin-11-up-1 and cb-lin-11-down-2 (Table S1) were used. Whole RNA was prepared from the mixed stage animals using a previously described TRIZOL method (Burdine and Stern 1996). The *C. elegans lin-11*-rescuing plasmid pGF50 (Freyd 1991) was injected at 20 ng/μL. pGF50 contains a 19-kb subclone of cosmid ZK273 that was previously shown to rescue *C. elegans lin-11* mutants (Freyd 1991). Two stable lines (*bhEx78* and *bhEx148*) were generated for pGF50 (20 ng/μL), both of which rescued *Egl* and vulval invagination defects in *sy5336* animals.

Sequencing

All primer sequences are listed in Table S1. The exons of *Cbr-unc-84* were amplified using primer pairs GL793/GL795, GL800/GL801, GL806/812, and GL809/810. To sequence the intermediate regions, primers GL802, GL807, and GL808 were used. A 403-bp deletion between

exons 6 and 7 (genomic location +5006 and +5408) was identified that introduces an in-frame stop codon downstream of the deleted region.

Cbr-lin-39 exons were amplified from *bh20* and *bh23* alleles using primer pairs GL380/GL381, GL382/GL383, GL384/GL385, GL389/GL390, and GL391/GL392. The *bh23* mutation contains a 364-bp deletion overlapping with the 5' region of the *Cbr-lin-39* coding sequence. The deletion is located between -158 (upstream of the ATG start site) and +207 (in exon 1). The *bh20* allele carries a point mutation in exon 3 (G9427 to A) that corresponds to the homeodomain region.

The *Cbr-lin-11* ORF was amplified in two fragments using primer pairs cb-lin-11-up-1/cb-lin-11-down-7 and cb-lin-11-up-5/cb-lin-11-down-1. Sequencing primers were cb-lin-11-up-1, cb-lin-11-up-4, cb-lin-11-up-6, cb-lin-11-up-7, cb-lin-11-up-8, cb-lin-11-up-9, cb-lin-11-down-1, cb-lin-11-down-5, cb-lin-11-down-7, and cb-lin-11-down-8. Both *lin-11* alleles, *sy5336* and *sy5368*, affect splicing. *sy5336* causes a G to A transition (G4403 to A) in the splicing acceptor site of intron 7 and is likely to disrupt intron 7 splicing. The *sy5368* mutation affects the splicing donor site of intron 6 (G3340 to A) and is predicted to introduce a premature in-frame stop codon 52 nucleotides downstream.

Statistical analysis

Statistical analyses were performed using InStat 2.0 (GraphPad) Software. Two-tailed *P* values were calculated in unpaired *t*-tests, and values less than 0.05 were considered statistically significant.

RESULTS

Overview of the genetic screen

We screened for egg-laying defective (*Egl*) mutants after EMS mutagenesis of AF16 animals (see *Materials and Methods* for details). Of 39 *Egl* mutants identified, we report the characterization of 19 mutants. Seventeen of these fell into 13 complementation groups and were placed into four distinct phenotypic categories (Table 4). Of the remaining 2, *lin*(*sy5212*) and *lin*(*sy5426*), *sy5212* is a fully penetrant Vul mutant and could not be outcrossed. In rare circumstances, VPC induction in *sy5212* animals was observed only for P6.p. All other VPCs fused to hyp7 during the L2 and L3 stages. The other mutant, *sy5426*, has variable vulva defects (a combination of missing VPCs, uninduced VPCs, and abnormal morphogenesis) and could not be

■ Table 4 Overview of *C. briggsae* egg-laying defective mutants

Class	Features	Gene	Alleles	Mutation	Egl Penetrance (%)			n
					Non-Egl	Semi-Egl	Egl	
1	Wild-type vulva	<i>egl(bh2)^a</i>	2	<i>bh2</i>	0	69	31	103
		<i>egl(bh21)</i>	1	<i>bh21</i>	0	41	59	120
		<i>egl(sy5395)</i>	1	<i>sy5395</i>	6	32	62	244
2	Fewer Pn.p cells	<i>unc(sy5505)</i>	1	<i>sy5505</i>	22	17	61	127
		<i>Cbr-unc-84</i>	1	<i>sy5506</i>	56	21	23	100
3	Reduced VPC induction	<i>lin(bh7)</i>	1	<i>bh7</i>	81	12	7	137
		<i>lin(bh14)</i>	1	<i>bh14</i>	39	32	29	133
		<i>Cbr-lin-39</i>	2	<i>bh20</i>	0	4	96	140
4	Abnormal vulval invagination	<i>Cbr-lin-11</i>	2	<i>bh23</i>	0	0	100	41
				<i>sy5336</i>	0	0	100	100
				<i>sy5368</i>	0	0	100	100
		<i>lin(bh13)^a</i>	2	<i>bh13</i>	1	1	98	102
		<i>lin(bh26)</i>	1	<i>bh26</i>	0	0	100	100
		<i>lin(bh25)</i>	1	<i>bh25</i>	1	23	76	105
–	Unclassified	<i>lin(sy5425)</i>	1	<i>sy5425</i>	36	25	39	104
		<i>lin(sy5212)</i>	–	<i>sy5212</i>	0	0	100	49
		<i>lin(sy5426)</i>	–	<i>sy5426</i>	0	0	100	29

Egl, animals did not lay eggs at all; n: number of animals scored; Non-Egl, animals continued to lay eggs throughout their reproductive life; Semi-Egl, animals laid eggs initially but became Egl afterward.

^aThe phenotype of the other allele of this locus was not characterized in detail.

uniquely classified. We used indel-based BSA, snip-SNP, and SNP-chip mapping approaches (Koboldt *et al.* 2010; Zhao *et al.* 2010) to localize the mutations to chromosomes (Table 3).

Class 1 mutants consist of three loci, each of which shows morphologically wild-type vulval development and a vulva-uterine connection (*utse*). The Egl phenotype of these animals is likely to result from defects in neuronal and/or muscle components of the egg-laying system. Class 2 is composed of two mutants, both of which are uncoordinated and frequently lack VPCs. In some cases, these animals lack a functional vulva and develop an Egl phenotype. Class 3 mutants are represented by three loci, each of which shows reduced VPC induction. The strongest allele in this class, *bh23*, causes a fully penetrant Egl defect. The largest phenotypic category, class 4, is composed of five loci. Mutations belonging to this class do not affect VPC induction but cause abnormal vulval invagination and morphology. The adults frequently have Pvl and Egl phenotypes.

Class 1 mutants have defects in egg-laying components other than the vulva and *utse*

The examination of vulval phenotype in class 1 mutants revealed that VPCs and their progeny were unaffected. Vulval cells invaginated correctly and gave rise to a morphology characteristic of the wild-type animals. Furthermore, the *utse* was normal and was located on the top of the vulval apex (data not shown). To examine defects in other components of the egg-laying system, we treated animals with drugs that affect neuronal and muscle activities. In *C. elegans*, hermaphrodite-specific neurons (HSNs) control egg-laying behavior (Croll 1975; Horvitz *et al.* 1982; Weinshenker *et al.* 1995). In response to external cues, such as food, HSNs release serotonin (*i.e.*, 5-hydroxytryptamine or 5-HT) into the neuromuscular synapse, which then acts on the postsynaptic receptors in the vulval muscle to stimulate the release of eggs. Authors investigating the role of HSNs have used serotonin and fluoxetine [a serotonin reuptake inhibitor that increases the amount of neurotransmitter available to post-synaptic receptors (Baldessarini 1996; Dempsey *et al.* 2005)] to characterize the neuronal basis of the Egl phenotype. Serotonin and fluoxetine drug assays can distinguish between pre- and postsynaptic defects (*i.e.*, between HSN and

vulva muscle). Mutants resistant to fluoxetine that lay eggs in the presence of exogenous serotonin are likely to have abnormal HSNs, whereas resistance to both drugs suggests a postsynaptic signaling defect. We found that *egl(sy5395)* animals, when exposed to serotonin, had a modest but consistent increase in the number of eggs laid compared with the control, but *egl(bh21)* and *egl(bh2)* were unaffected (Figure 1). Fluoxetine exposure had no obvious effect on any of the strains. These results suggest that the Egl phenotype in *sy5395* animals may be caused by abnormal differentiation of HSNs. In the case of *bh21* and *bh2* mutants, the cellular basis of the Egl phenotype remains to be identified.

Class 2 mutants have defects in nuclear migration and include *Cbr-unc-84*

The class 2 mutants *unc(sy5505)* and *unc(sy5506)* have fewer and more variable numbers of P cells in the ventral hypodermal region. Animals homozygous for either of these mutations move in a slow and uncoordinated manner. Microscopic observations revealed fewer than 12 P-cell nuclei in the ventral hypodermal region (Figure 2A). This phenotype was temperature sensitive, such that the loss of P cells was greater at higher temperatures (Figure 2A and data not shown). Nearly two-thirds of the animals had an Egl phenotype due to the absence of some or all of the P(5-7).p VPCs (Tables 4 and 5, Figure 3A). We also observed a *hyp7* nuclear migration defect in the *sy5506* strain. Unlike wild-type animals where no *hyp7* nuclei are observed in the dorsal hypodermis, *sy5506* worms had many *hyp7* nuclei in this region (Figure 2, B and C).

In *C. elegans*, similar phenotypes are caused by mutations in two genes, *unc-83* (KASH domain) and *unc-84* (SUN domain), which affect nuclear migration during development (Malone *et al.* 1999; Starr *et al.* 2001; Sulston and Horvitz 1981). One of these, *unc-84*, is located on the right arm of chromosome X. We found that *sy5506* also maps to the right arm of chromosome X close to the *bhP27* polymorphism (see *Materials and Methods*), a region that contains *Cbr-unc-84* (CBG07416 and is syntenic to *unc-84*).

To further confirm that *unc(sy5506)* defines the *Cbr-unc-84* gene, we generated transgenic *sy5506* animals carrying an *unc-84* rescuing

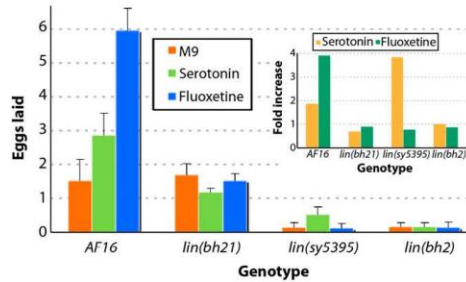


Figure 1 Egg-laying responses of class 1 mutants. The graph shows the average number of eggs laid by animals in M9 buffer (control) and serotonin and fluoxetine drug-containing solutions. The fold increase in egg laying in drug solution (over M9 buffer control) is plotted in the inset graph.

plasmid called pSL38 (McGee *et al.* 2006). The transgenic animals showed rescue of the hyp7 and P-cell nuclear migration defects (51% *bhEx139* animals with normal hyp7 nuclear migration, n = 35, and 90% P nuclei present in ventral cord, n = 91, at 20°C, compared with 100% abnormal hyp7 nuclear migration and 42% P-cell nuclei, n = 23, in *sy5506*). The Egl and VPC induction defects in mutants also were rescued (69% of *bhEx139* animals laying eggs, n = 94, compared with 56% in *sy5506*, n = 100; see Table 5 for VPC induction).

Finally, we sequenced the *Cbr-unc-84* genomic region in *unc(sy5506)* animals and identified a 403-bp deletion covering parts of exons 6 and 7 (Figure 2D, also see *Materials and Methods*). These results demonstrate that *sy5506* is an allele of *Cbr-unc-84*. In *C. elegans*, UNC-84 protein contains a SUN domain, a transmembrane domain and an intervening linker region (Malone *et al.* 1999; McGee *et al.* 2006). Based on the sequence alignment, the *sy5506* mutation is

located in the linker region of Cbr-UNC-84. In *C. elegans*, this region interacts with UNC-83 to facilitate localization of other cytoskeletal components that are crucial for nuclear positioning in hyp7 and P cells.

The phenotype of *sy5505* animals differs from *Cbr-unc-84(sy5506)* in two respects. First, they are more sensitive to increased temperature as evidenced by their inability to grow at 29°C (Figure 2A). Second, no hyp7 migration defect was observed in *sy5505* animals (data not shown). We also generated transgenic *sy5505* strains carrying the *unc-84* plasmid pSL38 (*bhEx141* and *bhEx142*) but did not observe rescue of the mutant phenotype (Table 5 and data not shown). These results together with linkage data (Table 3) suggest that *sy5505* is not allelic to *Cbr-unc-84* and is likely a different gene. The phenotype of *sy5505* is similar to mutations in *unc-83* in *C. elegans*; however, the possibility that *sy5505* is an allele of *Cbr-unc-83* has not been tested.

Class 3 mutants exhibit reduced VPC induction

Four mutations define class 3 genes, all of which cause a reduction in the number of vulval progeny (see VPC induction score in Table 5) and abnormal invagination (Figure 3). In these animals, some or all P (3-8).p fail to divide and fuse with surrounding hypodermis ('F' fate; Table 5). The phenotype is weakest in *lin(bh7)* (only one VPC uninduced; Figure 3B) but fully penetrant in *lin(bh23)* (all VPCs uninduced; Figure 3E). The other two alleles, *lin(bh14)* and *lin(bh20)*, are intermediate (Figure 3, C and D), with *bh20* being somewhat more severe as determined by fewer cases of P6.p induction (15%; see Table 5) and rudimentary vulval invagination. This observation agrees well with the vulval induction score, cell lineage, and Egl penetrance of the animals (Tables 4, 5, and 6). The *bh20* and *bh23* mutations also cause abnormal folding of gonad arms and subtle uncoordinated phenotypes (data not shown).

Next, we examined the VPC induction defect in some detail. As the defect in *bh7*, *bh14*, and *bh20* animals is predominantly limited to 2° precursors (P5.p and P7.p), we wanted to determine whether these two VPCs lack the potential to respond to an external signal and are

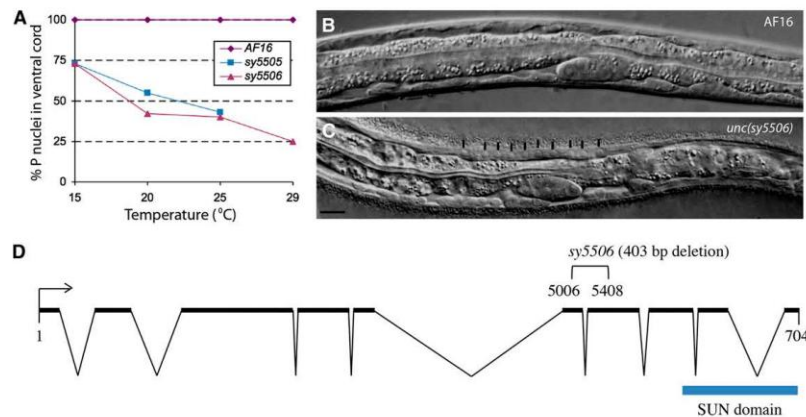


Figure 2 Nuclear migration defects in class 2 mutants and molecular analysis of *Cbr-unc-84*. (A) P-cell nuclei in the ventral cord region of mutants vary with temperature. At greater temperatures, fewer nuclei are visible. *sy5505* animals are very sick at 29°C and could not be examined. Each data point consists of 25 or more animals. (B, C) Wild-type AF16 and *sy5506* L1 stage animals, respectively. The hyp7 nuclei in the *sy5506* animals fail to migrate and are located in the dorsal region (marked with vertical lines). Scale bar is 10 µm. (D) Open reading frame of *Cbr-unc-84*. *sy5506* causes a 403-bp deletion.

■ Table 5 Vulval induction pattern in Class 2 and 3 mutants

Class	Genotype	VPC Induction Score	% VPC Fate Pattern (F/3°/I)						n
			P3.p	P4.p	P5.p	P6.p	P7.p	P8.p	
2	AF16	3	61/39/0	0/100/0	0/0/100	0/0/100	0/0/100	0/100/0	101
	<i>unc(sy5505)</i>	1.7 ± 1.3	39/4/0	0/35/0	0/0/50	0/0/75	0/0/48	2/37/0	52
	<i>sy5505; bhEx141</i>	1.2 ± 1.2	25/2/00	8/8/00	0/0/31	0/0/62	0/0/31	4/13/0	52
	<i>sy5505; bhEx142</i>	1.4 ± 1.1	24/4/0	2/18/0	0/0/38	0/0/62	0/0/38	4/11/0	45
	<i>Cbr-unc-84(sy5506)</i>	1.9 ± 1.2	31/14/0	10/18/0	0/0/53	0/0/82	0/0/51	14/25/0	51
	<i>sy5506; bhEx139</i>	2.9 ± 0.4 ^a	54/30/0	0/86/0	0/0/96	0/0/100	0/0/94	0/93/0	91
	<i>sy5506; bhEx152</i>	2.9 ± 0.4 ^a	57/31/0	2/90/0	0/0/94	0/0/100	0/0/96	0/94/0	51
3	<i>lin(bh7)</i>	2.3 ± 1	77/23/0	54/46/0	28/4/68	5/0/95	32/2/66	43/57/0	56
	<i>lin(bh14)</i>	2.3 ± 1	91/9/0	71/29/0	35/0/65	1/0/99	33/0/67	65/35/0	78
	<i>Cbr-lin-39(bh20)</i>	0.2 ± 0.4	100/0/0	100/0/0	100/0/0	85/0/15	100/0/0	100/0/0	155
	<i>bh20; bhEx134</i>	1 ± 0.9 ^a	100/0/0	97/3/0	93/0/7	40/0/60	71/0/29	99/1/0	88
	<i>bh20; bhEx132</i>	0.5 ± 0.5 ^a	100/0/0	100/0/0	99/0/1	54/0/46	100/0/0	100/0/0	81
	<i>Cbr-lin-39(bh23)</i>	0	96/4/0	96/4/0	88/12/0	96/4/0	96/4/0	100/0/0	50

VPC fates are classified into three categories: F, fused with *hyp7* without division, 3°, fused with *hyp7* after one cell division, I, induced (either 1°, 2°, or a hybrid fate that could not be uniquely classified). See Materials and Methods for details. For *sy5505* and *sy5506* animals missing VPCs were excluded from the analysis. VPC, vulval precursor cells.

^aVPC induction is significantly higher compared to the parental strain, $P < 0.0001$.

unable to adopt an induced fate. In *C. elegans*, AC is necessary for VPC induction because it secretes LIN-3/EGF ligand that activates the LET-23/EGFR-LET-60/RAS-MPK-1/MAPK pathway in VPCs (Hill and Sternberg 1992; Kimble 1981). To this end, we ablated the central VPC, *i.e.*, P6.p, during the L2 stage and examined the fates of the remaining VPCs. We predicted that P5.p and P7.p would receive greater levels of AC signal, perhaps triggering VPC induction. In wild-type animals, P6.p ablation causes full induction of P5.p and P7.p, whereas P4.p and P8.p adopt vulval fates in some cases (Table 7). In our experiment, *bh7* animals exhibited an induction pattern similar to AF16. Thus, P5.p and P7.p were induced in all cases (Table 7) compared with intact *bh7* animals in Table 5). The frequencies of induced VPCs were much lower in *bh14* animals (Table 7). In total, five of nine animals had some vulval tissue as a result of P5.p and P7.p induction (P5.p adopted 1° fate in three cases and P7.p in the remaining two). Only one of these animals had induction of both P5.p and

P7.p (P5.p 1° and P7.p 2°). The remaining VPCs adopted an 'F' fate. Similar manipulations in *bh20* animals also caused P5.p and P7.p to be induced, albeit rarely (Table 7). Of the 19 cases, 4 had few vulval progeny. In two of these, P5.p appeared to adopt a 1°-like fate (no P7.p induction), whereas the other two had a hybrid 1°/2° lineage. This result is in contrast to intact *bh20* animals in which P5.p and P7.p are never induced (Table 5). Taken together, these results suggest that in the absence of the central P6.p, the neighboring VPCs in these three mutants can be induced by the AC-mediated signal, and they can give rise to vulval tissue.

Overexpression of *lin-3* suppresses the VPC induction defect in a subset of class 3 mutants

In *C. elegans*, LIN-3 signaling plays a role in maintaining the competence of VPCs by preventing their fusion with *hyp7* (Myers and Greenwald 2007). This allows unfused VPCs to initiate Ras-MAPK

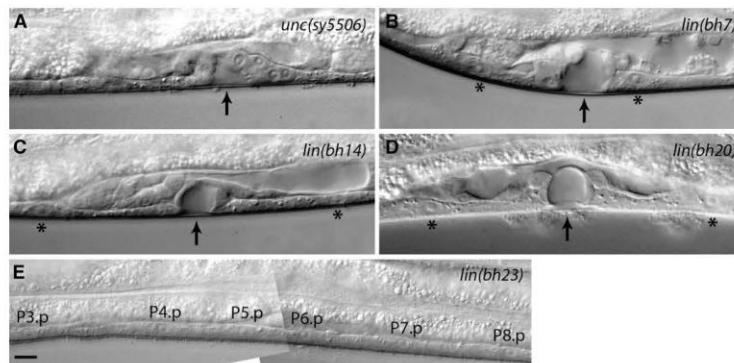


Figure 3 Vulva phenotypes of class 2 and 3 mutants. Arrows point to the center of invagination. Animals were examined at the mid-L4 stage. (A) Fewer VPCs are present in *sy5506* animals due to a defect in P-cell nuclear migration. In this case P6.p and P7.p are induced to form the vulva. P5.p and P8.p are missing. (B) One or more VPCs in *bh7* animals remain uninduced. In this example, P5.p and P6.p are induced. P4.p and P7.p have adopted an F fate (asterisks). (C, D) *bh14* and *bh20* animals showing a similar vulval morphology defect. In both cases invagination is formed by P6.p progeny, whereas P5.p and P7.p have adopted an F fate (asterisks). (E) A *bh23* animal showing no vulval induction. All VPCs have adopted an F fate. Scale bar is 10 μ m.

■ Table 6 Vulval cell lineage analysis of class 3 and 4 mutants

Genotype	VPCs						n	
	P3.p	P4.p	P5.p	P6.p	P7.p	P8.p		
<i>AF16</i>	S/SS	SS	<u>LLTN</u>	TTTT	<u>NTLL</u>	SS	>50	
<i>lin(bh7)</i>	SS	SS	<u>LLTN</u>	TTTT	<u>NTLL</u>	SS	4	
	S	SS	<u>LLTN</u>	TTTT	<u>NTLL</u>	SS	1	
	S	S	S	TTTT	<u>NTLL</u>	SS	1	
	S	SS	<u>LLTN</u>	TTTT	<u>NTLL</u>	OOLL	1	
	S	S	SS	TTTT	<u>NTLL</u>	SS	1	
	S	SS	<u>LLTN</u>	TOOT	S	SS	1	
	S	S	S	TTTT	S	S	1	
	<i>lin(bh14)</i>	S	S	S	TTTT	OTLL	S	1
		S	S	<u>LLTN</u>	TTTT	<u>NTLL</u>	S	2
		S	S	<u>LLTN</u>	TTTT	<u>NTLL</u>	SS	1
S		S	S	TTTT	S	S	2	
S		SS	<u>NTOL</u>	TTTT	S	S	1	
S		S	S	OOTT	S	S	1	
S		S	S	TTTT	S	S	1	
S		S	<u>LLTN</u>	TTTT	S	S	2	
<i>lin(bh20)</i>		S	S	S	S	S	S	13
		S	S	S	TTTT	S	S	3
	S	S	S	Oooo	S	S	1	
	S	S	S	TTTT	S	S	1	
	S	S	S	OOTT	S	S	1	
<i>lin(bh23)</i>	S	S	S	S	S	S	12	
<i>lin(sy5336)</i>	SS	SS	<u>LLLL</u>	LTTT	<u>LLLL</u>	SS	2	
	SS	SS	<u>LLLL</u>	ODTO	<u>LLLL</u>	SS	1	
	S	SS	<u>LLLL</u>	Oooo	<u>LLLL</u>	SS	1	
	SS	SS	<u>LLLL</u>	OOTO	<u>LLLL</u>	SS	1	
	S	SS	<u>LLLL</u>	OTOT	<u>LLLL</u>	SS	1	

Cells attached to the cuticle are underlined. D, division plane not observed; L, longitudinal; O, oblique; N, no cell division; n, number of animals scored; S, cell fused with syncytium; T, transverse plane of cell division.

signaling to promote vulval induction. A similar mechanism could operate in *C. briggsae* as well, which would be consistent with the results of our aforementioned cell ablation experiments in which P5.p and P7.p often were induced in the absence of P6.p, possibly by responding to a greater level of gonad-derived signal. To test this directly, we monitored the effect of increased doses of LIN-3/EGF on VPC induction in *bh7*, *bh14*, and *bh20* animals. A *C. elegans lin-3* transgene under the control of a heat shock promoter was introduced in *C. briggsae*. This transgene was previously used in *C. elegans* and causes a *Muv* phenotype (Katz *et al.* 1995). Heat shocks given during early stages (0-18 hr post-L1) and late stages (30 hr post-L1 and beyond) had no effect on vulval development (Figure 4A and data not shown). However, 20-28 hr post-L1, animals (VPC one-cell stage, Pn.p) developed a *Muv* phenotype when subjected to heat shock (Figure 4A). The *Muv* penetrance was highest at the 24 hr post-L1 time point (58%, see Figure 4A, AC visible in all cases at the time of heat shock), which corresponds to the late-L2/early-L3 stage and precedes the division of dorsal uterine precursors. All VPCs were in-

duced, although P3.p appeared to be somewhat refractory in this assay (Figure 4C).

Next, we examined the effect of *lin-3* overexpression in *bh7*, *bh14* and *bh20* animals. Heat shocks at the 24 hr post-L1 time point induced a *Muv* phenotype in *bh7* animals similar to the control (Figure 4B). The *bh14* animals showed a similar but reduced response (Figure 4B). In contrast, no *Muv* phenotype was observed in *bh20* animals (Figure 4B). Examination of cell fates revealed that greater doses of LIN-3 induced VPCs in all 3 genetic backgrounds, including *bh20* in which P6.p was threefold more likely to be induced compared to the control (Figure 4C). These results show that increased VPC induction in class 3 mutants is most likely caused by the activation of a pathway homologous to LIN-3/EGF signaling in *C. elegans*.

Class 3 mutations *bh20* and *bh23* are alleles of *Cbr-lin-39*

The cell fusion defect in class 3 mutants was similar to that of *C. elegans* with mutant Hox gene *lin-39* alleles that cause P(3-8).p cells to

■ Table 7 Effect of cell ablations on VPC fates in class 3 mutants

Genotype	VPC Fate (Induced/Uninduced)						n
	P3.p	P4.p	P5.p	P6.p	P7.p	P8.p	
<i>mfts5(egl-17::gfp)</i>	0/100	30/70	100/0	x	100/0	70/30	10
<i>lin(bh7)</i>	0/100	67/33	100/0	x	100/0	17/83	6
<i>lin(bh14)</i>	0/100	0/100	33/67	x	22/78	0/100	9
<i>lin(bh20)</i>	0/100	0/100	x	x	100/0	0/100	1
	0/100	0/100	15/85	x	5/95	0/100	19

'x' denotes VPCs that were ablated during the early-L2 stage. See Table 5 for a description of VPC fates. Uninduced refers to F and 3rd fates, n, number of animals scored; VPC, vulval precursor cells.

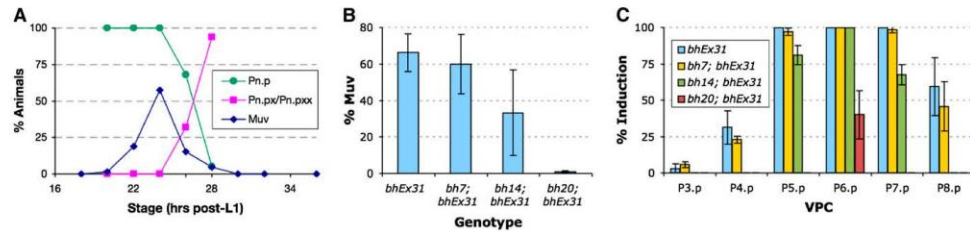


Figure 4 Effect of *lin-3* overexpression on VPC induction in class 3 mutants. The *bhEx31* transgenic strain carries a *hs::lin-3* plasmid from *C. elegans* (see *Materials and Methods* for details). (A) The graph shows the proportion of Pn.p (1-cell stage), Pn.px (2-cell stage), and Pn.pxx (4-cell stage) *bhEx31* animals at different time points of development (green and pink lines). The heat shock-induced Muv phenotype of *bhEx31* is also plotted (blue line). Almost 60% of animals, when subjected to heat shock at 24 hr after L1, develop a Muv phenotype. The Muv penetrance decreases rapidly after the VPCs start to divide such that by 30 hr, when all VPCs have divided, heat shock has no effect on VPC induction (no Muv phenotype develops). Pn.p and progeny stages were determined from a total of 16 to 20 animals for each time point. For Muv penetrance analysis, each time point contained (starting from the L1+18 hr stage) 25, 63, 328, 118, 300, 214, 86, 25, and 81 animals, respectively. (B) The graph shows the Muv phenotype in mutants after the heat shock at 24 hr. The Muv frequency in *bh7* animals is similar to the control (*bhEx31*), slightly reduced in *bh14*, and not present in *bh20* animals. The number of animals examined in each case was 154 (control), 50 (*bh7*), 159 (*bh14*), and 112 (*bh20*). (C) The pattern of VPC induction in animals plotted in graph B. Although all VPCs can be induced in the control and *bh7* to varying extents, only the central 3, P(5-7).p, do so in *bh14*, and only one (P6.p) is induced in *bh20* animals. For each genotype, we examined 32 (control), 70 (*bh7*), 37 (*bh14*), and 95 (*bh20*) animals.

fuse to surrounding hypodermis (Clark *et al.* 1993). Therefore, we wanted to determine whether any of these are alleles of *Cbr-lin-39*. Using Indel mapping, we had earlier placed *lin(bh20)* on the right arm of chromosome 3 (Koboldt *et al.* 2010). This region includes *C. elegans lin-39* ortholog (<http://www.wormbase.org>). Therefore, we took a candidate gene approach and sequenced the exonic regions of *Cbr-lin-39* in *bh20* animals. A single point mutation (G9427 to A) was found that is predicted to replace a conserved arginine (R) with glutamine (Q) at position 169 in the homeodomain region (Figure 5A). Considering that *lin(bh23)* animals show a similar but more severe VPC induction defect, we suspected that this could be another allele of *Cbr-lin-39*. Sequencing of the *Cbr-lin-39* region in this strain identified a 364 bp deletion affecting the promoter and translational start site (Figure 5A).

We also carried out a transgene rescue experiment for *lin(bh20)* animals using a *C. elegans lin-39*-rescuing genomic DNA clone. Examination of transgenic animals revealed a rescue of the VPC competence defect in both cases (Table 5). The *Egl* defect also was rescued in these lines (animals laying eggs: *bhEx132* 83%, $n = 29$ and *bhEx134* 24%, $n = 124$; compared with 4% in *bh20* alone, $n = 140$).

Pn.p cells lack competence and are irregularly placed in *Cbr-lin-39* mutants

In *C. elegans*, *lin-39* acts at multiple times during vulval development. In the L1 and L2 stages, it prevents Pn.p cells from fusing to hyp7 (Clark *et al.* 1993). Later on in stage L3, it is up-regulated by Ras signaling to promote vulval induction (Malooof and Kenyon 1998). To determine whether *Cbr-lin-39* mutants cause cell fusion defects in *C. briggsae*, we used a junction-associated marker *dlg-1::GFP* (Seetharaman *et al.* 2010). In wild-type *AF16*, P(3-8).p remain unfused in the late-L1 and L2 stages and become competent to form the vulval tissue (Figure 5B). In the majority of *bh20* animals, the corresponding cells were fused by early-to-mid-L2 stage (60.7%, $n = 28$). In the remaining cases, one or two Pn.p cells were protected (P5.p and P6.p 21.4% and P6.p alone 17.8%, $n = 28$; Figure 5C). The proportion of animals with unfused cells was much lower at later stages and was limited to P6.p (mid-L3 stage: P6.p 30.8%, $n = 13$; L4 stage: P6.p 12.5%, $n = 24$).

As it has been previously reported that the spacing of Pn.p cells in the ventral hypodermis is less regular in *C. elegans lin-39* mutants (Clark *et al.* 1993), we measured VPC spacing in *Cbr-lin-39* animals. Our results agreed with the findings in *C. elegans* and revealed that both *Cbr-lin-39* alleles cause greater variability in VPC placement (Figure 5, D and E). Although all inter-VPC distances were affected, the phenotype was most pronounced in the P6.p-P7.p pair. Interestingly, the P5.p-P6.p pair in *C. briggsae* showed the reverse of *C. elegans*.

bh20 is epistatic to *Cbr-pry-1(sy5353)*

We recently demonstrated a conserved role for *pry-1*-mediated Wnt signaling in 2° VPC fate specification (Seetharaman *et al.* 2010). In *Cbr-pry-1*, animals P5.p and P6.p are always induced, but P7.p often is not (Figure 5F). The inability of P7.p to contribute to vulval tissue is likely due to a change in cell fate as judged by its small nucleus and P12pa-like appearance. *Cbr-pry-1* mutants also exhibit ectopic induction of P3.p and P4.p and to some extent P8.p, resulting in the formation of multiple ventral protrusions (pseudovulvae). Thus, both a lack of induction (P7.p) and excessive induction phenotypes are observed in *Cbr-pry-1* animals.

Given that *lin-39* acts genetically downstream of *pry-1* in *C. elegans* (Gleason *et al.* 2002), we examined the genetic interaction of *Cbr-lin-39* with *Cbr-pry-1*. As expected, *Cbr-lin-39(bh20)* suppressed the increased induction phenotype of *Cbr-pry-1(sy5353)*. Ectopic vulval induction was inhibited due to VPCs frequently adopting F fates ($n = 42$; P6.p was induced in 24% cases; Figure 5G). However, the small nucleus phenotype of P7.p, P8.p, and P11.p was not suppressed by *bh20* (Figure 5G and data not shown). Therefore, one of the following may be true: either the residual activity of *Cbr-lin-39* in *bh20* animals is greater than the threshold needed for VPC size specification or *Cbr-lin-39* mediates only a subset of *Cbr-pry-1* function.

Class 4 mutations affect vulval invagination and morphology

This class consists of seven mutants, all of which have defective vulval morphology (Table 8). Microscopic observations revealed that the

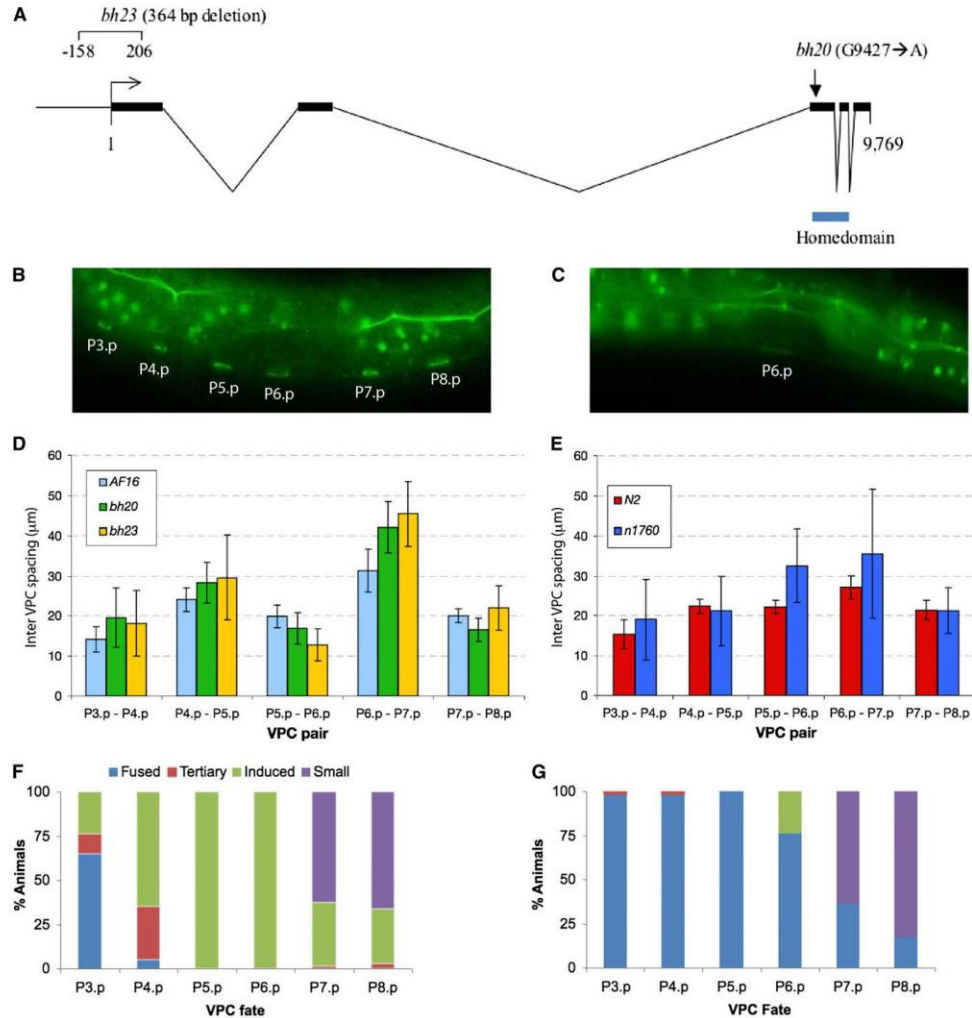


Figure 5 Genomic organization and mutant phenotypes of *lin-39*. (A) *C. briggsae lin-39* open reading frame. Exons are represented by thick lines. The positions of the homeodomain and two mutations are shown. (B, C) Unfused VPCs revealed by *dgl-1::GFP* expression. (B) Wild-type AF16 and (C) *bh20* L2 stage animals. In this *bh20* animal only P6.p ring is visible. (D, E) Inter-VPC spacing in *lin-39* alleles in *C. elegans* and *C. briggsae*. VPCs are irregularly spaced in mutants, which is reflected in greater SDs. (F, G) Excessive induction of VPC phenotype in *sy5353* animals is suppressed by *bh20*. (F) *sy5353* and (G) *bh20; sy5353* double mutant. VPC fates are shown as Fused, 3°, induced (1° and 2°) and small (P12.pa-like).

animals have the correct number of VPCs and their progeny but the cells fail to invaginate correctly (Figure 6). In addition to the *Egl* phenotype, the adults exhibit a *Pvl* phenotype (Table 8). Complementation and mapping experiments revealed a total of five loci, three of which are located on chromosome 1 with the others on chromosome 5 and the X chromosome (Table 3). Two of the chromosome 1 genes

have additional alleles (*bh13* and *sy5197* on the left arm, *sy5336* and *sy5368* close to the center).

The *sy5336* and *sy5368* mutations cause a fully penetrant *Egl* phenotype. A distinctive feature of these animals, with regards to egg laying, is rudimentary vulval invagination and defects in the connection of the vulva to the uterus (Figure 6B). The analysis of VPC

■ Table 8 Vulval morphology defects in class 4 mutants

Gene	Allele	Abnormal Vulval Morphology	Pvl
<i>lin(bh13)</i>	<i>bh13</i>	71% (69)	29% (110)
	<i>sy5197</i>	51% (39)	ND
<i>lin(bh25)</i>	<i>bh25</i>	47% (36)	7.4% (148)
<i>lin(bh26)</i>	<i>bh26</i>	86% (51)	51.8% (110)
<i>lin(sy5425)</i>	<i>sy5425</i>	83% (35)	17.9% (95)
<i>lin(sy5336)</i>	<i>sy5336</i>	100% (100)	83.9% (152)
	<i>sy5368</i>	100% (100)	51.2% (162)

Number of animals scored are shown inside parentheses. ND, not done; Pvl, protruding vulva.

lineages revealed errors in cell divisions and adherence properties of some of the 2° lineage cells (Table 6). Other phenotypes included low brood size (*sy5336*: 21 ± 5 , $n = 11$; *sy5368*: 10 ± 2 , $n = 12$) and defective mating. The hermaphrodites are unable to mate at all, whereas males can mate, although very poorly (data not shown).

The *bh13* and *sy5197* animals are small and mildly sluggish. Some also have abnormally folded gonad arms. These phenotypes accompany *Egl* and vulval invagination defects in both outcrossed strains (Tables 4 and 8, Figure 6C), suggesting they are linked to a single gene. We looked at the vulval morphology in L4 stage animals and found that the 1° lineage cell nuclei are abnormally placed. In addition, the utse cannot be clearly observed in these animals (Figure 6C). A combination of the vulva and utse defects appears to cause a physical block in the egg-laying passage.

The vulval morphology defect in *bh26* animals shares some similarity with that of *bh13* animals (Figure 6D compared with Figure 6C). Specifically, the nuclei of the 1° lineage cells fail to migrate correctly, thereby blocking the connection between the vulva and the uterus. We also observed defects in the migration of the AC and a lack of utse (Figure 6D). Other defects included abnormal gonad arms and sterility.

The remaining two class 4 mutants, *lin(bh25)* and *lin(sy5425)*, have weaker *Egl* and Pvl phenotypes compared with others in this category (Table 8). In both cases, vulval cells invaginate and form finger-like structures, but the overall morphology is abnormal (Figure 6, E and F). The penetrance of the vulval defect is greater in *sy5425* compared with *bh25*, although an opposite trend was observed for the *Egl* phenotype. We also noted that the utse is somewhat thicker in *bh25* animals (Figure 6E), although its contribution to the *Egl* phenotype is unclear. Interestingly, some *sy5425* animals showed ectopic P4.p and P8.p induction. This phenotype is present in the outcrossed strain, so it is either caused by the same mutation or another very closely linked mutation. More work is needed to distinguish between these two possibilities. We also observed significant embryonic and early larval lethality in the *sy5425* strain (18%, $n = 284$).

***Cbr-lin-11* mutations disrupt vulva and utse morphogenesis**

The vulva and utse defects of *lin(sy5336)* and *lin(sy5368)* animals strongly resemble those of *C. elegans lin-11* mutants (Ferguson *et al.* 1987; Newman *et al.* 1999). In addition, the thermotaxis defect of the animals is also similar [(Hobert *et al.* 1998) Figure 7B], which is reflected in their lack of preference to the cultivation temperature. Therefore, we carried out transgene rescue experiments to examine whether these two lines carry mutant alleles of *Cbr-lin-11*. Stable lines carrying a 19-kb genomic clone of *C. elegans lin-11* (*bhEx78* and *bhEx148*, on the *sy5336* genetic background) showed rescue of the vulva, utse, and *Egl* defects (*bhEx78*: 47% wild-type vulva and utse,

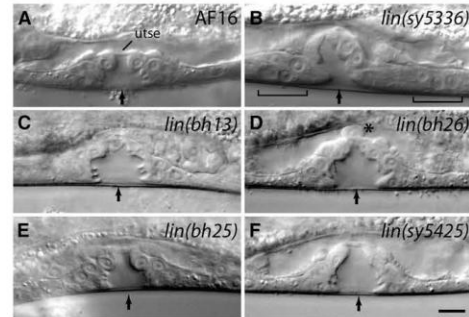


Figure 6 Vulval morphology defects in class 4 mutants. Animals were examined at mid-L4 stage. Arrows mark the center of invagination. (A) Wild type. The utse is visible as a thin line above the vulva. (B) The 2° lineage vulval cells fail to invaginate (shown by brackets). The utse cannot be clearly identified. (C, D) The vulval opening is blocked due to a failure in the migration of the 1° lineage cells. (E, F) Vulval invagination is abnormal. In addition, the utse in a *bh25* animal (E) is thicker compared with the wild type. Scale bar is 10 μ m.

$n = 32$, non-*Egl* 8%, $n = 25$; *bhEx148*: 71% wild-type vulva and utse, $n = 31$, non-*Egl* 12.5%, $n = 48$; compared with *Cbr-lin-11* mutants in Table 8). We also sequenced the *Cbr-lin-11* locus in both alleles and identified molecular changes that are predicted to disrupt splicing in the homeobox region (Figure 7A, also see *Materials and Methods*).

The aforementioned rescue experiments demonstrate that *C. elegans lin-11* can substitute for *Cbr-lin-11* function in *C. briggsae* and suggest that *lin-11* function is evolutionarily conserved. This is also supported by the analysis of the cDNA and protein sequences. The *lin-11* cDNA (*C. elegans*: 1218 bp, 10 exons; *C. briggsae*: 1239 bp, 10 exons) (see Figure S3 for *C. briggsae* sequence) is 80% conserved, and the corresponding proteins are 87% identical (94% similar).

To examine the vulval defect in *Cbr-lin-11* animals, we used the two GFP-based markers *Cbr-egl-17* (*mfls5*) and *Cbr-zmp-1* (*mfls8*). In *C. elegans*, *egl-17* and *zmp-1* have been used extensively in cell fate specification studies (Cui and Han 2003; Gupta *et al.* 2003; Inoue *et al.* 2002). The dissection of the regulatory regions of these genes has revealed evolutionarily conserved sequences (Kirouac and Sternberg 2003). In the wild-type *C. briggsae*, the earliest expression of *Cbr-egl-17::gfp* is observed in mid/late-L4 stage animals in the presumptive vulC and vulD (Seetharaman *et al.* 2010). In the case of *Cbr-zmp-1::gfp*, GFP fluorescence is primarily observed in the presumptive vulE (Seetharaman *et al.* 2010). We found that the expression of both markers was absent in *Cbr-lin-11(sy5336)* animals (Table 9). This result supports our previous findings and a crucial role of *lin-11* in vulval cell differentiation (Gupta *et al.* 2003).

Despite the high conservation in *lin-11* sequence and function, we did observe an interesting difference in the AC placement between the two species. Unlike *C. elegans lin-11* animals, in which ACs fail to migrate and are located on the vulval apex in most animals (*h389*: 81.1%, $n = 53$; Figure 7C), no such phenotype was observed in *C. briggsae* (*sy5336*: 0%, $n = 47$ and *sy5368*: 0%, $n = 52$; Figure 7D).

DISCUSSION

We report the isolation and characterization of mutations in 13 genes in *C. briggsae* that are involved in the development and function of the

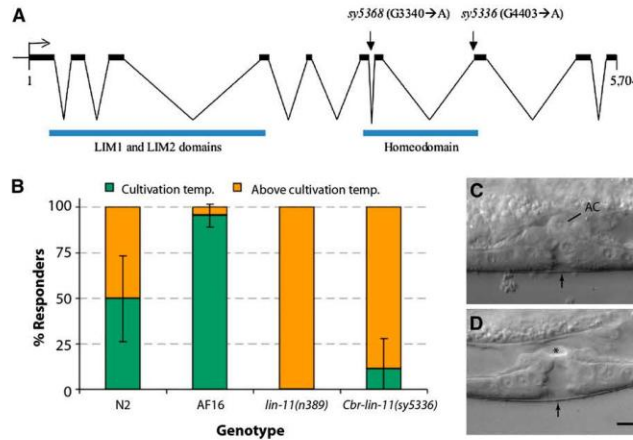


Figure 7 Genomic organization of *Cbr-lin-11* and mutant phenotypes. (A) *Cbr-lin-11* open reading frame showing LIM and homeodomain regions as well as mutations. Both alleles affect the homeodomain region. (B) Graph shows the thermotaxis response of the wild-type and *lin-11* animals. Wild-type animals prefer to live near the temperature at which they were initially grown, whereas *lin-11* animals do not demonstrate such behavior. Instead, they are thermophilic. (C) *lin-11*(n389). The AC is located at the vulval apex. (D) *Cbr-lin-11*(*sy5336*). No AC can be observed at the corresponding location (asterisk). Scale bar in C and D is 10 μ m.

egg-laying system. To date, this is the largest set of genes identified by a forward genetics approach in this species. Ten of these genes are involved in various steps of vulval development (Figure 8). Transgene rescue and molecular analyses have revealed that three genes are orthologs of *unc-84*, *lin-39*, and *lin-11*. Together, these mutant strains serve as valuable tools for comparative and evolutionary studies. Another genetic screen in *C. briggsae* was previously carried out to identify dauer pathway genes (Inoue *et al.* 2007). The screen identified several mutations, including alleles of *Cbr-daf-2* (insulin receptor), *Cbr-daf-3* (Smad), and *Cbr-daf-4* (TGF- β family receptor). Genetic studies revealed that although the functions of *C. elegans* orthologs are conserved in *C. briggsae*, the two species exhibit differences in their temperature sensitivities. Thus, comparative genetics approaches are useful for revealing the similarities and differences in biological processes between *C. elegans* and *C. briggsae*.

Egl phenotype-based genetic screens were first carried out in *C. elegans* and led to the identification of many genes involved in vulval development (Ferguson and Horvitz 1985; Trent *et al.* 1983). Characterization of their function revealed a genetic pathway for the formation of the vulva (Ferguson *et al.* 1987). During the past decade and a half, this knowledge has been extended to other distant species, such as *P. pacificus* and *O. tipulae*, resulting in a better understanding of the evolutionary changes in the mechanism of vulva formation. Screens in *O. tipulae* have identified several mutations affecting vulva formation. Although the majority of these cause defects in VPC division and competence (Dichtel *et al.* 2001; Louvet-Vallee *et al.* 2003), others affecting vulva centering and hyper- and hypo-induced phenotypes also have been identified (Dichtel *et al.* 2001). Similar mutant classes have been found in *P. pacificus* screens as well (Eizinger *et al.* 1999; Sommer 2005). Compared with *C. elegans*, the phenotypic spectrum in these two species is quite different. For example, mutations affecting P.n.p fate (e.g., 1 $^\circ$ converted to 2 $^\circ$ or 3 $^\circ$) were recovered quite frequently in *C. elegans* but not in *O. tipulae* or *P. pacificus*. Interestingly, our screens in *C. briggsae* also revealed differences from *C. elegans*. We did not find P.n.p fate mutants, and one-half of the mutants examined show defects in cell invagination and morphogenesis (Table 8, Figure 8). It is not clear whether this phenotypic distribution is typical in *C. briggsae* or whether it results from the lack of saturation in the screen or another reason. It is worth pointing out that in our experience, Egl

animals in *C. briggsae* are more difficult to identify in a standard F2 screen in the presence of predominantly non-Egl worms. This may be at least partly caused by the tendency of *C. briggsae* to retain fewer eggs in the uterus compared to *C. elegans* (B. P. Gupta, unpublished results; T. Inoue and M. A. Felix, personal communications). The difficulty in isolating Egl's could have limited the recovery of vulva-specific mutants and the phenotypic classes in our screens. Future genetic screens using different approaches will help to address this issue. Furthermore, combining a vulva-specific GFP reporter with an Egl phenotype may be a useful approach, as it will minimize the recovery of non-vulval mutations.

Phenotypic classes recovered in our screen

We have isolated four phenotypic classes of worms, all of which affect egg laying. Mutations in one of these (class 1) have normal vulva and uterine morphologies. To investigate the role of sex muscles and HSNs, we used serotonin and fluoxetine drugs to induce egg laying. *sy5395* mutants showed a mild but obvious increase in egg laying in response to serotonin, suggesting that the muscle function is intact. However, *bh2* and *bh21* did not respond to any of the drugs, suggesting that muscle function may be impaired.

The class 2 mutations *sy5505* and *sy5506* affect nuclear migration in a temperature-dependent manner. Both alleles cause animals to develop Egl and Unc phenotypes due to the failure of P nuclei to migrate into the ventral cord region. The phenotype of *unc*(*sy5506*) animals can be rescued by a *C. elegans unc-84* transgene, suggesting that *sy5506* is an allele of *Cbr-unc-84*. This conclusion is also supported by our mapping and allele sequencing data. The remaining two classes of mutations alter the number of vulval progeny and vulval invagination. *Cbr-lin-39* is required for the maintenance of VPC competence and appears to act

Table 9 Expression of vulval cell fate markers in *Cbr-lin-11* mutants

Genotype	GFP Fluorescence in Vulval Progeny	n
<i>mfls5</i> (<i>egl-17::gfp</i>)	vulC: 79%, vulC and vulD: 21%	113
<i>sy5336; mfls5</i>	None	104
<i>mfls8</i> (<i>zmp-1::gfp</i>)	vulA: 2%, vulE: 91%, vulA and vulE: 7%	128
<i>sy5336; mfls8</i>	None	61

GFP, green fluorescent protein; n, number of animals scored.

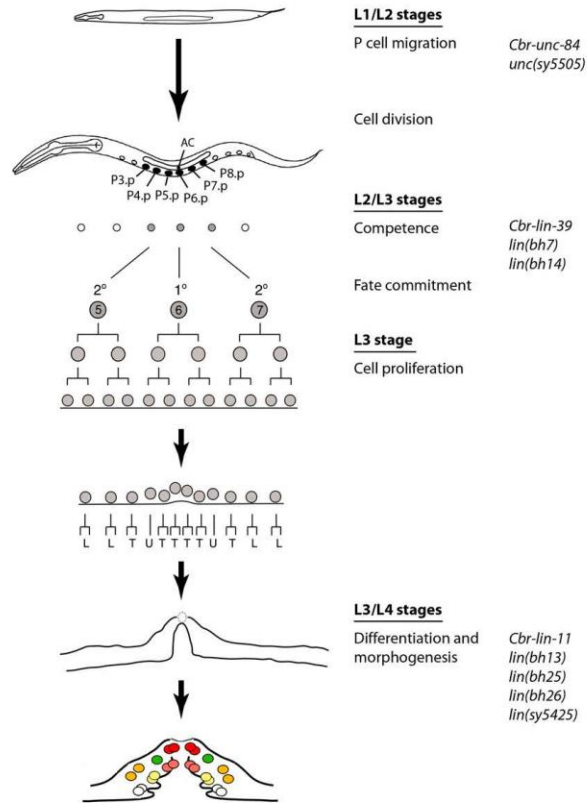


Figure 8 Vulval development in *C. briggsae* and the proposed roles of genes described in this study. P-cell migration into the ventral hypodermal region is mediated by the class 2 genes. Subsequently, P cells divide, and six of their posterior daughters (Pn.p, n = 3–8), termed VPCs, become capable of giving rise to the vulval tissue. Their competence appears to be regulated by the class 3 genes. VPC progeny differentiate and undergo morphogenetic changes during the L3 and L4 stages. The class 4 genes are required in these processes.

downstream of *Cbr-pry-1/axin*-mediated Wnt signaling, *Cbr-lin-11* controls vulval cell differentiation and tissue morphogenesis. Both genes belong to conserved families of transcription factors (the *Dfd/Scr*-related Hox family and the *LIM-Hox* family, respectively).

Nuclear migration in *C. briggsae* is mediated by a conserved SUN domain protein

Nuclear migration plays important roles in diverse cellular processes, including cell division, cell polarity and cell migration. In *C. elegans*, well-studied nuclear migration events are observed with the *hyp7* syncytium (dorsal side of the hypodermis) and a set of hypodermal blast cells (P cells) that form the vulva. Genetic analysis of these events has revealed that UNC-83 (KASH domain) and UNC-84 (SUN domain) proteins form a bridge-like structure to connect the nucleus to microtubules, motor proteins, and other cytoskeletal components. The movement of Kinesin and Dynein motors in a coordinated manner causes the nucleus to move in a specific direction. The vulval defects in *C. briggsae* *sy5505* and *sy5506* animals are typical of *unc-83* and *unc-84* mutants. Both alleles exhibit a temperature-sensitive phenotype and display *Egl* and *Unc* phenotypes. The phenotypes of *sy5506* animals can be efficiently rescued by a *C. elegans unc-84* genomic clone,

which demonstrates that *unc-84* plays a conserved role in nuclear migration in both species.

Genes affecting cell fusion in *C. briggsae*

We isolated two alleles of *Cbr-lin-39*, both of which prevent VPC induction. In *C. elegans*, P(3–8).p escape fusion in the L1 and L2 stages and remain competent to respond to induction during the L3 stage (Sternberg 2005). This process is regulated by *lin-39* (Clark *et al.* 1993). The expression of *lin-39* at the L2 stage appears to be partly controlled by BAR-1/ β -catenin-mediated Wnt signaling because in *bar-1* mutants, *lin-39* expression in VPCs is reduced, resulting in fusion of some VPCs to the *hyp7* syncytium (Eisenmann *et al.* 1998). Our experiments on *Cbr-lin-39* suggest that the function of *lin-39* in VPC competence is conserved in *C. briggsae*. This finding is supported by the analysis of mutant phenotype, rescue experiments, cell fusion studies using the *dlg-1::GFP* marker, and genetic interaction with *Cbr-pry-1* (Axin family). Our previous results involving RNA interference-mediated knockdown of *Cbr-lin-39* (Seetharaman *et al.* 2010) also support these findings.

lin-39 orthologs also have been identified in *O. tipulae* and *P. pacificus*. *Oti-lin-39* appears to control VPC competence by

preventing fusion of Pn.p cells in the late-L1/early-L2 stages (Louvet-Vallee *et al.* 2003). However, the function of *Ppa-lin-39* appears to have diverged. In *Ppa-lin-39* mutants, VPCs undergo programmed cell death instead of fusing with the hypodermis (Eizinger and Sommer 1997). Taken together, these findings suggest that although *lin-39* function is conserved in *Caenorhabditis* and *Oscheius* species, it has acquired new roles in *Pristionchus*. In the future, analysis of the role of *lin-39* in additional nematode species will allow for a more detailed comparison of its roles in vulval development.

In addition to *Cbr-lin-39*, we have uncovered two other loci, *lin(bh7)* and *lin(bh14)*, that control VPC competence. The phenotype of both mutants is weaker than that of *bh20* animals, perhaps due to weak hypomorphic alleles. Alternatively, these genes may have some redundant function. More alleles are required to distinguish between these two possibilities. The induction of P5.p and P7.p in *bh7* and *bh14* animals is frequently affected. To test the induction potential of these two VPCs, we carried out two complementary experiments. We examined their pattern of division after ablation of P6.p. Furthermore, the effect of *lin-3* overexpression was investigated. We found that in the absence of P6.p, the P5.p and P7.p cells were induced to various extents, suggesting that these VPCs can respond to inductive signal. This conclusion is strongly supported by the *lin-3* dosage experiments. High doses of *lin-3* during the L2 stage caused ectopic VPC induction, resulting in a Muv phenotype. We can therefore conclude that class 3 genes interact with a LIN-3-like inductive signal to regulate VPC competence in *C. briggsae*.

***lin-11* is a key regulator of vulval morphogenesis**

lin-11 is a founding member of the LIM homeobox family of genes. Mutations in *lin-11* were originally isolated in genetic screens for worms that failed to lay eggs (Ferguson and Horvitz 1985). Subsequently, phenotypic analyses showed a wide range of defects affecting vulval morphology (Freyd *et al.* 1990; Gupta *et al.* 2003), utse formation (Newman *et al.* 1999), and neuronal differentiation (Hobert *et al.* 1998; Sarafi-Reinach *et al.* 2001). *C. briggsae lin-11* mutants exhibit defects in the egg-laying system similar to those observed in *C. elegans lin-11* animals. Thus, vulval cells fail to invaginate, and a functional connection between the vulva and the uterus is not established. These phenotypes can be rescued by a *C. elegans lin-11* genomic fragment, suggesting that *lin-11* regulatory and coding sequences are evolutionarily conserved. This supports our previous conclusions on the conservation of *lin-11* regulation by Wnt and LIN-12/Notch signaling pathways in the vulva and π cell differentiation (Marri and Gupta 2009).

Outside the reproductive system, *lin-11* also is involved in the differentiation of several olfactory and chemosensory neurons (Sarafi-Reinach *et al.* 2001). We have not yet characterized the neuronal role of *Cbr-lin-11* in detail, but we have found that *Cbr-lin-11* mutants have a thermotaxis defect similar to that reported in *C. elegans lin-11* animals. Thus, similar to the egg-laying system, the role of *lin-11* in thermosensory behavior is also conserved. The recovery of *Cbr-lin-11* alleles provides a unique opportunity to investigate the mechanism of cell differentiation in *C. briggsae* and *C. elegans*.

DSD in *C. briggsae* vulva formation

Kiontke *et al.* 2007 had earlier reported variations in several steps of vulva formation in Rhabditid species. These included changes in Pn.p cell competence, cell division pattern, and vulva position. The phenotypic analysis of *C. briggsae* vulva mutants and molecular cloning of the 3 loci in which the mutations are located has revealed DSD in homologous processes. We observed interesting differences in at least three cases. First, the P5.p-P6.p inter-VPC distance in *lin-39* mutants

tends to be lower in *C. briggsae* than in *C. elegans*. Second, *lin-39* does not interact with *pry-1* to enhance the small nuclear size phenotype of posterior Pn.p cells in *C. briggsae* as it does in *C. elegans* (Penigault and Felix 2011b). Finally, *Cbr-lin-11* animals do not show AC migration defects, which is one of the hallmarks of *lin-11* mutants in *C. elegans*. These results reveal the differences in developmental mechanisms that exist despite conservation of vulval morphology in these two species.

***C. briggsae* as a model for the study of vulval development**

C. briggsae is increasingly being used in comparative developmental and evolutionary studies. In recent years, a number of publications have described processes such as sex determination (Guo *et al.* 2009; Hill *et al.* 2006; Kelleher *et al.* 2008), dauer formation (Inoue *et al.* 2007), pheromone receptor signaling (McGrath *et al.* 2011), embryogenesis (Lin *et al.* 2009; Zhao *et al.* 2008), and vulva formation in *C. briggsae* (Felix 2007; Hoyos *et al.* 2011; Marri and Gupta 2009; Penigault and Felix 2011a; Seetharaman *et al.* 2010). The findings have revealed similarities and differences in developmental processes.

The analysis of the vulval precursor fates in *C. briggsae* has revealed the role of conserved signaling pathway genes such as Ras, Notch, and Wnt. However, a detailed examination of gene function and pathways could not be carried out due to the lack of mutations affecting specific steps in the vulval development process. The mutations described in this study represent the first systematic effort in *C. briggsae* to investigate the genetic basis of vulva formation. Future work is needed to reveal the mechanism of gene function and to further compare *C. briggsae* to *C. elegans*. The results will ultimately help clarify how distinct processes form almost identical vulval structures in these two species.

ACKNOWLEDGMENTS

We thank Takao Inoue and Shahla Gharib for isolating *lin-11* alleles, Veena Deekonda, Nayasta Ademmana, and Carly Ching for assistance in experiments, and Takao Inoue for critical comments. Two of the transgenic strains *mfls5* and *mfls8* were kindly provided by Marie-Anne Felix (Institut Jacques Monod). The genetic screens were carried out in the laboratory of Paul Sternberg. This work was supported by the Natural Sciences and Engineering Research Council Discovery grant to B.P.G. Work in the laboratory of D.G.M. was supported by Genome Canada, Genome British Columbia and the Canadian Institutes for Health Research.

LITERATURE CITED

- Antoshechkin, L., and P. W. Sternberg, 2007 The versatile worm: genetic and genomic resources for *Caenorhabditis elegans* research. *Nat. Rev. Genet.* 8: 518–532.
- Avery, L., and H. R. Horvitz, 1987 A cell that dies during wild-type *C. elegans* development can function as a neuron in a *ced-3* mutant. *Cell* 51: 1071–1078.
- Baldessarini, R. J., 1996 Drugs and the treatment of psychiatric disorders: antimanic and antidepressant agents, pp. 249–263 in *Goodman and Gilman's Pharmacological Basis of Therapeutics*, Ed. 12, edited by L. L. Brunton, B. A. Chabner, and B. C. Knollmann. McGraw-Hill, New York.
- Benian, G. M., S. W. L'Hernault, and M. E. Morris, 1993 Additional sequence complexity in the muscle gene, *unc-22*, and its encoded protein, twitchin, of *Caenorhabditis elegans*. *Genetics* 134: 1097–1104.
- Brenner, S., 1974 The genetics of *Caenorhabditis elegans*. *Genetics* 77: 71–94.
- Burdine, R. D., and M. J. Stern, 1996 Easy RNA isolation from *C. elegans*: a TRIZOL based method. *Worm Breed. Gaz.* 14: 10.
- Clark, S. G., A. D. Chisholm, and H. R. Horvitz, 1993 Control of cell fates in the central body region of *C. elegans* by the homeobox gene *lin-39*. *Cell* 74: 43–55.

- Croll, N. A., 1975 Indolealkylamines in the coordination of nematode behavioral activities. *Can. J. Zool.* 53: 894-903.
- Cui, M., and M. Han, 2003 Cis regulatory requirements for vulval cell-specific expression of the *Caenorhabditis elegans* fibroblast growth factor gene *egl-17*. *Dev. Biol.* 257: 104-116.
- Cutter, A. D., 2008 Divergence times in *Caenorhabditis* and *Drosophila* inferred from direct estimates of the neutral mutation rate. *Mol. Biol. Evol.* 25: 778-786.
- Delattre, M., and M. A. Felix, 2001 Polymorphism and evolution of vulval precursor cell lineages within two nematode genera, *Caenorhabditis* and *Oscheius*. *Curr. Biol.* 11: 631-643.
- Dempsey, C. M., S. M. Mackenzie, A. Gargus, G. Blanco, and J. Y. Sze, 2005 Serotonin (5HT), fluoxetine, imipramine and dopamine target distinct 5HT receptor signaling to modulate *Caenorhabditis elegans* egg-laying behavior. *Genetics* 169: 1425-1436.
- Dichtel, M. L., S. Louvet-Vallee, M. E. Viney, M. A. Felix, and P. W. Sternberg, 2001 Control of vulval cell division number in the nematode *Oscheius/Dolichorhabditis* sp. CEW1. *Genetics* 157: 183-197.
- Eisenmann, D. M., 2005 Wnt signaling (June 25, 2005). WormBook, ed. The *C. elegans* Research Community WormBook, doi/10.1895/wormbook.1.7.1, <http://www.wormbook.org>.
- Eisenmann, D. M., J. N. Maloof, J. S. Simske, C. Kenyon, and S. K. Kim, 1998 The beta-catenin homolog BAR-1 and LET-60 Ras coordinately regulate the Hox gene *lin-39* during *Caenorhabditis elegans* vulval development. *Development* 125: 3667-3680.
- Eizinger, A., and R. J. Sommer, 1997 The homeotic gene *lin-39* and the evolution of nematode epidermal cell fates. *Science* 278: 452-455.
- Eizinger, A., B. Jungblut, and R. J. Sommer, 1999 Evolutionary change in the functional specificity of genes. *Trends Genet.* 15: 197-202.
- Felix, M. A., 2007 Cryptic quantitative evolution of the vulva intercellular signaling network in *Caenorhabditis*. *Curr. Biol.* 17: 103-114.
- Felix, M. A., and P. W. Sternberg, 1997 Two nested gonadal inductions of the vulva in nematodes. *Development* 124: 253-259.
- Felix, M. A., P. De Ley, R. J. Sommer, L. Frisse, S. A. Nadler *et al.*, 2000 Evolution of vulva development in the Cephalobina (Nematoda). *Dev. Biol.* 221: 68-86.
- Ferguson, E. L., and H. R. Horvitz, 1985 Identification and characterization of 22 genes that affect the vulval cell lineages of the nematode *Caenorhabditis elegans*. *Genetics* 110: 17-72.
- Ferguson, E. L., P. W. Sternberg, and H. R. Horvitz, 1987 A genetic pathway for the specification of the vulval cell lineages of *Caenorhabditis elegans*. *Nature* 326: 259-267.
- Flibotte, S., M. L. Edgley, J. Maydan, J. Taylor, R. Zapf *et al.*, 2009 Rapid high resolution single nucleotide polymorphism-comparative genome hybridization mapping in *Caenorhabditis elegans*. *Genetics* 181: 33-37.
- Freyd, G., 1991 Molecular analysis of the *Caenorhabditis elegans* cell lineage gene *lin-11*. Ph.D. Thesis, Massachusetts Institute of Technology, Boston.
- Freyd, G., S. K. Kim, and H. R. Horvitz, 1990 Novel cysteine-rich motif and homeodomain in the product of the *Caenorhabditis elegans* cell lineage gene *lin-11*. *Nature* 344: 876-879.
- Gleason, J. E., H. C. Korswagen, and D. M. Eisenmann, 2002 Activation of Wnt signaling bypasses the requirement for RTK/Bas signaling during *C. elegans* vulval induction. *Genes Dev.* 16: 1281-1290.
- Gleason, J. E., E. A. Szyleyko, and D. M. Eisenmann, 2006 Multiple redundant Wnt signaling components function in two processes during *C. elegans* vulval development. *Dev. Biol.* 298: 442-457.
- Greenwald, I., 2005 LIN-12/Notch signaling in *C. elegans* (August 4, 2005). WormBook, ed. The *C. elegans* Research Community WormBook, doi/10.1895/wormbook.1.10.1, <http://www.wormbook.org>.
- Guo, Y., S. Lang, and R. E. Ellis, 2009 Independent recruitment of F box genes to regulate hermaphrodite development during nematode evolution. *Curr. Biol.* 19: 1853-1860.
- Gupta, B. P., and P. W. Sternberg, 2003 The draft genome sequence of the nematode *Caenorhabditis briggsae*, a companion to *C. elegans*. *Genome Biol.* 4: 238.
- Gupta, B. P., M. Wang, and P. W. Sternberg, 2003 The *C. elegans* LIM homeobox gene *lin-11* specifies multiple cell fates during vulval development. *Development* 130: 2589-2601.
- Gupta, B. P., J. Liu, B. J. Hwang, N. Moghal, and P. W. Sternberg, 2006 *lin-3* negatively regulates the LET-23/epidermal growth factor receptor-mediated vulval induction pathway in *Caenorhabditis elegans*. *Genetics* 174: 1315-1326.
- Gupta, B. P., R. Johnsen, and N. Chen, 2007 Genomics and biology of the nematode *Caenorhabditis briggsae* (May 3, 2007). WormBook, ed. The *C. elegans* Research Community WormBook, doi/10.1895/wormbook.1.10.1, <http://www.wormbook.org>.
- Hill, R. J., and P. W. Sternberg, 1992 The gene *lin-3* encodes an inductive signal for vulval development in *C. elegans*. *Nature* 358: 470-476.
- Hill, R. C., C. E. de Carvalho, J. Salogiannis, B. Schlager, D. Pilgrim *et al.*, 2006 Genetic flexibility in the convergent evolution of hermaphroditism in *Caenorhabditis* nematodes. *Dev. Cell* 10: 531-538.
- Hillier, L. W., R. D. Miller, S. E. Baird, A. Chinwalla, L. A. Fulton *et al.*, 2007 Comparison of *C. elegans* and *C. briggsae* genome sequences reveals extensive conservation of chromosome organization and synteny. *PLoS Biol.* 5: e167.
- Hobert, O., T. D'Alberti, Y. Liu, and G. Ruvkun, 1998 Control of neural development and function in a thermoregulatory network by the LIM homeobox gene *lin-11*. *J. Neurosci.* 18: 2084-2096.
- Horvitz, H. R., and J. E. Sulston, 1980 Isolation and genetic characterization of cell-lineage mutants of the nematode *Caenorhabditis elegans*. *Genetics* 96: 435-454.
- Horvitz, H. R., M. Chalfie, C. Trent, J. E. Sulston, and P. D. Evans, 1982 Serotonin and octopamine in the nematode *Caenorhabditis elegans*. *Science* 216: 1012-1014.
- Hoyos, E., K. Kim, J. Milloz, M. Barkoulas, J. B. Penigault *et al.*, 2011 Quantitative variation in autocrine signaling and pathway cross-talk in the *Caenorhabditis* vulval network. *Curr. Biol.* 21: 527-538.
- Inoue, T., D. R. Sherwood, G. Aspöck, J. A. Butler, B. P. Gupta *et al.*, 2002 Gene expression markers for *Caenorhabditis elegans* vulval cells. *Mech. Dev.* 119(Suppl 1): S203-S209.
- Inoue, T., M. Ailion, S. Poon, H. K. Kim, J. H. Thomas *et al.*, 2007 Genetic analysis of dauer formation in *Caenorhabditis briggsae*. *Genetics* 177: 809-818.
- Katz, W. S., R. J. Hill, T. R. Clandinin, and P. W. Sternberg, 1995 Different levels of the *C. elegans* growth factor LIN-3 promote distinct vulval precursor fates. *Cell* 82: 297-307.
- Kelleher, D. F., C. E. de Carvalho, A. V. Doty, M. Layton, A. T. Cheng *et al.*, 2008 Comparative genetics of sex determination: masculinizing mutations in *Caenorhabditis briggsae*. *Genetics* 178: 1415-1429.
- Kimble, J., 1981 Alterations in cell lineage following laser ablation of cells in the somatic gonad of *Caenorhabditis elegans*. *Dev. Biol.* 87: 286-300.
- Kiontke, K., A. Barriere, I. Kolotuev, B. Podbilewicz, R. Sommer *et al.*, 2007 Trends, stasis, and drift in the evolution of nematode vulva development. *Curr. Biol.* 17: 1925-1937.
- Kirouac, M., and P. W. Sternberg, 2003 cis-Regulatory control of three cell fate-specific genes in vulval organogenesis of *Caenorhabditis elegans* and *C. briggsae*. *Dev. Biol.* 257: 85-103.
- Koboldt, D. C., J. Staisch, B. Thillainathan, K. Haines, S. E. Baird *et al.*, 2010 A toolkit for rapid gene mapping in the nematode *Caenorhabditis briggsae*. *BMC Genomics* 11: 236.
- Li, C., and M. Chalfie, 1990 Organogenesis in *C. elegans*: positioning of neurons and muscles in the egg-laying system. *Neuron* 4: 681-695.
- Lin, K. T., G. Broitman-Maduro, W. W. Hung, S. Cervantes, and M. F. Maduro, 2009 Knockdown of SKN-1 and the Wnt effector TCF/POP-1 reveals differences in endomesoderm specification in *C. briggsae* as compared with *C. elegans*. *Dev. Biol.* 325: 296-306.
- Louvet-Vallee, S., I. Kolotuev, B. Podbilewicz, and M. A. Felix, 2003 Control of vulval competence and centering in the nematode *Oscheius* sp. 1 CEW1. *Genetics* 163: 133-146.
- Malone, C. J., W. D. Fiksen, H. R. Horvitz, and M. Han, 1999 UNC-84 localizes to the nuclear envelope and is required for nuclear migration and anchoring during *C. elegans* development. *Development* 126: 3171-3181.
- Maloof, J. N., and C. Kenyon, 1998 The Hox gene *lin-39* is required during *C. elegans* vulval induction to select the outcome of Ras signaling. *Development* 125: 181-190.

- Marri, S., and B. P. Gupta, 2009 Dissection of lin-11 enhancer regions in *Caenorhabditis elegans* and other nematodes. *Dev. Biol.* 325: 402–411.
- Maydan, J. S., S. Flibotte, M. L. Edgley, J. Lau, R. R. Selzer *et al.*, 2007 Efficient high-resolution deletion discovery in *Caenorhabditis elegans* by array comparative genomic hybridization. *Genome Res.* 17: 337–347.
- McGee, M. D., R. Rillo, A. S. Anderson, and D. A. Starr, 2006 UNC-83 IS a KASH protein required for nuclear migration and is recruited to the outer nuclear membrane by a physical interaction with the SUN protein UNC-84. *Mol. Biol. Cell* 17: 1790–1801.
- McGrath, P. T., Y. Xu, M. Ailion, J. L. Garrison, R. A. Butcher *et al.*, 2011 Parallel evolution of domesticated *Caenorhabditis* species targets pheromone receptor genes. *Nature* 477: 321–325.
- Mello, C. C., J. M. Kramer, D. Stinchcomb, and V. Ambros, 1991 Efficient gene transfer in *C. elegans*: extrachromosomal maintenance and integration of transforming sequences. *EMBO J.* 10: 3959–3970.
- Miller, M. A., A. D. Cutter, I. Yamamoto, S. Ward, and D. Greenstein, 2004 Clustered organization of reproductive genes in the *C. elegans* genome. *Curr. Biol.* 14: 1284–1290.
- Myers, T. R., and I. Greenwald, 2007 Wnt signal from multiple tissues and lin-3/EGF signal from the gonad maintain vulval precursor cell competence in *Caenorhabditis elegans*. *Proc. Natl. Acad. Sci. USA* 104: 20368–20373.
- Newman, A. P., and P. W. Sternberg, 1996 Coordinated morphogenesis of epithelia during development of the *Caenorhabditis elegans* uterine-vulval connection. *Proc. Natl. Acad. Sci. USA* 93: 9329–9333.
- Newman, A. P., G. Z. Acton, E. Hartwig, H. R. Horvitz, and P. W. Sternberg, 1999 The lin-11 LIM domain transcription factor is necessary for morphogenesis of *C. elegans* uterine cells. *Development* 126: 5319–5326.
- Penigault, J. B., and M. A. Felix, 2011a Evolution of a system sensitive to stochastic noise: P3.p cell fate in *Caenorhabditis*. *Dev. Biol.* 357: 419–427.
- Penigault, J. B., and M. A. Felix, 2011b High sensitivity of *C. elegans* vulval precursor cells to the dose of posterior Wnts. *Dev. Biol.* 357: 428–438.
- Rudel, D., and J. Kimble, 2001 Conservation of glp-1 regulation and function in nematodes. *Genetics* 157: 639–654.
- Sarafi-Reinach, T. R., T. Melkman, O. Hobert, and P. Sengupta, 2001 The lin-11 LIM homeobox gene specifies olfactory and chemosensory neuron fates in *C. elegans*. *Development* 128: 3269–3281.
- Seetharaman, A., P. Cumbo, N. Bojanala, and B. P. Gupta, 2010 Conserved mechanism of Wnt signaling function in the specification of vulval precursor fates in *C. elegans* and *C. briggsae*. *Dev. Biol.* 346: 128–139.
- Sommer, R. J., 2005 Evolution of development in nematodes related to *C. elegans* (December 14, 2005). WormBook, ed. The *C. elegans* Research Community WormBook, doi/10.1895/wormbook.1.10.1, <http://www.wormbook.org>.
- Sommer, R. J., and P. W. Sternberg, 1996 Evolution of nematode vulval fate patterning. *Dev. Biol.* 173: 396–407.
- Sommer, R. J., L. K. Carta, and P. W. Sternberg, 1994 The evolution of cell lineage in nematodes. *Dev. Suppl.* 1994: 85–95.
- Starr, D. A., 2011 Watching nuclei move: insights into how kinesin-1 and dynein function together. *BioArchitecture* 1: 9–13.
- Starr, D. A., G. J. Hermann, C. J. Malone, W. Fixsen, J. R. Priess *et al.*, 2001 *unc-83* encodes a novel component of the nuclear envelope and is essential for proper nuclear migration. *Development* 128: 5039–5050.
- Stein, L. D., Z. Bao, D. Blasiar, T. Blumenthal, M. R. Brent *et al.*, 2003 The genome sequence of *Caenorhabditis briggsae*: a platform for comparative genomics. *PLoS Biol.* 1: E45.
- Sternberg, P. W., 2005 Vulval development (June 25, 2005). WormBook, ed. The *C. elegans* Research Community WormBook, doi/10.1895/wormbook.1.10.1, <http://www.wormbook.org>.
- Sternberg, P. W., and H. R. Horvitz, 1986 Pattern formation during vulval development in *C. elegans*. *Cell* 44: 761–772.
- Sulston, J. E., 1976 Post-embryonic development in the ventral cord of *Caenorhabditis elegans*. *Philos. Trans. R. Soc. Lond. B. Biol. Sci.* 275: 287–297.
- Sulston, J. E., and H. R. Horvitz, 1981 Abnormal cell lineages in mutants of the nematode *Caenorhabditis elegans*. *Dev. Biol.* 82: 41–55.
- Sulston, J. E., and J. G. White, 1980 Regulation and cell autonomy during postembryonic development of *Caenorhabditis elegans*. *Dev. Biol.* 78: 577–597.
- Trent, C., N. Tsuing, and H. R. Horvitz, 1983 Egg-laying defective mutants of the nematode *Caenorhabditis elegans*. *Genetics* 104: 619–647.
- True, J., and E. Haag, 2001 Developmental system drift and flexibility in evolutionary trajectories. *Evol. Dev.* 3: 109–119.
- Weinschenker, D., G. Garriga, and J. H. Thomas, 1995 Genetic and pharmacological analysis of neurotransmitters controlling egg laying in *C. elegans*. *J. Neurosci.* 15: 6975–6985.
- Wood, W. B., 1988 *The nematode Caenorhabditis elegans*. Cold Spring Harbor Laboratory Press, New York.
- Zhao, Z., T. J. Boyle, Z. Bao, J. I. Murray, B. Mericle *et al.*, 2008 Comparative analysis of embryonic cell lineage between *Caenorhabditis briggsae* and *Caenorhabditis elegans*. *Dev. Biol.* 314: 93–99.
- Zhao, Z., S. Flibotte, J. I. Murray, D. Blick, T. J. Boyle *et al.*, 2010 New tools for investigating the comparative biology of *Caenorhabditis briggsae* and *C. elegans*. *Genetics* 184: 853–863.

Communicating editor: D. S. Fay

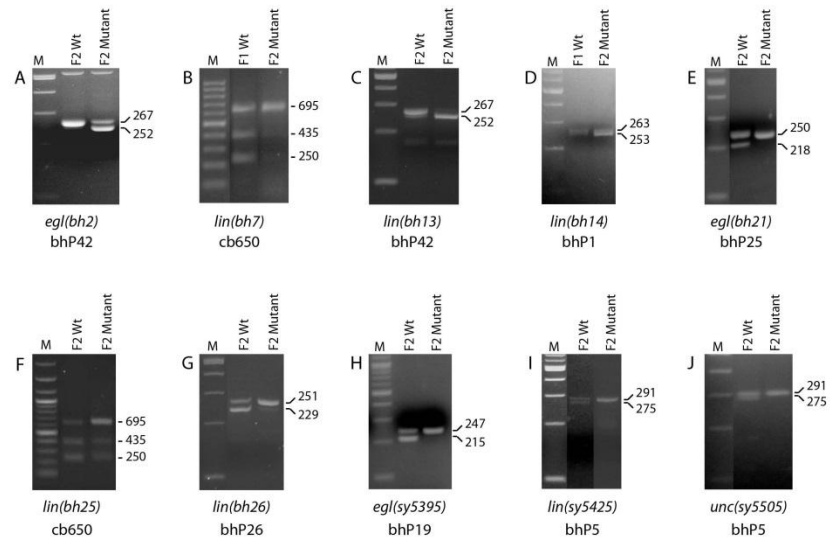


Figure S1 Mutation mapping using indel and snip-SNP polymorphisms. The images show DNA bands on 4% (for indels) and 1% (for snip-SNPs) agarose gels. The polymorphisms have been previously described (KOBOLDT *et al.* 2010). See Materials and Methods and Table 3 for details. M: DNA molecular weight marker, F1 Wt: DNA from F1 heterozygous animals, F2 Wt: DNA from phenotypically wild type pool of F2 animals, F2 Mutant: DNA from phenotypically mutant pool of F2 animals.

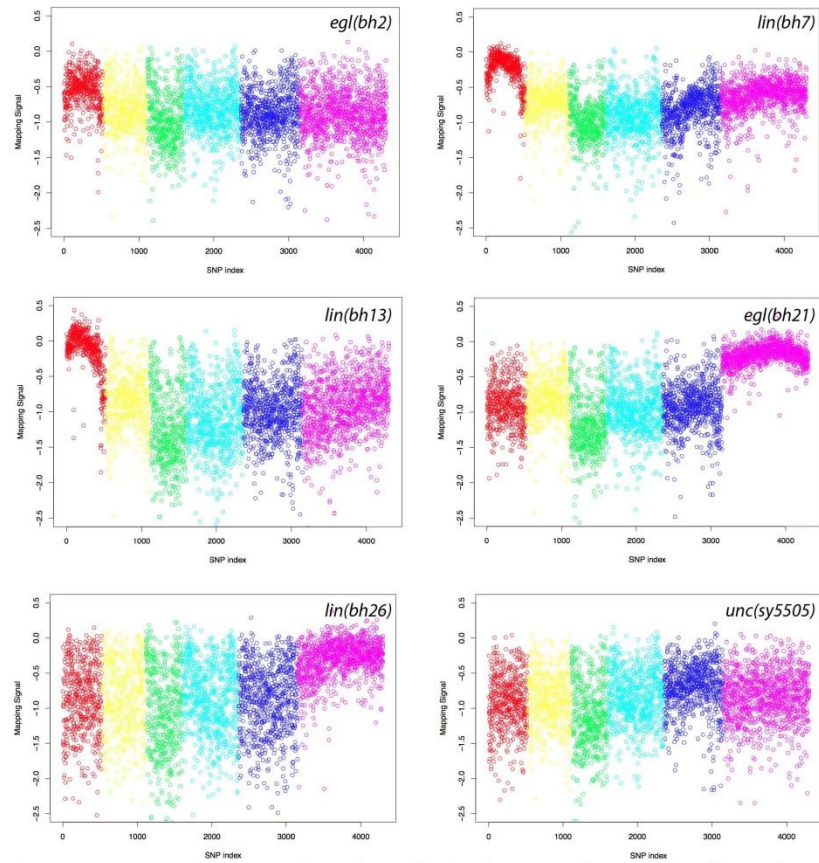


Figure S2 Mutation mapping using SNP-chip. Each tiny colored circle represents the mapping signal for a single SNP. Chromosomes are color coded (starting from 1 to 5 and X, in that order). See Materials and Methods and Zhao et al. study (ZHAO et al. 2010) for details.

Cbr-lin-11 cDNA sequence (1239 bp)

```

1  ATGCATTCTT  CTTCTGCCAT  CATCACCACC  CTGGAAGAAG  AAGAGAAGAA  GCCTCCTGCT
61  CATCTTCATC  AATATCATCA  TCATCTTCAT  CAACAGTCAG  TAGAAGACGT  CCGAAGTGCC
121  ACCTCATCAG  CCACGTGCT  TCTTCTGGAT  ACTTCCGCTG  CCACGTGGAT  GATGCCGTCC
181  TCGACGACGC  ACCCTCAAAT  CTCCGAGATA  AGCGGAAATG  AATGCGCTGC  ATGTGCACAG
241  CCTATTCTTG  ACAGATATGT  ATTCACCGTT  CTGGCAAAT  GTTGGCATCA  ATCATGTCTC
301  CGATGTTGCG  ATTGTGCGAGC  TCCAATGTCTG  ATGACTTGTT  TCAGTAAAGA  TGGCCTGATA
361  TTGTGTAATA  CAGACTATTC  AAGAGGTAC  GGCATCGAT  GCGCTGGATG  TGATGGAAAA
421  CTGGAATAAG  AGGATTTAGT  AAGGAGAGCA  AGAGACAAAG  TATTTTCATAT  TCGATGTTTT
481  CAATGTTTCA  TATGTCAAAG  GCTCTTGGAT  ACGGGTGATC  AGCTTTATAT  CATGGAGGGA
541  AATCGATTCA  TGTGTCAAAA  TGATTTTCAA  ACGGCTACCA  AAACATCGAC  TCCACATCA
601  ATGCACCGTC  CAATATCCAA  TGGATCCGAA  TGTAATTCCG  ATATCGAGGA  AGATAACGTG
661  GATGCTTGTC  ACAGCGTGG  TCTTGACGAC  GTTGATGGTG  ACTGTGGAAA  GGATAACTCT
721  GATGACTCAA  ACTCTGCAA  ACGGCGGGGT  CCTCGAACA  CAATCAAAGC  TAAACAGTTT
781  GAAACATTGA  AAAATGCATT  CGCTGCGACC  CCGAAACCAA  CTCGACACAT  CCGTGAACAA
841  CTTGCTGCCG  AGACAGGGCT  GAACATGAGA  GTCATTCAAG  TGTGGTTCCA  AAATCGACGA
901  AGCAAGGAAC  GTCGAATGAA  ACAGCTTCGA  TACGGTGGAT  ATCGTCAATC  CAGAAGACAA
961  CGTCGAGAGG  ATATCGTTGA  TATGTTTCCG  AATGACCAAC  AGTCTACCC  TCCACCACCT
1021  CCATCAAACG  TTCAATTCTT  CTGTGACCCA  TATGGAAGTC  CTCCAAATAA  CGGAGAGTCG
1081  ATGCAAAATC  CATCACAATT  CACAGTACCT  CCGGAGACTA  TGAATATGGT  GCCAGAACCA
1141  TATGCCGAAT  CATCGTCAAC  ACCACCAGAG  TTCAATGAAG  ATGCATTCAC  ATGCATTTAT
1201  TCCACTGATG  TCGGAAAACC  AACTCCAGTT  TCATGGTAG

```

Exon 1:	254 bp	(1 - 254)
2:	129 bp	(255 - 383)
3:	139 bp	(384 - 522)
4:	91 bp	(523 - 613)
5:	62 bp	(614 - 675)
6:	102 bp	(676 - 777)
7:	102 bp	(778 - 879)
8:	115 bp	(880 - 994)
9:	141 bp	(995 - 1135)
10:	104 bp	(1136 - 1239)

Figure S3 *Cbr-lin-11* cDNA sequence. The positions of exon-intron boundaries are marked.

Table S1 List of PCR and sequencing primers used in this study.

Oligo	Sequence (5' to 3')
GL380	GCTTCCCAATTCTCTGAGACGTCACA
GL381	GCCAAATTGCACAATTCAGTTCAG
GL382	GTCCCGTTGAGACACACTTACATTG
GL383	CTCTGCTAGCTCCGACCACATTTT
GL384	AGGCTACTGTAGTTCTCATTTTAGGACCTA
GL385	GGTCAAAGCTAGAAGCCTATTAGAGCG
GL389	TTACGGTATTGACGCCTAGGTAACC
GL390	GAGAAGTTCACACCTGCTGAGCTAC
GL391	GCAACAATGGAGCATCTACAGTAAGATCCC
GL392	AACAGGATACTGTGGTCTGCTCCAATC
GL793	AGCTTCACATCTTGGTTCG
GL795	AAGAAACTCTGGATGGGCTC
GL800	CGGGAAGTTTGGAACG
GL801	GACAGAGTGCAGGAACGC
GL802	GGCTCTCCTAATACATTCACG
GL806	TCCGAATAAGCGTAGGAGAC
GL807	AGCAGTCACTGCTCCTCC
GL808	AGATCCGTGTTGTCCAAGG
GL809	AGCTTCTGTCTACGGTC
GL810	GAGGTAGCGCCAATTTATG
GL812	CCTCTATTCCAGCCAGAAACC
cb-lin-11-up-1	CCATGCATTCTTCTCGTCCATCATCAC
cb-lin-11-up-2	TCTTCTGCAGTTCGGTTCGTTTCATTTTCC
cb-lin-11-up-4	GGAAGTCTCCAAATAACGGAGAG
cb-lin-11-up-5	GTCTTGACGACGTTGATGGTGACTGTG
cb-lin-11-up-6	GGAATGAATGCGCTGCATGTGCAC
cb-lin-11-up-7	GATTCTACCATCTTCCACGCTGTAG
cb-lin-11-up-8	CTGGCTCTCCTCATCTAACTG
cb-lin-11-up-9	CTGGTCAATCGTACAGGGTTC
cb-lin-11-down-1	CCCTGCAGTGAAACTGGAGTTGGTTTTCC
cb-lin-11-down-2	GTGATGATGGACGAAGAAGATGCATG
cb-lin-11-down-5	CTGAAAATGAAATGACTGGTCCGAGGG
cb-lin-11-down-7	GAACCCGTGTGTCTCTCTACTTC
cb-lin-11-down-8	GATAACTGACTCCAATAGACGTAGGC

CHAPTER 4: MUTATIONS IN *CAENORHABDITIS BRIGGSAE* IDENTIFY NEW GENES IMPORTANT FOR LIMITING THE RESPONSE TO EGF SIGNALING DURING VULVAL DEVELOPMENT

Preface:

This chapter includes the following article in its originally published format: “*Mutations in Caenorhabditis briggsae identify new genes important for limiting the response to EGF signaling during vulval development*” by Devika Sharanya, Cambree J. Fillis, Jaeyoung Kim, Edward M. Zitnik Jr., Kelly A. Ward, Molly E. Gallagher, Helen M. Chamberlin, and Bhagwati P. Gupta (Evolution & Development, 17: 34–48. doi: 10.1111/ede.12105). This article is available online open access under the terms of the Creative Commons Licenses which permits use, distribution and reproduction in any medium, provided the original work is properly cited.

This study describes seven new *C. briggsae* Muv genes that inhibit appropriate division of vulval precursors. Three of the Muv genes include orthologs of *Cel-lin-1*, *Cel-lin-31* of the EGF-Ras pathway and *Cel-pry-1* of the Wnt pathway. The remaining four genes lack orthologs of known *C. elegans* Muv genes. We have determined that these four genes are dependent on the EGF pathway kinase MEK. Based on their *Cbr-lin-3* levels, it is likely *Cbr-ivp-2(gu167)* acts upstream of *Cbr-lin-3/EGF*, while the remaining three influence the pathway either downstream or parallel to EGF. A new cost effective genetic mapping method by introgression has also been reported to map mutations and improve gene identification in *C. briggsae* alongside technologies like whole genome sequencing and SNP-chip assays.

Contributions:

This work was done in collaboration between Dr. Bhagwati Gupta lab at McMaster University and Dr. Helen Chamberlin lab at Ohio State University. Mutagenesis screens were done independently in both labs. I generated data for Figures 2, 6, 8 and Tables 1, 2, 3, 4. Mapping experiments along with data for tables 3 and 4 were generated with assistance from Bavithra Thillainathan. Jaeyoung Kim performed all the ablation experiments. Dr. Helen Chamberlin and members in her lab Cambree J. Fillis, Edward M. Zitnik Jr., Kelly A. Ward, and Molly E. contributed to the genetic and molecular analysis of *gu* alleles (*gu138*, *gu162* and *gu137*) described in Tables 1, 2; Figures 4, 5, 7; and Supplementary Tables 1, 2, 3, 4. I contributed to the writing of the manuscript along with Dr. Helen Chamberlin and Dr. Bhagwati Gupta.

Mutations in *Caenorhabditis briggsae* identify new genes important for limiting the response to EGF signaling during vulval development[†]

Devika Sharanya,^a Cambree J. Fillis,^b Jaeyoung Kim,^a Edward M. Zitnik Jr.,^b Kelly A. Ward,^b Molly E. Gallagher,^{b,1} Helen M. Chamberlin,^{b,*} and Bhagwati P. Gupta^{a,*}

^a Department of Biology, McMaster University, Hamilton ON, Canada

^b Department of Molecular Genetics, Ohio State University, Columbus OH, USA

*Authors for correspondence (e-mail: chamberlin.27@osu.edu; guptab@mcmaster.ca)

[†]Current address: Department of Ecology & Evolution, University of Chicago, Chicago, IL, USA

¹The four new genes reported in this study, *Cbr-lin(gu163)*, *Cbr-lin(gu167)*, *Cbr-lin(sy5216)* and *Cbr-lin(gu102)*, are now named as *ivp-1*, *ivp-2*, *ivp-3* and *ivp-4*, respectively.

SUMMARY Studies of vulval development in the nematode *C. elegans* have identified many genes that are involved in cell division and differentiation processes. Some of these encode components of conserved signal transduction pathways mediated by EGF, Notch, and Wnt. To understand how developmental mechanisms change during evolution, we are doing a comparative analysis of vulva formation in *C. briggsae*, a species that is closely related to *C. elegans*. Here, we report 14 mutations in 7 Multivulva (Muv) genes in *C. briggsae* that inhibit inappropriate division of vulval precursors. We have developed a new efficient and cost-effective gene mapping method to localize Muv mutations to small genetic intervals on chromosomes, thus facilitating cloning and functional studies. We demonstrate the utility of our method by determining molecular identities of

three of the Muv genes that include orthologs of *Cel-lin-1* (ETS) and *Cel-lin-31* (Winged-Helix) of the EGF-Ras pathway and *Cel-pry-1* (Axin), of the Wnt pathway. The remaining four genes reside in regions that lack orthologs of known *C. elegans* Muv genes. Inhibitor studies demonstrate that the Muv phenotype of all four new genes is dependent on the activity of the EGF pathway kinase, MEK. One of these, *Cbr-lin(gu167)*, shows modest increase in the expression of *Cbr-lin-3/EGF* compared to wild type. These results argue that while *Cbr-lin(gu167)* may act upstream of *Cbr-lin-3/EGF*, the other three genes influence the EGF pathway downstream or in parallel to *Cbr-lin-3*. Overall, our findings demonstrate that the genetic program underlying a conserved developmental process includes both conserved and divergent functional contributions.

INTRODUCTION

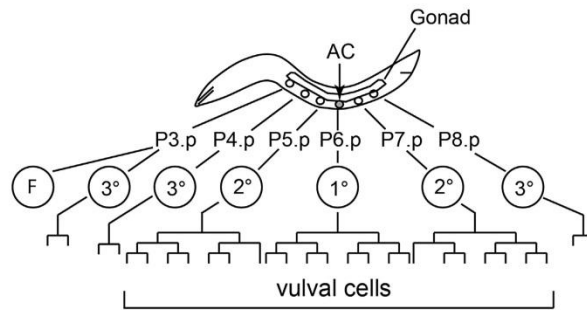
All biological systems incorporate changes in their genome that are shaped by evolutionary forces and functional selection. Such changes could lead to phenotypic differences between species, or between individuals within a species (Stern and Orgogozo 2008). In addition, the genome also undergoes other, more cryptic alterations that could change the relative importance of genes, or their regulatory relationships, in certain biological processes without leading to overt phenotypic differences. These changes could result in phenotypically conserved biological traits in different individuals that are produced from distinct or divergent sets of underlying genes and gene regulatory networks (e.g., Tsong et al. 2006). Understanding the genomic differences that nevertheless combine to yield similar phenotypes is important, as these differences influence the potential of genomes to evolve novel traits, or to withstand different functional perturbations resulting from genetic mutation, environmental disruptions, or disease conditions.

To better understand the functional flexibility and constraints of genomes, we are using an unbiased genetic analysis of the

nematode *Caenorhabditis briggsae*, for comparison to the related and well-characterized nematode *Caenorhabditis elegans*. The two species diverged roughly 30 million years ago, yet retain many phenotypic similarities, and occupy similar environmental niches (Cutter 2008). Of particular note, the two species exhibit almost identical patterns of developmental cell division, morphogenesis, and differentiation (Gupta et al. 2007; Zhao et al. 2010; Sharanya et al. 2012). This suggests that the development of both species is subject to a similar phenotypic selection. However, whether this conservation of phenotype results from conservation of the underlying genetic programs is not clear.

To characterize genes and gene networks important for development in *C. briggsae*, the current work focuses on the development of the vulva structure of the egg-laying system. In both *C. elegans* and *C. briggsae*, the vulva comprises 22 cells derived from three epidermal precursor cells termed Vulval Precursor Cells (VPCs; Fig. 1) (Sternberg 2005). Also in both species, experiments using a laser beam to ablate one or more cells demonstrate that the process of vulval development results from a reproducible set of cell interactions (Sulston and White 1980; Felix 2007; Seetharaman et al. 2010; Sharanya et al. 2012). In

Sharanya et al.

Multivulva mutants in *C. briggsae* 35A L3 stage vulval cell lineage in *C. elegans* and *C. briggsae*

B L4 stage vulval anatomy

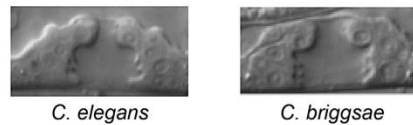


Fig. 1. Wild-type vulval development in *C. elegans* and *C. briggsae*. A, Three of six VPCs are induced to adopt primary and secondary fates. The induced VPCs divide to produce vulval progeny during the third larval stage (L3) of development. The remaining VPCs acquire uninduced tertiary fate. B, The cells and morphology of the vulva in the fourth larval stage (L4) are similar in the two species.

particular, a cell in the somatic gonad (the Anchor Cell, AC) provides an inductive signal in the form of LIN-3 EGF ligand that activates LET-23 EGF receptor (EGFR) in VPCs. The components of LIN-3-LET-23 pathway include LET-60 (Ras) and MPK-1 (MAP kinase) (Sternberg 2005; Sundaram 2013). Among the targets of MPK-1 two transcription factors LIN-1 (ETS family) and LIN-31 (Winged-Helix family) have been studied in some detail (Sundaram 2013). In addition to the inductive signal, a lateral signal, initiated by LIN-12/Notch, facilitates inter-VPC communication (Sternberg 2005). Finally, Wnt signaling is also required to promote VPC competence and cell fates (Sawa and Korswagen 2013). Together, these three evolutionarily conserved pathways function to generate a reproducible pattern of 3° – 3° – 2° – 1° – 2° – 3° VPC fates (Fig. 1). More distal VPCs adopt non-vulval fates, although they have the potential to produce vulval cells when the more proximal VPCs are removed (Sulston and White 1980). While some genetic studies demonstrate that these three pathways are also important for vulval development in *C. briggsae* (Felix 2007; Seetharaman et al. 2010; Sharanya et al. 2012), previous work has provided evidence for some quantitative differences in gene function between the two species (Felix 2007; Braendle and Felix 2008).

To systematically investigate the genes and genetic networks important for vulval development in *C. briggsae*, we have conducted genetic screens for mutants. In this article, we report characterization of a set of 14 *C. briggsae* mutants that exhibit inappropriate division of the distal VPCs (Multivulva, or Muv,

mutants). Our genetic experiments have revealed that these mutations define seven different genes and each of the genes acts independent of the gonad-derived inductive signal to promote cell proliferation. We have mapped these mutations to specific regions of chromosomes using a combination of phenotypic markers and molecular polymorphisms. The mutations have been localized to small genetic intervals using a new streamlined mapping method. The map data enabled us to clone three of the genes that likewise mutate to the Muv phenotype in *C. elegans*: *Cbr-lin-1*, *Cbr-lin-31*, and *Cbr-pry-1*. The remaining four genes do not appear to represent orthologs of known *C. elegans* Muv genes in *C. briggsae*. We further examined the role of all four new genes in vulva formation and found that their activity depends on the EGF pathway kinase, MEK. Interestingly, all but *Cbr-lin(gu167)* show no obvious increase in *Cbr-lin-3/EGF* transcript abundance, suggesting that the genes act downstream of or in parallel to *Cbr-lin-3*, but upstream of MEK. In summary, our results provide evidence for the conservation and divergence of developmental mechanisms in nematode vulva formation.

MATERIALS AND METHODS

Worm husbandry

C. briggsae strains were cultured under standard conditions used for *C. elegans* (Brenner 1974; Stiernagle 2006). The *C. briggsae* Muv mutations described in this study are listed in

36 EVOLUTION & DEVELOPMENT Vol. 17, No. 1, January–February 2015

Table 1. An overview of *C. briggsae* Muv mutants described in this study

Gene/Complementation Group	Location	Alleles	Type of mutation ¹
<i>Cbr-pry-1</i>	Chr 1	<i>gu137</i>	<i>gu137</i> (splice site mutation in intron 7)
<i>Cbr-lin-31</i>	Chr 2	<i>sy5342</i> , <i>sy5344</i> , <i>gu138</i> , <i>gu162</i>	<i>gu138</i> (missense mutation in exon 3), <i>gu162</i> (splice site mutation in intron 1) <i>gu198</i> (190 bp deletion in exon 2), <i>sa993</i> (nonsense mutation in exon 3), <i>bh9</i> (same as <i>sa993</i>)
<i>Cbr-lin-1</i>	Chr 4	<i>gu198</i> , <i>sa993</i> , <i>bh9</i>	<i>bh9</i> (same as <i>sa993</i>)
<i>Cbr-lin(gu163)</i>	Chr 1	<i>gu163</i>	n/a
<i>Cbr-lin(sy5216)</i>	Chr 4	<i>sy5216</i> , <i>sy5392</i>	n/a
<i>Cbr-lin(gu167)</i>	Chr 4	<i>gu167</i>	n/a
<i>Cbr-lin(gu102)</i>	Chr 5	<i>gu102</i> , <i>gu168</i>	n/a

¹See Methods for details. n/a: uncloned genes.

Table 1. All experiments were performed at 20°C, unless otherwise noted. Two of the mutations, *gu102* and *gu167*, are cold sensitive (Table 2). The wild-type *C. briggsae* strain used was AF16, and the polymorphism genetic mapping strain used was HK104.

C. briggsae markers and mapping strains used in genetic experiments: *Cbr-sma(sy5330) I*, *Cbr-sma-6(sy5148) II*, *Cbr-unc-4(sy5341) II*, *Cbr-dpy-1(sy5022) III*, *Cbr-daf-4(sa973) III*, *Cbr-unc-22(s1270) IV*, *Cbr-unc-22(gu205) IV*, *Cbr-dpy(sy5027) IV*, *Cbr-unc(sy5329) X*, *bhEx166[Cel-daf-6::YFP+Cel-myo-2::GFP]* (this study), *mfls5[Cbr-egl-17::GFP + Cel-myo-2::GFP]* (Felix 2007), *mfls8[Cbr-zmp-1::GFP + Cel-myo-2::GFP]* (Felix 2007).

C. elegans strains: N2 (wild type), *Cel-lin-31(n301) II* (Ferguson and Horvitz 1985), *Cel-lin-1(e1777) IV* (Ferguson and Horvitz 1985), *Cel-lin-15AB(n309) X* (Ferguson and Horvitz 1985). Transgenes: *ayls4[Cel-dpy-20(+)+Cel-egl-17::gfp]* (Burdine et al. 1998), *bhEx53[Cel-unc-119(+)+pGLC9 (Cel-daf-6::YFP+Cel-myo-2::GFP)]* (Seetharaman et al. 2010).

Table 2. The Muv phenotype of *Cbr-lin(gu102)* and *Cbr-lin(gu167)* is temperature sensitive

Strain	Temperature	% Muv	N
<i>Cbr-lin(gu167)</i>	25° C	33.4%	464
	20° C	66.2%	133
	15° C	ND	
<i>Cbr-lin(gu102)</i>	25° C	3.2%	158
	20° C	96.9%	381
	15° C	97.8%	91

ND, not determined, as parent animals are sterile. N, number of animals.

Genetic screens

AF16 animals were mutagenized by incubating in a 25 mM M9 buffer solution of Ethyl Methane Sulfonate (EMS) for up to 4 h using standard methods (Brenner 1974). Muv animals were isolated in the F2 generation and their progeny were evaluated. The lines exhibiting a heritable phenotype were retained for further study. Each strain was outcrossed at least three times before initiating genetic experiments. The 13 Muv strains reported in this article were recovered from a screen of the offspring of approximately 40000 F1 animals (80000 mutagenized gametes). The additional mutation, *sa993*, was kindly provided by Takao Inoue (National University of Singapore).

Complementation and mapping

Mutations were mapped to linkage groups using a combination of visible phenotypic markers (Table S1) and DNA polymorphisms (indels and snip-SNPs) (see below). In two cases, 3-factor mapping experiments were also carried out. *Cbr-lin(sy5342)* was crossed to double mutant worms *Cbr-sma-6(sy5148) Cbr-unc-4(sy5341)* and *Cbr-lin(sy5216)* was crossed to *Cbr-dpy(sy5027) Cbr-unc-22(s1270)*. The following recombinants were recovered:

sy5342: 17/27 Dpy non-Unc segregated Muv and 10/23 Unc non-Dpy segregated Muv.

sy5216: 5/5 Dpy non-Unc segregated Muv and 0/2 Unc non-Dpy segregated Muv.

Complementation tests were performed using visible recessive (e.g., Dpy or Unc) or *gfp*-based markers to identify the cross progeny. Heterozygous males were used to avoid the mating defects associated with many of the male mutants (data not shown). Complementation results, based on vulval morphology in L4 and adults, are shown in Table S2. Based on these findings,

Sharanya et al.

Multivulva mutants in *C. briggsae* 37

the mutations have been placed into seven complementation groups. Four genes, *Cbr-lin-31*, *Cbr-lin-1*, *Cbr-lin(sy5216)*, and *Cbr-lin(gu102)*, are represented by more than one allele.

Genetic mapping using polymorphism markers

Two genetic mapping methods were used to map mutations: a bulk segregant method and a genetic introgression method. The polymorphisms used were both indel and snip-SNPs (Koboldt et al. 2010) (www.briggsae.org), either verified previously or predicted based on genome sequence. The bulk segregant method was carried out as described previously for both *C. elegans* and *C. briggsae* (Wicks et al. 2001; Koboldt et al. 2010; Sharanya et al. 2012).

The genetic introgression method was performed as follows: Males from HK104 were crossed with hermaphrodite individuals from the AF16-derived Muv mutant strain. F1 cross animals were selected and allowed to self-cross. Several Muv animals were selected individually from the F2 generation and allowed to self-cross to establish lines representing independent “round-1” backcross lines. Muv hermaphrodites from each of these lines were crossed again with HK104 males, and the process repeated to establish round-2 backcross lines. Introgression of the AF16-derived mutation into the HK104 background was carried out in independently derived lines for a minimum of five rounds, allowing replacement of much of the genome with HK104 DNA except for DNA near the mutation responsible for the Muv phenotype. Genomic DNA was recovered from round-5 (or later) strains and genotyped using polymorphism analysis. Initial genotyping used DNA pooled from all introgressed lines and three polymorphisms from each chromosome to establish chromosomal linkage (Table S3). After assigning a mutation to a chromosome, DNA from individual lines was genotyped for additional polymorphisms to establish chromosomal “breakpoints” that delimit the physical position of the mutation. To aid in identifying cross- from self-progeny, an unlinked Dpy mutation (*gul09*) or a *Cel-myo-2::gfp*-expressing array was introduced in the background of strains. The marker was selected against in the final generation. Detailed map data are in Table S4.

Molecular biology and transgenics

The primers are listed in Table S5. To identify the mutations in *Cbr-lin-1*, *Cbr-lin-31*, and *Cbr-pry-1* in different Muv strains, genomic DNA corresponding to the gene from mutants was amplified by PCR. The PCR products were sequenced either by the Plant-Microbe Genomics Facility at The Ohio State University or by the McMaster University MOBIX facility. Characterization of three alleles of *Cbr-pry-1* has been reported previously (Seetharaman et al. 2010). In this study, we report a new *Cbr-pry-1* allele for completeness in considering all of the products of a genome-wide genetic screen.

Mutations associated with each allele are as follows:

Cbr-lin-1: gul98 is a 190 bp deletion within exon 2. The mutation shifts the frame and immediately introduces a stop codon. Flanking sequence and the site of the deletion are indicated: ACCCAATCAATGTCAAACGC/GTGAGACACCAAGTCCCAC.

sa993 is a C to T transition, nonsense mutation in exon 3. The mutation is indicated in bold italic: CCATTACTGCAACAATAAATTGGGCAGTTGT. The *bh9* allele is identical to *sa993*.

Cbr-lin-31: gul62 is a G to A transition that disrupts the splice donor site between exon 1 and intron 1. The mutation is indicated in bold italic: GAAAAATACGCAAAGATAGAGGGATTGAA.

gul38 is a C to T transition missense mutation that changes codon CGT to TGT. The mutation is indicated in bold italic: AACGGCAGTTGTCTGTGTCGCGGAAACGCT.

The precise nature of mutation in *sy5342* and *sy5344* alleles has not been determined since the exon 1 could not be successfully amplified. It is formally possible that this is due to a deletion overlapping exon 1 and the upstream region since we failed to amplify *Cbr-lin-31* cDNA in mutant worms as well. The other three exons were sequenced and showed no mutation.

Cbr-pry-1: gul37 is a G to A transition that disrupts the splice donor site between exon 7 and intron 7. The mutation is indicated in bold italic: GAGTATCGAAGATGATGAGATTCAAGACCT

Cbr-lin-1 and *Cbr-lin-31* full-length cDNA were sequenced to identify open reading frames and exon-intron boundaries. Whole RNA was extracted from mixed stage animals using the TRIZOL method. mRNA was reverse transcribed (NEB Protoscript AMV first strand cDNA synthesis kit #E6500S) and cDNA amplification was performed using primer pairs GL929/GL730 for *Cbr-lin-1* and GL926/GL928 for *Cbr-lin-31*. cDNA was purified (Invitrogen PureLink Quick Gel extraction kit K210012) and sequenced at McMaster MOBIX facility. This cDNA sequencing confirmed the gene structure predictions in Wormbase (www.wormbase.org).

C. briggsae daf-6::YFP transgenic strains, *bhEx165* and *bhEx166*, were generated by standard microinjection technique (Mello et al. 1991). The *daf-6* genomic fragment and *unc-119(+)* rescue DNA were from *C. elegans*. The construction of *Cel-daf-6::YFP* plasmid (pGLC9) has been described earlier (Seetharaman et al. 2010). Concentrations of plasmids were 100 ng/μl (pGLC9) and 40 ng/μl (*Cel-unc-119(+)*). *bhEx166* was used in experiments described here.

38 EVOLUTION & DEVELOPMENT Vol. 17, No. 1, January–February 2015

Microscopy

The Muv phenotype was scored in adults at plate-level using a stereomicroscope, as well as in L4 animals using a compound microscope and Nomarski optics. Adults with two or more protrusions on their ventral surface were scored as Muv. Animals with a single protrusion were scored as Pvl (protruding vulva). In cases where only Muv or non-Muv animals are indicated, the Pvl animals were included in the non-Muv category. For Nomarski examination, animals were mounted on agar pads in the presence of 1 mM Sodium Azide (Wood 1988).

VPC induction was examined at the mid-L4 stage. In wild-type animals, P5.p, P6.p, and P7.p VPCs are induced to divide and produce vulval cells (induction score 3.0, corresponding to 3 cells producing vulval cell progeny). Induction is apparent based on the presence of seven (for 2° lineages) or eight (for 1° lineages) progeny cells produced from a single VPC. In Muv animals, some or all of the remaining three VPCs (P3.p, P4.p, and P8.p) are also induced to produce vulval progeny, and result in an induction score > 3.

For fluorescent reporter studies, epifluorescence was visualized by using Zeiss AxioImager D1 and Nikon Eclipse 80i microscopes equipped with GFP filters from Chroma Technology.

Gonad ablation experiments

Gonad precursors (Z1 to Z4) were ablated in the L1 stage (Kimble 1981). Except the two temperature sensitive strains, *Cbr-lin(gu167)* and *Cbr-lin(gu102)*, which were maintained at 20 °C, all others were kept at room temperature (23 °C). Cells were ablated in anesthetized animals (by treating with 1–10 mM sodium azide) using a class IIb laser system (Photonic Instruments Inc.) attached to a Nikon Eclipse 80i Nomarski fluorescence microscope. Operated animals were recovered and allowed to grow to mid-L4 stage. The VPC induction pattern was examined under Nomarski optics, as described above.

U0126 assays

Animals were treated with the MEK inhibitor U0126 using a plate assay (Reiner et al. 2008). A stock of a 10 mM U0126 solution in DMSO was diluted with 1X M9, with 150 µl of the solution spread on NGM plates (5 ml NGM in 35 mm petri plates). The solution was allowed to absorb into the agar overnight at room temperature, with final concentration of drug calculated for the whole plate volume. Three drops of OP50 *E. coli* were added to the center of each plate on day two, and allowed to dry overnight at room temperature. On day three, approximately 20 L1 worms were added to each plate. All plates were then moved to 20 °C. After three days, the adult worms were scored for the Muv phenotype.

Quantitative RT-PCR assays

The *lin-3* transcript was quantified in late-L2 to early-L3 stage worms (Saffer et al. 2011). L1 larvae were grown on NGM plates for approximately 24 h at 20 °C following bleach synchronization (Wood 1988). The developmental stage of animals in each culture was confirmed by observing a sample of animals under the Nomarski microscope, using gonad size and presence of the anchor cell as indicators of stage.

Total RNA was extracted using the TRIZOL method. All samples were DNase treated (Ambion Turbo DNA-free, AM1907) prior to preparing cDNA (NEB Protoscript AMV first strand cDNA synthesis kit, E6500S). Reaction mixes were prepared using LuminoCt SYBR Green qPCR ReadyMix (Sigma, L6544). *lin-3* fragment was amplified using primer pairs GL909/GL910 (*C. elegans*) and GL911/GL912 (*C. briggsae*). The reference genes were *Cbr-pmp-3* and CBG22375 in *C. briggsae* and *Cel-pmp-3* and Y45F10d.4 in *C. elegans*. *Cel-pmp-3* and *Cbr-pmp-3* were used in the final analyses. Primer sequences are listed in Table S5. Data were generated and analyzed using BioRad CFX manager software 3.1.

RESULTS

A genetic screen for Multivulva mutants in *C. briggsae* identifies alleles of seven genes

In *C. elegans*, formation of the vulva results from a balance between genes that promote vulval development, and genes that inhibit the production of vulval cells in the absence of specific inductive signal information. Genes in these two classes have been identified based on their reduction- and loss-of-function phenotypes: genes that promote vulval development exhibit a Vulvaless (Vul) phenotype, and genes that inhibit vulval development exhibit a Multivulva (Muv) phenotype (Ferguson and Horvitz 1985). Although previous studies have identified Vul mutants in *C. briggsae* (Sharanya et al. 2012), a systematic analysis of genes important for inhibiting or restricting production of vulval tissue has not been reported. Thus, we carried out a set of genetic screens for mutations that confer the Muv phenotype as an unbiased method to identify *C. briggsae* genes that inhibit vulval development.

In this study, we describe 14 mutations that confer a Muv phenotype, visible as the presence of abnormal ventral protrusions under low magnification, and reflecting the inappropriate division of VPCs apparent under higher magnification (Tables 3 and 4 and Tables S3 and S4). Inter se complementation tests showed that all mutations are recessive to the wild-type allele, and that the alleles correspond to seven complementation groups (Table 1 and Table S2). Mutations in five of the genes exhibit a maternal rescue phenotype when the alleles segregate in a self-cross

Sharanya et al.

Multivulva mutants in *C. briggsae* 39**Table 3. Vulval defects in Muv animals derived from homozygous and heterozygous mothers**

Strain	Muv progeny of m/m (N)	Muv progeny of m/+ het (N)
<i>Cbr-pry-1(gu137)</i>	36% (161)	3.9% (355)
<i>Cbr-lin-31(sy5342)</i>	96.6% (291)	24.4% (283)
<i>Cbr-lin-31(sy5344)</i>	99% (95)	ND
<i>Cbr-lin-31(gu138)</i>	70.8% (89)	21.1% (147)
<i>Cbr-lin-31(gu162)</i>	96.6% (59)	24.7% (178)
<i>Cbr-lin-1(gu198)</i>	88% (200)	21.9% (269)
<i>Cbr-lin-1(sa993)</i>	98% (200)	21.3% (267)
<i>Cbr-lin-1(bh9)</i>	79.5% (210)	19.8% (101)
<i>Cbr-lin(gu163)</i>	90.1% (146)	10.2% (294)
<i>Cbr-lin(sy5216)</i>	100% (86)	2.2% (321)
<i>Cbr-lin(sy5392)</i>	100% (20)	0% (42)
<i>Cbr-lin(gu167)</i>	49.8% (289)	1.3% (302)
<i>Cbr-lin(gu102)</i>	97.6% (381)	0.02% (377)
<i>Cbr-lin(gu168)</i>	ND	15.1% (284)

Alleles of each locus are grouped together. The number of animals for each strain is shown in the parenthesis. ND, not determined; N, total number of animals examined (i.e., m/m, m/+, +/+).

from a heterozygous mother (Table 3). No such phenotype was observed in *Cbr-lin-31* and *Cbr-lin-1* mutants, although the numbers of Muvs in some cases are slightly lower than the expected one-quarter segregation. This is most likely due to animals exploding and the phenotype not being fully penetrant.

Ectopic vulval cells in *C. briggsae* Muv mutants can adopt primary as well as secondary vulval cell fates

We examined L3 and L4 animals using Nomarski optics to characterize the cellular defects in the mutants. All mutants exhibit ectopic division of VPCs and increased numbers of induced cells (Fig. 2). In all strains, the P3.p cell was capable of adopting a vulval cell fate. A similar phenotype was reported earlier in *Cbr-pry-1* mutants (Seetharaman et al. 2010). In contrast, cell ablation experiments in wild-type *C. briggsae* animals have shown that the P3.p cell does not respond to inductive signal when isolated, as it does in *C. elegans* (Delattre and Felix 2001). The phenotype of the Muv mutants argues that these distinct experimental observations could reflect species differences in the AC-derived signal, anatomy of the animals, or capacity of the P3.p to migrate toward the signal source, not just capacity of the P3.p cell to adopt a vulval cell fate.

We used 1° and 2° lineage markers, *mfls5* (*Cel-egl-17::gfp*), *mfls8* (*Cel-zmp-1::gfp*), and *bhEx166* (*Cel-daf-6::yfp*) (Felix 2007; Seetharaman et al. 2010), to assess the fates of induced VPCs. In contrast to the previously described *Cbr-pry-1* mutants (Seetharaman et al. 2010) and with exception of *Cbr-lin-31(sy5342)*, the Muv mutants reported in this study can produce ectopic 1° cell fates from precursors in addition to the P6.p VPC. This is similar to the phenotype in non-*pry-1* Muv mutants in *C. elegans* (Ferguson et al. 1987; Sternberg and Horvitz 1989). Interestingly, ectopic VPCs in *lin-31* mutants in both species (*Cbr-lin-31(sy5342)* and *Cel-lin-31(n301)*) exhibited only 2° cell fates (Fig. 2).

Table 4. Analysis of the VPC induction pattern in Muv mutants

Genotype	% Induction of VPCs						Avg ind	N
	P3.p	P4.p	P5.p	P6.p	P7.p	P8.p		
<i>Cbr-lin-31(sy5342)</i>	36.4	82.5	100.0	100.0	97.1	72.9	4.9	140
<i>Cbr-lin-31(sy5344)</i>	60.0	90.0	100.0	100.0	100.0	90.0	5.4	10
<i>Cel-lin-31(n301)</i>	27.7	51.8	98.8	100.0	100.0	30.7	4.1	83
<i>Cbr-lin-1(gu198)</i>	2.8	13.4	100.0	100.0	100.0	62.7	3.8	71
<i>Cbr-lin-1(sa993)</i>	2.8	27.8	100.0	100.0	100.0	62.8	3.9	90
<i>Cbr-lin-1(bh9)</i>	0.0	12.2	100.0	100.0	100.0	38.4	3.5	82
<i>Cbr-lin(gu163)</i>	0.6	11.2	100.0	100.0	100.0	28.7	3.4	89
<i>Cbr-lin(sy5216)</i>	19.6	86.1	100.0	100.0	96.1	91.3	4.9	115
<i>Cbr-lin(sy5392)</i>	29.0	29.0	100.0	100.0	100.0	100.0	4.6	7
<i>Cbr-lin(gu167)</i>	1.5	11.1	100.0	100.0	100.0	17.2	3.3	99
<i>Cbr-lin(gu167)*</i>	6.4	43.6	100.0	100.0	100.0	51.1	4.0	94
<i>Cbr-lin(gu102)</i>	2.4	18.3	100.0	100.0	100.0	31.1	3.5	82
<i>Cbr-lin(gu102)*</i>	14.8	87.5	99.5	100.0	100.0	92.6	4.9	108

Animals were examined at room temperature (23 °C) or at 20 °C (marked with star). Avg ind, average VPC induction of each strain. N, number of animals examined.

40 EVOLUTION & DEVELOPMENT Vol. 17, No. 1, January–February 2015

A Primary VPC fates in Muv mutants

Genotype	transgene	P3.p	P4.p	P5.p	P6.p	P7.p	P8.p	n
wild type	<i>daf-6::yfp</i>	0	0	0	98	0	0	43
	<i>zmp-1::gfp</i>	0	0	0	100	0	0	43
<i>Cbr-lin-31(sy5342)</i>	<i>daf-6::yfp</i>	0	0	0	92.9	0	0	42
	<i>zmp-1::gfp</i>	0	0	0	100	0	0	41
<i>Cel-lin-31(n301)</i>	<i>daf-6::yfp</i>	0	0	0	98	0	0	42
<i>Cbr-lin-1(gu198)</i>	<i>daf-6::yfp</i>	0	3.3	0	90	0	6.7	30
<i>Cbr-lin(gu163)</i>	<i>zmp-1::gfp</i>	0	1.1	0	81.8	0	6.8	44
<i>Cbr-lin(sy5216)</i>	<i>daf-6::yfp</i>	2.5	15	2.5	72.5	0	47.5	40
	<i>zmp-1::gfp</i>	5.7	30	11.4	91.4	0	38.6	35
<i>Cbr-lin(gu167)</i>	<i>zmp-1::gfp</i>	0	1.1	0	88.6	0	2.3	44
<i>Cbr-lin(gu102)</i>	<i>zmp-1::gfp</i>	0	0	0	97.6	0	21.4	42

B Secondary VPC fates in Muv mutants

wild type	<i>egl-17::gfp</i>	0	0	100	0	100	0	43
<i>Cbr-lin-31(sy5342)</i>	<i>egl-17::gfp</i>	55.3	82.5	98.2	0	98.2	71.1	57
<i>Cel-lin-31(n301)</i>	<i>egl-17::gfp</i>	31.7	52.4	97.6	0	95.1	18.3	41
<i>Cbr-lin-1(gu198)</i>	<i>egl-17::gfp</i>	2.4	8.5	87.8	0	82.9	23.2	41
<i>Cbr-lin(gu163)</i>	<i>egl-17::gfp</i>	1.1	4.4	95.6	0	97.8	23.3	45
<i>Cbr-lin(sy5216)</i>	<i>egl-17::gfp</i>	5	48.8	92.5	0	82.5	42.5	40
<i>Cbr-lin(gu167)</i>	<i>egl-17::gfp</i>	0	7.3	92.7	0	96.4	6.4	55
<i>Cbr-lin(gu102)</i>	<i>egl-17::gfp</i>	0	16.3	90	0	87.5	8.8	40

Marker	75-100%	50-74%	25-49%	1-24%	0%
Primary					
Secondary					

Fig. 2. *C. briggsae* Muv mutants exhibit ectopic development of primary and secondary vulval cells. For each VPC, the frequency of cell fate is shown in shades of green (primary) and red (secondary) colors. All transgenes are from *C. elegans*.

In *C. elegans*, lateral signaling to inhibit the production of adjacent VPCs adopting the primary fate is active in Muv mutants (Stemberg 1988; Beitel et al. 1995). To ask whether this is also the case in *C. briggsae*, we evaluated the cell type marker data. We observed no adjacent primaries in all mutants except for *Cbr-lin-1(sa993)* and *Cbr-lin(sy5216)* (6% and 2%, out of 126 and 143 pairs that adopted induced fates, respectively) (Table S6). The *sa993* result is consistent with the observations for *Cel-lin-1* mutants (Beitel et al. 1995). Overall, the data are consistent with the idea that lateral signaling is functional during the specification of VPC fates in *C. briggsae* Muv mutants.

Genetic mapping and a streamlined approach for gene mapping in *C. briggsae*

To establish the genetic location of each gene, we mapped representative alleles to a specific chromosome or chromosomal region using genetic linkage tests. While two genes were mapped with respect to available visible genetic markers, polymorphism mapping was used to map with respect to a larger set of available loci on the genetic map. In particular, we utilized genetic sequence polymorphisms that distinguish AF16

from HK104 strains of *C. briggsae*, and were previously identified through whole genome sequencing methods (Koboldt et al. 2010). These genetic mapping methods allowed us to identify physically distinct locations for each of the genes in a two-step approach (first linking to chromosomes and then to sub-chromosomal regions), with the exception of *Cbr-lin(gu167)* and the gene defined by *sy5216* and *sy5392* (Fig. 3, Tables S3 and S4).

To streamline gene-mapping methods for *C. briggsae*, we developed a new introgression method that can be used to efficiently assign chromosomal linkage as well as define the physical region containing a genetic mutation. For the introgression method, we established independent lines from each AF16-derived Muv mutation that had been crossed into the HK104 genetic background, identified homozygous Muv mutants in the F2, and then crossed again to HK104 (see Materials and Methods). This process results in increasingly more of the genome represented by HK104-derived DNA, with the exception of sequences proximal to the mutation responsible for the Muv phenotype. Subsequent evaluation of the polymorphisms present in each line allows inference of both chromosomal linkage and chromosomal

Sharanya et al.

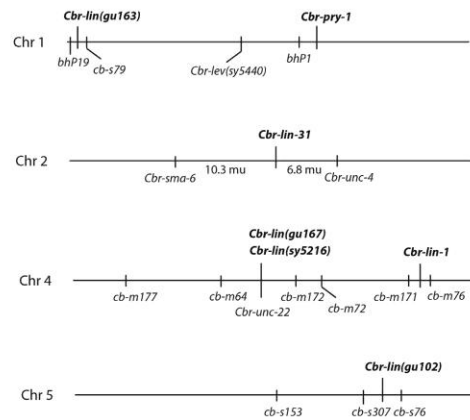
Multivulva mutants in *C. briggsae* 41

Fig. 3. Genetic linkage map of *C. briggsae* Muv genes described in this study. The approximate positions of selected markers and known *C. elegans* orthologs are also shown. Only the chromosomes that include identified Muv genes are included.

recombination points that delimit the physical location of the mutation. Using these combined methods, we determined the chromosomal linkage and genetic position of alleles of all seven *C. briggsae* Muv genes (Table S4).

Mutations in three *C. elegans* Muv gene orthologs also confer a Muv phenotype in *C. briggsae*

Although the Muv phenotype in *C. elegans* can result from perturbation of a number of genes, only three genes have been identified that are both 1) non-essential and 2) confer the Muv phenotype when disrupted singly with a loss-of-function or null allele. One gene, *pry-1/Axin*, that acts in the canonical Wnt signaling pathway has been shown previously to also exhibit a Muv phenotype when mutant in *C. briggsae* (Seetharaman et al. 2010). The gene set from the current study includes the new allele of *Cbr-pry-1 (gu137)*. Two additional genes (*lin-1/Ets* and *lin-31/Hnf3*) act in response to the EGF pathway, but their function has not been previously studied in *C. briggsae*. Other *C. elegans* genes for which a loss-of-function phenotype is Muv fall into the synthetic multivulva (synMuv) gene class, and require mutations in two (rather than one) genes simultaneously to produce the Muv phenotype (Ferguson and Horvitz 1989; Lu and Horvitz 1998; Ceol and Horvitz 2001; Thomas et al. 2003). We experimentally address whether any of the *C. briggsae* Muv mutants could result from “single hit” mutations of the synMuv gene class below.

As a proof of concept for applying the introgression mapping strategy leading to molecular identification of a gene, we considered *Cbr-lin-1* that is linked to Chr 4. Map data from four independent introgression lines placed *gu198* on the right arm of

Chr 4, between *bhP11* and *cb-s221* (Fig. 4). Subsequent sequencing of the DNA from *gu198* identified a 190 bp deletion within exon 2 of CBG13868/*Cbr-lin-1*, and a nonsense mutation in DNA from *sa993* and *bh9* (see Methods). We conclude that these alleles genetically define *Cbr-lin-1*, and demonstrate that the Muv phenotype can result from mutation of this gene.

Only one Muv gene exhibited linkage to Chr 2, where *Cbr-lin-31* is located. Sequencing of CBG18439/*Cbr-lin-31* from mutants assigned to this complementation group identified mutations predicted to disrupt or reduce the function of the gene (Fig. 5). We conclude that these alleles genetically define *Cbr-lin-31* and demonstrate that the Muv phenotype could result from mutation of this gene. Thus, three genes predicted to participate in either the Wnt pathway or the EGF pathway, and known from genetic analysis in *C. elegans* to mutate to a Muv phenotype in that species, exhibit a similar phenotype when disrupted in *C. briggsae*.

The Muv phenotype of *C. briggsae* mutants is gonad independent

In *C. elegans* (as well as in *C. briggsae*), the anchor cell of the somatic gonad is the source of an inductive signal that is necessary for vulval development (Kimble 1981; Felix 2007). This gonad-dependence of vulval development is lost in many *C. elegans* Muv mutants, as disruption of the affected genes bypasses the requirement for the inductive signal (Sternberg 1988; Sternberg and Horvitz 1989). However, in principle, a Muv phenotype can result in either species from overproduction of *lin-3/EGF* from the anchor cell (Katz et al., 1995; Felix 2007), which would result in a gonad-dependent Muv phenotype. To test whether the Muv phenotype of the *C. briggsae* mutants is dependent on the anchor cell, we used a laser to remove the gonad (and therefore the precursor to the anchor cell) in animals from each mutant strain, and subsequently examined vulval development in L4 larvae. The Muv phenotype for mutants of all six tested genes (as well as *Cbr-pry-1* previously reported in [Seetharaman et al. 2010]) is not dependent on the presence of the gonad (and therefore, the anchor cell) (Fig. 6). These results are consistent with the phenotype observed for *C. elegans lin-1* and *lin-31* mutants, as well as other *C. elegans* Muv mutants (Sternberg 1988; Sternberg and Horvitz 1989; Miller et al. 1993; Beitel et al. 1995). We interpret that disruption of each affected gene can bypass the normal dependence of vulval development on the anchor cell.

The Muv phenotype of new *C. briggsae* mutants is dependent on MEK

Beyond the three genes predicted from studies on *C. elegans*, our screen identified mutations in four additional *C. briggsae* genes for which mutations confer a Muv phenotype. Although the

42 EVOLUTION & DEVELOPMENT Vol. 17, No. 1, January–February 2015

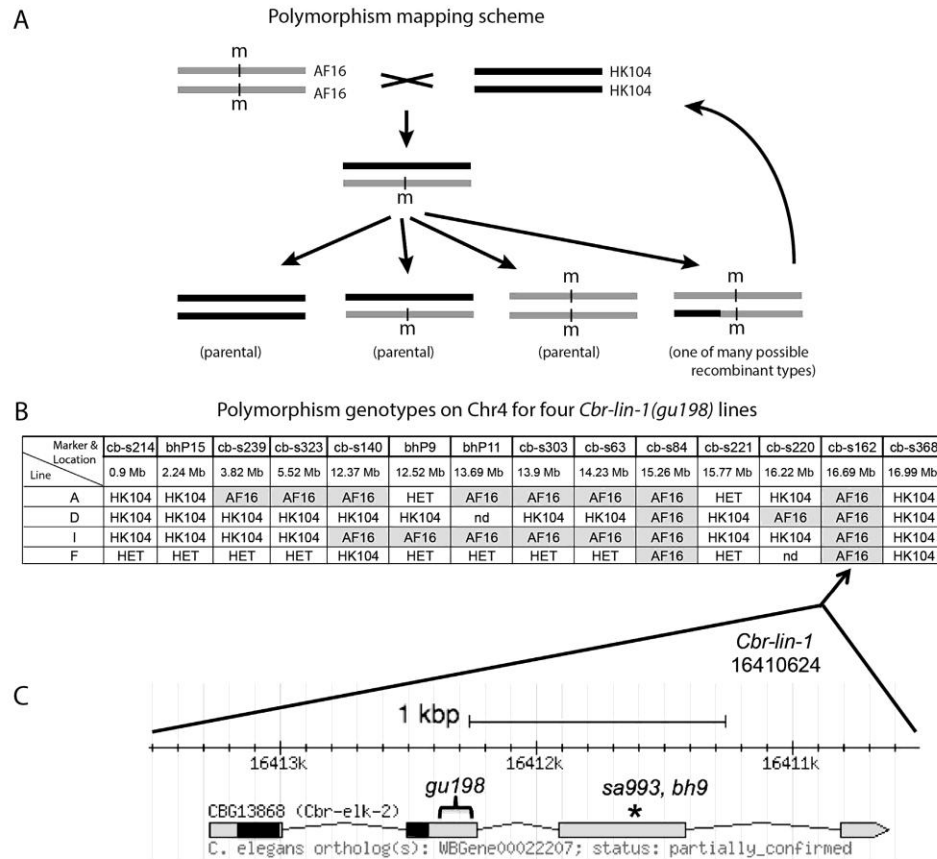


Fig. 4. A streamlined genetic mapping method allows for efficient genetic mapping and gene identification of *Cbr-lin-1*. **A.** A genetic crossing scheme to introduce the Muv mutation (m) isolated in the AF16 genetic background into the HK104 genetic background. The HK104 and AF16 chromosomes are represented by black and gray lines, respectively. The F2 progeny include both parental types and recombinants. Only one of the many possible recombinants carrying the Muv mutation is shown. The F2 Muv animals are crossed back to HK104 and the cross cycle is repeated for five or more introgression rounds. The crossing process for all lines is completed in parallel. **B.** Example of data from four independent lines after five rounds of introgression of the *Cbr-lin-1(gu198)* allele. A polymorphism that retains the AF16 alleles in all four lines maps close to the *Cbr-lin-1* locus. **C.** The *C. briggsae lin-1* locus (from Wormbase) indicating the gene structure and the position of mutant alleles.

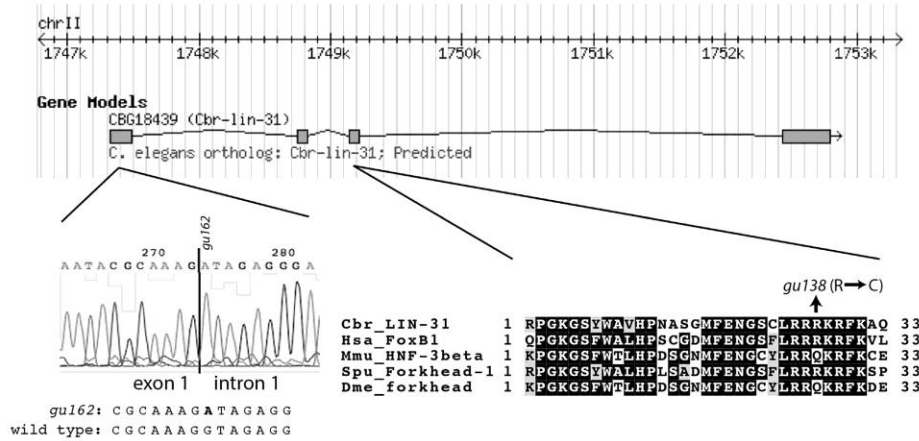
gonad ablation experiments demonstrate that a mutation in each of these genes can bypass the requirement for the inductive signal, these experiments do not address how each gene might function with respect to the EGF pathway, which functions as the inductive signal in *C. elegans* and can promote ectopic vulval cell induction in both species (Katz et al. 1995; Felix 2007). To test whether the Muv phenotype associated with the four new *C. briggsae*

genes results from activation of the EGF pathway or from a functionally distinct mechanism, we utilized the selective MEK inhibitor U0126 (Goueli et al. 1998). This inhibitor has been used successfully to inhibit EGF signaling during vulval development in nematodes, including *C. elegans* and *O. tipulae*, and can specifically inhibit the Muv phenotype associated with *C. elegans* mutants with active EGF signaling, such as

Sharanya et al.

Multivulva mutants in *C. briggsae* 43

A *Cbr-lin-31*



B *Cbr-pry-1*

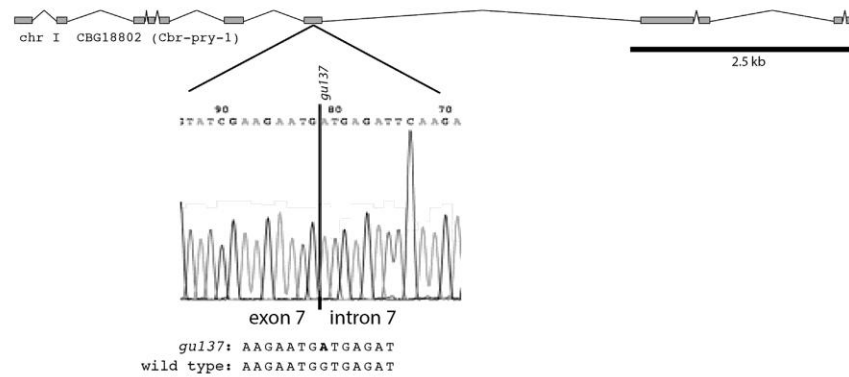


Fig. 5. Genetic mutations associated with *Cbr-lin-31* and *Cbr-pry-1* are identified from the set of *C. briggsae* Muv mutants. A, The gene structure of *Cbr-lin-31* (from Wormbase), and the locations of two alleles, *gu162* and *gu138*. B, The gene structure of *Cbr-pry-1* (Seetharaman et al. 2010), and the location of the allele *gu137*. Additional *Cbr-pry-1* alleles have been reported previously (Seetharaman et al. 2010).

Cel-let-60(n1046)/Ras (Dichtel-Danjoy and Felix 2004; Reiner et al. 2008). We observed that the Muv phenotype was suppressed by treatment with U0126 in a dose-dependent way in mutants for each of the four new genes, whereas the Muv phenotype of *Cbr-lin-1(gu198)* (which is predicted to act downstream of MEK

in the EGF pathway) was unchanged (Fig. 7). This result argues that although the *C. briggsae* genome includes genes that mutate to a Muv phenotype that are not clearly predicted from genetic studies in *C. elegans*, the four new genes depend on the conserved EGF pathway to promote vulval development.

44 EVOLUTION & DEVELOPMENT Vol. 17, No. 1, January–February 2015

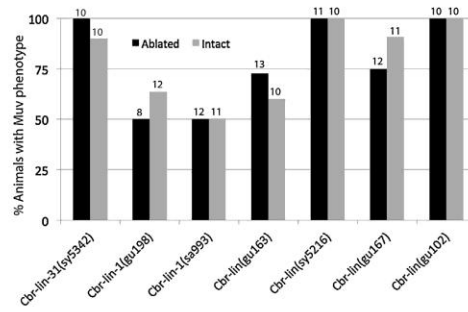


Fig. 6. The Muv phenotype associated with *C. briggsae* mutants is gonad-independent. The vulval phenotype of animals was examined at L4 and young adult stages. The Y-axis depicts the percentage of animals exhibiting the Muv phenotype. The number of animals in each condition is indicated above each bar.

The Muv phenotype of some new *C. briggsae* mutants does not result from increased transcript abundance of *lin-3/EGF*

The *C. elegans* synMuv genes are a group of genes that negatively regulate cell proliferation and confer a Muv phenotype when mutant (Ferguson and Horvitz 1989; Clark et al. 1994; Lu and Horvitz 1998; Thomas et al. 2003). However, unlike *Cel-lin-1*, *Cel-lin-31*, and *Cel-pry-1*, synMuv mutants show the Muv phenotype with a high frequency only when

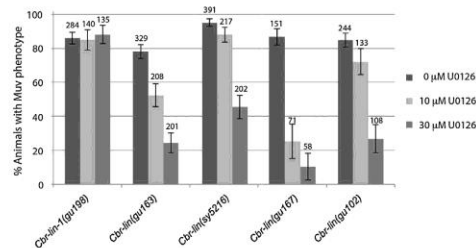


Fig. 7. The Muv phenotype of four new *C. briggsae* mutants is dependent on MEK. The MEK inhibitor U0126 blocks the Muv phenotype associated with all four *C. briggsae* Muv mutants that define new genes. While all four exhibit a reduced Muv phenotype in the presence of 30 μM U0126, *Cbr-lin(gu163)* and *Cbr-lin(gu167)* are also sensitive to a lower, 10 μM dose. The Muv phenotype associated with *Cbr-lin-1(gu198)* mutants is not reduced in the presence of U0126, a result consistent with the expectation that *Cbr-lin-1/Ets* acts downstream of MEK in the EGF pathway. Error bars designate the 95% confidence interval for population proportion (π) based on sample proportion (p). The number of animals in each condition is indicated above each bar. The number of trials for each mutant was between 2 and 5.

genes from two distinct classes (A and B) are simultaneously disrupted. While in the case of one locus (*Cel-lin-15*) these two genes are located adjacent to each other (*Cel-lin-15A* and *Cel-lin-15B*, as part of a single operon) (Clark, Lu, and Horvitz 1994), the other synMuv genes are distributed across the genome, and the genes from each class behave as distinct loci.

We tested the possibility that the four *C. briggsae* Muv genes that are not clearly predicted from *C. elegans* genetic studies represent synMuv genes. Such genes might be identified in our screen if we were to find additional synMuv genes that are part of a single locus, or because *C. briggsae* VPCs have different sensitivity to perturbation of synMuv genes, and single-gene mutants could therefore exhibit the Muv phenotype. *C. elegans* synMuv genes act to restrict the expression pattern and abundance of the *Cel-lin-3/EGF* transcript (Cui et al. 2006). This increased and ectopic expression of the inductive signal in synMuv double mutants is the cause of ectopic vulval development. To ask whether the *C. briggsae* Muv mutants exhibit a similar dysregulation of *Cbr-lin-3*, we utilized qRT-PCR to measure *Cbr-lin-3* abundance in both wild type and Muv mutant strains (Fig. 8) during late-L2 and early-L3 stages (Sternberg and Horvitz 1986; Sharanya et al. 2012). A similar method in *C. elegans* synMuv double mutants has showed an increase in *Cel-lin-3* transcript abundance (Cui et al. 2006). This was also confirmed by our analysis of *Cel-lin-15AB(n309)* synMuv that affects both A and B transcripts (~2.5-fold, Fig. 8C). We found no increase in *Cbr-lin-3* transcript levels in any of our new uncloned *C. briggsae* Muv mutants except *Cbr-lin(gu167)* that exhibited a modest but statistically significant increase at 20 °C (~1.5-fold, Fig. 8B). Indeed, *Cbr-lin-3* transcripts are reduced compared to wild type in *Cbr-lin(gu163)* and *Cbr-lin(sy5216)* mutants.

DISCUSSION

We have carried out a genetic mutagenesis screen for *C. briggsae* mutants with abnormal, ectopic vulval development (Muv mutants). Our screen recovered alleles of seven genes, including three that are predicted to mutate to a Muv phenotype based on genetic studies in *C. elegans*. We developed and applied a streamlined genetic mapping method to map the genes to chromosomal regions and to facilitate molecular identification of the genes. Our cellular and molecular studies argue that the screen has identified four *C. briggsae* Muv genes for which the molecular identity is not easily predicted based on phenotypic overlap with *C. elegans* genes. We interpret these genes to act through the EGF pathway, as their Muv phenotype is dependent on MEK. However, at least some of them do not behave as synMuv genes, as expression of the *Cbr-lin-3/EGF* transcript is not de-repressed in these mutants. Altogether, this work argues that similar biological outcomes in different species can result from a combination of conserved and divergent genetic inputs and provides a framework for future studies on the flexibility and constraints of genetic pathways in animal development.

Sharanya et al.

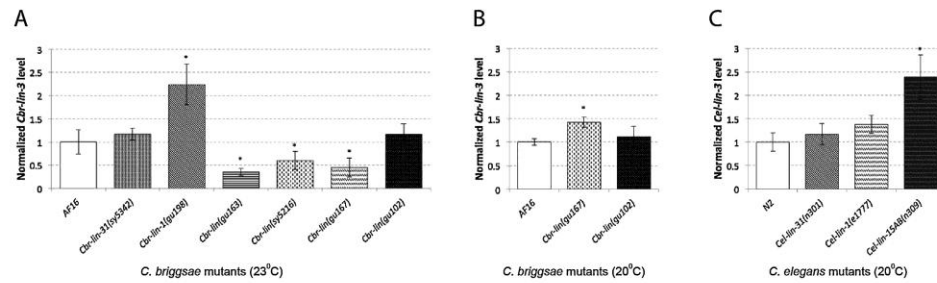
Multivulva mutants in *C. briggsae* 45

Fig. 8. The abundance of *lin-3/EGF* transcripts in *C. briggsae* and *C. elegans* Muv mutants determined by qRT-PCR. Relative fold changes of *lin-3* transcripts have been plotted. Error bars represent the standard error of the mean. P values were calculated using student's T test. Stars mark data that are statistically significant ($P < 0.05$). A, At room temperature (23 °C) *Cbr-lin-3* transcript levels are high in *Cbr-lin-1(gu198)* and low in *Cbr-lin(gu163)*, *Cbr-lin(sy5216)*, and *Cbr-lin(gu167)* animals. B, At 20 °C, *Cbr-lin(gu167)* shows an opposite trend, and a modest increase in *Cbr-lin-3* transcript abundance compared to the control. C, In *C. elegans*, *Cel-lin-3* levels are unchanged in *Cel-lin-1* and *Cel-lin-31* mutants but high in *Cel-lin-15AB* (a synMuv double mutant).

Genetic mapping for the molecular identification of mutant genes in *C. briggsae*

C. briggsae has many strengths that make it a preferred nematode model for comparative genetic and genomic studies involving *C. elegans*. Like *C. elegans*, *C. briggsae* animals are hermaphroditic, and they have a complete genomic sequence as well as a physical map that is supported by genetic recombination data (Stein et al. 2003; Hillier et al. 2007; Koboldt et al. 2010; Ross et al. 2011). Consequently, classical genetic screens and analysis of genomic information are as straightforward and efficient as with *C. elegans*. However, a limitation to linking genetic and genomic information, and to positional cloning of genetically identified loci in *C. briggsae*, is that relatively few mutations that confer a visible phenotype are available, and fewer still are anchored to the physical map (Koboldt et al. 2010; Zhao et al. 2010; Sharanya et al. 2012; Wei et al. 2014) (www.briggsae.org). Thus, defining genomic “boundaries” that limit the physical position of new genes defined by mutation is more challenging than in *C. elegans*.

We had earlier applied F2 generation bulk segregant analysis (BSA) assay for *C. briggsae* to rapidly map new mutations. The BSA technique is effective in linking mutations to chromosomal arms (Koboldt et al. 2010) but it lacks resolution. Another assay, involving SNP-chip, offers more sensitivity, but is not readily accessible to all labs (Zhao et al. 2010).

To address the shortcomings of the BSA technique and SNP-chip assay, and to provide a sensitive and affordable mapping method, we have developed a genetic introgression method that uses polymorphic *C. briggsae* strains, and a strategy of producing multiple parallel isolates to both assign genetic linkage and delimit the map position of mutations. We find that this method can reliably limit the mutations to chromosomal regions of a few megabases of sequence, with greater resolution likely possible with larger numbers of parallel isolates. However, this method, on

its own, is not sufficient to uniquely identify the gene affected in the mutant. In addition, we frequently observed recombinant chromosomes that appear to retain more than one region of AF16 DNA, separated by HK104 sequences (as in Fig. 4B). It is unclear whether this reflects a feature or error of the mapping method, or inaccuracies in the current *C. briggsae* genomic assembly. Despite these limitations, we anticipate that this mapping approach, combined with molecular analyses such as whole genome sequencing methods, will allow efficient molecular identification of genes in *C. briggsae*.

Discovery of new genes that limit vulval formation in *C. briggsae*

Our genetic screen for *C. briggsae* Muv mutants has identified new genes that limit proliferation potential of vulval precursors. We identified mutations in three *C. briggsae* genes known to restrict vulval development in *C. elegans*, and these genes are in conserved signaling pathways (Wnt and EGF) predicted to participate in vulval development. However, we also identified alleles of four additional genes that are dependent on the EGF pathway, but for which the molecular identity is not readily predicted from *C. elegans* studies. In the case of *Cbr-lin(gu167)*, we observed a slight increase in *Cbr-lin-3* transcript, a phenotype observed in *C. elegans* synMuv mutants. However, the remaining mutants exhibited normal or decreased levels of *Cbr-lin-3* transcript abundance. It is also worth noting that *Cbr-lin(gu167)* and *Cbr-lin(gu102)* are cold sensitive, which is different from *C. elegans* synMuv. Additional work is required to determine whether the new *C. briggsae* genes represent orthologs of genes known to modulate *C. elegans* vulval development or new genes that have no apparent function in homologous processes in *C. elegans*. In either case, the recovery of multiple additional genes argues that despite the similarity

between the species in their normal development, there are differences in the interactions and the relative functional contributions of the underlying genes and gene networks.

Although we have identified mutations in genes not predicted from work in *C. elegans*, we also failed to identify alleles of other genes. For example, we did not recover any dominant mutations that confer a Muv phenotype, such as *Cel-lin-12/Notch* or *Cel-lin-60/Ras* orthologs, as were recovered in *C. elegans* genetic screens (Greenwald et al. 1983; Beitel et al. 1990; Han et al. 1990). In *C. elegans*, a wide range of missense mutations in *Cel-lin-12/Notch* can confer a Muv phenotype, and at least seven distinct dominant *Cel-lin-12* alleles (*Cel-lin-12(d)*) have been recovered (Greenwald, Sternberg, and Horvitz 1983; Ferguson and Horvitz 1985; Greenwald and Seydoux 1990). Although the frequency of these alleles is unknown, recovery of such a large number of mutations suggests that the *Cel-lin-12* locus can be readily mutated in *C. elegans* to give rise to a Muv phenotype. One explanation for our failure to recover such alleles in *C. briggsae* could be the smaller size of our genetic screens and consequently fewer genomes that were searched. However, we did recover multiple alleles of four genes (see Table 1). Future experiments to engineer alleles into the *C. briggsae* genome that confer a dominant Muv phenotype in *C. elegans* will definitively test whether the absence of these alleles reflects sampling, or functional differences between the two species.

Genetic screens in two other leading nematode models, *Pristionchus pacificus* and *Oscheius tipulae*, have recovered mutations affecting vulval development (reviewed in Sommer 2005; Felix 2006). Such screens have demonstrated that EGF, Notch and Wnt signaling contribute to vulval development in these species as they do in *C. elegans* (Dichtel-Danjoy and Felix 2004; Zheng et al. 2005; Tian et al. 2008; Kienle and Sommer 2013). However in these species many differences in the specific effects or the relative contribution of different pathways, as well as the importance of other genes not identified in *C. elegans* screens, have been observed. Our work with *C. briggsae* argues that these features that reflect evolutionary constraints and flexibility are also apparent in species comparisons where there are not overt differences in the normal (wild type) developmental processes. Furthermore, we report the results from a systematic screen for genes that mutate to the Muv phenotype, rather than characterization of specific genes or mutants. This allows direct comparison to genetic screens in *C. elegans*, and a consideration of the potential of evolutionarily distinct genomes to yield mutants of a particular type.

Genomic evolution and functional genetic polymorphisms

Our work on *C. briggsae* vulval development genes addresses a long-standing question in comparative genomics of how the genotypes of different individuals or species lead to their phenotypes. In general, the well-established principle that sequence conservation relates to functional conservation guides

many analyses and interpretations of comparative data. However, application of this principle identifies only a subset of the genetic regions (and genes) that contribute to conserved phenotype. Indeed, much experimental work argues that many biological processes have a number of alternative but equal solutions, which allow for species to solve the same problem with different underlying genetic architecture. For example, hermaphroditism has evolved independently in *C. elegans* and *C. briggsae*, and some of the critical genetic changes responsible for this trait are distinct in the different species (Hill et al. 2006; Guo et al. 2009). In contrast, our work addresses the question of the potential for genomic evolution in the case where phenotype is conserved between species, termed as Developmental System Drift (DSD) (True and Haag 2001). We anticipate that further studies of the vulval development process between *C. elegans* and *C. briggsae* will uncover additional differences that underlie a common biological output.

ACKNOWLEDGMENTS

We thank many individuals who contributed to the generation of reagents and subsequent genetic analyses during the course of this study. These include Shahla Gharib, Jennifer Li, Keith Brown, Takao Inoue, Steven J. Billups, Bavithra Thillainathan, Nagagireesh Bojanala, and Ria Oommen. This work was supported by grants from the National Science and Engineering Research Council (NSERC) of Canada to BPG. Other funding sources include Pelotonia Undergraduate Research Fellowship to CJF, EMZ, KAW, and MEG; Research for Undergraduates in Mathematics and Biology Applications Fellowship (RUMBA) to CJF and EMZ; Ohio State Arts & Sciences Undergraduate Research Fellowship to KAW and MEG.

REFERENCES

- Beitel, G. J., Clark, S. G., Horvitz, H. R. 1990. *Caenorhabditis elegans* ras gene *let-60* acts as a switch in the pathway of vulval induction. *Nature* 348 (6301): 503–509.
- Beitel, G. J., Tuck, S., Greenwald, I., Horvitz, H. R. 1995. The *Caenorhabditis elegans* gene *lin-1* encodes an ETS-domain protein and defines a branch of the vulval induction pathway. *Genes Dev.* 9 (24): 3149–3162.
- Braendle, C., Felix, M. A. 2008. Plasticity and errors of a robust developmental system in different environments. *Dev. Cell* 15 (5): 714–724.
- Brenner, S. 1974. The genetics of *Caenorhabditis elegans*. *Genetics* 77: 71–94.
- Burdine, R. D., Branda, C. S., Stern, M. J. 1998. EGL-17(FGF) expression coordinates the attraction of the migrating sex myoblasts with vulval induction in *C. elegans*. *Development* 125 (6): 1083–1093.
- Ceol, C. J., Horvitz, H. R. 2001. *dpl-1* DP and *efl-1* E2F act with *lin-35* Rb to antagonize Ras signaling in *C. elegans* vulval development. *Mol. Cell* 7 (3): 461–473.
- Clark, S. G., Lu, X., Horvitz, H. R. 1994. The *Caenorhabditis elegans* locus *lin-15*, a negative regulator of a tyrosine kinase signaling pathway, encodes two different proteins. *Genetics* 137 (4): 987–997.
- Cui, M., Chen, J., Myers, T. R., Hwang, B. J., Sternberg, P. W., Greenwald, I., Han, M. 2006. SynMuv genes redundantly inhibit *lin-3/EGF* expression to prevent inappropriate vulval induction in *C. elegans*. *Dev. Cell* 10 (5): 667–672.
- Cutter, A. D. 2008. Divergence times in *Caenorhabditis* and *Drosophila* inferred from direct estimates of the neutral mutation rate. *Mol. Biol. Evol.* 25 (4): 778–786.
- Delattre, M., Felix, M. A. 2001. Polymorphism and evolution of vulval precursor cell lineages within two nematode genera, *Caenorhabditis* and *Oscheius*. *Curr. Biol.* 11 (9): 631–643.

Sharanya et al.

Multivulva mutants in *C. briggsae* 47

- Dichtel-Danjoy, M. L., Felix, M. A. 2004. The two steps of vulval induction in *Oscheius tipulae* CEW1 recruit common regulators including a MEK kinase. *Dev. Biol.* 265 (1): 113–126.
- Felix, M. A. 2006. *Oscheius tipulae*. WormBook ed. The C. elegans Research Community, WormBook, doi/10.1895/wormbook.1.119.1, <http://www.wormbook.org>.
- . 2007. Cryptic quantitative evolution of the vulva intercellular signaling network in *Caenorhabditis*. *Curr. Biol.* 17 (2): 103–114.
- Ferguson, E. L., Horvitz, H. R. 1985. Identification and characterization of 22 genes that affect the vulval cell lineages of the nematode *Caenorhabditis elegans*. *Genetics* 110 (1): 17–72.
- . 1989. The multivulva phenotype of certain *Caenorhabditis elegans* mutants results from defects in two functionally redundant pathways. *Genetics* 123 (1): 109–121.
- Ferguson, E. L., Sternberg, P. W., Horvitz, H. R. 1987. A genetic pathway for the specification of the vulval cell lineages of *Caenorhabditis elegans*. *Nature* 326 (6110): 259–267.
- Goneli, S. A., Hsiao, K., Lu, T., Simpson, D. 1998. U0126: A novel, selective and potent inhibitor of MAP kinase kinase (MEK). *Promega Notes* 69.
- Greenwald, I., Seydoux, G. 1990. Analysis of gain-of-function mutations of the *lin-12* gene of *Caenorhabditis elegans*. *Nature* 346 (6280): 197–199.
- Greenwald, I. S., Sternberg, P. W., Horvitz, H. R. 1983. The *lin-12* locus specifies cell fates in *Caenorhabditis elegans*. *Cell* 34 (2): 435–444.
- Guo, Y., Lang, S., Ellis, R. E. 2009. Independent recruitment of F box genes to regulate hermaphrodite development during nematode evolution. *Curr. Biol.* 19 (21): 1853–1860.
- Gupta, B. P., Johnsen, R., Chen, N. 2007. Genomics and biology of the nematode *Caenorhabditis briggsae*. WormBook ed. The C. elegans Research Community, WormBook, doi/10.1895/wormbook.1.136.1, <http://www.wormbook.org>.
- Han, M., Aroian, R. V., Sternberg, P. W. 1990. The *let-60* locus controls the switch between vulval and nonvulval cell fates in *Caenorhabditis elegans*. *Genetics* 126 (4): 899–913.
- Hill, R. C., de Carvalho, C. E., Salogiannis, J., Schlager, B., Pilgrim, D., Haag, E. S. 2006. Genetic flexibility in the convergent evolution of hermaphroditism in *Caenorhabditis* nematodes. *Dev. Cell* 10 (4): 531–538.
- Hillier, L. W., et al. 2007. Comparison of *C. elegans* and *C. briggsae* genome sequences reveals extensive conservation of chromosome organization and synteny. *PLoS Biol.* 5 (7): e167.
- Katz, W. S., Hill, R. J., Clandinin, T. R., Sternberg, P. W. 1995. Different levels of the *C. elegans* growth factor LIN-3 promote distinct vulval precursor fates. *Cell* 82 (2): 297–307.
- Kienle, S., Sommer, R. J. 2013. Cryptic variation in vulva development by cis-regulatory evolution of a HAIRY-binding site. *Nat. Commun.* 4: 1714.
- Kimble, J. 1981. Alterations in cell lineage following laser ablation of cells in the somatic gonad of *Caenorhabditis elegans*. *Dev. Biol.* 87 (2): 286–300.
- Koboldt, D. C., et al. 2010. A toolkit for rapid gene mapping in the nematode *Caenorhabditis briggsae*. *BMC Genomics* 11 (1): 236.
- Lu, X., Horvitz, H. R. 1998. *lin-35* and *lin-53*, two genes that antagonize a *C. elegans* Ras pathway, encode proteins similar to Rb and its binding protein RbAp48. *Cell* 95 (7): 981–991.
- Mello, C. C., Kramer, J. M., Stinchcomb, D., Ambros, V. 1991. Efficient gene transfer in *C. elegans*: Extrachromosomal maintenance and integration of transforming sequences. *EMBO J.* 10 (12): 3959–3970.
- Miller, L. M., Gallegos, M. E., Morisseau, B. A., Kim, S. K. 1993. *lin-31*, a *Caenorhabditis elegans* HNF-3/fork head transcription factor homolog, specifies three alternative cell fates in vulval development. *Genes Dev.* 7 (6): 933–947.
- Reiner, D. J., Gonzalez-Perez, V., Der, C. J., Cox, A. D. 2008. Use of *Caenorhabditis elegans* to evaluate inhibitors of Ras function *in vivo*. *Methods Enzymol.* 439: 425–449.
- Ross, J. A., et al. 2011. *Caenorhabditis briggsae* recombinant inbred line genotypes reveal inter-strain incompatibility and the evolution of recombination. *PLoS Genet.* 7 (7): e1002174.
- Saffer, A. M., Kim, D. H., van Oudenaarden, A., Horvitz, H. R. 2011. The *Caenorhabditis elegans* synthetic multivulva genes prevent ras pathway activation by tightly repressing global ectopic expression of *lin-3* EGF. *PLoS Genet.* 7 (12): e1002418.
- Sawa, H., Korswagen, H. C. 2013. Wnt signaling in *C. elegans*. WormBook ed. The C. elegans Research Community, WormBook, doi/10.1895/wormbook.1.7.2, <http://www.wormbook.org>.
- Seetharaman, A., Cumbo, P., Bojarala, N., Gupta, B. P. 2010. Conserved mechanism of Wnt signaling function in the specification of vulval precursor fates in *C. elegans* and *C. briggsae*. *Dev. Biol.* 346 (1): 128–139.
- Sharanya, D., et al. 2012. Genetic control of vulval development in *Caenorhabditis briggsae*. *G3 (Bethesda)* 2 (12): 1625–1641.
- Sommer, R. J. 2005. Evolution of development in nematodes related to *C. elegans*. WormBook ed. The C. elegans Research Community, WormBook, doi/10.1895/wormbook.1.46.1, <http://www.wormbook.org>.
- Stein L.D., et al. 2003. The genome sequence of *Caenorhabditis briggsae*: a platform for comparative genomics. *PLoS Biol.* 1 (2): E45.
- Stern, D. L., Orgogozo, V. 2008. The loci of evolution: how predictable is genetic evolution?. *Evolution* 62 (9): 2155–2177.
- Sternberg, P. W. 1988. Lateral inhibition during vulval induction in *Caenorhabditis elegans*. *Nature* 335 (6190): 551–554.
- . 2005. Vulval development. WormBook ed. The C. elegans Research Community, Wormbook doi/10.1895/wormbook.1.6.1, <http://www.wormbook.org>.
- Sternberg, P. W., Horvitz, H. R. 1986. Pattern formation during vulval development in *C. elegans*. *Cell* 44 (5): 761–772.
- . 1989. The combined action of two intercellular signaling pathways specifies three cell fates during vulval induction in *C. elegans*. *Cell* 58 (4): 679–693.
- Stiernagle, T. 2006. Maintenance of *C. elegans*. WormBook 1–11.
- Sulston, J. E., White, J. G. 1980. Regulation and cell autonomy during postembryonic development of *Caenorhabditis elegans*. *Dev. Biol.* 78 (2): 577–597.
- Sundaram M. V. 2013. Canonical RTK-Ras-ERK signaling and related alternative pathways. WormBook ed. The C. elegans Research Community, Wormbook doi/10.1895/wormbook.1.80.2 <http://www.wormbook.org>.
- Thomas, J. H., Ceol, C. J., Schwartz, H. T., Horvitz, H. R. 2003. New genes that interact with *lin-35* Rb to negatively regulate the *let-60* ras pathway in *Caenorhabditis elegans*. *Genetics* 164 (1): 135–151.
- Tian, H., Schlager, B., Xiao, H., Sommer, R. J. 2008. Wnt signaling induces vulva development in the nematode *Pristionchus pacificus*. *Curr. Biol.* 18 (2): 142–146.
- True, J., Haag, E. 2001. Developmental system drift and flexibility in evolutionary trajectories. *Evol. Dev.* 3: 109–119.
- Tsong, A. E., Tuch, B. B., Li, H., Johnson, A. D. 2006. Evolution of alternative transcriptional circuits with identical logic. *Nature* 443 (7110): 415–420.
- Wei, Q., Shen, Y., Chen, X., Shifman, Y., Ellis, R. E. 2014. Rapid creation of forward-genetics tools for *C. briggsae* using TALENs: Lessons for nonmodel organisms. *Mol. Biol. Evol.* 31 (2): 468–473.
- Wicks, S. R., Yeh, R. T., Gish, W. R., Waterston, R. H., Plasterk, R. H. 2001. Rapid gene mapping in *Caenorhabditis elegans* using a high density polymorphism map. *Nat. Genet.* 28 (2): 160–164.
- Wood, W. B. 1988. *The nematode Caenorhabditis elegans*. In W. B. Wood (ed.), Cold Spring Harbor Laboratory Press, New York.
- Zhao, Z., et al. 2010. New tools for investigating the comparative biology of *Caenorhabditis briggsae* and *C. elegans*. *Genetics* 184 3 853–863.
- Zheng, M., Messerschmidt, D., Jungblut, B., Sommer, R. J. 2005. Conservation and diversification of Wnt signaling function during the evolution of nematode vulva development. *Nat. Genet.* 37 3 300–304.

SUPPORTING INFORMATION

Additional supporting information may be found in the online version of this article at the publisher's web-site.

Table S1. Linkage tests for three of the Muv mutants using phenotypic markers.

48 EVOLUTION & DEVELOPMENT Vol. 17, No. 1, January–February 2015

Table S2. Complementation matrix of *C. briggsae* Muv mutants used in this study.

Table S3. Map data for HK104 introgressed *C. briggsae* Muv mutant strains (pooled DNA from at least 3 different lines, each 5 times introgressed).

Table S4. Map data for HK104 introgressed *C. briggsae* Muv mutants.

Table S5. List of primers and sequences used in this study.

Table S6. Lateral signaling is mostly intact in Muv mutants.

Supplementary Table 1.

Linkage tests for three of the Muv mutants using phenotypic markers. The phenotype was scored in the F2 generation.

Chr	Marker	<i>sy5342</i>	<i>sa993</i>	<i>sy5216</i>	<i>gul67</i>
1	<i>Cbr-sma(sy5330)</i>	5 of 18 Muv 12 of 48 Muv*	7 of 28 Muv	-	-
2	<i>Cbr-unc-4(sy5341)</i>	0 of 29 Muv	-	-	-
	<i>Cbr-dpy(sy5148)</i>	4 of 100 Muv	13 of 51 Muv	-	-
3	<i>Cbr-dpy-1(sy5022)</i>	10 of 42 Muv	10 of 27 Muv	-	-
	<i>Cbr-daf-4(sa973)</i>	-	-	-	-
4	<i>Cbr-unc-22(s1270)</i>	-	5 of 53 Muv	7 of 15 non-Unc	0 of 53 Muv 0 of 367 Muv**
X	<i>Cbr-unc(sy5329)</i>	6 of 34 Muv	8 of 31 Muv	-	-

*used *sy5344* allele

**used *Cbr-unc-22(gu205)* allele

Supplementary Table 2.
Complementation matrix of *C. briggsae* Muv mutants used in this study.

	<i>gu137</i>	<i>sy5353</i>	<i>sy5342</i>	<i>sy5344</i>	<i>gu138</i>	<i>gu162</i>	<i>gu198</i>	<i>sa993</i>	<i>gu163</i>	<i>sy5216</i>	<i>gu167</i>	<i>gu102</i>	<i>gu168</i>
<i>gu137/+</i>	11 (190)					0 (36)	0 (28)				0 (55)	0 (53)	0 (33)
<i>sy5353/+</i>	25 (20), 10 (82)	X	0 (32)	X				0 (24) ²	0 (88)	X			
<i>sy5342/+</i>			X	46 (28) ⁵	8 (60)	36 (22)		0 (13) ²					
<i>sy5344/+</i>			0 (37), 0 (34) ⁶	X		51 (45)				X			0 (33)
<i>gu138/+</i>			47 (100) ⁴		X	0 (40)	X			0 (76)	0 (44)		0 (44)
<i>lin9/+</i>					0 (47)		7.7 (65)	X					
<i>sa993/+</i>		0 (36) ⁵					18 (33) ⁹	X	0 (98)	X	0 (57)		
<i>gu163/+</i>					48 (23)	0 (41)		0 (98)	44 (160)				0 (40)
<i>sy5216/+</i>		0 (30) ⁷	0 (35) ⁴	0 (30) ⁵			X	0 (15)	0 (101)	X	0 (102)	0 (111)	
<i>sy5392/+</i>		0 (28)	0 (36)	0 (36)				0 (20) ²		44 (106) ⁸			
<i>gu167/+</i>						0 (23)	0 (48)	0 (22), 0 (168) ²		0 (37), 3 (118) ³	26 (243)	21 (73)	0 (39)
<i>gu102/+</i>						0 (39)	0 (36)					6 (53)	37 (49)
<i>gu168/+</i>			X		0 (31)	0 (45)							
	<i>gu137</i>	<i>sy5353</i>	<i>sy5342</i>	<i>sy5344</i>	<i>gu138</i>	<i>gu162</i>	<i>gu198</i>	<i>sa993</i>	<i>gu163</i>	<i>sy5216</i>	<i>gu167</i>	<i>gu102</i>	<i>gu168</i>

Complementation experiments were performed for several, but not all, mutants. In each case data is represented as the percentage of animals showing mutant phenotype. The number of animals examined in each case is inside the parenthesis. 'X' denotes combinations that were either irrelevant or tested in reciprocal crosses.

¹*Cbr-sma-6(sy5148) Cbr-lin-31(sy5344)*
²*Cbr-unc-22(s1270) Cbr-lin-1(sa993)*
³*Cbr-dpy(sy5027) Cbr-lin(sy5216)*
⁴*Cbr-sma-6(sy5148) Cbr-lin-31(sy5342)*
⁵*Cbr-unc-22(s1270) Cbr-lin-31(sy5344)*
⁶*Cbr-sma-6(sy5148) Cbr-dpy-1(sy5411)*
⁷*Cbr-unc-22(s1270) Cbr-dpy-1(sy5353)*
⁸*Cbr-unc-4(sy5341); Cbr-lin(sy5216)*
⁹*Cbr-lin-1(gu198); Cbr-dpy(gu109)*

Supplementary Table 3.

Map data for HK104 introgressed *C. briggsae* Muv mutant strains (pooled DNA from at least 3 different lines, each 5 times introgressed). The pooled strains are the same as those evaluated individually in Supplementary Table 4. Markers linked to each mutation are highlighted.

	I			II			III			IV			V		
	LEFT (bhP19)	CENTER (bhP1)	RIGHT (bhP29)	LEFT (bhP2)	CENTER (bhP21)	RIGHT (bhP8)	LEFT (bhP14)	CENTER (bhP12)	RIGHT (bhP40)	LEFT (bhP15)	CENTER (bhP11)	RIGHT (bhP9)	LEFT (bhP31)	CENTER (bhP5)	RIGHT (bhP24)
<i>gu198</i>	HK104	HK104	HK104	HET	HK104	HK104	HET	HK104	HET	HK104	AF16	AF16	HET	HK104	HK104
<i>gu163</i>	AF16	HK104	HK104	HET	HET	HK104	HET	HET	HK104	N/A	HET	N/A	N/A	HK104	HK104
<i>gu167</i>	N/A	N/A	N/A	N/A	N/A	N/A	N/A	N/A	N/A	N/A	AF16	AF16	N/A	HK104	N/A
<i>gu102</i>	N/A	HK104	N/A	HET	HK104	HK104	HET	HET	HK104	HET	N/A	N/A	HET	AF16	HK104

N/A no mapping data available
HET both AF16 and HK104 PCR product
AF16 AF16 PCR product
HK104 HK104 PCR product

Supplementary Table 4.Map data for HK104 introgressed *C. briggsae* Muv mutants.

Individual lines were tested for their linkage with selected polymorphisms described in Kobaltdt et al. (2008) study.

Grey-shaded regions indicate the location of the mutation.

N/A No data available
 AF16 AF16 PCR product
 HK104 HK104 PCR product
 HET AF16 and HK104 PCR products

gu163 (total 5 lines, each 5 rounds introgressed)

LGI	bhP19	cb-s179	cb-s13	cb-s79	cb-s360	bhP43	cb-s71	cb-s191	cb-s211
line	0.02 Mb	0.26 Mb	0.59 Mb	1.47 Mb	2.55 Mb	3.31 Mb	5.77 Mb	10.03 Mb	11.58 Mb
B	AF16	HK104	HK104						
C	AF16	AF16	AF16	AF16	HK104	HK104	HK104	N/A	HK104
E	AF16	HK104	HK104						
F	AF16	N/A	HK104						
G	AF16	AF16	AF16	HK104	HK104	AF16	AF16	N/A	AF16

sy5216 (total 9 lines, each 6 rounds introgressed)

LGI	cb-m177	cb-m167	cb-m64	cb-m172	cb-m72	cb-m171
line	2.6 Mb	5.1 Mb	8.7 Mb	10.3 Mb	11.1 Mb	14.5 Mb
C2-6	AF16	AF16	AF16	AF16	AF16	HK104
5-4	HK104	HK104	AF16	AF16	AF16	HET
2-1	HK104	HK104	AF16	AF16	AF16	AF16
C6-2	HK104	AF16	AF16	AF16	AF16	HK104
C6-3	HK104	HK104	AF16	AF16	AF16	AF16
4-4	HK104	AF16	AF16	AF16	AF16	AF16
1-1	HK104	HK104	AF16	AF16	AF16	AF16
C1-2	HK104	AF16	AF16	AF16	AF16	HK104
C6-1	HK104	AF16	AF16	AF16	AF16	HK104

gu167 (total 3 lines, each 5 rounds introgressed)

LGI	cb-s323	cb-s87	cb-s96	cb-s98	cb-s40	cb-s140	bhP9	bhP11	cb-s84
line	5.52 Mb	6.70 Mb	7.72 Mb	8.69 Mb	11.26 Mb	12.37 Mb	12.52 Mb	13.68 Mb	15.46 Mb
A	HK104	AF16	AF16	AF16	AF16	AF16	AF16	AF16	HK104
C	HK104	HK104	HK104	AF16	AF16	HET	AF16	AF16	HET
E	AF16	AF16	AF16	AF16	AF16	HET	AF16	AF16	HK104

gu102 (total 7 lines, each 5 rounds introgressed)

LGI	cb-s381	bhP37	cb-s154	cb-s153	cb-s307	cb-s310	cb-s76	bhP5	bhP48
line	9 Mb	9 Mb	10.34 Mb	11.05 Mb	12.45 Mb	13.29 Mb	14.54 Mb	14.72 Mb	16.12 Mb
A	AF16	AF16	AF16	AF16	AF16	AF16	AF16	AF16	AF16
B	HK104	HK104	AF16						
C	AF16	AF16	AF16	HK104	AF16	AF16	AF16	AF16	AF16
E	AF16	AF16	AF16	HK104	HK104	AF16	HK104	HK104	HK104
I	AF16	AF16	N/A	AF16	AF16	AF16	AF16	AF16	HET
J	N/A	HK104	N/A	HK104	AF16	AF16	AF16	AF16	HET
K	AF16	AF16	N/A	AF16	HK104	AF16	HK104	HK104	HK104

Supplementary Table 5.

List of primers and sequences used in this study.

GL729	GAGATGAACGTCTCGGAACTGA
GL730	CATTTTTATAGGTACAGTCGGTG
GL731	GACGCCTATCACCTCTGGA
GL732	CTCGCGTTAAAATTGAGCTAGAG
GL733	CTCAGCTTAAAATTGAGCTAGA
GL734	AGCTAGAGATATGAAAATAGTACCG
GL824	AGGGCTGTAACCTCGCTTC
GL909	GTACCCGGTGTTGGGATAG
GL910	TATGTGCCACCAGAAGC
GL911	GTGGTTCCTTCTTGCCATTGTCC
GL912	GAACGAAGAGTTGCGCCGTG
GL926	ATGCCGAGACCCGAAAAGACTCT TACGATG
GL927	AGGAGCCGAGATAATTGAGCTCAAAC TTC
GL928	GATTCAATACTAAACGACGAGTTGAACCCAGCG
GL929	ATGCACCACTCCTCTTCTC

Supplementary Table 6.

Lateral signaling is mostly intact in Muv mutants.

Adjacent 1^o VPCs, as judged by the expression of molecular markers *Cel-zmp-1::gfp* and *Cel-daf-6::yfp*, are rarely observed in mutant animals.

Strain	Adjacent 1 ^o *	Adjacent 2 ^o ^S
<i>Cbr-lin-31(sy5342)</i>	0% (0/146) 0% (0/152) [#]	60% (120/200)
<i>Cel-lin-31(n301)</i>	0% (0/123) [#]	28.5% (39/137)
<i>Cbr-lin-1(sa993)</i>	6.3% (8/126)	9.5% (14/147)
<i>Cbr-lin-1(gu198)</i>	0% (0/75) [#]	12.8% (14/109)
<i>Cbr-lin(gu163)</i>	0% (0/111)	13.5% (15/111)
<i>Cbr-lin(sy5216)</i>	2.1% (3/143) 0.6% (1/162) [#]	24.7% (39/158)
<i>Cbr-lin(gu167)</i>	0% (0/143)	6.8% (10/147)
<i>Cbr-lin(gu167)[†]</i>	0% (0/102)	6% (8/133)
<i>Cbr-lin(gu102)</i>	0% (0/150)	19.5% (36/185)
<i>Cbr-lin(gu102)[†]</i>	0% (0/116)	10.7% (11/103)

[†]Grown at room temperature (23° C)

*based on *Cel-zmp-1::gfp*

[#]based on *Cel-daf-6::yfp*

^Sbased on *Cel-egl-17::gfp*

CHAPTER 5: GENOME EDITING IN *CAENORHABDITIS BRIGGSAE* USING THE CRISPR/CAS9 SYSTEM

Preface:

This chapter consists of the manuscript in preparation for publication entitled “*Genome Editing in Caenorhabditis briggsae using the CRISPR/Cas9 System*” by Elizabeth Culp, Cory Richman, Devika Sharanya and Bhagwati P Gupta (doi: <http://dx.doi.org/10.1101/021121>). This article has been made available in the preprint server bioRxiv, an online archive and distribution service for unpublished preprints until it is ready for publication.

This study describes how CRISPR/cas9 system can be used to generate targeted mutations in *C. briggsae* and the various limitations in the methodology. We show that CRISPR/Cas9 works in *C. briggsae* resulting in the generation of loss of function mutants for genes *Cbr-unc-22*, *Cbr-unc-119*, *Cbr-bar-1* and *Cbr-dpy-1* through NHEJ. As in *C. elegans*, the presence of sgRNA with 3'GG motif adjacent to the PAM site improved the efficiency of targeted mutations and interestingly the frequency of insertion events was higher in *C. briggsae* compared to *C. elegans*. A PCR-based screening approach has also been established to increase screening sensitivity for mutants like *Cbr-vit-2* which have no obvious phenotypes. Some limitations have been identified with respect of sgRNA design and targeted mutagenesis with homology directed repair.

Contributions:

The CRIPSR protocol was earlier developed in the Gupta lab by Cory Richman who generated mutant alleles for *Cbr-unc-22* and *Cbr-dpy-1*. Subsequently, Elizabeth Culp performed experiments involving donor vectors, single stranded oligonucleotides (ssODN) with restriction enzyme sites, PCR screening, 3'GG motif sgRNAs along with microinjections for *Cbr-bar-1*, *Cbr-unc-119*, *Cbr-lin-2*, *Cbr-lin-7*, *Cbr-lin-10*, *Cbr-lin-17*, *Cbr-lin-18* and *Cbr-vit-2*. I provided technical guidance and generated the expression plasmid for the donor vector for *Cbr-bar-1* and data for ssODN for *Cbr-lin-17* along with the microinjections. The manuscript was written by Elizabeth Culp and Bhagwati Gupta, with inputs from myself, Cory Richman and Ayush Ranawade.

bioRxiv preprint first posted online June 18, 2015; doi: <http://dx.doi.org/10.1101/021121>; The copyright holder for this preprint is the author/funder. It is made available under a [CC-BY 4.0 International license](#).

1 **Genome Editing in *Caenorhabditis briggsae* using the CRISPR/Cas9 System**

2

3 Elizabeth Culp¹, Cory Richman¹, Devika Sharanya and Bhagwati P Gupta *

4 Department of Biology, McMaster University, 1280 Main Street West, Hamilton, ON L8S-4K1,

5 Canada

6

7

8 ¹Co-first authors

9 *Corresponding author. Email: guptab@mcmaster.ca, Phone: 905-525-9140 x26451

10

11 **Keywords:** CRISPR/Cas9, genome editing, nematode, *C. briggsae*

12

bioRxiv preprint first posted online June 18, 2015; doi: <http://dx.doi.org/10.1101/021121>; The copyright holder for this preprint is the author/funder. It is made available under a [CC-BY 4.0 International license](#).

1 **Author Summary**

2 The CRISPR/Cas9 system has recently emerged as a powerful tool to engineer the genome of an
3 organism. The system is adopted from bacteria where it confers immunity against invading
4 foreign DNA. This work reports the first successful use of the CRISPR/Cas9 system in *C.*
5 *briggsae*, a cousin of the well-known nematode *C. elegans*. We used two plasmids, one
6 expressing Cas9 endonuclease and the other an engineered CRISPR RNA corresponding to the
7 DNA sequence to be cleaved. Our approach allows for the generation of loss-of-function
8 mutations in *C. briggsae* genes thereby facilitating a comparative study of gene function between
9 nematodes.

10

11

12 **Abstract**

13 The CRISPR/Cas9 system is an efficient technique for generating targeted alterations in an
14 organism's genome. Here we describe a methodology for using the CRISPR/Cas9 system to
15 generate mutations via non-homologous end joining in the nematode *Caenorhabditis briggsae*, a
16 sister species of *C. elegans*. Evidence for somatic mutations and off-target mutations are also
17 reported. The use of the CRISPR/Cas9 system in *C. briggsae* will greatly facilitate comparative
18 studies to *C. elegans*.

bioRxiv preprint first posted online June 18, 2015; doi: <http://dx.doi.org/10.1101/021121>; The copyright holder for this preprint is the author/funder. It is made available under a [CC-BY 4.0 International license](#).

1 Linking genotype and phenotype is an important step in the characterization of a gene. Targeted
2 genome editing, defined as the creation of alterations at specific sites in an organism's genome, is
3 a powerful means to study the relationship between gene and phenotype. Genome editing
4 techniques are based on guiding an endonuclease to a specific target in the genome in order to
5 generate a double strand break (DSB) [1-3]. Breaks are subsequently repaired by either error
6 prone non-homologous end joining (NHEJ) or template-directed homologous recombination
7 (HR) [4]. While the former introduces random mutations at the point of cleavage, the latter can
8 be used to generate specific alterations based on the presence of a donor sequence. Although
9 several technologies currently exist for genome editing, such as zinc finger nucleases (ZFN) and
10 transcription activator-like effector nucleases (TALEN), these techniques leave room for
11 improvement in their ease of use, as each new sequence to be targeted requires the labor intensive
12 process of generating a new protein construct [2].

13 Clustered, regularly interspaced, short palindromic repeats (CRISPR) and CRISPR-
14 associated (Cas) systems are adaptive immune mechanisms evolved by archaea and bacteria to
15 defend against foreign plasmids and viral DNA [5]. Manipulation of the *Streptococcus pyrogenes*
16 type II CRISPR/Cas system has been used to develop an efficient genome editing technique.
17 First, a 20 bp sequence in a gene of interest is selected to act as a guide for the *S. pyrogenes*
18 nuclease, Cas9. This sequence, termed the CRISPR RNA (crRNA), has the only requirement that
19 it must precede a Protospacer Adjacent Motif (PAM) of the form 3'NGG [6]. Next, a second
20 RNA molecule, termed the trans-activating crRNA (tracrRNA), is used for binding to Cas9 [6].
21 For the purpose of experimental simplification, the crRNA and tracrRNA sequences can be fused
22 into a single guide RNA (sgRNA) [7]. By expressing this sgRNA along with Cas9 in germ line
23 cells, heritable genome mutations can be created.

24 The CRISPR/Cas9 system has been successfully established in two leading nematode
25 models – *C. elegans* and *Pristionchus pacificus* [2, 8]. Friedland *et al.* [9] developed a simple
26 protocol for *C. elegans* that involved injecting plasmids into the gonad of adult hermaphrodites.
27 The authors modified Cas9 to include a SV40 NLS to ensure nuclear localization and expressed
28 under an *eft-3* translation elongation factor promoter, chosen for its effectiveness in germ line
29 expression. The sgRNAs were expressed under a U6 small nuclear RNA polymerase III

bioRxiv preprint first posted online June 18, 2015; doi: <http://dx.doi.org/10.1101/021121>; The copyright holder for this preprint is the author/funder. It is made available under a [CC-BY 4.0 International license](#).

1 promoter, chosen for its ability to drive expression of small RNAs. As the optimal expression
2 from this promoter requires the first base to be a purine, the sgRNA target sequence is restricted
3 to the form (G/A)(N)₁₉NGG [9, 10].

4 Adaptation of CRISPR/Cas9 to *C. briggsae*, a species that is closely related to *C. elegans*,
5 would provide a powerful tool to investigate the function of any given gene. *C. briggsae* is used
6 routinely by many laboratories in comparative evolutionary studies. The two animals diverged
7 less than 30 million years ago yet share similar morphology [11]. A comparison of their genome
8 sequences has revealed that roughly one-quarter of their genes lack clear orthologs including
9 many that are highly divergent and species-specific [12]. This suggests that underlying gene
10 networks have evolved substantially without an obvious change in phenotype [13]. Such changes
11 are likely to have significant impacts and may confer unique advantages on animals to withstand
12 genetic and environmental fluctuations. By generating mutations in *C. briggsae* genes and
13 characterizing phenotypes, we can learn the functional relevance of genomic differences,
14 including any alterations in genetic pathways and developmental mechanisms between the two
15 species. With this goal in mind, we set out to develop a method for using this system in *C.*
16 *briggsae*.

17 The wild type AF16 strain was used as a reference strain in all experiments. Strains
18 generated as part of this study include DY503 *Cbr-unc-22(bh29)*, DY504 *Cbr-dpy-1(bh30)*,
19 DY530 *Cbr-bar-1(bh31)*, DY544 *Cbr-unc-119(bh34)* and DY545 *Cbr-unc-119(bh35)*.

20 We first used the CRISPR/Cas9 system in *C. briggsae* in an attempt to generate targeted
21 loss-of-function mutations by employing NHEJ. For this, two conserved genes were chosen
22 based on visible phenotypes, *Cbr-dpy-1*, a cuticle protein causing a dumpy (Dpy) phenotype, and
23 *Cbr-unc-22*, a twitchin homolog causing an uncoordinated (Unc) phenotype [14-16]. Target
24 sgRNA sequences following the form G/A(N)₁₉NGG were searched for in the exonic regions of
25 these genes using the ZiFiT Targeter Version 4.2 software [17]. The sgRNA sites were screened
26 based on predicted efficiency using empirically based scoring algorithms. Off-target sites were
27 minimized using the sgRNAs9 software package developed by Xie *et al.* [18].

28 The plasmids containing the *C. elegans* U6 promoter and sgRNA target sequences were
29 generated by site-directed mutagenesis. This was accomplished using either two-step overlap-

4

bioRxiv preprint first posted online June 18, 2015; doi: <http://dx.doi.org/10.1101/021121>; The copyright holder for this preprint is the author/funder. It is made available under a [CC-BY 4.0 International license](https://creativecommons.org/licenses/by/4.0/).

1 extension PCR on a *pU6::Cbr-unc-119_sgrNA* template (gift from John Calarco, Addgene
2 plasmid #46169) [9], or Q5 site-directed mutagenesis on a *pU6::Cbr-lin-10_sgrNA* template [19]
3 using the NEB Q5 site-directed mutagenesis kit (E0554). The target site substitution was
4 confirmed by *AclI* digestion. See Tables S1 and S2 for sgRNA sites and primers used in this
5 study.

6 The plasmids sgRNA and Cas9 (*Peft-3::Cas9-SV40 NLS::tbb-2 3'UTR*, also from John
7 Calarco, Addgene #46168) were injected into the germline of young adults using standard
8 methods [20] and F1 progeny displaying the co-injection marker, pharyngeal expression of GFP,
9 were isolated onto separate plates. Injection mixes contained *pU6::sgRNA* (100 ng/ul), *Peft-*
10 *3::Cas9-SV40 NLS::tbb-2 3'UTR* (100 ng/ul), and *myo-2::GFP* (10 ng/ul).

11 Following microinjection, F2 worms were screened for desired phenotypes. We
12 successfully isolated mutants for both *Cbr-dpy-1* and *Cbr-unc-22* at comparable frequencies to
13 those observed in *C. elegans* (Table 1) [9]. Sequencing of the alleles of each of these genes
14 revealed insertions and deletions at the sgRNA target sites (Table 2). The phenotypes of mutant
15 animals are indistinguishable from those in *C. elegans* corresponding to orthologous genes,
16 demonstrating conservation of gene function. Together, these results show that the CRISPR/Cas9
17 system works in *C. briggsae* and can utilize conserved *C. elegans* promoters to express sgRNAs
18 and Cas9.

19 Next, we targeted six other conserved genes of the Wnt and Ras pathways (*Cbr-lin-2*,
20 *Cbr-lin-7*, *Cbr-lin-10*, *Cbr-lin-17*, *Cbr-lin-18* and *Cbr-vit-2*). For the PCR-based assay [19] F1s
21 were allowed to lay eggs for 24-36 hours, and then picked and lysed in pools of two. A region of
22 the genomic DNA spanning the sgRNA site (~200 bp) was amplified and examined on a 4%
23 high-resolution agarose gel (Invitrogen UltraPure Agarose-1000, Catalog #16550-100) for
24 changes in band sizes (Figure S2). In some cases we recovered mutations as determined by
25 phenotypic as well as PCR-based screening approaches but none were found to be heritable
26 (Table 1). It is unclear to us whether it was due to sgRNAs being non-functional, less efficient or
27 requiring much larger F1s to be screened. Similar results were previously reported in *C. elegans*
28 [21]. In one case, *Cbr-lin-17*, we sequenced the animal that showed bi-vulva phenotype and
29 found possible evidence for a somatic mutation (T/A transversion causing M482L substitution).

5

bioRxiv preprint first posted online June 18, 2015; doi: <http://dx.doi.org/10.1101/021121>; The copyright holder for this preprint is the author/funder. It is made available under a [CC-BY 4.0 International license](https://creativecommons.org/licenses/by/4.0/).

1 The bi-vulva phenotype in this line was lost in subsequent generations. Evidence of somatic
2 mutations has also been described in *C. elegans* [21].

3

Screening Approach	Targeted Gene	3' Target bases	Visible phenotype	Frequency of mutations	Animals screened
Phenotypic screening	<i>Cbr-bar-1</i>	GG	Egl	9.5%	22
	<i>Cbr-dpy-1</i>	GA	Dpy	2.8%	35
	<i>Cbr-lin-2</i>	UA	Vul	0	40
	<i>Cbr-lin-7</i>	GA	Vul*	0	44
	<i>Cbr-lin-10</i>	AC	Vul	0	161
	<i>Cbr-lin-17</i>	AC	Bivulva	0	63
	<i>Cbr-lin-17</i> (linear sgRNA)	AC	Bivulva [#]	0	3
	<i>Cbr-lin-18</i>	AG	Bivulva [§]	0	65
	<i>Cbr-unc-22</i>	UC	Unc	2.5%	40
	<i>Cbr-unc-119</i> (sgRNA #1)	TT	Unc	0	48
	<i>Cbr-unc-119</i> (sgRNA #2)	GG	Unc	11.1%	54
	PCR-based screening	<i>Cbr-lin-7</i>	GA	Vul	0
<i>Cbr-lin-10</i>		AC	Vul	0	126
<i>Cbr-vit-2</i>		AG	WT [@]	1.3%	78

Table 1. Phenotypes of transgenic animals generated using the CRISPR/Cas9 technique. The 3' target bases are those at positions 19 and 20 in the sgRNA target sequence. *One F2 showed Dpy phenotype. [#]3 bivulva worms were recovered in F3 but the phenotype was not heritable. [§]One F2 showed protruding vulva (Pvl) phenotype. [@]wild type based on the *C. elegans vit-2* mutant phenotype.

4

5 Interestingly, our screens also recovered worms with unexpected phenotypes, e.g., Dpy in
6 *Cbr-lin-7* screen (Table 1). Sequencing of these worms revealed no disruption in targeted genes,
7 raising the possibility of off-target effects of CRISPR/Cas9. Off target effects have been reported
8 in *C. elegans* as well as several other models including *Drosophila*, mice, zebrafish, and human
9 cell lines [22-25].

10 The sgRNAs with a 3'GG motif at positions 19 and 20 were recently shown to
11 significantly enhance the efficiency of targeted mutations in *C. elegans* [21](23). To test whether
12 a similar sequence structure could be effective in *C. briggsae* we selected two conserved genes

6

bioRxiv preprint first posted online June 18, 2015; doi: <http://dx.doi.org/10.1101/021121>; The copyright holder for this preprint is the author/funder. It is made available under a [CC-BY 4.0 International license](#).

1 *Cbr-unc-119* and *Cbr-bar-1*. Mutations in *Cbr-unc-119* with Unc phenotype were recovered at a
 2 frequency of 11.1% (Tables 1 and 2). In contrast, another sgRNA for *Cbr-unc-119* that lacked 3'
 3 GG motif did not give rise to any mutation (Table 1). In the case of *Cbr-bar-1*, a β -catenin
 4 homolog [26], the 3'GG motif sgRNA resulted in a disruption efficiency of 9.5% (Tables 1 and
 5 2). The enhanced efficiency of the 3'GG motif sgRNA sites for these two genes suggests that
 6 such an approach in *C. briggsae* could improve the frequency of targeted mutations in genes of
 7 interest.

8

Strain	Sequence	Mutation
<i>Cbr-bar-1(bh31)</i>	AAGGTCAAGTTTGTGAAGATGGG AGG ACC ACAGAA	8bp deletion
<i>Cbr-bar-1(bh33)</i>	TTGTGAAGA ACTCCTTGATGACGTTTTTC TTGGGAGG	21bp insertion
<i>Cbr-bar-1(bh36)</i> *	GTCAAGTTTGTGAAGA [147 bases] TGGGT ATCGG AC	150bp insertion, 3bp deletion
<i>Cbr-dpy-1(bh30)</i>	GTGCTGATCATTGTGAATCTCAGTTCGGT GTAGGTCGTTTCGCTCCA ACTGATGG	31bp insertion, 1bp deletion
<i>Cbr-unc-22(bh29)</i>	GTTGAGAACTCTGTTGGATCTGATTC TGGA ATCG	5bp deletion
<i>Cbr-unc-119(bh34)</i>	CGACGGGAAGGTCGCCGAGCGACGGGAAGG TCGCCGACGGG TGGA ATC	17bp insertion, 1bp deletion
<i>Cbr-unc-119(bh35)</i>	GCGACGGGAAGGTCGCCGAGCTTTCGGG TG GAATC	3bp insertion, 1bp deletion

Table 2. Alleles generated by the CRISPR/Cas9 approach. The DNA sequence includes the sgRNA target. The PAM site is bolded. Insertion and deletion sequences are underlined (dotted underline: insertion, solid underline: deletion). For clarity the 147 base pair inserted sequence in *bh36* allele has been omitted. This long sequence matches with the *E. coli* gene EF-Tu. *The allele was recovered in a separate screen along with another allele *bh32* that has small deletion. The exact base change in *bh32* has not been determined.

9

10 In addition to the CRISPR-mediated NHEJ approach we also attempted the HR method of
 11 gene editing in *C. briggsae*. For this donor templates were designed to either disrupt a gene (by
 12 inserting a single-stranded oligonucleotide) or tag genes using double-stranded linear PCR

7

bioRxiv preprint first posted online June 18, 2015; doi: <http://dx.doi.org/10.1101/021121>; The copyright holder for this preprint is the author/funder. It is made available under a [CC-BY 4.0 International license](#).

1 amplicons (or plasmids) of fluorescent reporters (GFP and dsRED). Specifically, the single strand
 2 oligonucleotide donor templates were intended to insert a 22 bp sequence containing an *NcoI*
 3 restriction enzyme site into *Cbr-bar-1* and *Cbr-lin-15B* (Figure S1B). Homology arms of length
 4 75 and 49 bases were chosen directly overlapping the sgRNA site, based on previous results [19].
 5 The double-stranded linear donor templates of *GFP* (864 bp) and *dsRED* (830 bp) containing
 6 short microhomology arms were generated by PCR to create translational fusions with *Cbr-bar-1*
 7 and *Cbr-vit-2*, respectively (Figure S1C). The donor vector *myo-2::dsRED::unc-54 3'UTR* was
 8 designed to insert a *myo-2::dsRED* reporter into the *Cbr-bar-1* (Figure S1A) [27]. The vector
 9 contained a 2 kb transgene flanked on either side by 1 kb of sequence homologous to *Cbr-bar-1*
 10 (Gibson Assembly Cloning Kit NEB catalog #E5510). The templates were included in the
 11 injection mix (donor plasmid 200 ng/μl, linear PCR amplicons 50 ng/μl, single-stranded
 12 oligonucleotides 30 ng/μl) along with other DNA components as mentioned above. Although
 13 none of these HR approaches were successful, in some cases we did observe expected genomic
 14 changes in F1 and F2 animals (as determined by sequencing), which were not inherited in
 15 subsequent generations (Table 3).
 16

Targeted Gene	Expected phenotype	sgRNA Efficiency	HR Efficiency
<i>Cbr-bar-1</i>	Egl	25/219 (11.4%)	0/219
<i>Cbr-bar-1</i>	Egl	18/211 (8.5%)	0/211
<i>Cbr-bar-1</i>	Egl	Not Determined	0/202
<i>Cbr-lin-15B</i>	WT [#]	Not Determined	0/68
<i>Cbr-vit-2</i>	WT [#]	1/78 (1.3%)	0/78

Table 3. Genome editing events detected using CRISPR-mediated HR. The sgRNA efficiency shows all genome editing events, including those repaired by NHEJ and HR, based on phenotypic and PCR-based screens. HR efficiency indicates the number of HR events detected in F2 out of the total F1s screened. [#]Wild type based on the phenotype of *C. elegans* orthologs.

17
 18 In conclusion, we have shown that the CRISPR/Cas9 system can be effectively employed
 19 in *C. briggsae* to alter a gene of interest. Similar to *C. elegans* the 3' GG motif appears to
 20 increase the frequency of NHEJ events. Interestingly, we observed a significant bias towards

bioRxiv preprint first posted online June 18, 2015; doi: <http://dx.doi.org/10.1101/021121>; The copyright holder for this preprint is the author/funder. It is made available under a [CC-BY 4.0 International license](#).

1 insertion NHEJ events in *C. briggsae*. Of the total of 8 alleles recovered, for 4 different genes,
2 62% had insertion of bases of varying length (range 3 to 150). Similar screens in *C. elegans* have
3 reported 26% frequency of such events (n = 86 from 5 different studies) [9, 21, 28-30]. More
4 work is needed to ascertain if such a bias in *C. briggsae* holds true in a larger sample size.

5 Together with the recently developed TALEN-based genome editing approach [3], the
6 CRISPR/Cas9 approach described here provides a powerful means to investigate the functions of
7 conserved as well as divergent genes in *C. briggsae*. This promises to accelerate comparative
8 studies with *C. elegans* thereby leading to a greater understanding of the flexibility of genetic and
9 molecular mechanisms during animal development.

10

11 **Acknowledgements**

12 We thank all members of the Gupta lab, particularly Scott Amon, Ayush Ranawade and Anand
13 Adhikari, for their input and assistance throughout this project. We also thank John Calarco for
14 two plasmids and initial advice in microinjection experiments. This work was supported by funds
15 from the Natural Sciences and Engineering Research Council of Canada (NSERC) Discovery
16 program to BPG.

17

18 **Competing interests**

19 The authors declare no competing interests.

20

21 **References:**

- 22 1. Gaj, T., C.A. Gersbach, and C.F. Barbas, 3rd, *ZFN, TALEN, and CRISPR/Cas-based*
23 *methods for genome engineering*. Trends Biotechnol, 2013. **31**(7): p. 397-405.
- 24 2. Frokjaer-Jensen, C., *Exciting prospects for precise engineering of Caenorhabditis elegans*
25 *genomes with CRISPR/Cas9*. Genetics, 2013. **195**(3): p. 635-42.
- 26 3. Wei, C., et al., *TALEN or Cas9 - rapid, efficient and specific choices for genome*
27 *modifications*. J Genet Genomics, 2013. **40**(6): p. 281-9.

bioRxiv preprint first posted online June 18, 2015; doi: <http://dx.doi.org/10.1101/021121>; The copyright holder for this preprint is the author/funder. It is made available under a [CC-BY 4.0 International license](#).

- 1 4. Wyman, C. and R. Kanaar, *DNA double-strand break repair: all's well that ends well*.
2 Annu Rev Genet, 2006. **40**: p. 363-83.
- 3 5. Terns, M.P. and R.M. Terns, *CRISPR-based adaptive immune systems*. Curr Opin
4 Microbiol, 2011. **14**(3): p. 321-7.
- 5 6. Mojica, F.J., et al., *Short motif sequences determine the targets of the prokaryotic*
6 *CRISPR defence system*. Microbiology, 2009. **155**(Pt 3): p. 733-40.
- 7 7. Jinek, M., et al., *A programmable dual-RNA-guided DNA endonuclease in adaptive*
8 *bacterial immunity*. Science, 2012. **337**(6096): p. 816-21.
- 9 8. Witte, H., et al., *Gene inactivation using the CRISPR/Cas9 system in the nematode*
10 *Pristionchus pacificus*. Dev Genes Evol, 2015. **225**(1): p. 55-62.
- 11 9. Friedland, A.E., et al., *Heritable genome editing in C. elegans via a CRISPR-Cas9*
12 *system*. Nat Methods, 2013. **10**(8): p. 741-3.
- 13 10. Fruscoloni, P., et al., *Mutational analysis of the transcription start site of the yeast*
14 *tRNA(Leu3) gene*. Nucleic Acids Res, 1995. **23**(15): p. 2914-8.
- 15 11. Cutter, A.D., *Divergence times in Caenorhabditis and Drosophila inferred from direct*
16 *estimates of the neutral mutation rate*. Mol Biol Evol, 2008. **25**(4): p. 778-86.
- 17 12. Uyar, B., et al., *RNA-seq analysis of the C. briggsae transcriptome*. Genome Res, 2012.
18 **22**(8): p. 1567-80.
- 19 13. True, J. and E. Haag, *Developmental system drift and flexibility in evolutionary*
20 *trajectories*. Evol. Dev., 2001. **3**: p. 109-119.
- 21 14. Benian, G.M., et al., *Sequence of an unusually large protein implicated in regulation of*
22 *myosin activity in C. elegans*. Nature, 1989. **342**(6245): p. 45-50.
- 23 15. Brenner, S., *The genetics of Caenorhabditis elegans*. Genetics, 1974. **77**: p. 71-94.
- 24 16. *Caenorhabditis briggsae Research Resource*. Available from: <http://www.briggsae.org>.
- 25 17. Sander, J.D., et al., *Zinc Finger Targeter (ZiFiT): an engineered zinc finger/target site*
26 *design tool*. Nucleic Acids Res, 2007. **35**(Web Server issue): p. W599-605.
- 27 18. Xie, S., et al., *sgRNAs9: a software package for designing CRISPR sgRNA and*
28 *evaluating potential off-target cleavage sites*. PLoS One, 2014. **9**(6): p. e100448.

bioRxiv preprint first posted online June 18, 2015; doi: <http://dx.doi.org/10.1101/021121>; The copyright holder for this preprint is the author/funder. It is made available under a [CC-BY 4.0 International license](#).

- 1 19. Paix, A., et al., *Scalable and versatile genome editing using linear DNAs with*
2 *microhomology to Cas9 Sites in Caenorhabditis elegans*. Genetics, 2014. **198**(4): p. 1347-
3 56.
- 4 20. Mello, C.C. and A. Fire, *DNA transformation, in Caenorhabditis elegans: modern*
5 *biological analysis of an organism*, H.F. Epstein and D.C. Shakes, Editors. 1995,
6 Academic Press: San Diego. p. 452-482.
- 7 21. Farboud, B. and B.J. Meyer, *Dramatic Enhancement of Genome Editing by CRISPR/Cas9*
8 *Through Improved Guide RNA Design*. Genetics, 2015. **199**(4): p. 959-71.
- 9 22. Wu, Y., et al., *Correction of a genetic disease in mouse via use of CRISPR-Cas9*. Cell
10 Stem Cell, 2013. **13**(6): p. 659-62.
- 11 23. Hruscha, A., et al., *Efficient CRISPR/Cas9 genome editing with low off-target effects in*
12 *zebrafish*. Development, 2013. **140**(24): p. 4982-7.
- 13 24. Yu, Z., et al., *Highly efficient genome modifications mediated by CRISPR/Cas9 in*
14 *Drosophila*. Genetics, 2013. **195**(1): p. 289-91.
- 15 25. Fu, Y., et al., *High-frequency off-target mutagenesis induced by CRISPR-Cas nucleases*
16 *in human cells*. Nat Biotechnol, 2013. **31**(9): p. 822-6.
- 17 26. Seetharaman, A., et al., *Conserved mechanism of Wnt signaling function in the*
18 *specification of vulval precursor fates in C. elegans and C. briggsae*. Dev Biol, 2010.
19 **346**(1): p. 128-39.
- 20 27. Tzur, Y.B., et al., *Heritable custom genomic modifications in Caenorhabditis elegans via*
21 *a CRISPR-Cas9 system*. Genetics, 2013. **195**(3): p. 1181-5.
- 22 28. Katic, I. and H. Grosshans, *Targeted heritable mutation and gene conversion by Cas9-*
23 *CRISPR in Caenorhabditis elegans*. Genetics, 2013. **195**(3): p. 1173-6.
- 24 29. Waaijers, S., et al., *CRISPR/Cas9-targeted mutagenesis in Caenorhabditis elegans*.
25 Genetics, 2013. **195**(3): p. 1187-91.
- 26 30. Chen, C., L.A. Fenk, and M. de Bono, *Efficient genome editing in Caenorhabditis elegans*
27 *by CRISPR-targeted homologous recombination*. Nucleic Acids Res, 2013. **41**(20): p.
28 e193.

29

bioRxiv preprint first posted online June 18, 2015; doi: <http://dx.doi.org/10.1101/021121>; The copyright holder for this preprint is the author/funder. It is made available under a [CC-BY 4.0 International license](#).

1 **Supplementary Materials**

2 **Table S1. sgRNA target sites.**

3

Gene	sgRNA Target
<i>Cbr-bar-1</i>	GTCAAGTTTGTGAAGATGGG AGG
<i>Cbr-dpy-1</i>	GTGCTGATCATTGTGACTGAT TGG
<i>Cbr-lin-2</i>	GATTAGAGACAAAGAGCATAT TGG
<i>Cbr-lin-7</i>	GGTTCGAGAGGTTTATGAGAC CGG
<i>Cbr-lin-10</i>	GTCCACAGCAACAAGAAAC AGG
<i>Cbr-lin-15B</i>	GCCGTCAACAACACTACACCTAT TGG
<i>Cbr-lin-17</i>	GTGTTGTCCAGTTGACCACT TGG
<i>Cbr-lin-18</i>	GCTCCGGAAGCAATTGCTAG AGG
<i>Cbr-unc-22</i>	AACTCTGTTGGATCTGATTCT TGG
<i>Cbr-unc-119</i> #1	GGAAAGTGCTAAAACGTCGT TCCGG
<i>Cbr-unc-119</i> #2	GGGAAGGTCGCCGAGCCGG TGG
<i>Cbr-vit-2</i>	AATGATGCACACCCGCC AGG
Bold indicates the PAM site.	

4

5

bioRxiv preprint first posted online June 18, 2015; doi: <http://dx.doi.org/10.1101/021121>; The copyright holder for this preprint is the author/funder. It is made available under a [CC-BY 4.0 International license](https://creativecommons.org/licenses/by/4.0/).

1 **Table S2. List of Primers.**

2

Gene	Purpose	Name	Direction	Sequence
<i>Cbr-bar-1</i>	sgRNA (OE)	GL964	F	GTCAAGTTTGTGAAGATGGGGTT TTAGAGCTAGAAATAGCAAGTTA
		GL965	R	CCCATCTTCACAAAATTGACAAA CATTAGATTTGCAATTCAATTAT ATAG
	5' homology arm for Gibson Assembly	GL991	F	CGAGGTCGACGGTATCGATATCT GAGCAGCCACGCTAA
		GL992	R	TCTCTACTTGTCTAGAAGCTAAG ATTATGCGGTAATAGTCTAATA ATTG
	3' homology arm for Gibson Assembly	GL1001	F	AAGTCGAAAAAATTAAGCTTTT TGAAAGACACTATATTTGGCTCG
		GL1002	R	GCTGCAGGAATTCGATATCAACC TAGTTATCAACCATGACGATAC
	Sequencing	GL1009	F	CATCTTGCTAGGCACATCACTTA TA
		GL1010	R	GGCAACAAGATGCGATCATTG
	PCR amplicon for direct HR	GL1039	F	GAATACTGACCAAAAGGTCAAGT TTGTGAAGATGGGAAAAGGAGA AGAACTTTTCACTGG
		GL1040	R	GTTGTTGCAGAATATGGAGCAGT TTCTGTGGTCCCTATTTGTATAGT TCATCCATGCC
	single stranded oligonucleotide donor template	GL1058	N/A	CTTCTCCTGTTATCGTCGACTTG ATCAGAGTTCTATGTGAAAAGAA TACTGACCAAAAAGGTCAAGTTG TGAAGGACCATGGGCTGGGAGG GTAAGATGGGAGGACCACAGAA ACTGCTCCATATTCTGCAACAAC GAGGATATG
	PCR screening	GL1059	R	CATGGGCTGGGAGGGTAAG
	<i>Cbr-dpy-1</i>	PCR stitching	GL954	F
GL955			R	TCAGTCACAATGATCAGCACAAA CATTAGATTTGCAATTCAATTAT ATAG
Sequencing		GL968	F	GGAGGAAGCCAACCTACCAAG
		GL969	R	CAGCTCGATTTCCAGACAATTC
<i>Cbr-lin-2</i>	sgRNA (OE)	GL974	F	GATTAGAGACAAAAGAGCATAGTT TTAGAGCTAGAAATAGCAAGTT

13

bioRxiv preprint first posted online June 18, 2015; doi: <http://dx.doi.org/10.1101/021121>; The copyright holder for this preprint is the author/funder. It is made available under a [CC-BY 4.0 International license](https://creativecommons.org/licenses/by/4.0/).

		GL975	R	TATGCTCTTTGTCTCTAATCAAAC ATTTAGATTTGCAATTCAATTAT ATAG
<i>Cbr-lin-7</i>	sgRNA (OE)	GL976	F	GGTTCGAGAGGTTTATGAGAGTT TTAGAGCTAGAAATAGCAAGTT
		GL977	R	TCTCATAAACCTCTCGAACCAAA CATTAGATTTGCAATTCAATTAT ATAG
	PCR-based screening and sequencing	GL1024	F	TGGGCCAATTCTATATCGATT
		GL1025	R	TTGCAGTCGAAATATGGGAT
<i>Cbr-lin-10</i>	sgRNA (OE)	GL978	F	GTCCACAGCAACAAGAAACGTT TTAGAGCTAGAAATAGCAAGTT
		GL979	R	GTTTCTTGTGCTGTGGGACAAA CATTAGATTTGCAATTCAATTAT ATAG
	PCR-based screening	GL1043	F	CAAGCCAATGCATAATATGCTCA ATAG
		GL1044	R	CTTCTTGATATTGTGCCGGCGAG
<i>Cbr-lin-15B</i>	sgRNA #1	GL1065	F	GCCGTCACAACACTACCTAGTT TTAGAGCTAGAAATAGCAAG
	sgRNA #2	GL1066	F	GTTGTTGACGGCACGACGGAGTT TTAGAGCTAGAAATAGCAAG
	PCR-based screening	GL1067	F	CGACGATCAGAAGTACCTCGTG
		GL1068	R	CGGCATCTGTGGAATGTATTTC
	Single stranded oligonucleotide donor template	GL1064	N/A	GTATCGAAGCGGAAACATTGCTC ACTTCCATGTGTCGTGCCCATGG GCTGGGAGGGTAAGCTAGTCAAC AACTACACCTATCGAACTGTGAA ATTGAGTAACATCGTCTGCCCA ATGAATCG
<i>Cbr-lin-17</i>	sgRNA #1 (OE)	GL960	F	GTGTTGTCCAGTTTGACCACGTTT TAGAGCTAGAAATAGCAAGTTA
		GL961	R	GTGGTCAAACCTGGACAACACAA ACATTTAGATTTGCAATTCAATT ATATAG
	sgRNA #2	GL1076	F	GGAACCTGCTTTATTGTGCGGGTTT TAGAGCTAGAAATAGCAAG
	PCR-based screening and sequencing	GL1077	F	CGGTGGGAAACCTGAATTCGATC
GL1078		R	GTATAGTCTCACCTTGTCTG	
<i>Cbr-lin-18</i>	sgRNA (OE)	GL962	F	GCTCCGGAAGCAATTGCTAGGTT TTAGAGCTAGAAATAGCAAGTTA
		GL963	R	CTAGCAATTGCTCCCGAGCAAA CATTAGATTTGCAATTCAATTAT ATAG
		GL1011	F	GCTCTTGCCACTCAGTTATCC

14

bioRxiv preprint first posted online June 18, 2015; doi: <http://dx.doi.org/10.1101/021121>; The copyright holder for this preprint is the author/funder. It is made available under a [CC-BY 4.0 International license](https://creativecommons.org/licenses/by/4.0/).

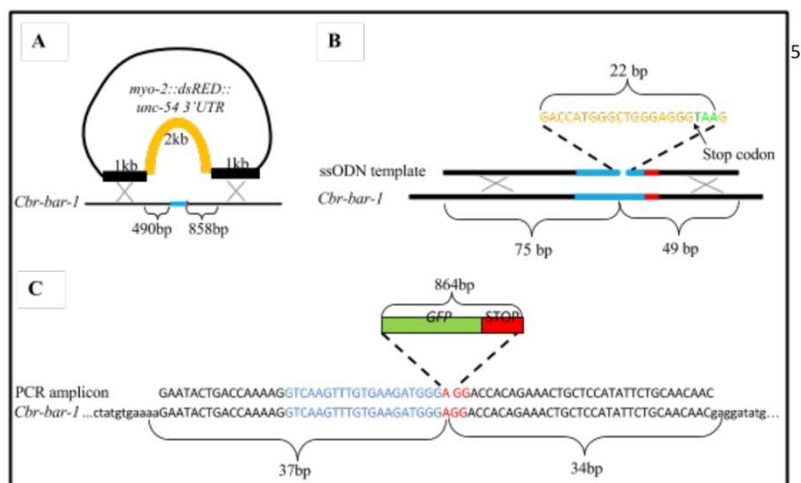
	Sequencing	GL1012	R	CACATGAGCACTCCTAGGGAC
<i>Cbr-unc-22</i>	PCR stitching	GL942	F	AACTCTGTTGGATCTGATTCGTTT TAGAGCTAGAAATAGCAAGTTA
		GL943	R	GAATCAGATCCAACAGAGTTAAA CATTAGATTTGCAATTCAATTAT ATAG
		GL966	F	GGAGAAACCGTTGAGTTGAAG
	Sequencing	GL967	R	CCATGATCCTCCCATAGCTTC
<i>Cbr-unc-119</i>	sgRNA #1	GL1047	F	GGAAGTGCTAAAAACGTCGTTGTT TTAGAGCTAGAAATAGCAAG
	sgRNA #2	GL1079	F	GGAAGGTCGCCGAGCCGGGT TTTAGAGCTAGAAATAGCAAG
	Sequencing	GL1099	F	GGCACCTCTAATTACCATT
		GL1100	R	GATTCCTTGTTCCGGTGCTTG
	sgRNA (OE)	GL940	F	CGGGAATTCCTCCAAGAACTCGT ACAAAAATGCTCT
		GL941	R	CGGAAGCTTCACAGCCGACTATG TTTGGCGT
	sgRNA (Q5)	GL1048	R	AAACATTTAGATTTGCAATTCAA TTATAT
<i>Cbr-vit-2</i>	sgRNA #1 (OE)	GL1029	F	AATGATGCACACCCGCCAGGTT TTAGAGCTAGAAATAGCAAGTT
		GL1030	R	CTGGGCGGGTGTGCATCATTTAAA CATTAGATTTGCAATTCAATTAT ATAG
	sgRNA #2 (OE)	GL1033	F	GGCGGCCTCGACGGTCAAAGTT TTAGAGCTAGAAATAGCAAGTT
		GL1034	R	TTTGACCGTCGAGCCCGCCAAA CATTAGATTTGCAATTCAATTAT ATAG
	PCR-based screening (sgRNA #1)	GL1049	F	ACCGTCAATACGAGCCAGAA
		GL1050	R	TAGCACACTCAGTGGCAACA
	PCR amplicon to direct HR	GL1053	F	GCCAGAAATCCGATTCTTGCTC TCTGGAGAATGATGCACATGGTG CGCTCCTCCAAGAA
		GL1054	R	GAGAGACGACTTGAACGAGGAG TGGCTCCTCTGGGCGGGTGAAC CAGTTTAAACTTACT
F indicates forward, R indicates reverse. sgRNA plasmids were either generated by overlap extension PCR (OE), or Q5 site directed mutagenesis (Q5).				

1

15

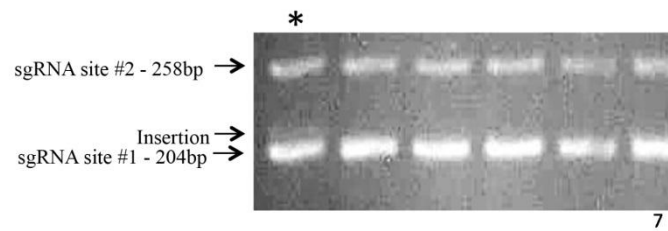
bioRxiv preprint first posted online June 18, 2015; doi: <http://dx.doi.org/10.1101/021121>; The copyright holder for this preprint is the author/funder. It is made available under a [CC-BY 4.0 International license](https://creativecommons.org/licenses/by/4.0/).

- 1 **Figure S1. Donor sequence approaches generated as templates for HR for *Cbr-bar-1*.**
- 2 Templates may take the form of a donor vector (A), ssODN (B) or PCR amplicons (C). Blue
- 3 letters represent the sgRNA target sequence while red letters represent the PAM site.



bioRxiv preprint first posted online June 18, 2015; doi: <http://dx.doi.org/10.1101/021121>; The copyright holder for this preprint is the author/funder. It is made available under a [CC-BY 4.0 International license](https://creativecommons.org/licenses/by/4.0/).

- 1 **Figure S2. PCR amplicons of the *Cbr-vit-2* genomic region flanking the sgRNA target site.**
- 2 An insertion can be seen at sgRNA site #1 in the lane marked with *.



8

17

CHAPTER 6: DISCUSSION AND FUTURE DIRECTIONS

The work described in this thesis focuses on the identification of genes involved in vulval development in *C. briggsae*, with an emphasis on comparative evo-devo analysis using *C. elegans*. The mutants used in my work were previously isolated in forward genetic screens performed in the Gupta lab. Among the 20 genes examined in this thesis, 17 are involved in processes that affect VPC number, cell proliferation and vulval morphology. Rescue experiments and molecular analyses have revealed that six of these genes are orthologs of *C. elegans unc-84*, *lin-39*, *lin-11*, *pry-1*, *lin-1*, and *lin-31*. The molecular identity of the remaining genes (14) is unknown and, based on the mapping data, may include novel genes. In my study of Multivulva mutants (Chapter 4), the identity of four uncloned genes could not be predicted from *C. elegans* based on genetic and molecular studies. Altogether, the work in this thesis reports the largest collection of genes involved in vulval development isolated through forward genetic screens in *C. briggsae*. The genetic analysis of mutants has provided evidence that the development of the reproductive system in *C. briggsae* utilizes both conserved and divergent processes. Additionally, my thesis has generated useful biological and technical resources in the form of mutants in addition to new mapping protocols and a CRISPR-based platform for targeted mutagenesis in *C. briggsae* (Chapter 5). The genes discussed below are based upon their sequential involvement during the vulval development process.

6.1. Genes involved in P-cell migration

Nuclear migration is central to many cellular processes like fertilization, cell polarity, differentiation, migration and cell organization during organ development (Starr, 2009; Starr and Fridolfsson, 2010). Mutations in UNC-83 (KASH domain) and UNC-84 (SUN domain) that disrupt nuclear migration in *hyp7* and P-cells were first isolated in *C. elegans* genetic screens aimed at identifying lineage mutants (Horvitz and Sulston, 1980; Ferguson and Horvitz, 1985). Since a subset of P-cells give rise to VPCs, lack of nuclear migration in these mutants leads to vulval abnormalities (Malone *et al.*, 1999). Additionally, P-cells contribute to neuronal lineages, therefore the migration defects in *unc-83* and *unc-84* mutants are due to the disruption of neuronal and muscular systems (Malone *et al.*, 1999).

Similar to *C. elegans unc-83* and *unc-84* mutants, we observed defects in P-cell and *hyp7* nuclear migration in two *C. briggsae* class 2 mutant strains-*Cbr-unc-84(sy5506)* and *Cbr-unc(sy5505)* (Chapter 3). These animals were uncoordinated and often lacked the vulva, leading to an Egl phenotype. Transgene rescue analysis revealed that the SUN domain protein UNC-84 is functionally conserved between *C. elegans* and *C. briggsae*, as *Cel-UNC-84* expression in *Cbr-unc-84* mutants rescued the Egl phenotype. In contrast, the phenotype of *sy5505* was not rescued by *C. elegans unc-84*. It is possible that *Cbr-unc(sy5505)* defines a new locus on chromosome 5, e.g., *Cbr-unc-83*, but this possibility needs to be tested by further rescue and allele sequencing experiments. It is interesting to note that unlike *C. elegans unc-83* mutants, *Cbr-unc(sy5505)* animals do not display *hyp7* migration defects. The future identification of the causal mutation in *Cbr-unc(sy5505)*

will reveal if it is indeed an allele of *Cbr-unc-83* or if it represents a novel gene that has acquired new function in *C. briggsae*. Furthermore, it would allow us to study similarities and differences in nuclear migration process between the two species.

6.2. Genes affecting cell proliferation

6.2.1. Vulvaless genes

My work has resulted in the identification of three class 3 mutants *Cbr-lin(bh7)*, *Cbr-lin(bh14)*, and *Cbr-lin-39*, whose loss of function result in VPC competence and induction defects. In one case, i.e., *Cbr-lin-39*, I have shown that uninduced VPCs fuse to the surrounding hypodermal syncytium prior to receiving an inductive signal, as judged by the expression of a cell junction associated marker DLG-1 (MAGUK family). Previous work in our lab has demonstrated that *Cbr-lin-39* is a downstream target of the *Cbr-bar-1-Cbr-pop-1*-mediated canonical Wnt signaling pathway required to regulate VPC competence and fate specification (Seetharaman *et al.*, 2010), similar to what has been observed in *C. elegans* (Eisenmann *et al.*, 1998).

Despite the conserved role of *lin-39* in regulating VPC competence, *Cbr-lin-39* mutants exhibit slight phenotypic differences compared to *C. elegans lin-39* animals. The Pn.p spacing defect is more severe in *Cbr-lin-39* alleles, especially between the P5.p and P6.p pair. When the interaction between *Cbr-lin-39* and *Cbr-pry-1* was examined to determine if overactivation of Wnt signal can bypass *Cbr-lin-39* activity, there was no change in small nucleus phenotype-like fate on the posterior side between the single and double mutant, despite the reduction in induction level. It is likely *Cbr-lin-39* is not

involved in preventing fate transformation in the posterior VPCs by Wnt overactivation (Seetharaman *et al.*, 2010). Also, immunostaining with MH27 antibody and anti-LIN-39 antibody has revealed that there is a higher posterior competence in *C. briggsae* AF16 compared to *C. elegans* N2 (Pénigault and Félix, 2011b). This contrast in competence is further supported by differences in P3.p division frequency and the observation that LIN-39 levels are lower in *C. briggsae* compared to *C. elegans* (Delattre and Félix, 2001a; Pénigault and Félix, 2011a). This competence variation in P3.p is likely caused by the long range Wnt signals CWN-1 and EGL-20, which establish a concentration gradient from the posterior region to P3.p (Pénigault and Félix, 2011b).

It is not clear how the *Cbr-lin(bh7)* and *Cbr-lin(bh14)* genes function in regulating VPC competence. However, since the VPCs fuse to the hyp7 without dividing, it is likely that the genes responsible are components of a novel pathway, or function with the conserved Wnt pathway to converge on LIN-39 in regulating competence (Eisenmann *et al.*, 1998). Future studies aimed at identifying their molecular identities will enable us to design experiments to investigate these possibilities.

6.2.2. *Multivulva genes*

6.2.3. *Identification of conserved C. elegans orthologs in C. briggsae*

Chapter 4 describes the identification and characterization of new Muv genes in *C. briggsae* whose loss of function results in excessive cell proliferation. This study has revealed three conserved orthologs of *C. elegans lin-1*, *lin-31* and *pry-1*. The role of *pry-1* in both *C. elegans* and *C. briggsae* was investigated previously in the Gupta lab

(Seetharaman *et al.*, 2010), therefore I focused on the analysis of *Cbr-lin-1* and *Cbr-lin-31*.

My work has shown that loss of *Cbr-lin-31* gene function results in a Muv phenotype and that ectopic VPC induction is independent of the gonad derived signal. Previous studies in *C. elegans* have shown that *lin-31* is required for VPC fate specification and that VPCs in *lin-31* mutants are induced to adopt anyone of the three possible fates (1^o, 2^o or 3^o). However, these experiments were based on cell lineage analysis rather than lineage-specific molecular markers (Miller *et al.*, 1993). Using two different GFP-based 1^o and 2^o cell fate markers, I have shown for the first time that ectopically induced VPCs in both *C. briggsae* and *C. elegans lin-31* mutants acquire a 2^o cell fate. In the future it will be interesting to investigate the interaction of LIN-31 with LIN-12/Notch signaling, which is also involved in conferring 2^o fates on VPCs (Sternberg, 1988; Chen and Greenwald, 2004).

In collaboration with the Chamberlin lab, I have characterized three alleles of *Cbr-lin-1* (*bh9*, *sa993* and *gu198*). *Cbr-lin-1* mutant hermaphrodites exhibit both Muv and Pvl phenotypes on plate level. Upon examination under Nomarski, I found that the Pvl phenotype is due to multiple VPCs inducing to form a single protrusion, indicative of a Muv phenotype. The analysis of cell fates in *Cbr-lin-1* mutants revealed that ectopic VPCs adopt both 1^o and 2^o cell fates. In no case did we find adjacent ectopic 1^o cells, indicating that the lateral signal is functional in the VPCs. A similar phenotype was also observed in *C. elegans lin-1* mutants. Overall, the role of LIN-1 in vulval development appears to be conserved between *C. elegans* and *C. briggsae*.

6.2.4. New genes that function in an EGF dependent manner

In addition to known EGF signaling pathway components *Cbr-lin-1*, *Cbr-lin-31* and *Cbr-pry-1*, the genetic screen performed in collaboration with the Chamberlin lab (Ohio State University) yielded four new genes that do not have any obvious candidates in *C. elegans* based on mapping and phenotypic studies (*Cbr-ivp-1*, *Cbr-ivp-2*, *Cbr-ivp-3*, *Cbr-ivp-4*). In these *C. briggsae* mutants, VPC fate specification occurs independent of the gonadal signal. However, when compared to wildtype control animals, we find that some animals exhibit patterns where three or less VPCs are induced, indicating some dependency on the gonadal derived EGF signal despite displaying a Muv phenotype. For instance, when the gonad was ablated in *Cbr-lin-1(gu198)* the resulting vulval phenotype looked similar to the intact mutant strain, except in rare cases where P7.p did not fully divide. Similarly, two animals had reduced induction after gonad ablation in *Cbr-lin-1(sa993)*, however in this case P6.p remained undivided. Further, Muv penetrance was also reduced in *gu167* gonad ablated animals. In *gu102*, *sy5216* and *gu163* animals, we find that there is no difference in the Muv penetrance between ablated and intact animals, indicating that these mutants can bypass the requirement for the gonad signal.

Their dependency on EGF signaling is further demonstrated in an experiment carried out by the Chamberlin lab in which the Muv penetrance was reduced with the U0126 EGF-inhibitor. However, it is interesting to note that Muv penetrance is not completely suppressed even at high concentrations of U0126 (30 μ M). Studies with *Cel-let-60(n1046)* have shown that the Muv phenotype caused by constitutive activation of

Ras is completely eliminated with 10 μ M of U0126 (Zitnik, 2014). Further tests with increasing doses of U0126 have also shown that VPC induction in P5.p, P6.p and P7.p is not completely suppressed in wild type *C. briggsae*, indicating that EGF pathway is more robust to perturbations than *C. elegans* (Zitnik, 2014). Altogether, these results imply that EGF-dependent and independent signaling pathways contribute to vulval development in *C. briggsae* (Zitnik, 2014).

In addition, 2^o cell fate expression was also observed more frequently among the ectopic VPCs in the four Muv mutants described in this thesis. These observations suggest that these Muv genes may play an important role in regulating notch signaling. This possibility could be tested by suppressing Notch signaling in these mutants to determine if this can suppress excessive VPC induction.

In summary, these four genes are likely to represent novel regulators of cell proliferation in *C. briggsae*. At present the molecular identity of these genes is unknown, which precludes us from making a definitive statement about their possible mechanism of action. If these genes lack orthologs in *C. elegans* then their role in *C. briggsae* vulva development could indicate novel function after the divergence of two species from the common gonochoristic ancestor (Kiontke *et al.*, 2004). Alternatively if the genes are conserved in *C. elegans*, then these variations could be due to evolution of gene function and regulation or gene network regulators.

6.3. Genes affecting vulval morphology

One of the larger category of mutants described in this thesis (chapter 3) have normal vulval induction but show defects in processes such as vulval invagination, vulval-uterine connection, anchor cell migration, and vulval cell division axes. These mutations give rise to a protruding vulva phenotype and are Egl.

We described two alleles of *Cbr-lin-11* that display egg laying defects similar to those seen in *C. elegans lin-11* mutants. These animals possess the correct number of VPCs, but exhibit altered division axes and abnormal vulval cell differentiation indicating that *Cbr-lin-11* plays a pivotal role in vulval morphogenesis as in *C. elegans* (Ferguson *et al.*, 1987; Gupta and Sternberg, 2002; Gupta, 2003). Transgene rescue experiments have shown that *Cbr-lin-11* mutants can be rescued by *Cel-lin-11*, demonstrating that *Cel-lin-11* is functionally similar to *Cbr-lin-11* in the *C. briggsae* egg-laying system. Interestingly, AC migration defects present in *Cel-lin-11* mutants were not observed in two different *Cbr-lin-11* mutants. This may suggest subtle differences in *lin-11* function between the two species. Thus, the recovery of *Cbr-lin-11* alleles in our forward genetic screens provides a unique opportunity to explore its functional conservation and divergence in *C. briggsae*.

6.4. Genetic variations underlying a robust system

Vulval development studies performed in other nematode species have revealed extensive differences in various steps of the developmental process (True and Haag, 2001; Kiontke *et al.*, 2007; Milloz *et al.*, 2008). These variations could be the result of

stochastic noise, environmental and genetic changes, which in turn could be a basis for new adaptations in the long term (Waddington C. H., 1942; Kiontke *et al.*, 2007; Félix and Wagner, 2008; Félix and Barkoulas, 2012). In such a system, cryptic variations could accumulate even with an invariant outcome (Félix, 2007; Braendle and Felix, 2009).

Several cell fate deviations have been observed upon anchor cell ablation, heat shock, and starvation in a number of different nematode species (Félix, 2007; Braendle and Félix, 2008; Félix and Barkoulas, 2012). For example, anchor cell ablation at early L3 stage caused P6.p to predominantly adopt 1° cell fates in *C. elegans* and 2° cell fates in *C. briggsae* (Félix, 2007). Also, the examination of VPC fates in *C. elegans* and *C. briggsae* following a period of starvation demonstrated deviations from the 2°-1°-2° invariant fate pattern, as the vulva was centered mostly on P5.p in *C. elegans* N2, the vulva was centered on P7.p in *C. briggsae* AF16 (Félix, 2007). Another study using *C. elegans* and *C. briggsae* animals has shown that orthologous genes can have different RNAi phenotypes, indicating that the underlying molecular function of the genes has diverged (Adrian *et al.*, 2014).

In our study, we have also observed several instances of DSD. Among the *lin-39* mutants in both nematode species, we find greater variability in VPC spacing in *Cbr-lin-39* mutants compared to *Cel-lin-39*. The significance of inter-VPC differences in *lin-39* is not well understood, however it should be mentioned that spatial patterning of VPCs is important for vulval positioning by ensuring that P6.p is located closest to the AC.

Subtle differences in *lin-11* function were also observed. As mentioned in section 6.3, the AC migration defect observed in *Cel-lin-11* mutants is absent in both *Cbr-lin-11* mutants. It is likely that LIN-11 function has diverged in *C. briggsae* compared to *C. elegans*. Further comparative analysis of new *C. briggsae lin-11* mutants with similar base changes as in *C. elegans* could confirm if the functions have diverged between these two species.

Another example of variation in these two phenotypically similar species is the isolation of four new *C. briggsae* Muv genes that lack orthologs in the *C. elegans* genome. It is possible that these are novel regulators of cell proliferation whose functions have diverged in *C. briggsae*.

The phenotypic differences described above could be in part attributed to DSD either through acquisition of new mechanisms or evolution of independent hermaphroditic lineages. More work involving gene identification along with comparison with gonochoristic species could explain the source of novelty. These examples provide ample evidence of evolutionary changes in cellular and molecular processes in *C. briggsae*. However, it should be noted that these differences do not lead to an obvious change in the position of vulval centering, vulval progeny number, vulval invagination and overall morphology. Such cryptic variations in genes can only be uncovered when the system is perturbed.

Outside of the *Caenorhabditis* genus, in species like *Oscheius*, variations have been found with respect to vulval competence group, cell fate specification, and VPC

induction (Delattre and Félix, 2001a; Dichtel *et al.*, 2001a, 2001b; Dichtel-Danjou and Félix, 2004). In *Oscheius sp.* CEW1, the VPC group lacks P3.p, containing only P4.p-P8p (Félix and Sternberg, 1997; Dichtel-Danjou and Félix, 2004). In this species the spatial pattern of vulval precursor fates is specified by the anchor cell and requires two successive rounds of inductions (Félix and Sternberg, 1997; Dichtel-Danjou and Félix, 2004). The 2^o and 3^o cells have similar cell lineages. Each generate four progenies, with the vulva forming from the P(5,7).p VPC progeny. The progeny of the remaining VPCs (P4.p and P8.p) fuse with the surrounding hypodermis (Louvet-Vallée *et al.*, 2003). It has also been shown that the anchor cell can induce vulval cell divisions independently without specifying VPC fates (Dichtel *et al.*, 2001b), a phenomenon not observed in *C. elegans* and *C. briggsae*.

In a more distantly related nematode species such as *P. pacificus*, significant alterations have occurred in the vulval development process (Wang and Sommer, 2011). The VPC group in this nematode consists of P3.p-P8.p, however unlike *C. elegans* and *C. briggsae* where uninduced Pn.p cells fuse with surrounding hypodermal syncytium, the uninduced Pn.p cells in *P. pacificus* undergo programmed cell death (Sommer and Sternberg, 1996; Sommer *et al.*, 1998). Furthermore, vulval induction in this species requires continuous interaction with multiple cells in the gonad (Sommer *et al.*, 1998; Sigrist and Sommer, 1999). Ablation studies have identified a novel cell interaction among the VPCs. Specifically, P8.p provides an inhibitory signal along with mesoblast to determine the competence of P5.p and P7.p (Jungblut *et al.*, 2001). Overall, these results

suggest that signaling pathways underlying cell competence and cell-cell interactions have diverged in this species.

Additional evidence for differences in signaling pathways governing vulval development comes from the analysis of Wnt pathway components. In *C. elegans* and *C. briggsae* Wnt signaling acts in regulate the competence of vulval precursors, but Wnt signaling in *P. pacificus* functions to repress vulval cell fates (Sigrist and Sommer, 1999; Tian *et al.*, 2008; Wang and Sommer, 2011). Specifically, mutants of Wnt pathway genes in *P. pacificus* cause a Muv phenotype independent of the gonad-derived signal (Tian *et al.*, 2008; Wang and Sommer, 2011). Furthermore, the frizzled receptor Ppa-LIN-17 plays a novel role in sequestering Wnt ligand Ppa-EGL-20 to restrict excessive vulval induction (Wang and Sommer, 2011). While these findings are exciting, they also raise questions about the divergence of Wnt signaling in *P. pacificus*. In this context it is worth pointing out that the role of Wnt signaling in *C. briggsae* vulval development is conserved when compared to *C. elegans* (Sharanya *et al.*, 2012, 2015). Whether the pathway is conserved in *Caenorhabditis* species and diverged in distant non-*Caenorhabditis* nematodes remains to be determined.

6.5. Phenotypic spectrum of mutants obtained in different nematode species

Comparisons of mutant phenotypes among *Caenorhabditis* species (*C. elegans* and *C. briggsae*) and non-*Caenorhabditis* nematodes like *O. tipulae* and *P. pacificus* have revealed differences that may be attributed to genetic backgrounds, developmental

changes or pleiotropic effects of the genes involved (Eizinger *et al.*, 1999; Dichtel *et al.*, 2001a; Louvet-Vallée *et al.*, 2003).

In *Oscheius* sp. CEW1 screens, vulval induction mutants were rare, but a high number of cell division mutants were obtained, revealing that vulva cell cycle regulation and fate specification may be uncoupled (Dichtel *et al.*, 2001b; Louvet-Vallée *et al.*, 2003). In the distantly related nematode *P. pacificus*, several Vul and Muv mutants have been isolated, however they differ in cell fate specification mechanisms and phenotypic range in comparison to *C. elegans* and *C. briggsae* (Sommer and Sternberg, 1996; Eizinger *et al.*, 1999).

In *C. elegans*, initial genetic screens yielded several mutations that lead to Egl, Vul and Muv phenotypes (Trent *et al.*, 1983; Ferguson and Horvitz, 1985; Ferguson *et al.*, 1987). Cell lineage studies revealed cell competence, induction and cell fate transformation defects in these mutants (Ferguson *et al.*, 1987). In *C. briggsae*, no induction mutants were recovered in spite of the fact that LIN-3/EGF-LET-23/EGFR-LET-60/RAS pathway is highly conserved (Section 1.6, Figure 3). However, we did recover several mutants showing defects in cell competence, cell invagination and morphogenesis. Molecular cloning of *C. briggsae* vulval genes has resulted in the identification of *C. elegans* orthologs, namely *lin-39*, *pry-1*, *lin-31*, *lin-1*, *unc-84* and *lin-11*. The remaining uncloned genes include several that act to restrict vulval proliferation and others that control cell differentiation and morphogenesis. In cases such as *Cbr-ivp-3(sy5216)*, the map location does not reveal an obvious *C. elegans* ortholog involved in vulval development, raising the possibility that these novel genes may have acquired new

function in *C. briggsae*. Future studies involving molecular cloning as well as a targeted approach of the CRISPR genome editing technique (Chapter 5) should help us uncover functional similarities and differences in the vulval development process in *C. briggsae* and *C. elegans*.

6.6. Concluding remarks

The nematode *C. briggsae*, a close relative of *C. elegans*, is a leading animal model to investigate evolutionary changes in gene function and signaling pathways. The findings of this thesis highlight the important roles of several conserved and novel genes involved in vulval development. In some cases, genes interact with conserved signaling pathways like Ras, Wnt and Notch but in other cases their mechanism of action appears divergent and remains to be characterized. Overall, this thesis reports the genetic analysis of 13 Egl genes, including orthologs of *C. elegans unc-84* (SUN domain), *lin-39* (*Dfd/Scr*-related homeobox), and *lin-11* (LIM-homeobox). Additionally, we have discovered differences in homologous processes indicating developmental system drift. Further, we have isolated alleles of seven *C. briggsae* multivulva genes that function to inhibit inappropriate cell proliferation. Two of these Muv genes have been cloned and found to be orthologs of *lin-1* (ETS) and *lin-31* (Winged-Helix) that act downstream of the EGF-Ras pathway. The *pry-1* (Axin) Muv gene, previously described by Seetharaman *et al.* 2010, is a component of the Wnt pathway. The remaining four Muv genes are likely novel regulators of cell proliferation in *C. briggsae*. Lastly, we have demonstrated that the CRISPR/cas9 system can be used to create targeted mutations in the *C. briggsae* genome

thereby accelerating the comparative study of vulval development in nematodes. The exciting discoveries from this study have helped lay the basis for future genetic studies in *C. briggsae*, while also providing a unique platform to investigate genetic changes that shape developmental diversity among living organisms.

6.7. Future directions

My work has made significant contributions to understanding the genetic basis of vulval formation in *C. briggsae* and serves as an important platform to make new discoveries in the future. While we have characterized the phenotypes and molecular identities of many genes, more work is needed to ascertain their exact role during development. For example, the identity of many of the Vul genes still needs to be resolved by mapping and whole genome sequencing. For the *Cbr-lin(bh7)* and *Cbr-lin(bh14)* Vul genes exhibiting reduced cell proliferation, epistasis experiments can be carried out with available *C. briggsae* Wnt pathway mutants to determine if they play a role in the pathway. Expression analysis using different fluorescent markers specific for vulval cells will also facilitate a better understanding of gene function. Additionally, there is a need to determine the identification of novel multivulva genes in *C. briggsae* and their tumor suppressor-like role in regulating cell proliferation.

My preliminary work involving the Muv mutants has resulted in the identification of a few putative candidates through whole genome sequencing. This includes CBG03376, a RNase H-like domain gene, that is a good candidate for *Cbr-ivp-3*. This gene contains and encodes for the *C. elegans* ortholog Y67D8C.3. Previous work on *C.*

elegans Y67D8C.3 demonstrated a role in reproduction and growth (Maeda *et al.*, 2001; Sönnichsen *et al.*, 2005). However, the results are not well established and significantly more work is need to understand if Y67D8C.3 plays a role in vulval development. Future work may include careful analysis of the mutant phenotypes of CBG03376 in *C. briggsae* and Y67D8C.3 in *C. elegans*. This could be done by RNAi as well as generating new alleles using the CRISPR technique. Additional work may involve phenotypic rescue using wild-type copy of the genes. The CRISPR alleles will allow us to complement the RNAi data, and determine the precise role of Y67D8C.3/CBG03376 in vulval development.

To investigate how Y67D8C.3/CBG03376 regulates cell proliferation, one approach may involve screening for protein-protein interactions. Identification of interacting proteins by a yeast 2 hybrid assay approach (Walhout *et al.*, 2000; Walhout and Vidal, 2001) may provide valuable information about their molecular function and also lead up to discovery of new proteins involved in vulval development process in *C. briggsae*.

The other area of future investigation is to generate targeted vulval mutants in *C. briggsae* using CRISPR technology. Several genes of the three conserved signaling pathways (EGF, Wnt and Notch) such as *lin-3(EGF)*, *lin-17(Frizzled)*, *lin-18(Ryk)*, *lin-12(Notch)* remain to be characterized in *C. briggsae*. Adapting the CRISPR technology would provide a powerful tool to generate genetic resources for *C. briggsae*. This could include generating knockout mutants for genes with visible and no obvious phenotypes, introducing fluorescent knock ins to improve genetic screening strategies and using

homologous recombination (HR) to generate gene fusions which would allow for *in vivo* observations (e.g., Muv, Pvl and Egl genes). In addition, the development of these resources will facilitate comparative studies with *C. elegans* enabling a better understanding of the robustness and flexibility of genetic and molecular mechanisms during vulval development.

APPENDIX

Transgenic lines were created by microparticle bombardment in *Cbr-unc-119(st20000)* using the protocol described. The outlined procedure below has been adapted with protocols used in Sarov, Seydoux and Waterston labs.

Preparation of worms for one bombardment session

For all bombardment sessions, use nematode growth media (NGM) plates with concentrated OP50.

1. Start with two small (6cm) NGM plates and continue to propagate till 12-15 plates of young adult *Cbr-unc-119(st20000)* is obtained.
2. On the day of bombardment or a day before, collect all the worms by washing the plates with M9 or sterile water. Resuspend the collected worms in a 15ml tube with M9 or sterile water to make a total of 10 ml.
3. Using a 5ml pipette, take 2ml of worms and add them to the surface of a dry one week post bacterial spreading enriched peptone plate (10cm). Add them drop wise starting at the center and then spiraling around until you reach the edge of the plate. Repeat until all worms are plated. The goal is to have five plates (10cm) of worms for each fosmid.
4. Leave the covers off the plates to evaporate the liquid. This should take no more than 15min.

For our purpose the BioRad Biolistic PDS-1000/He particle delivery system (with Hepta adaptor) at Mount Sinai Hospital was used for bombardments.

Preparation of the gold particles and DNA for bombardment

1. Before preparing the gold particles, use the small petri plates (6cm) to immerse the macrocarriers, stopping screens and rupture disks (mock and test) in 100% ethanol for sterilization. Leave them to dry by leaning them sideways on the petri plate cover.
2. Then weigh 30mg of 1 μ M gold beads (BioRad) in the balance and transfer into a siliconized 1.5ml eppendorf tube.
3. Wash the gold beads in 1ml of 70% ethanol. Vortex for five minutes and soak for 15 minutes. Then pellet by centrifuging for 20-25seconds and remove supernatant
4. Add 1ml of sterile water. Vortex for one minute and soak for one minute. Again pellet by centrifuging for 20-25seconds and remove supernatant. Repeat this step two more times to get a well suspended solution.
5. Finally, resuspend the gold particles in 500 μ L of sterile 50% glycerol. This bead stock can be used for two weeks (or more and should be stored at 4C).
6. If the bombardment is being planned the same day, vortex the mix continuously for five minutes. Pipette immediately 100 μ L of bead suspension into three siliconized eppendorf tubes. Take care to keep the gold beads in suspension.
7. For each of three tubes, then add in order while vortexing on medium speed:

- 30 μL fosmid DNA (Starting concentration should be atleast $1\mu\text{g}/\mu\text{L}$),
 - 100 μL 2.5M Calcium chloride (CaCl_2) and
 - 40 μL 0.1M spermidine,
8. Vortex for two more minutes once the spermidine has been added. Then soak the mixture for one minute. Pellet again by centrifuging for 20-25seconds and remove supernatant.
 9. To the pellet, add 280 μL 70% ethanol. Flick tube to mix. Pellet and remove supernatant.
 10. Add 280 μL of 100% ethanol. Flick tube to mix. Pellet and remove supernatant. Add 100 μL 100% ethanol and resuspend by gently flicking tube. This is your prepped DNA. On the middle of each microcarrier, pipet 11 μL of prepped DNA.
 11. Allow the macrocarriers to dry using a vacuum set up. Turn on the WC faucet in the Dennis lab. Connect the tube to the vacuum equipment. Make sure to close the tap of the vacuum holder and let it run till you hear a hissing sound. The gold particles will take a few minutes to dry.
 12. In the bombardment room (Room 886), before placing the macrocarrier in the target plate, open the tap to release vacuum.

Setting up the bombardment chamber

1. Wipe down the bombardment chamber and chamber door with 70% ethanol. Open the helium tank valve and check to make sure the He tank pressure is >2200psi).
2. Using the two regulators, main pressure valve and secondary regulator adjust the setting as outlined below.

- TO OPEN

Open the main pressure valve >2200psi and then check if the secondary regulator is open. Open clockwise till you feel resistance and psi is over 2200. Make sure the secondary regulator is open always.

- TO CLOSE:

Close main pressure value and then leave the secondary regulator open. Press the vacuum button and continuously fire till the psi is 0. Only then switch of the machine. Wipe the machine before you leave

3. Open the pressure valve has been set to open, place the rupture disk into the rupture disk retaining cap.
4. Screw the holder into the machine. Use the torque to tighten the holder.
5. Place the stopping screen into the target plate shelf.
6. Place the macrocarrier (Gold particles should be in the centre and should be dry at this point) into the macrocarrier holder exactly in the centre.

7. Slide the macrocarrier launch assembly in and close the door. (The apparatus has to slide in completely. Keep an eye on the side in which you are sliding otherwise the door cannot be closed).
8. For turning on the machine, Press the power button in the motor below. Then press the power in the heptaadapter. There are 3 options in the middle button- Vac, Vent and Hold. Press vacuum button till it reaches to 27 In. of Hg. Once it reaches 27 In. of Hg press hold. Then press the fire button and hold until disk ruptures. At this point, the pressure gauge on top will read 1200psi. Once this is done, release vacuum by pressing vent button. Open door now. Unscrew retaining cap and discard rupture disk.
9. Repeat the same procedure for all the five plates that have been prepared for the fosmid bombardment.

Transgenic lines and expression analysis

Three fosmid clones (*C. briggsae nhr-67*, *egl-43*, *eor-1*) were chosen based on their role in vulval morphogenesis in *C. elegans* studies (Howard and Sundaram, 2002; Rocheleau *et al.*, 2002; Fernandes and Sternberg, 2007; Hwang *et al.*, 2007; Rimann and Hajnal, 2007; Verghese *et al.*, 2011) and were used to streamline the bombardment protocol and to obtain transgenic lines for expression analysis.

After bombardment, three integrated lines were obtained for *Cbr-nhr-67*, two 2 lines (1 stable and 1 integrated) for *Cbr-eor-1* and one stable line for *Cbr-egl-43*. Using

GFP fluorescence microscopy, the expression of the tagged protein was observed during vulval development for all the three genes.

In *C. elegans*, *tailless* homolog *nhr-67* plays a major role during uterus development (Verghese *et al.*, 2011) and functions to regulate patterning of cell fates in several vulval cells (Fernandes and Sternberg, 2007). In *C. briggsae*, *nhr-67* is expressed in the gonadal precursor cells that form the ventral uterus AC and VU from late L2 stage. This expression disappears at mid L4 when the AC is fused with the uterine seam cell (utse). This expression pattern in *C. briggsae* during uterus patterning is similar to *C. elegans nhr-67*.

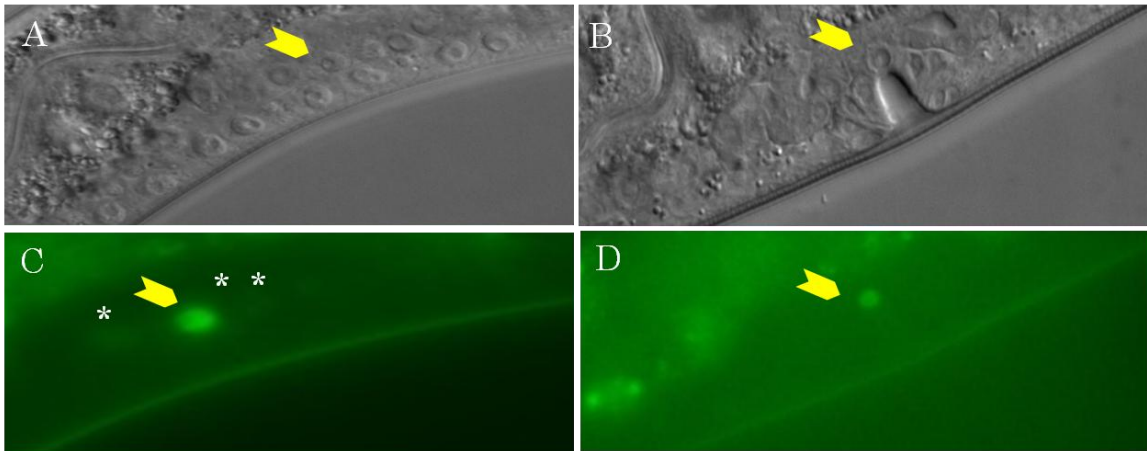


Figure 1. Expression of *nhr-67* in *C. briggsae* at L3 (A and C) and early L4 stages (B and D). A and B are DIC images, while C and D are GFP fluorescent images. The yellow arrow highlights the anchor cell in while the asterisk shows the ventral uterine cells (VU).

In *C. elegans*, *eor-1* expression is present in the all P-cells, precursors to the VPCs and in their descendants, anchor cell and ventral cord neurons. In contrast, no expression is

observed in anchor cell, ventral cord neurons or VPCs for *Cbr-eor-1*. For *Cbr-egl-43* gene, diffused expression was observed in the uterus around late L4 stage in a few of the animals. However this expression needs to be validated as only one transgenic line was obtained for this gene.

Table A1. Main components and targets of Ras, Wnt and Notch signaling pathways in *C. elegans* and *C. briggsae*. The percent of amino acid identity is based on UnitProtKB results and WormBase BlastP results.

Ras pathway		
Gene	Description	Percent identity
<i>lin-3</i>	EGF family Inductive signal	73%
<i>let-23</i>	RTK for <i>lin-3</i> , induces vulval development through <i>let-60/Ras</i>	69%
<i>sem-5</i>	RTK-binding adaptor. Contains a Src homology (SH) domain 2 and 3-containing protein	90%
<i>sos-1</i>	Guanine nucleotide exchange factor	72%
<i>let-60</i>	Ras, Small GTPase	99%
<i>lin-45</i>	Raf homolog. Serine/threonine kinase. Binds Ras-GTP, phosphorylates MEK-2	90%
<i>mek-2</i>	Phosphorylates MPK-1	96%
<i>mpk-1</i>	Serine/Threonine kinase	81%
<i>ksr-1</i>	Scaffold for Raf/MEK/MPK	76%
<i>ksr-2</i>	Scaffold for Raf/MEK/MPK	57%
<i>lin-1</i>	ETS domain transcription factor. Target of MPK-1	73%
<i>lin-31</i>	WH transcription factor. Target of MPK-1	80%
<i>lin-39</i>	HOX transcription factor	81%

Notch pathway		
Gene	Description	Percent identity
<i>lag-2</i>	DSL ligand	62%
<i>apx-1</i>	DSL ligand	52%
<i>dsl-1</i>	DSL ligand	51%
<i>osm-11</i>	DOS ligand	86%
<i>lin-12</i>	Notch receptor	59%
<i>glp-1</i>	Notch receptot	51%

<i>lag-1</i>	Transcription factor, CSL family (mammalian CBF1 and Drosophila Su(H) as well as LAG-1)	69%
<i>lip-1</i>	Mitogen-activated protein (MAP) kinase phosphatase. Negatively regulates MPK-1	91%
<i>lst-1</i>	Negative regulator. Novel MPK-1 binding protein	50%
<i>lst-2</i>	Negative regulator. Zinc finger transcription factor	82%
<i>lst-3</i>	Negative regulator. SAF-A/B, Acinus and PIAS domain protein	40%
<i>lst-4</i>	Negative regulator. SNX9 family of sorting nexins	70%

Wnt pathway		
Gene	Description	Percent identity
<i>mom-2</i>	Wnt ligands	85%
<i>lin-44</i>	Wnt ligands	93%
<i>egl-20</i>	Wnt ligands	91%
<i>cwn-1</i>	Wnt ligands	90%
<i>cwn-2</i>	Wnt ligands	97%
<i>mom-5</i>	Frizzled receptor. G protein-coupled receptor protein family	92%
<i>lin-17</i>	Frizzled receptor. G protein-coupled receptor protein family	92%
<i>mig-1</i>	Frizzled receptor. G protein-coupled receptor protein family	85%
<i>cfz-2</i>	Frizzled receptor. G protein-coupled receptor protein family	87%
<i>lin-18</i>	Ryk/Derailed family of tyrosine kinase-related receptors	87%
<i>mig-5</i>	Wnt signaling effector protein-Dishevelled	84%
<i>dsh-1</i>	Wnt signaling effector protein-Dishevelled	72%
<i>dsh-2</i>	Wnt signaling effector protein-Dishevelled	58%
<i>kin-19</i>	Destruction complex CK1 α	94%
<i>gsk-3</i>	Destruction complex GSK3 β	96%
<i>pry-1</i>	Destruction complex Axin	68%

<i>axl-1</i>	Destruction complex Axin	83%
<i>apr-1</i>	Destruction complex APC	77%
<i>bar-1</i>	Transcriptional activator. β -Catenin	80%
<i>pop-1</i>	TCF/LEF family of transcription factors	60%

REFERENCES

- Amit, S., Hatzubai, A., Birman, Y., Andersen, J.S., Ben-Shushan, E., Mann, M., Ben-Neriah, Y., and Alkalay, I. 2002. Axin-mediated CKI phosphorylation of beta-catenin at Ser 45: a molecular switch for the Wnt pathway. *Genes Dev.* *16*, 1066–1076.
- Andersen, E.C., and Horvitz, H.R. 2007. Two *C. elegans* histone methyltransferases repress *lin-3* EGF transcription to inhibit vulval development. *Development* *134*, 2991–2999.
- Baird, S.E., and Chamberlin, H.. 2006. *Caenorhabditis briggsae* methods. In *Wormbook*,.
- Barrière, A., and Félix, M.-A. 2005. High Local Genetic Diversity and Low Outcrossing Rate in *Caenorhabditis elegans* Natural Populations. *Curr. Biol.* *15*, 1176–1184.
- Battu, G. 2003. The *C. elegans* G-protein-coupled receptor SRA-13 inhibits RAS/MAPK signalling during olfaction and vulval development. *Development* *130*, 2567–2577.
- Beitel, G.J., Tuck, S., Greenwald, I., and Horvitz, H.R. 1995. The *Caenorhabditis elegans* gene *lin-1* encodes an ETS-domain protein and defines a branch of the vulval induction pathway. *Genes Dev.* *9*, 3149–3162.
- Belting, H.-G., Shashikant, C.S., and Ruddle, F.H. 1998. Modification of expression and cis-regulation of *Hoxc8* in the evolution of diverged axial morphology. *Proc. Natl. Acad. Sci.* *95*, 2355–2360.
- Bender, L.B., Cao, R., Zhang, Y., and Strome, S. 2004. The MES-2/MES-3/MES-6 complex and regulation of histone H3 methylation in *C. elegans*. *Curr. Biol.* *14*, 1639–1643.
- Bergmann, S., Ihmels, J., and Barkai, N. 2004. Similarities and differences in genome-wide expression data of six organisms. *PLoS Biol.* *2*, E9.
- Berset, T., Hoier, E.F., Battu, G., Canevascini, S., and Hajnal, a 2001. Notch inhibition of RAS signaling through MAP kinase phosphatase LIP-1 during *C. elegans* vulval development. *Science* *291*, 1055–1058.
- Bettinger, J.C., Euling, S., and Rougvie, A.E. 1997. The terminal differentiation factor LIN-29 is required for proper vulval morphogenesis and egg laying in *Caenorhabditis elegans*. *Development* *124*, 4333–4342.

Bhanot, P., Brink, M., Samos, C.H., Hsieh, J.C., Wang, Y., Macke, J.P., Andrew, D., Nathans, J., and Nusse, R. 1996. A new member of the frizzled family from *Drosophila* functions as a Wingless receptor. *Nature* 382, 225–230.

Bhattacharyya, R.P., Reményi, A., Yeh, B.J., and Lim, W.A. 2006. Domains, motifs, and scaffolds: the role of modular interactions in the evolution and wiring of cell signaling circuits. *Annu. Rev. Biochem.* 75, 655–680.

Blencowe, B.J. 2006. Alternative splicing: new insights from global analyses. *Cell* 126, 37–47.

Braendle, C., and Felix, M.-A. 2009. The other side of phenotypic plasticity: a developmental system that generates an invariant phenotype despite environmental variation. *J. Biosci.* 34, 543–551.

Braendle, C., and Félix, M.-A. 2008. Plasticity and errors of a robust developmental system in different environments. *Dev. Cell* 15, 714–724.

Brenner, S. 1973. The genetics of behaviour. *Br. Med. Bull.* 29, 269–271.

Brenner, S. 1974. The genetics of *Caenorhabditis elegans*. 71–94.

Bruinsma, J.J., Jirakulaporn, T., Muslin, A.J., and Kornfeld, K. 2002. Zinc Ions and Cation Diffusion Facilitator Proteins Regulate Ras-Mediated Signaling. *Dev. Cell* 2, 567–578.

Bülow, H.E., Boulin, T., and Hobert, O. 2004. Differential Functions of the *C. elegans* FGF Receptor in Axon Outgrowth and Maintenance of Axon Position. *Neuron* 42, 367–374.

Burdine, R.D., Branda, C.S., and Stern, M.J. 1998. EGL-17(FGF) expression coordinates the attraction of the migrating sex myoblasts with vulval induction in *C. elegans*. *Development* 125, 1083–1093.

Byerly, L., Cassada, R.C., and Russell, R.L. 1976. The life cycle of the nematode *Caenorhabditis elegans*. *Dev. Biol.* 51, 23–33.

Cadigan, K.M., and Nusse, R. 1997. Wnt signaling: a common theme in animal development. *Genes Dev.* 11, 3286–3305.

Carroll, S.B., Grenier, J.K., and Weatherbee, S.D. 2013. *From DNA to Diversity: Molecular Genetics and the Evolution of Animal Design* (John Wiley & Sons).

- Cavallo, R.A., Cox, R.T., Moline, M.M., Roose, J., Polevoy, G.A., Clevers, H., Peifer, M., and Bejsovec, A. 1998. *Drosophila* Tcf and Groucho interact to repress Wingless signalling activity. *Nature* 395, 604–608.
- Ceol, C.J., and Horvitz, H.R. 2001. *dpl-1* DP and *efl-1* E2F act with *lin-35* Rb to antagonize Ras signaling in *C. elegans* vulval development. *Mol. Cell* 7, 461–473.
- Ceol, C.J., and Horvitz, H.R. 2004. A new class of *C. elegans* synMuv genes implicates a Tip60/NuA4-like HAT complex as a negative regulator of Ras signaling. *Dev. Cell* 6, 563–576.
- Chamberlin, H.M., and Sternberg, P.W. 1994. The *lin-3/let-23* pathway mediates inductive signalling during male spicule development in *Caenorhabditis elegans*. *Development* 120, 2713–2721.
- Chang, C., Hopper, N. a, and Sternberg, P.W. 2000. *Caenorhabditis elegans* SOS-1 is necessary for multiple RAS-mediated developmental signals. *EMBO J.* 19, 3283–3294.
- Chang, C., Newman, a P., and Sternberg, P.W. 1999. Reciprocal EGF signaling back to the uterus from the induced *C. elegans* vulva coordinates morphogenesis of epithelia. *Curr. Biol.* 9, 237–246.
- Chen, N., and Greenwald, I. 2004. The lateral signal for LIN-12/Notch in *C. elegans* vulval development comprises redundant secreted and transmembrane DSL proteins. *Dev. Cell* 6, 183–192.
- Chitwood, B.G., and Chitwood, M.B.H. 1974. *Introduction to Nematology* (University Park Press).
- Church, D.L., Guan, K.L., and Lambie, E.J. 1995. Three genes of the MAP kinase cascade, *mek-2*, *mpk-1/sur-1* and *let-60 ras*, are required for meiotic cell cycle progression in *Caenorhabditis elegans*. *Development* 121, 2525–2535.
- Cinar, H.N., Richards, K.L., Oommen, K.S., and Newman, A.P. 2003. The EGL-13 SOX Domain Transcription Factor Affects the Uterine {pi} Cell Lineages in *Caenorhabditis elegans*. *Genetics* 165, 1623–1628.
- Clark, S.G., Chisholm, a D., and Horvitz, H.R. 1993. Control of cell fates in the central body region of *C. elegans* by the homeobox gene *lin-39*. *Cell* 74, 43–55.

- Clark, S.G., Lu, X., and Horvitz, H.R. 1994. The *Caenorhabditis elegans* locus *lin-15*, a negative regulator of a tyrosine kinase signaling pathway, encodes two different proteins. *Genetics* *137*, 987–997.
- Clark, S.G., Stern, M.J., and Horvitz, H.R. 1992. *C. elegans* cell-signalling gene *sem-5* encodes a protein with SH2 and SH3 domains. *Nature* *356*, 340–344.
- Clevers, H., and Nusse, R. 2012. Wnt/ β -catenin signaling and disease. *Cell* *149*, 1192–1205.
- Cohn, M.J., and Tickle, C. 1999. Developmental basis of limblessness and axial patterning in snakes. *Nature* *399*, 474–479.
- Cox, A.D., and Der, C.J. 2010. Ras history: The saga continues. *Small GTPases* *1*, 2–27.
- Cui, M., Chen, J., Myers, T.R., Hwang, B.J., Sternberg, P.W., Greenwald, I., and Han, M. 2006a. SynMuv genes redundantly inhibit *lin-3*/EGF expression to prevent inappropriate vulval induction in *C. elegans*. *Dev. Cell* *10*, 667–672.
- Cui, M., Chen, J., Myers, T.R., Hwang, B.J., Sternberg, P.W., Greenwald, I., and Han, M. 2006b. SynMuv Genes Redundantly Inhibit Short Article *lin-3* / EGF Expression to Prevent Inappropriate Vulval Induction in *C. elegans*. 667–672.
- Cutter, A.D. 2008. Divergence times in *Caenorhabditis* and *Drosophila* inferred from direct estimates of the neutral mutation rate. *Mol. Biol. Evol.* *25*, 778–786.
- Cutter, A.D., Félix, M.-A., Barrière, A., and Charlesworth, D. 2006. Patterns of nucleotide polymorphism distinguish temperate and tropical wild isolates of *Caenorhabditis briggsae*. *Genetics* *173*, 2021–2031.
- Delattre, M., and Félix, M. a 2001a. Microevolutionary studies in nematodes: a beginning. *Bioessays* *23*, 807–819.
- Delattre, M., and Félix, M.A. 2001b. Polymorphism and evolution of vulval precursor cell lineages within two nematode genera, *Caenorhabditis* and *Oscheius*. *Curr. Biol.* *11*, 631–643.
- Denouel-Galy, A., Douville, E.M., Warne, P.H., Papin, C., Laugier, D., Calothy, G., Downward, J., and Eychène, A. 1998. Murine Ksr interacts with MEK and inhibits Ras-induced transformation. *Curr. Biol.* *8*, 46–55.

Deshpande, R., Inoue, T., Priess, J.R., and Hill, R.J. 2005. lin-17/Frizzled and lin-18 regulate POP-1/TCF-1 localization and cell type specification during *C. elegans* vulval development. *Dev. Biol.* 278, 118–129.

Dichtel, M., Louvet-valle, S., Viney, M.E., Fe, M., and Sternberg, P.W. 2001a. Control of Vulval Cell Division Number in the Nematode.

Dichtel, M.-L., Louvet-Vallee, S., Viney, M.E., Felix, M.-A., and Sternberg, P.W. 2001b. Control of Vulval Cell Division Number in the Nematode *Oscheius/Dolichorhabditis* sp. CEW1. *Genetics* 157, 183–197.

Dichtel-Danjoy, M.-L., and Félix, M.-A. 2004. The two steps of vulval induction in *Oscheius tipulae* CEW1 recruit common regulators including a MEK kinase. *Dev. Biol.* 265, 113–126.

Dickinson, D.J., Pani, A.M., Heppert, J.K., Higgins, C.D., and Goldstein, B. 2015. Streamlined Genome Engineering with a Self-Excising Drug Selection Cassette. *Genetics*.

Dickinson, D.J., Ward, J.D., Reiner, D.J., and Goldstein, B. 2013. Engineering the *Caenorhabditis elegans* genome using Cas9-triggered homologous recombination. *Nat. Methods* 10, 1028–1034.

Doench, J.G., Hartenian, E., Graham, D.B., Tothova, Z., Hegde, M., Smith, I., Sullender, M., Ebert, B.L., Xavier, R.J., and Root, D.E. 2014. Rational design of highly active sgRNAs for CRISPR-Cas9-mediated gene inactivation. *Nat. Biotechnol.* 32, 1262–1267.

Dolgin, E.S., Félix, M.-A., and Cutter, A.D. 2008. Hakuna Nematoda: genetic and phenotypic diversity in African isolates of *Caenorhabditis elegans* and *C. briggsae*. *Heredity (Edinb)*. 100, 304–315.

Doyle, T.G., Wen, C., and Greenwald, I. 2000. SEL-8, a nuclear protein required for LIN-12 and GLP-1 signaling in *Caenorhabditis elegans*. *Proc. Natl. Acad. Sci. U. S. A.* 97, 7877–7881.

Dueber, J.E., Yeh, B.J., Chak, K., and Lim, W.A. 2003. Reprogramming control of an allosteric signaling switch through modular recombination. *Science* 301, 1904–1908.

Egeblad, M., Nakasone, E.S., and Werb, Z. 2010. Tumors as organs: complex tissues that interface with the entire organism. *Dev. Cell* 18, 884–901.

Eisenmann, D.M. 2005. Wnt signaling. In *Wormbook*,

- Eisenmann, D.M., and Kim, S.K. 2000. Protruding vulva mutants identify novel loci and Wnt signaling factors that function during *Caenorhabditis elegans* vulva development. *Genetics* *156*, 1097–1116.
- Eisenmann, D.M., Maloof, J.N., Simske, J.S., Kenyon, C., and Kim, S.K. 1998. The beta-catenin homolog BAR-1 and LET-60 Ras coordinately regulate the Hox gene *lin-39* during *Caenorhabditis elegans* vulval development. *Development* *125*, 3667–3680.
- Eizinger, a. 1997. The Homeotic Gene *lin-39* and the Evolution of Nematode Epidermal Cell Fates. *Science* (80-.). *278*, 452–455.
- Eizinger, A., Jungblut, B., and Sommer, R.J. 1999. Evolutionary change in the functional specificity of genes. *Trends Genet.* *15*, 197–202.
- Elion, E.A. 2001. The Ste5p scaffold. *J. Cell Sci.* *114*, 3967–3978.
- Ellisen, L.W., Bird, J., West, D.C., Soreng, A.L., Reynolds, T.C., Smith, S.D., and Sklar, J. 1991. TAN-1, the human homolog of the *Drosophila* notch gene, is broken by chromosomal translocations in T lymphoblastic neoplasms. *Cell* *66*, 649–661.
- Fahed, A.C., Gelb, B.D., Seidman, J.G., and Seidman, C.E. 2013. Genetics of congenital heart disease: the glass half empty. *Circ. Res.* *112*, 707–720.
- Farboud, B., and Meyer, B.J. 2015. Dramatic Enhancement of Genome Editing by CRISPR/Cas9 Through Improved Guide RNA Design. *Genetics* *genetics.115.175166* – .
- Fay, D.S., and Han, M. 2000. The synthetic multivulval genes of *C. elegans*: functional redundancy, Ras-antagonism, and cell fate determination. *Genesis* *26*, 279–284.
- Fay, D.S., and Yochem, J. 2007. The SynMuv genes of *Caenorhabditis elegans* in vulval development and beyond. *Dev. Biol.* *306*, 1–9.
- Félix, M.-A. 2004. Genomes: A Helpful Cousin for Our Favourite Worm. *Curr. Biol.* *14*, R75–R77.
- Félix, M.-A. 2007. Cryptic quantitative evolution of the vulva intercellular signaling network in *Caenorhabditis*. *Curr. Biol.* *17*, 103–114.
- Félix, M.-A., and Barkoulas, M. 2012. Robustness and flexibility in nematode vulva development. *Trends Genet.* *28*, 185–195.
- Félix, M.-A., and Dubeau, F. 2012. Population dynamics and habitat sharing of natural populations of *Caenorhabditis elegans* and *C. briggsae*. *BMC Biol.* *10*, 59.

- Félix, M.A., and Sternberg, P.W. 1996. Symmetry breakage in the development of one-armed gonads in nematodes. *Development* *122*, 2129–2142.
- Félix, M.A., and Sternberg, P.W. 1997. Two nested gonadal inductions of the vulva in nematodes. *Development* *124*, 253–259.
- Félix, M.-A., and Wagner, A. 2008. Robustness and evolution: concepts, insights and challenges from a developmental model system. *Heredity (Edinb)*. *100*, 132–140.
- Ferguson, E.L., and Horvitz, H.R. 1985. Identification and characterization of 22 genes that affect the vulval cell lineages of the nematode *Caenorhabditis elegans*. *Genetics* *110*, 17–72.
- Ferguson, E.L., and Horvitz, H.R. 1989. The multivulva phenotype of certain *Caenorhabditis elegans* mutants results from defects in two functionally redundant pathways. *Genetics* *123*, 109–121.
- Ferguson, E.L., Sternberg, P.W., and Horvitz, H.R. 1987. A genetic pathway for the specification of the vulval cell lineages of *Caenorhabditis elegans*. *Nature* *326*, 259–267.
- Fernandes, J.S., and Sternberg, P.W. 2007. The tailless Ortholog *nhr-67* Regulates Patterning of Gene Expression and Morphogenesis in the *C. elegans* Vulva. *PLoS Genet.* *3*, e69.
- Fixsen, W., Sternberg, P., Ellis, H., and Horvitz, R. 1985. Genes that affect cell fates during the development of *Caenorhabditis elegans*. *Cold Spring Harb. Symp. Quant. Biol.* *50*, 99–104.
- Flibotte, S., Edgley, M.L., Maydan, J., Taylor, J., Zapf, R., Waterston, R., and Moerman, D.G. 2009. Rapid high resolution single nucleotide polymorphism-comparative genome hybridization mapping in *Caenorhabditis elegans*. *Genetics* *181*, 33–37.
- Francois, V., Solloway, M., O’Neill, J.W., Emery, J., and Bier, E. 1994. Dorsal-ventral patterning of the *Drosophila* embryo depends on a putative negative growth factor encoded by the short gastrulation gene. *Genes Dev.* *8*, 2602–2616.
- Freyd, G.A. 1991. Molecular analysis of the *Caenorhabditis elegans* cell, lineage gene *lin-11*.
- Friedland, A.E., Tzur, Y.B., Esvelt, K.M., Colaiácovo, M.P., Church, G.M., and Calarco, J. a 2013. Heritable genome editing in *C. elegans* via a CRISPR-Cas9 system. *Nat. Methods* *10*, 741–743.

- Frøkjær-Jensen, C. 2013. Exciting prospects for precise engineering of *Caenorhabditis elegans* genomes with CRISPR/Cas9. *Genetics* 195, 635–642.
- Galant, R., and Carroll, S.B. 2002. Evolution of a transcriptional repression domain in an insect Hox protein. *Nature* 415, 910–913.
- Gaul, U., Mardon, G., and Rubin, G.M. 1992. A putative Ras GTPase activating protein acts as a negative regulator of signaling by the Sevenless receptor tyrosine kinase. *Cell* 68, 1007–1019.
- Gellon, G., and McGinnis, W. 1998. Shaping animal body plans in development and evolution by modulation of Hox expression patterns. *Bioessays* 20, 116–125.
- Gilbert, S. 1997. *Embryology: Constructing The Organism*.
- Gleason, J.E., Korswagen, H.C., and Eisenmann, D.M. 2002. Activation of Wnt signaling bypasses the requirement for RTK/Ras signaling during *C. elegans* vulval induction. *Genes Dev.* 16, 1281–1290.
- Gleason, J.E., Szyleyko, E.A., and Eisenmann, D.M. 2006. Multiple redundant Wnt signaling components function in two processes during *C. elegans* vulval development. *Dev. Biol.* 298, 442–457.
- Greenwald, I. 2005. LIN-12/Notch signaling in *C. elegans*. In *Wormbook*,.
- Greenwald, I.S., Sternberg, P.W., and Robert Horvitz, H. 1983. The *lin-12* locus specifies cell fates in *caenorhabditis elegans*. *Cell* 34, 435–444.
- Gupta, B.P. 2003. The *C. elegans* LIM homeobox gene *lin-11* specifies multiple cell fates during vulval development. *Development* 130, 2589–2601.
- Gupta, B.P., Hanna-Rose, W., and Sternberg, P.W. 2012a. Morphogenesis of the vulva and the vulval-uterine connection. *WormBook* 1–20.
- Gupta, B.P., Liu, J., Hwang, B.J., Moghal, N., and Sternberg, P.W. 2006. *sli-3* Negatively Regulates the LET-23/Epidermal Growth Factor Receptor-Mediated Vulval Induction Pathway in *Caenorhabditis elegans*. *Genetics* 174, 1315–1326.
- Gupta, B.P., and Sternberg, P.W. 2002. Tissue-specific regulation of the LIM homeobox gene *lin-11* during development of the *Caenorhabditis elegans* egg-laying system. *Dev. Biol.* 247, 102–115.

- Gupta, B.P., and Sternberg, P.W. 2003. The draft genome sequence of the nematode *Caenorhabditis briggsae*, a companion to *C. elegans*. *Genome Biol.* 4, 238.
- Gupta, B.P., Wendy Hanna-Rose, A., and Sternberg, P.W. 2012b. Morphogenesis of the vulva and the vulval-uterine connection. In *Wormbook*,.
- Hajnal, A., Whitfield, C.W., and Kim, S.K. 1997. Inhibition of *Caenorhabditis elegans* vulval induction by *gap-1* and by *let-23* receptor tyrosine kinase. *Genes Dev.* 11, 2715–2728.
- Han, M., Golden, A., Han, Y., and Sternberg, P.W. 1993. *C. elegans* *lin-45* *raf* gene participates in *let-60* *ras*-stimulated vulval differentiation. *Nature* 363, 133–140.
- Han, M., and Sternberg, P.W. 1990. *let-60*, a gene that specifies cell fates during *C. elegans* vulval induction, encodes a *ras* protein. *Cell* 63, 921–931.
- Hanna-Rose, W., and Han, M. 1999. *COG-2*, a *sox* domain protein necessary for establishing a functional vulval-uterine connection in *Caenorhabditis elegans*. *Development* 126, 169–179.
- Hart, M.J., de los Santos, R., Albert, I.N., Rubinfeld, B., and Polakis, P. 1998. Downregulation of beta-catenin by human Axin and its association with the APC tumor suppressor, beta-catenin and GSK3 beta. *Curr. Biol.* 8, 573–581.
- Hayashizaki, S., Iino, Y., and Yamamoto, M. 1998. Characterization of the *C. elegans* *gap-2* gene encoding a novel Ras-GTPase activating protein and its possible role in larval development. *Genes Cells* 3, 189–202.
- Heffer, A., and Pick, L. 2013. Conservation and variation in Hox genes: how insect models pioneered the evo-devo field. *Annu. Rev. Entomol.* 58, 161–179.
- Hillier, L.W., Miller, R.D., Baird, S.E., Chinwalla, A., Fulton, L. a, Koboldt, D.C., and Waterston, R.H. 2007. Comparison of *C. elegans* and *C. briggsae* genome sequences reveals extensive conservation of chromosome organization and synteny. *PLoS Biol.* 5, e167.
- Hirsh, D., Oppenheim, D., and Klass, M. 1976. Development of the reproductive system of *Caenorhabditis elegans*. *Dev. Biol.* 49, 200–219.
- Hong, R.L., and Sommer, R.J. 2006. *Pristionchus pacificus*: a well-rounded nematode. *Bioessays* 28, 651–659.

- Hopper, N.A., Lee, J., and Sternberg, P.W. 2000. ARK-1 Inhibits EGFR Signaling in *C. elegans*. *Mol. Cell* 6, 65–75.
- Horvitz, H.R., and Sulston, J.E. 1980. Isolation and genetic characterization of cell-lineage mutants of the nematode *Caenorhabditis elegans*. *Genetics* 96, 435–454.
- Howard, P.L., Chia, M.C., Del Rizzo, S., Liu, F.-F., and Pawson, T. 2003. Redirecting tyrosine kinase signaling to an apoptotic caspase pathway through chimeric adaptor proteins. *Proc. Natl. Acad. Sci. U. S. A.* 100, 11267–11272.
- Howard, R.M., and Sundaram, M. V 2002. *C. elegans* EOR-1/PLZF and EOR-2 positively regulate Ras and Wnt signaling and function redundantly with LIN-25 and the SUR-2 Mediator component. *Genes Dev.* 16, 1815–1827.
- Huang, L.S., Tzou, P., and Sternberg, P.W. 1994. The *lin-15* locus encodes two negative regulators of *Caenorhabditis elegans* vulval development. *Mol. Biol. Cell* 5, 395–411.
- Hwang, B.J., Meruelo, A.D., and Sternberg, P.W. 2007. *C. elegans* EVI1 proto-oncogene, EGL-43, is necessary for Notch-mediated cell fate specification and regulates cell invasion. *Development* 134, 669–679.
- Inoue, T., Wang, M., Ririe, T.O., Fernandes, J.S., and Sternberg, P.W. 2005. Transcriptional network underlying *Caenorhabditis elegans* vulval development. *Proc. Natl. Acad. Sci.* 102, 4972–4977.
- Jacobs, D., Beitel, G.J., Clark, S.G., Horvitz, H.R., and Kornfeld, K. 1998. Gain-of-function mutations in the *Caenorhabditis elegans* *lin-1* ETS gene identify a C-terminal regulatory domain phosphorylated by ERK MAP kinase. *Genetics* 149, 1809–1822.
- Jiang, L.I., and Sternberg, P.W. 1998. Interactions of EGF, Wnt and HOM-C genes specify the P12 neuroectoblast fate in *C. elegans*. *Development* 125, 2337–2347.
- Jongeward, G.D., Clandinin, T.R., and Sternberg, P.W. 1995. *sli-1*, a negative regulator of *let-23*-mediated signaling in *C. elegans*. *Genetics* 139, 1553–1566.
- Jungblut, B., Pires-dasilva, A., and Sommer, R.J. 2001. Formation of the egg-laying system in *Pristionchus pacificus* requires complex interactions between gonadal, mesodermal and epidermal tissues and does not rely on single cell inductions V ulva Induction. 3404, 3395–3404.

- Kao, G., Tuck, S., Baillie, D., and Sundaram, M. V 2004. *C. elegans* SUR-6/PR55 cooperates with LET-92/protein phosphatase 2A and promotes Raf activity independently of inhibitory Akt phosphorylation sites. *Development* *131*, 755–765.
- Kataoka, T., Broek, D., and Wigler, M. 1985. DNA sequence and characterization of the *S. cerevisiae* gene encoding adenylate cyclase. *Cell* *43*, 493–505.
- Katz, W.S., Hill, R.J., Clandinin, T.R., and Sternberg, P.W. 1995. Different Levels of the *C. elegans* growth factor LIN-3 promote distinct vulval precursor fates. *Cell* *82*, 297–307.
- Kimble, J. 1981. Alterations in cell lineage following laser ablation of cells in the somatic gonad of *Caenorhabditis elegans*. *Dev. Biol.* *87*, 286–300.
- Kimble, J., and Hirsh, D. 1979. The postembryonic cell lineages of the hermaphrodite and male gonads in *Caenorhabditis elegans*. *Dev. Biol.* *70*, 396–417.
- Kiontke, K., Barrière, A., Kolotuev, I., Podbilewicz, B., Sommer, R., Fitch, D.H. a, and Félix, M.-A. 2007. Trends, stasis, and drift in the evolution of nematode vulva development. *Curr. Biol.* *17*, 1925–1937.
- Kiontke, K., Gavin, N.P., Raynes, Y., Roehrig, C., Piano, F., and Fitch, D.H.A. 2004. *Caenorhabditis* phylogeny predicts convergence of hermaphroditism and extensive intron loss. *Proc. Natl. Acad. Sci. U. S. A.* *101*, 9003–9008.
- Kirouac, M., and Sternberg, P.W. 2003. cis-Regulatory control of three cell fate-specific genes in vulval organogenesis of *Caenorhabditis elegans* and *C. briggsae*. *Dev. Biol.* *257*, 85–103.
- Kishida, S., Yamamoto, H., Ikeda, S., Kishida, M., Sakamoto, I., Koyama, S., and Kikuchi, A. 1998. Axin, a negative regulator of the wnt signaling pathway, directly interacts with adenomatous polyposis coli and regulates the stabilization of beta-catenin. *J. Biol. Chem.* *273*, 10823–10826.
- Koboldt, D.C., Staisch, J., Thillainathan, B., Haines, K., Baird, S.E., Chamberlin, H.M., Haag, E.S., Miller, R.D., and Gupta, B.P. 2010. A toolkit for rapid gene mapping in the nematode *Caenorhabditis briggsae*. *BMC Genomics* *11*, 236.
- Kornfeld, K., Guan, K.L., and Horvitz, H.R. 1995. The *Caenorhabditis elegans* gene mek-2 is required for vulval induction and encodes a protein similar to the protein kinase MEK. *Genes Dev.* *9*, 756–768.

- Krause, M., Harrison, S.W., Xu, S.Q., Chen, L., and Fire, a 1994. Elements regulating cell- and stage-specific expression of the *C. elegans* MyoD family homolog *hlh-1*. *Dev. Biol.* *166*, 133–148.
- Lackner, M.R., Kornfeld, K., Miller, L.M., Horvitz, H.R., and Kim, S.K. 1994. A MAP kinase homolog, *mpk-1*, is involved in ras-mediated induction of vulval cell fates in *Caenorhabditis elegans*. *Genes Dev.* *8*, 160–173.
- Lambie, E.J., and Kimble, J. 1991. Two homologous regulatory genes, *lin-12* and *glp-1*, have overlapping functions. *Development* *112*, 231–240.
- Langer, R., and Vacanti, J.P. 1993. Tissue engineering. *Science* *260*, 920–926.
- Lappin, T.R.J., Grier, D.G., Thompson, A., and Halliday, H.L. 2006. HOX genes: seductive science, mysterious mechanisms. *Ulster Med. J.* *75*, 23–31.
- Lee, J., Jongeward, G.D., and Sternberg, P.W. 1994. *unc-101*, a gene required for many aspects of *Caenorhabditis elegans* development and behavior, encodes a clathrin-associated protein. *Genes Dev.* *8*, 60–73.
- Leon, G., Sanchez-Ruiloba, L., Perez-Rodriguez, A., Gragera, T., Martinez, N., Hernandez, S., Anta, B., Calero, O., Garcia-Dominguez, C.A., Dura, L.M., *et al.* 2014. *Shoc2/Sur8* protein regulates neurite outgrowth. *PLoS One* *9*, e114837.
- Lesca, G.M., and Sternberg, P.W. 1997. Positive and negative tissue-specific signaling by a nematode epidermal growth factor receptor. *Mol. Biol. Cell* *8*, 779–793.
- Lewis, E.B. 1978. A gene complex controlling segmentation in *Drosophila*. *Nature* *276*, 565–570.
- Li, C., and Chalfie, M. 1990. Organogenesis in *C. elegans*: Positioning of neurons and muscles in the egg-laying system. *Neuron* *4*, 681–695.
- Li, W., Han, M., and Guan, K.L. 2000. The leucine-rich repeat protein SUR-8 enhances MAP kinase activation and forms a complex with Ras and Raf. *Genes Dev.* *14*, 895–900.
- Lin, K.T.-H., Broitman-Maduro, G., Hung, W.W.K., Cervantes, S., and Maduro, M.F. 2009. Knockdown of *SKN-1* and the Wnt effector *TCF/POP-1* reveals differences in endomesoderm specification in *C. briggsae* as compared with *C. elegans*. *Dev. Biol.* *325*, 296–306.

Liu, C., Li, Y., Semenov, M., Han, C., Baeg, G.H., Tan, Y., Zhang, Z., Lin, X., and He, X. 2002. Control of beta-catenin phosphorylation/degradation by a dual-kinase mechanism. *Cell* 108, 837–847.

Lopez-Rios, J., Duchesne, A., Speziale, D., Andrey, G., Peterson, K.A., Germann, P., Unal, E., Liu, J., Floriot, S., Barbey, S., *et al.* 2014. Attenuated sensing of SHH by Ptch1 underlies evolution of bovine limbs. *Nature* 511, 46–51.

Louvet-Vallée, S., Kolotuev, I., Podbilewicz, B., and Félix, M.-A. 2003. Control of vulval competence and centering in the nematode *Oscheius* sp. 1 CEW1. *Genetics* 163, 133–146.

Lu, X., and Horvitz, H.R. 1998a. *lin-35* and *lin-53*, Two Genes that Antagonize a *C. elegans* Ras Pathway, Encode Proteins Similar to Rb and Its Binding Protein RbAp48. *Cell* 95, 981–991.

Lu, X., and Horvitz, H.R. 1998b. *lin-35* and *lin-53*, two genes that antagonize a *C. elegans* Ras pathway, encode proteins similar to Rb and its binding protein RbAp48. *Cell* 95, 981–991.

Maeda, I., Kohara, Y., Yamamoto, M., and Sugimoto, A. 2001. Large-scale analysis of gene function in *Caenorhabditis elegans* by high-throughput RNAi. *Curr. Biol.* 11, 171–176.

Maekawa, M., Li, S., Iwamatsu, A., Morishita, T., Yokota, K., Imai, Y., Kohsaka, S., Nakamura, S., and Hattori, S. 1994. A novel mammalian Ras GTPase-activating protein which has phospholipid-binding and Btk homology regions. *Mol. Cell. Biol.* 14, 6879–6885.

Malone, C.J., Fixsen, W.D., Horvitz, H.R., and Han, M. 1999. UNC-84 localizes to the nuclear envelope and is required for nuclear migration and anchoring during *C. elegans* development. *Development* 126, 3171–3181.

Maloof, J.N., and Kenyon, C. 1998. The Hox gene *lin-39* is required during *C. elegans* vulval induction to select the outcome of Ras signaling. *Development* 125, 181–190.

Malumbres, M., and Barbacid, M. 2003. RAS oncogenes: the first 30 years. *Nat. Rev. Cancer* 3, 459–465.

Mao, J., Wang, J., Liu, B., Pan, W., Farr, G.H., Flynn, C., Yuan, H., Takada, S., Kimelman, D., Li, L., *et al.* 2001. Low-Density Lipoprotein Receptor-Related Protein-5 Binds to Axin and Regulates the Canonical Wnt Signaling Pathway. *Mol. Cell* 7, 801–809.

- Marri, S., and Gupta, B.P. 2009. Dissection of *lin-11* enhancer regions in *Caenorhabditis elegans* and other nematodes. *Dev. Biol.* 325, 402–411.
- McEwan, D.L., Weisman, A.S., and Hunter, C.P. 2012. Uptake of extracellular double-stranded RNA by *SID-2*. *Mol. Cell* 47, 746–754.
- Mcgee, M.D., Rillo, R., Anderson, A.S., and Starr, D.A. 2006. *UNC-83* Is a KASH Protein Required for Nuclear Migration and Is Recruited to the Outer Nuclear Membrane by a Physical Interaction with the SUN Protein *UNC-84*. *17*, 1790–1801.
- McGinnis, W., Garber, R.L., Wirz, J., Kuroiwa, A., and Gehring, W.J. 1984. A homologous protein-coding sequence in *Drosophila* homeotic genes and its conservation in other metazoans. *Cell* 37, 403–408.
- McGinnis, W., and Krumlauf, R. 1992. Homeobox genes and axial patterning. *Cell* 68, 283–302.
- Miller, L.M., Gallegos, M.E., Morisseau, B. a, and Kim, S.K. 1993. *lin-31*, a *Caenorhabditis elegans* HNF-3/fork head transcription factor homolog, specifies three alternative cell fates in vulval development. *Genes Dev.* 7, 933–947.
- Miller, M.A., Cutter, A.D., Yamamoto, I., Ward, S., and Greenstein, D. 2004. Clustered organization of reproductive genes in the *C. elegans* genome. *Curr. Biol.* 14, 1284–1290.
- Milloz, J., Duveau, F., Nuez, I., and Félix, M.-A. 2008. Intraspecific evolution of the intercellular signaling network underlying a robust developmental system. *Genes Dev.* 22, 3064–3075.
- Moghal, N. 2003. The epidermal growth factor system in *caenorhabditis elegans*. *Exp. Cell Res.* 284, 150–159.
- Mora, C., Tittensor, D.P., Adl, S., Simpson, A.G.B., and Worm, B. 2011. How many species are there on Earth and in the ocean? *PLoS Biol.* 9, e1001127.
- Morgan, T.H. 1917. The theory of the gene. *Am Nat.* 1917;51:513–544 (The American Naturalist).
- Müller, J., Ory, S., Copeland, T., Piwnicka-Worms, H., and Morrison, D.K. 2001. *C-TAK1* Regulates Ras Signaling by Phosphorylating the MAPK Scaffold, *KSR1*. *Mol. Cell* 8, 983–993.

Myers, T.R., and Greenwald, I. 2007. Wnt signal from multiple tissues and *lin-3*/EGF signal from the gonad maintain vulval precursor cell competence in *Caenorhabditis elegans*. *Proc. Natl. Acad. Sci. U. S. A.* *104*, 20368–20373.

Nayak, S., Goree, J., and Schedl, T. 2005. *fog-2* and the evolution of self-fertile hermaphroditism in *Caenorhabditis*. *PLoS Biol.* *3*, e6.

Newman, a P., Inoue, T., Wang, M., and Sternberg, P.W. 2000. The *Caenorhabditis elegans* heterochronic gene *lin-29* coordinates the vulval-uterine-epidermal connections. *Curr. Biol.* *10*, 1479–1488.

Newman, a P., and Sternberg, P.W. 1996. Coordinated morphogenesis of epithelia during development of the *Caenorhabditis elegans* uterine-vulval connection. *Proc. Natl. Acad. Sci. U. S. A.* *93*, 9329–9333.

Newman, a P., White, J.G., and Sternberg, P.W. 1995. The *Caenorhabditis elegans* *lin-12* gene mediates induction of ventral uterine specialization by the anchor cell. *Development* *121*, 263–271.

Newman, a P., White, J.G., and Sternberg, P.W. 1996. Morphogenesis of the *C. elegans* hermaphrodite uterus. *Development* *122*, 3617–3626.

Newman, A., Acton, G., Hartwig, E., Horvitz, H., and Sternberg, P. 1999. The *lin-11* LIM domain transcription factor is necessary for morphogenesis of *C. elegans* uterine cells. *Development* *126*, 5319–5326.

Nilsson, L., Li, X., Tiensuu, T., Auty, R., Greenwald, I., and Tuck, S. 1998. *Caenorhabditis elegans* *lin-25*: cellular focus, protein expression and requirement for *sur-2* during induction of vulval fates. *Development* *125*, 4809–4819.

Nusse, R. 2005. Wnt signaling in disease and in development. *Cell Res.* *15*, 28–32.

Nüsslein-Volhard, C., and Wieschaus, E. 1980. Mutations affecting segment number and polarity in *Drosophila*. *Nature* *287*, 795–801.

Ohmachi, M., Rocheleau, C.E., Church, D., Lambie, E., Schedl, T., and Sundaram, M. V. 2002. *C. elegans* *ksr-1* and *ksr-2* Have Both Unique and Redundant Functions and Are Required for MPK-1 ERK Phosphorylation. *Curr. Biol.* *12*, 427–433.

Oommen, K.S., and Newman, A.P. 2007. Co-regulation by Notch and Fos is required for cell fate specification of intermediate precursors during *C. elegans* uterine development. *Development* *134*, 3999–4009.

- Paix, A., Wang, Y., Smith, H.E., Lee, C.-Y.S., Calidas, D., Lu, T., Smith, J., Schmidt, H., Krause, M.W., and Seydoux, G. 2014. Scalable and Versatile Genome Editing Using Linear DNAs with Micro-Homology to Cas9 Sites in *Caenorhabditis elegans*. *Genetics* *198*, 1347–1356.
- Palmer, R. 2002. *Caenorhabditis elegans cog-1* Locus Encodes GTX/Nkx6.1 Homeodomain Proteins and Regulates Multiple Aspects of Reproductive System Development. *Dev. Biol.* *252*, 202–213.
- Park, S.-H., Zarrinpar, A., and Lim, W.A. 2003. Rewiring MAP kinase pathways using alternative scaffold assembly mechanisms. *Science* *299*, 1061–1064.
- Pénigault, J.-B., and Félix, M.-A. 2011a. Evolution of a system sensitive to stochastic noise: P3.p cell fate in *Caenorhabditis*. *Dev. Biol.* *357*, 419–427.
- Pénigault, J.-B., and Félix, M.-A. 2011b. High sensitivity of *C. elegans* vulval precursor cells to the dose of posterior Wnts. *Dev. Biol.* *357*, 428–438.
- Polakis, P. 2000. Wnt signaling and cancer. *Genes Dev.* *14*, 1837–1851.
- Poulson, D.F. 1937. Chromosomal Deficiencies and the Embryonic Development of *Drosophila Melanogaster*. *Proc. Natl. Acad. Sci. U. S. A.* *23*, 133–137.
- Poulson, D.F. 1940. The effects of certain X-chromosome deficiencies on the embryonic development of *Drosophila melanogaster*. *J. Exp. Zool.* *83*, 271–325.
- Riddle, D.L., Blumenthal, T., Barbara J Meyer, and Priess, J.R. 1997. *C. elegans* II, 2nd edition (Cold Spring Harbor Laboratory Press).
- Rimann, I., and Hajnal, A. 2007. Regulation of anchor cell invasion and uterine cell fates by the *egl-43* Evi-1 proto-oncogene in *Caenorhabditis elegans*. *Dev. Biol.* *308*, 187–195.
- Rocheleau, C.E., Howard, R.M., Goldman, A.P., Volk, M.L., Girard, L.J., and Sundaram, M. V 2002. A *lin-45* raf enhancer screen identifies *eor-1*, *eor-2* and unusual alleles of Ras pathway genes in *Caenorhabditis elegans*. *Genetics* *161*, 121–131.
- Rocheleau, C.E., Rönnlund, A., Tuck, S., and Sundaram, M. V 2005. *Caenorhabditis elegans* CNK-1 promotes Raf activation but is not essential for Ras/Raf signaling. *Proc. Natl. Acad. Sci. U. S. A.* *102*, 11757–11762.
- Roelink, H., Porter, J.A., Chiang, C., Tanabe, Y., Chang, D.T., Beachy, P.A., and Jessell, T.M. 1995. Floor plate and motor neuron induction by different concentrations of the amino-terminal cleavage product of sonic hedgehog autoproteolysis. *Cell* *81*, 445–455.

- Romagnolo, B., Jiang, M., Kiraly, M., Breton, C., Begley, R., Wang, J., Lund, J., and Kim, S.K. 2002. Downstream targets of let-60 Ras in *Caenorhabditis elegans*. *Dev. Biol.* 247, 127–136.
- Ross, J.A., Koboldt, D.C., Staisch, J.E., Chamberlin, H.M., Gupta, B.P., Miller, R.D., Baird, S.E., and Haag, E.S. 2011. *Caenorhabditis briggsae* recombinant inbred line genotypes reveal inter-strain incompatibility and the evolution of recombination. *PLoS Genet.* 7, e1002174.
- Rudel, D., and Kimble, J. 2002. Evolution of discrete Notch-like receptors from a distant gene duplication in *Caenorhabditis*. *Evol. Dev.* 4, 319–333.
- Rudel, D., and Sommer, R.J. 2003. The evolution of developmental mechanisms. *Dev. Biol.* 264, 15–37.
- Saffer, A.M., Kim, D.H., van Oudenaarden, A., and Horvitz, H.R. 2011a. The *Caenorhabditis elegans* synthetic multivulva genes prevent ras pathway activation by tightly repressing global ectopic expression of lin-3 EGF. *PLoS Genet.* 7, e1002418.
- Saffer, A.M., Kim, D.H., van Oudenaarden, A., and Horvitz, H.R. 2011b. The *Caenorhabditis elegans* synthetic multivulva genes prevent ras pathway activation by tightly repressing global ectopic expression of lin-3 EGF. *PLoS Genet.* 7, e1002418.
- Sander, J.D., Zaback, P., Joung, J.K., Voytas, D.F., and Dobbs, D. 2007. Zinc Finger Targeter (ZiFiT): an engineered zinc finger/target site design tool. *Nucleic Acids Res.* 35, W599–W605.
- Sarov, M., Murray, J.I., Schanze, K., Pozniakovski, A., Niu, W., Angermann, K., Hasse, S., Rupprecht, M., Vinis, E., Tinney, M., *et al.* 2012. A genome-scale resource for in vivo tag-based protein function exploration in *C. elegans*. *Cell* 150, 855–866.
- Sarov, M., Schneider, S., Pozniakovski, A., Roguev, A., Ernst, S., Zhang, Y., Hyman, A.A., and Stewart, A.F. 2006. A recombineering pipeline for functional genomics applied to *Caenorhabditis elegans*. *Nat. Methods* 3, 839–844.
- Sawa, H., and Korswagen, H.C. 2013. Wnt signaling in *C. elegans*.
- Saxen, L., and Sariola, H. 1987. Early organogenesis of the kidney. *Pediatr. Nephrol.* 1, 385–392.

Seetharaman, A., Cumbo, P., Bojanala, N., and Gupta, B.P. 2010. Conserved mechanism of Wnt signaling function in the specification of vulval precursor fates in *C. elegans* and *C. briggsae*. *Dev. Biol.* *346*, 128–139.

Seydoux, G., and Greenwald, I. 1989. Cell autonomy of *lin-12* function in a cell fate decision in *C. elegans*. *Cell* *57*, 1237–1245.

Sharanya, D., Fillis, C.J., Kim, J., Zitnik, E.M., Ward, K.A., Gallagher, M.E., Chamberlin, H.M., and Gupta, B.P. 2015. Mutations in *Caenorhabditis briggsae* identify new genes important for limiting the response to EGF signaling during vulval development. *Evol. Dev.* *17*, 34–48.

Sharanya, D., Thillainathan, B., Marri, S., Bojanala, N., Taylor, J., Flibotte, S., Moerman, D.G., Waterston, R.H., and Gupta, B.P. 2012. Genetic control of vulval development in *Caenorhabditis briggsae*. *G3 (Bethesda)*. *2*, 1625–1641.

Sharma-Kishore, R., White, J.G., Southgate, E., and Podbilewicz, B. 1999. Formation of the vulva in *Caenorhabditis elegans*: a paradigm for organogenesis. *Development* *126*, 691–699.

Shaye, D.D., and Greenwald, I. 2002. Endocytosis-mediated downregulation of LIN-12/Notch upon Ras activation in *Caenorhabditis elegans*. *Nature* *420*, 686–690.

Shemer, G., Kishore, R., and Podbilewicz, B. 2000. Ring formation drives invagination of the vulva in *Caenorhabditis elegans*: Ras, cell fusion, and cell migration determine structural fates. *Dev. Biol.* *221*, 233–248.

Shemer, G., and Podbilewicz, B. 2002. LIN-39/Hox triggers cell division and represses EFF-1/fusogen-dependent vulval cell fusion. *Genes Dev.* *16*, 3136–3141.

Sherwood, D.R., and Sternberg, P.W. 2003. Anchor cell invasion into the vulval epithelium in *C. elegans*. *Dev. Cell* *5*, 21–31.

Shim, J., Sternberg, P.W., and Lee, J. 2000. Distinct and redundant functions of mu1 medium chains of the AP-1 clathrin-associated protein complex in the nematode *Caenorhabditis elegans*. *Mol. Biol. Cell* *11*, 2743–2756.

Sieburth, D.S., Sun, Q., and Han, M. 1998. SUR-8, a Conserved Ras-Binding Protein with Leucine-Rich Repeats, Positively Regulates Ras-Mediated Signaling in *C. elegans*. *Cell* *94*, 119–130.

Sigrist, C.B., and Sommer, R.J. 1999. Vulva formation in *Pristionchus pacificus* relies on continuous gonadal induction. *Dev. Genes Evol.* 209, 451–459.

Singh, N., and Han, M. 1995. *sur-2*, a novel gene, functions late in the *let-60* ras-mediated signaling pathway during *Caenorhabditis elegans* vulval induction. *Genes Dev.* 9, 2251–2265.

Skorobogata, O., Escobar-Restrepo, J.M., and Rocheleau, C.E. 2014. An AGEF-1/Arf GTPase/AP-1 ensemble antagonizes LET-23 EGFR basolateral localization and signaling during *C. elegans* vulva induction. *PLoS Genet.* 10, e1004728.

Skorobogata, O., and Rocheleau, C.E. 2012. RAB-7 antagonizes LET-23 EGFR signaling during vulva development in *Caenorhabditis elegans*. *PLoS One* 7, e36489.

Solnica-Krezel, L., and Sepich, D.S. 2012. Gastrulation: making and shaping germ layers. *Annu. Rev. Cell Dev. Biol.* 28, 687–717.

Sommer, R.J., Eizinger, a, Lee, K.Z., Jungblut, B., Bubeck, a, and Schlak, I. 1998. The *Pristionchus* HOX gene *Ppa-lin-39* inhibits programmed cell death to specify the vulva equivalence group and is not required during vulval induction. *Development* 125, 3865–3873.

Sommer, R.J., and Sternberg, P.W. 1996. Apoptosis and change of competence limit the size of the vulva equivalence group in *Pristionchus pacificus*: a genetic analysis. *Curr. Biol.* 6, 52–59.

Sönnichsen, B., Koski, L.B., Walsh, A., Marschall, P., Neumann, B., Brehm, M., Alleaume, A.-M., Artelt, J., Bettencourt, P., Cassin, E., *et al.* 2005. Full-genome RNAi profiling of early embryogenesis in *Caenorhabditis elegans*. *Nature* 434, 462–469.

Starr, D. a, Hermann, G.J., Malone, C.J., Fixsen, W., Priess, J.R., Horvitz, H.R., and Han, M. 2001. *Unc-83* Encodes a Novel Component of the Nuclear Envelope and Is Essential for Proper Nuclear Migration. *Development* 128, 5039–5050.

Starr, D.A. 2009. A nuclear-envelope bridge positions nuclei and moves chromosomes. *J. Cell Sci.* 122, 577–586.

Starr, D.A., and Fridolfsson, H.N. 2010. Interactions between nuclei and the cytoskeleton are mediated by SUN-KASH nuclear-envelope bridges. *Annu. Rev. Cell Dev. Biol.* 26, 421–444.

- Stein, L.D., Bao, Z., Blasiar, D., Blumenthal, T., Brent, M.R., Chen, N., Chinwalla, A., Clarke, L., Clee, C., Coghlan, A., *et al.* 2003. The genome sequence of *Caenorhabditis briggsae*: a platform for comparative genomics. *PLoS Biol.* *1*, E45.
- Sternberg, P.W. 1988. Lateral inhibition during vulval induction in *Caenorhabditis elegans*. *Nature* *335*, 551–554.
- Sternberg, P.W. 2005. Vulval development. In *WormBook*, B.J. Meyer, ed.
- Sternberg, P.W., and Han, M. 1998. Genetics of RAS signaling in *C. elegans*. *Trends Genet.* *14*, 466–472.
- Sternberg, P.W., and Horvitz, H.R. 1986. Pattern formation during vulval development in *C. elegans*. *Cell* *44*, 761–772.
- Sternberg, P.W., and Horvitz, H.R. 1989. The combined action of two intercellular signaling pathways specifies three cell fates during vulval induction in *C. elegans*. *Cell* *58*, 679–693.
- Stetak, A., Gutierrez, P., and Hajnal, A. 2008. Tissue-specific functions of the *Caenorhabditis elegans* p120 Ras GTPase activating protein GAP-3. *Dev. Biol.* *323*, 166–176.
- Stothard, P., and Pilgrim, D. 2003. Sex-determination gene and pathway evolution in nematodes. *Bioessays* *25*, 221–231.
- Strange, K. 2006. *C. Elegans: Methods and Applications* (Springer Science & Business Media).
- Sulston, J.E., and Horvitz, H.R. 1977. Post-embryonic cell lineages of the nematode, *Caenorhabditis elegans*. *Dev. Biol.* *56*, 110–156.
- Sundaram, M. V 2005. The love-hate relationship between Ras and Notch. *Genes Dev.* *19*, 1825–1839.
- Sundaram, M. V 2006. RTK/Ras/MAPK signaling. In *Wormbook*,.
- Sundaram, M., Yochem, J., and Han, M. 1996. A Ras-mediated signal transduction pathway is involved in the control of sex myoblast migration in *Caenorhabditis elegans*. *Development* *122*, 2823–2833.
- Takemaru, K.-I. 2000. The Transcriptional Coactivator CBP Interacts with beta-Catenin to Activate Gene Expression. *J. Cell Biol.* *149*, 249–254.

- Tan, P.B., Lackner, M.R., and Kim, S.K. 1998. by the LIN-1 Ets / LIN-31 WH Transcription Factor Complex during *C. elegans* Vulval Induction. *93*, 569–580.
- Tapley, E.C., and Starr, D.A. 2013. Connecting the nucleus to the cytoskeleton by SUN-KASH bridges across the nuclear envelope. *Curr. Opin. Cell Biol.* *25*, 57–62.
- Tax, F.E., Thomas, J.H., Ferguson, E.L., and Horvitz, H.R. 1997. Identification and characterization of genes that interact with *lin-12* in *Caenorhabditis elegans*. *Genetics* *147*, 1675–1695.
- Thesleff, I. 1996. Tooth morphogenesis and cell differentiation. *Curr. Opin. Cell Biol.* *8*, 844–850.
- Thomas, C.G., Li, R., Smith, H.E., Woodruff, G.C., Oliver, B., and Haag, E.S. 2012. Simplification and desexualization of gene expression in self-fertile nematodes. *Curr. Biol.* *22*, 2167–2172.
- Tian, H., Schlager, B., Xiao, H., and Sommer, R.J. 2008. Wnt signaling induces vulva development in the nematode *Pristionchus pacificus*. *Curr. Biol.* *18*, 142–146.
- Tickle, C. 1995. Vertebrate limb development. *Curr. Opin. Genet. Dev.* *5*, 478–484.
- Tickle, C., and Barker, H. 2013. The Sonic hedgehog gradient in the developing limb. *Wiley Interdiscip. Rev. Dev. Biol.* *2*, 275–290.
- Trent, C., Tsuing, N., and Horvitz, H.R. 1983. Egg-laying defective mutants of the nematode *Caenorhabditis elegans*. *Genetics* *104*, 619–647.
- True, J.R., and Haag, E.S. 2001. Developmental system drift and flexibility in evolutionary trajectories. *Evol. Dev.* *3*, 109–119.
- Tuck, S., and Greenwald, I. 1995. *lin-25*, a gene required for vulval induction in *Caenorhabditis elegans*. *Genes Dev.* *9*, 341–357.
- Unhavaithaya, Y., Shin, T.H., Miliaras, N., Lee, J., Oyama, T., and Mello, C.C. 2002. MEP-1 and a Homolog of the NURD Complex Component Mi-2 Act Together to Maintain Germline-Soma Distinctions in *C. elegans*. *Cell* *111*, 991–1002.
- Uyar, B., Chu, J.S.C., Vergara, I.A., Chua, S.Y., Jones, M.R., Wong, T., Baillie, D.L., and Chen, N. 2012. RNA-seq analysis of the *C. briggsae* transcriptome. *Genome Res.* *22*, 1567–1580.

- Vastenhouw, N.L., Brunschwig, K., Okihara, K.L., Müller, F., Tijsterman, M., and Plasterk, R.H.A. 2006. Gene expression: long-term gene silencing by RNAi. *Nature* 442, 882.
- Verghese, E., Schocken, J., Jacob, S., Wimer, A.M., Royce, R., Nesmith, J.E., Baer, G.M., Clever, S., McCain, E., Lakowski, B., *et al.* 2011. The tailless ortholog *nhr-67* functions in the development of the *C. elegans* ventral uterus. *Dev. Biol.* 356, 516–528.
- Verster, A.J., Ramani, A.K., McKay, S.J., and Fraser, A.G. 2014. Comparative RNAi screens in *C. elegans* and *C. briggsae* reveal the impact of developmental system drift on gene function. *PLoS Genet.* 10, e1004077.
- Waddington C. H. 1942. Canalization of Development and the Inheritance of Acquired Characters. *Nature* 563–565.
- Wagmaister, J. a, Miley, G.R., Morris, C. a, Gleason, J.E., Miller, L.M., Kornfeld, K., and Eisenmann, D.M. 2006. Identification of cis-regulatory elements from the *C. elegans* Hox gene *lin-39* required for embryonic expression and for regulation by the transcription factors LIN-1, LIN-31 and LIN-39. *Dev. Biol.* 297, 550–565.
- Walhout, A.J., Boulton, S.J., and Vidal, M. 2000. Yeast two-hybrid systems and protein interaction mapping projects for yeast and worm. *Yeast* 17, 88–94.
- Walhout, A.J., and Vidal, M. 2001. High-throughput yeast two-hybrid assays for large-scale protein interaction mapping. *Methods* 24, 297–306.
- Wang, D., Kennedy, S., Conte, D., Kim, J.K., Gabel, H.W., Kamath, R.S., Mello, C.C., and Ruvkun, G. 2005. Somatic misexpression of germline P granules and enhanced RNA interference in retinoblastoma pathway mutants. *Nature* 436, 593–597.
- Wang, M., and Sternberg, P.W. 2000. Patterning of the *C. elegans* 1 degrees vulval lineage by RAS and Wnt pathways. *Development* 127, 5047–5058.
- Wang, X., and Chamberlin, H.M. 2002. Multiple regulatory changes contribute to the evolution of the *Caenorhabditis* *lin-48* ovo gene. *Genes Dev.* 16, 2345–2349.
- Wang, X., and Sommer, R.J. 2011. Antagonism of LIN-17/Frizzled and LIN-18/Ryk in nematode vulva induction reveals evolutionary alterations in core developmental pathways. *PLoS Biol.* 9, e1001110.
- Wanninger, A. 2015. *Evolutionary Developmental Biology of Invertebrates 3: Ecdysozoa I: Non-Tetraconata* (Springer Vienna).

- Wehrli, M., Dougan, S.T., Caldwell, K., O'Keefe, L., Schwartz, S., Vaizel-Ohayon, D., Schejter, E., Tomlinson, A., and DiNardo, S. 2000. arrow encodes an LDL-receptor-related protein essential for Wingless signalling. *Nature* *407*, 527–530.
- Wei, Q., Shen, Y., Chen, X., Shifman, Y., and Ellis, R.E. 2014. Rapid creation of forward-genetics tools for *C. briggsae* using TALENs: lessons for nonmodel organisms. *Mol. Biol. Evol.* *31*, 468–473.
- Wharton, K.A., Johansen, K.M., Xu, T., and Artavanis-Tsakonas, S. 1985. Nucleotide sequence from the neurogenic locus notch implies a gene product that shares homology with proteins containing EGF-like repeats. *Cell* *43*, 567–581.
- White, J.G., Southgate, E., Thomson, J.N., and Brenner, S. 1986. The Structure of the Nervous System of the Nematode *Caenorhabditis elegans*. *Philos. Trans. R. Soc. B Biol. Sci.* *314*, 1–340.
- Whitsett, J.A., Wert, S.E., and Trapnell, B.C. 2004. Genetic disorders influencing lung formation and function at birth. *Hum. Mol. Genet.* *13 Spec No*, R207–R215.
- Wilkinson, H.A., and Greenwald, I. 1995. Spatial and temporal patterns of lin-12 expression during *C. elegans* hermaphrodite development. *Genetics* *141*, 513–526.
- Witte, H., Moreno, E., Rödelsperger, C., Kim, J., Kim, J.-S., Streit, A., and Sommer, R.J. 2015. Gene inactivation using the CRISPR/Cas9 system in the nematode *Pristionchus pacificus*. *Dev. Genes Evol.* *225*, 55–62.
- Wong, H.-C., Bourdelas, A., Krauss, A., Lee, H.-J., Shao, Y., Wu, D., Mlodzik, M., Shi, D.-L., and Zheng, J. 2003. Direct Binding of the PDZ Domain of Dishevelled to a Conserved Internal Sequence in the C-Terminal Region of Frizzled. *Mol. Cell* *12*, 1251–1260.
- Wood, W. 1988. *The Nematode Caenorhabditis elegans*.
- Xie, S., Shen, B., Zhang, C., Huang, X., and Zhang, Y. 2014. sgRNACas9: A Software Package for Designing CRISPR sgRNA and Evaluating Potential Off-Target Cleavage Sites. *PLoS One* *9*, e100448.
- Yochem, J., Sundaram, M., and Han, M. 1997. Ras is required for a limited number of cell fates and not for general proliferation in *Caenorhabditis elegans*. *Mol. Cell. Biol.* *17*, 2716–2722.

- Yoder, J.H., Chong, H., Guan, K.-L., and Han, M. 2004. Modulation of KSR activity in *Caenorhabditis elegans* by Zn ions, PAR-1 kinase and PP2A phosphatase. *EMBO J.* *23*, 111–119.
- Yoo, A.S., Bais, C., and Greenwald, I. 2004a. Crosstalk between the EGFR and LIN-12/Notch pathways in *C. elegans* vulval development. *Science* *303*, 663–666.
- Yoo, A.S., Bais, C., and Greenwald, I. 2004b. Crosstalk between the EGFR and LIN-12/Notch pathways in *C. elegans* vulval development. *Science* *303*, 663–666.
- Yost, C., Torres, M., Miller, J.R., Huang, E., Kimelman, D., and Moon, R.T. 1996. The axis-inducing activity, stability, and subcellular distribution of beta-catenin is regulated in *Xenopus* embryos by glycogen synthase kinase 3. *Genes Dev.* *10*, 1443–1454.
- Zhao, Z., Flibotte, S., Murray, J.I., Blick, D., Boyle, T.J., Gupta, B., Moerman, D.G., and Waterston, R.H. 2010. New tools for investigating the comparative biology of *Caenorhabditis briggsae* and *C. elegans*. *Genetics* *184*, 853–863.
- Zheng, M., Messerschmidt, D., Jungblut, B., and Sommer, R.J. 2005. Conservation and diversification of Wnt signaling function during the evolution of nematode vulva development. *Nat. Genet.* *37*, 300–304.
- Zitnik, E. 2014. Variation in EGF/Ras signaling in *C. elegans* and *C. briggsae* vulval development.
- Zorn, A.M., and Wells, J.M. 2009. Vertebrate endoderm development and organ formation. *Annu. Rev. Cell Dev. Biol.* *25*, 221–251.